CHARACTERISATION OF CARDIAC REMODELING ASSOCIATED WITH PREGNANCY: PROVIDING INSIGHTS TO PERIPARTUM CARDIOMYOPATHY

Vitaris Kodogo

Student number: kdgvit001

University of Cape Town

A thesis submitted in partial fulfilment of the requirements for the degree

Doctor of Philosophy

PhD

(Medicine)

Department of Medicine

Faculty of Health Sciences

University of Cape Town South Africa

December 2020

Supervisors: Prof Karen Sliwa,

Prof Sandrine Lecour

Dr Feriel Azibani

The copyright of this thesis vests in the author. No quotation from it or information derived from it is to be published without full acknowledgement of the source. The thesis is to be used for private study or non-commercial research purposes only.

Published by the University of Cape Town (UCT) in terms of the non-exclusive license granted to UCT by the author.

University of Cape Town

Declaration

I, **Vitaris Kodogo** hereby declare that the work on which this dissertation/thesis is based is my original work (except where acknowledgements indicated otherwise). I declare that neither the whole work nor any part of it has been, is being, or is to be submitted for another degree in this or any other university. I empower the university to reproduce for the purpose of research either the whole or any portion.

Signature:

Date:

Acknowledgements

I would like to thank the following people who played a key role in bringing this work together.

Firstly, I would like to thank my supervisor, Prof Karen Sliwa, for the fantastic insight into Cardiovascular Research and the guidance and mentorship.

Dr Feriel Azibani, my co-supervisor, for your encouragement, mentorship and great insights into basic science research.

Prof Sandrine Lecour, for the invaluable opportunity to work in the laboratory under your guidance.

Dr Nkanyiso Hadebe, for your assistance with training in echocardiography in murine models.

Sister Olivia Briton, for your friendship and generosity.

Sylvia Dennis for your helping hand in proof reading and formatting of the thesis

All the HATTER students and staff for their time and support in making the journey easier and more comfortable.

I would also like to extend a very special thank you to my family for enduring time away and to Samantha Kodogo for your whole-hearted and endless support and patience.

I would like to also thank the University of Cape Town Faculty of Health Sciences for institutional support.

Finally, I would like to thank NRF and MRC for funding the project.

Abstract

Introduction: Maternal cardiovascular changes that occur in pregnant women are usually well tolerated by most women experiencing an uncomplicated pregnancy and are reversable postpartum. However, pregnancy can induce adverse cardiac events in previously healthy women without any known cardiovascular disease. Understanding of the maternal cardiovascular adaptation during healthy pregnancy is important to identify deviations from regular patterns caused by pathological conditions. The main objective of this study was to explore the functional, structural and molecular cardiovascular changes that are involved in healthy pregnancy with the goal to delineate possible mechanisms involved in the lack of reverse cardiovascular remodeling observed in peripartum cardiomyopathy (PPCM).

Methods: Cardiovascular functional, morphological and molecular changes during pregnancy and postpartum were assessed in pregnant wild type mice (C57/BL6) and healthy women. An invitro model of cardiac hypertrophy was then used to explore the involvement of pregnancy hormones in the regulation of cardiac hypertrophy. Finally, we assessed the circulatory level of growth differentiation 15 (GDF-15) in PPCM patients and matched healthy controls.

Results: Cardiac structural, functional and morphological changes were observed in mice and all the parameters were resolved postpartum. Strikingly, volume load, cardiac hypertrophy and fibrosis were sustained for a longer period postpartum than previously reported. Proteomics profiling confirmed the prolongation of cardiac hypertrophy in the postpartum and the involvement of the ubiquitin proteasome system (UPS) in the reverse remodeling of cardiac changes that occur during pregnancy. We also identified a set of transcription factors that regulates the protein expression in the postpartum. Left ventricular systolic function was significantly reduced in late pregnancy in humans. Finally, the serum level of GDF-15 was significantly lower in PPCM patients compared to healthy controls

Conclusion: We conclude that pregnancy induces cardiac stress which is sustained in the postpartum period. The heart remodels and adapts to meet the demand by both the mother and the fetus. Cardiac changes that occur during pregnancy are strictly regulated and reversed postpartum. However, the postpartum period is a period of intense cardiac stress and activity which requires monitoring for any deviation that may lead to pathological conditions.

TABLE OF CONTENTS

List of Figures

List of Tables

List of Appendices

Supplementary Tables

List of Abbreviations

ACTH-	Adrenocorticotropic hormone
AT-	Angiotensin
ANF-	Atrial natriuretic factor
AET-	Aortic ejection time
ACN-	Acetonitrile
bHCG-	Beta human chorionic gonadotropin
BCA-	Bicinchoninic acid
BMI-	Body mass index
CNTF-	Ciliary neurotrophic factor
CT-1-	Cardiotrophin-like cytokine
CHD-	Congenital heart disease
CRP-	C-reactive protein
CCL2-	Cchemokine ligand 2
cAMP-PKA -	Cyclic AMP- protein kinase A
ChEA-	ChIP-seq/chip Enrichment Analysis
cDNA-	Complementary DNA
CVD-	Cardiovascular disease
CHF-	Chronic heart failure
CNTF-	Ciliary neurotrophic factor
CT-1-	Cardiotrophin-like cytokine
CHD-	Congenital heart disease
CRP-	C-reactive protein
DBP-	Diastolic blood pressure
DDA-	Data dependent acquisition
DTT -	Dithiothreitol
DBP-	Diastolic blood pressure
ESR-	Erythrocyte sedimentation
EF-	Ejection fraction
ECM-	Extracellular matrix
eNOS-	Endothelial nitric oxide synthase
ECC-	Excitation-contraction coupling
ESI-	Electrospray ionisation
ESR-	Erythrocyte sedimentation
FA-	Formic acid
GRF-	Glomerular filtration rate
GRSR-	Global radial strain rate
GLSR-	Global longitudinal strain rate
GPCR-	G-protein coupled receptor
Gal3-	Galectin-3
GAPDH-	Glyceraldehyde 3-phosphate dehydrogenase
GRF-	Glomerular filtration rate
HPL-	Human placental lactogen
HCG-	Human chorionic gonadotrophin
HIF-1-	Hypoxia inducible factor-1
HF-	Heart failure
HC-	Healthy control
HREC-	Human Research Ethics Committee
HPL-	Human placental lactogen

HCG-	Human chorionic gonadotrophin
IFNc -	Interferon gamma
IVRT-	Isovolumic relaxation time
IVCT-	Isovolumetric contraction time
LV-	Left ventricle
LVEDD-	Left ventricle end-diastolic dimension
LVESD-	Left ventricle end-systolic dimension
IGF-	Insulin like growth factor
LIF-	Leukemia inhibitory factor
MCV-	Mean corpuscular volume
MCHC-	Mean corpuscular haemoglobin concentration
mTOR-	Mammalian target of rapamycin
MMPs-	Matrix metalloproteinases
MnSOD-	Manganese sodium dismutase
MAPK-	Mitogen-activated protein kinases
MEF2-	Myocyte enhancer factor-2
MRI-	Magnetic resonance imaging
MCV-	Mean corpuscular volume
NHBPEPWG-	National High Blood Pressure Education Program Working Group on High Blood Pressure in Pregnancy
NFAT-	Nuclear factor of activated T cells
NYHA FC-	New York Heart Association Functional Classification
OPN-	Osteopontin
OD-	Optical Density
PPCM-	Peripartum Cardiomyopathy
PlGF -	Placental growth factor
PINP-	Procollagen type-I N-terminal propeptide
PIIINP-	Procollagen type-III N-terminal propeptide
PLAX-	Parasternal long axis
PSAX -	Parasternal short axis view
PVDF-	Polyvinylidene fluoride
PLAB-	Placental bone morphogenetic protein
RV-	Right ventricle
RTK -	Receptor tyrosine kinase
ROS-	Reactive oxygen species
RT-	Reverse transcription
RWT-	Relative wall thickness
SBP-	Systolic blood pressure
SERCA-	Sarco/endoplasmic reticulum Ca2+-ATPase
SKA-	Skeletal alpha actin
sST2-	Soluble ST2
TBG-	Thyroid binding globulin
TSH-	Thyroid stimulating hormone
T3-	Triiodothyronine
T4-	Thyroxine
TTP-	Time to peak
TRPC-	Transient receptor potential channel
TAC-	Transverse aortic constriction
TIMPs -	Tissue Inhibitor of Metalloproteinases

TNFa-	Tumour necrosis factor-a
TTE-	Transthoracic echocardiography
TRPC-	Transient receptor potential channel
TAC-	Transverse aortic constriction
VEGF-	Vascular endothelial growth factor
VT-	Ventricular tachycardia
VTI-	Velocity time integral
WHO	World Health Organisation

Chapter summary

Chapter 1: Maternal cardiovascular system goes through important changes during pregnancy to support the growing fetus. The changes are usually well tolerated by most women experiencing an uncomplicated pregnancy and are reversable postpartum. However, pregnancy can provoke adverse cardiovascular incidents in healthy women without any known previous cardiovascular disease. Cardiac disease account for up to 15% of maternal death and continues to be a main cause of morbidity and mortality in pregnant and postpartum women.

It can be more difficult to diagnose cardiovascular diseases during pregnancy as most symptoms are like changes that occur due to normal pregnancy induced biochemical changes. Hence, a deep understanding of the maternal cardiovascular adaptation during pregnancy is important to identify deviations from regular patterns caused by pathological conditions.

Chapter 2: The main objective of this study was to describe the functional, structural and molecular cardiovascular changes that are involved in pregnancy with the goal to delineate possible mechanisms involved in the lack of reverse cardiac remodeling observed in peripartum cardiomyopathy.

Chapter 3: This study was conducted on wild type mice model, cell culture model, healthy mothers and peripartum cardiomyopathy (PPCM) patients. Firstly, cardiac changes were assessed by echocardiography in a healthy pregnant wild type mouse model (C57/BL6) at different time points during pregnancy and postpartum. Blood and hearts were collected at each time point for hormone measurements, proteomics, fibrosis measurements and mRNA expression analysis. Bioinformatic tool (Expression2Kinases) was used to predict the transcription factors and kinases which control the expression of proteins upregulated in the postpartum period.

Cardiomyocytes (H9C2) invitro model of cardiac hypertrophy was then used to assess the potential role of pregnancy hormones in the modulation of cardiac hypertrophy. H9C2 cells were treated with isoproterenol, oestrogen, progesterone or cotreated with a combination of the hormones. Cell morphology, and mRNA expression of fetal gene program were assessed as markers of hypertrophy. Protein kinase B (AKT), signal transducer and activator of transcription 3 (STAT3) and STAT5 levels were also measured to explore the potential signaling mechanisms implicated in the control of cardiomyocytes hypertrophy.

We then assessed the cardiovascular structural and functional changes using conventional echocardiograph in 63 pregnant healthy mothers who were recruited consecutively from 2nd trimester until 6 months postpartum. Furthermore, we conducted a crossectional measurement of growth differentiation 15 (GDF-15) in PPCM patients and matched postpartum controls.

Results and Discussions

Chapter 4: Assessment of healthy pregnant mice showed a gradual increase in body weight, heart weight and stroke volume during pregnancy. Changes in the heart morphology and loading conditions were also observed in pregnant mice. We also observed eccentric cardiac hypertrophy starting in the late pregnancy phase. Strikingly, cardiac hypertrophy was sustained for about 2 weeks after parturition and had not reverted to normal level by Day 28 postpartum (pp). Other studies have published controversial findings on the time of reversal of cardiac hypertrophy in mice postpartum. Reports ranges from immediate resolving to 7 days postpartum. Systolic and diastolic cardiac functions were normal and did not change significantly at all stages.

Subsequently, we explored the potential signaling pathways that may be involved in the regulation of physiological cardiac hypertrophy during pregnancy in mice. Our results suggest that the PI3K/AKT signaling pathway modulates physiological hypertrophy during pregnancy whilst the janus kinase (JAK)-signal transducer and activator of transcription (STAT) (JAK/STAT) pathway may be responsible for maintaining physiological conditions in the postpartum phase when AKT is downregulated.

We also investigated the mRNA expression of a cardiac derived hormone GDF-15 during pregnancy. GDF-15 expression was induced from late pregnancy and throughout the postpartum period. Our finding suggest that GDF-15 could be induced by stretch or cardiac stress but not by pregnancy hormones. Surprisingly, GDF-15 expression was reduced in STAT3 KO mice hearts.

To gain insight on the molecular modifications that happen in pregnancy. We performed in-depth global protein expression profiling of pregnant mice hearts proteome at different time points during pregnancy and postpartum. 1190 proteins that were identified in all animals. Only 14 proteins were significantly varied across all groups. The significant proteins included proteins involved in hormone transport and metabolism, cardiac anatomical morphogenesis, angiogenesis, acute inflammation and immunological response.

The greatest proteomic response occurred between the late pregnancy group and the postpartum groups. We then assessed differential expressions between late pregnancy group (Day 14) and the 2 postpartum groups Day 14pp and Day 28pp. There was a clear functional difference between the proteins upregulated on Day 14pp and Day 28pp. The most significant proteins upregulated on Day 14pp are proteins that were involved in cardiac hypertrophy and muscle contraction, whilst proteins involved in proteasome system were upregulated on Day 28pp.

Specificity protein 1 (SP1), hepatocyte nuclear factor 4 alpha (HNF4A), interferon regulatory factor 1 (IRF1) and (IFR3) were the most significant transcriptional factors that regulated the expression of proteins on Day14pp whilst yin yang 1 (YY1), nuclear transcription factor Y alpha (NFYA), transcription initiation factor TFIID subunit 1 (TAF1), nuclear transcription factor Y beta (NFYB), and lysine Acetyltransferase 2A (KAT2A) regulated the expression on Day 28pp. Transcription factors on Day 14 pp regulated pro-hypertrophic signaling pathways whilst the transcription factors on Day 28pp are known to be repressors of cardiac hypertrophy and fibrosis.

Chapter 5: Our findings from the invitro model suggested that oestrogen (E2) through the instigation of the PI3K/AKT signaling pathway modulates physiological cardiomyocytes hypertrophy. E2 also has antihypertrophic properties which abrogated both physiological and pathological hypertrophy. Progesterone induced physiological cardiomyocytes hypertrophy.

Chapter 6: Data from healthy pregnant mothers substantiated the haemodynamic changes that occur during pregnancy. Blood pressure increased gradually peaking in the postpartum phase. Heart rate was significantly reduced in the early postpartum phase when compared to the late pregnancy group. Left ventricular ejection fraction was significantly reduced in the third trimester. Contradicting results were reported on left ventricular systolic function during pregnancy mainly because ejection fraction measurement is highly affected by the loading conditions of the heart.

Based on our finding on the level of GDF-15 in STAT3 KO mice we assessed the level of GDF-15 in serum of peripartum cardiomyopathy (PPCM) patients. The circulatory level of GDF-15 was significantly lower in PPCM patients when compared to controls. This finding contradicts with previous studies that suggested GDF-15 as a marker of pathological cardiac conditions. However, we suggest further studies on a bigger sample size.

Chapter 7: We concluded that cardiac structural and functional changes occur in mice during pregnancy. However, measurements like left ventricular ejection fraction may vary as they

are affected by other parameters such as preload and afterload. We also conclude that normal pregnancy in mice induces physiological cardiac hypertrophy which is sustained for weeks postpartum before reverting to normal level. Ubiquitin proteasome system (UPS) upregulated in the postpartum phase could be the important mechanism involved in reversing cardiac hypertrophy and fibrosis. However, further investigations are required to delineate the actual role played by proteasome system during pregnancy induced cardiovascular remodeling. Furthermore, the involvement of GDF-15 in physiological pregnancy and the downstream mechanisms needs to be investigated.

CHAPTER 1

INTRODUCTION

Section 1: Maternal physiological changes associated with pregnancy

The maternal body progressively adapts throughout pregnancy to sustain the mother and the developing fetus. Expected physiological modifications are often interconnected and affect the entire body systems [1]. Affected systems include the neurological, cardiovascular, metabolic, renal and respiratory system.

The pregnant woman's placenta also produces many hormones that have expansive effects during the pregnancy [2][3]. **Figure 1** is a central illustration of the changes that take place in several organs and systems during pregnancy. These projected physiological transformations may lead to decompensation in mothers without preceding co-morbidities or uncover pre-pregnancy diseases. Hence, an understanding of normal physiologic adaptations during pregnancy is essential to identify and manage diseases in pregnancy.

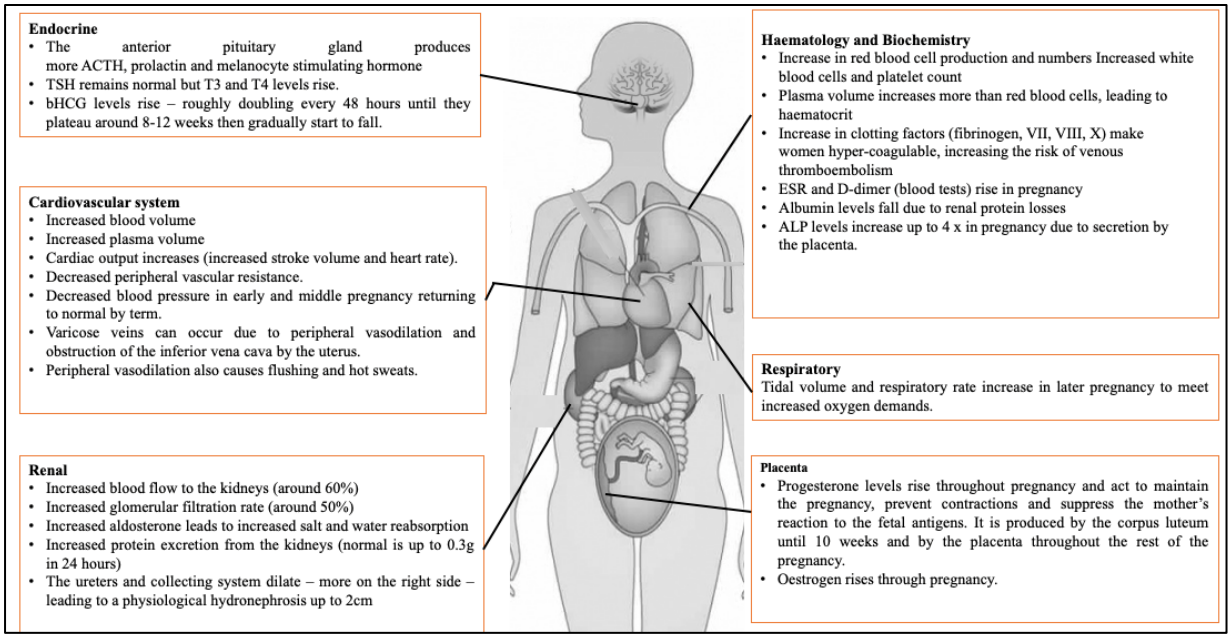

Figure 1: Central illustration of physiological changes during pregnancy

A pregnant woman's body experiences numerous physical and biological modifications necessary to assist fetal development. Abbreviations: ACTH-adrenocorticotropic hormone, TSH-thyroid stimulating hormone, bHCG-beta human chorionic gonadotropin, ESR-erythrocyte sedimentation rate, ALP- alkaline phosphatase. Adapted from Pieper, 2015 [4].

1.1 Endocrine and metabolic changes

Numerous endocrine and metabolic changes that transpire during pregnancy are dominated by the hormonal signals starting from the feto-placental unit (FPU). Right through the gestation period progesterone and oestrogen levels increase [2]. Before implantation, oestrogen and progesterone are produced by the corpus luteum and later by the placenta if implantation is successful [5][6]. Raised oestrogen concentrations causes an increase in hepatic production of thyroid binding globulin (TBG) [7]. Consequently, triiodothyronine (T3) and thyroxine (T4) bind to the TBG, which triggers more thyroid stimulating hormone from the anterior pituitary gland. Subsequently, the free T3 and T4 levels stay unaltered whilst the total T3 and T4 levels elevates.

In addition, the placenta produces other hormones for example relaxin, human placental lactogen (HPL) and human chorionic gonadotrophin (HCG) [1].

HPL, prolactin, cortisol levels increase together with the boost in progesterone and oestrogen can result in gestational diabetes [4][8]. This is because HPL, prolactin and cortisol are anti-insulin hormone therefore, the increase insulin resistance in the mother and diminish peripheral uptake of glucose [9][10].

1.2 Respiratory changes

Pregnancy impacts respiratory status and function. Anatomically, the development of the fetus in pregnancy causes upward shift of the diaphragm [11]. Nonetheless, this does not significantly reduce the total lung capacity due to an increase in the transverse and anterior-posterior diameters of the thorax that also happen [11].

Woman also faces escalation in their metabolic rate which causes augmented demand for oxygen. Circulating progesterone excites the respiratory centre, causing an increase in minute ventilation, principally by an increase in tidal volume (~40% increase) and by an upsurge in respiratory rate (~15% increase) [12].

1.3 Renal changes

Kidneys and ureter may increase in size in pregnant women due to the upsurge in blood volume and vasculature [13]. Glomerular filtration rate (GFR) increases by almost by 50% during pregnancy and revert to normal in about 20 weeks postpartum [14]. The augmented GFR increases the excretion of protein, albumin, and glucose [13][14].

1.4 Blood changes

Apparent adaptations in the haematological system are observed in the peripartum period [1]. The peripartum period is hence, marked with increased risks including anaemia, thromboembolism and consumptive coagulopathies [1].

Plasma volume increases by 40-50% during pregnancy to carter for the enhanced metabolic requirements by tissues. Most of the increase in plasma volume occurs by 34 weeks [15][16]. Unfortunately, the rise in plasma volume causes haemodilution [15]. Haemodilution causes a reduction in haemoglobin concentration, haematocrit and red blood cell count [12][17]. However, the mean corpuscular volume (MCV) or mean corpuscular haemoglobin concentration (MCHC) remain unchanged [18]. **Figure 2** shows the relative changes in red cell, plasma and total blood volumes during pregnancy. Labour contractions push blood back in circulation, approximately 500ml of blood is squeezed back after delivery [1][18]. In most cases plasma volume reverts to pre-pregnancy volume beginning at 6 days post-delivery [19][20].

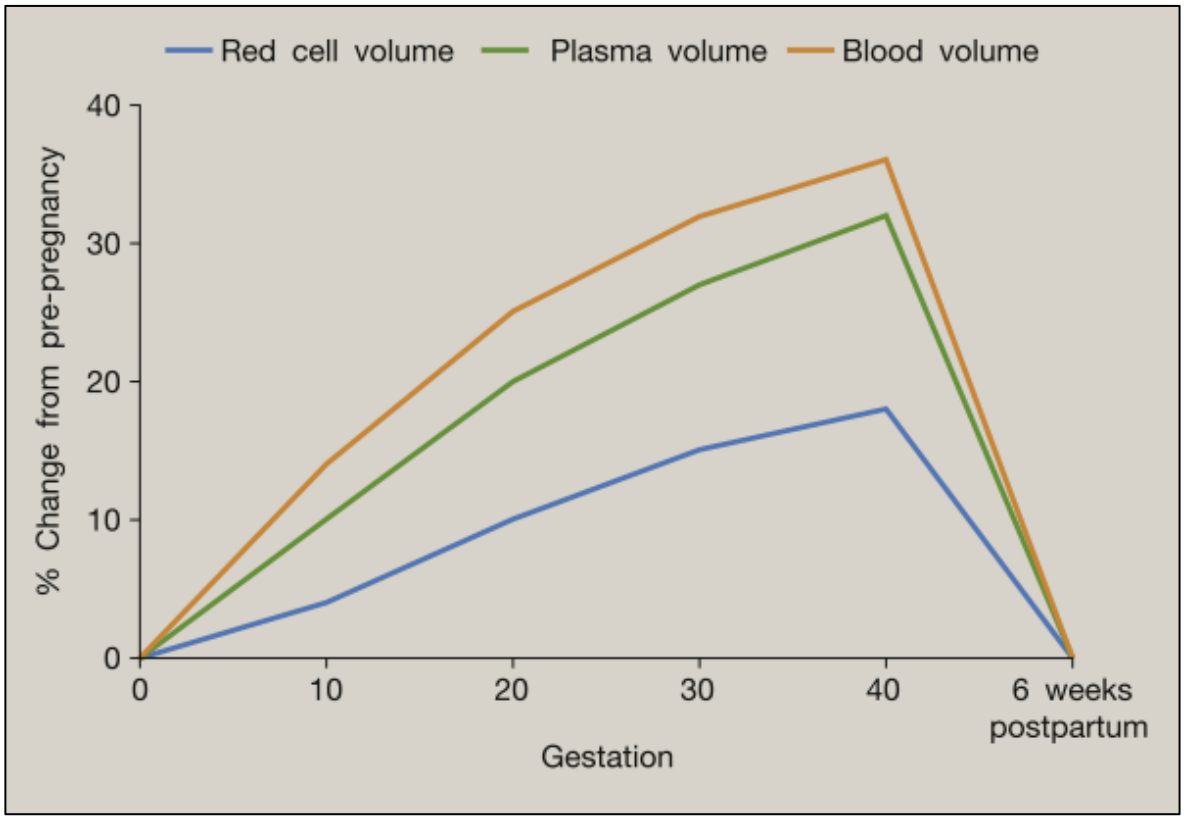

Figure 2: Relative changes in red cell, plasma and total blood volumes during pregnancy (*values approximate) Talbot et al, 2016 [18]*.

Pregnancy causes an increase in the iron demand for haemoglobin production of foetus [21]. There is a 10- to 20-fold rise in folate demand and a two-fold increase in vitamin B12 demand [22].

Pregnancy alters the balance within the coagulation system producing a physiological hypercoagulable state [1]. Most clotting factors excepting factors XI and XIII progressively rise during pregnancy with corresponding drop of thrombolytic factors such as antithrombin III [15]. There is a 4-5 times higher risk of developing a clot during pregnancy and in the postpartum period than non-pregnant [23]. Pregnancy known to cause a mild decline in platelet count [24][25]. However, others have reported no effect on platelets count [12][15]. The white blood cell count rises with sporadic presence of myelocytes or metamyelocytes in the blood. During labour, there is an upsurge in leukocyte count [16].

1.5 Vasculature changes

1.5.1 Angiogenesis changes

An equilibrium between the growth of cardiac muscle mass and coronary angiogenesis is an essential factor for physiological cardiac remodeling. During pregnancy, myocardial angiogenesis increases in early to mid-pregnancy, and revert to non-pregnant levels in late-pregnancy [26]. Studies in mice reported increased capillary density and upregulation of vascular endothelial growth factor (VEGF) in the late pregnant is an indication of strengthened neoangiogenesis [27]. The angiogenic process is instigated by growth factors such as basic fibroblast growth factor (bFGF), VEGF, or placental growth factor (PlGF) [28][29].

1.5.2 Systemic vasodilation changes

Systemic vasodilation is one of the earliest modifications which occur in the first six weeks of pregnancy peaking by the end of first trimester [17][30]. It has been proposed that systemic vasodilation direct most of the hemodynamic changes found in human pregnancy [31][32]. Increase in systemic vasodilation causes an ~35% to 40% drop in systemic vascular resistance (SVR) in the first trimester [17][33].

A number of important aspects are thought to aid to the vascular system changes that occur during pregnancy [34]. Substantial evidence points to the vasodilatory effect of progesterone, endothelium-dependent factors including nitric oxide synthesis, stimulated by estradiol and

perhaps vasodilatory prostaglandins (PGI2) [15] [34]. SVR revert to near-pre pregnancy levels close to the end of the second week postpartum in normal pregnancy [15][35].

1.5.3 Blood pressure changes

There are discrepancies on the conventional alterations of blood pressure in uncomplicated pregnancies. Although many studies have shown that women experience a mid-trimester drop, followed by a gradual increase in systolic blood pressure (SBP) and diastolic blood pressure (DBP) up to 30-45 postpartum days [36]. In numerous studies where the National High Blood Pressure Education Program Working Group on High Blood Pressure in Pregnancy (NHBPEPWG) references were employed to assess BP, SBP remained constant, whilst DBP and mean atrial pressure (MAP) dropped [37][38].

1.6 Heart rate changes

Heart rate rises from the seventh week of gestation and increases by up to 20% in the final three months [39][40]. Heart rate in normal uncomplicated pregnancy does not rise above 100 beats/minute [41]. The rise in heart rate is a compensatory response to falling SVR [33]. Heart rate returns to preconception levels within 10 days postpartum [17][33].

1.7 Cardiac output changes

During pregnancy, cardiac output increase by around 40% due to the added requirement for blood flow to the placenta, kidneys, breasts, skin and the heart itself [42]. Increase in cardiac output also compensate for reduced SVR during pregnancy [15]. Cardiac output upsurges during the first trimester, reaching its peak in the early third trimester [8].

Cardiac output follows a non-linear array of adaptation. Initially, it is facilitated by increases in stroke volume whereas, later, the increase is linked to heart rate [43][44]. Stroke volume (SV) rises steadily up until the second trimester and then stabilizes or decreases late in the third trimester [45]. It then yields to non-pregnant values momentarily postpartum [15].

Section 2: Physiological cardiac remodeling associated with pregnancy

Cardiac remodeling is a collection of molecular, cellular and interstitial changes that present clinically as changes in size, mass, geometry and function of the heart [46]. The etiologies of cardiac remodeling are different depending on the nature of upstream stimuli. However,

some pathways in terms of molecular, biochemical and mechanical events are shared [47][48][49].

Current evidence suggests that exercise and normal pregnancy typically elicits physiological remodeling [50][51]. Physiological cardiac remodeling during pregnancy is mostly prompted by haemodynamic load, neurohumoral activation and additional factors such as endothelin, cytokines, nitric oxide production and oxidative stress [52][53][54].

It is characterized by a tweaked and orchestrated process of favourable adaptations, which result in reduced cardiac wall stress, increased pumping performance and improved vascularisation [55][56][57]. At molecular level, physiological cardiac remodeling is linked to well-organized signaling pathways which tightly control cardiomyocytes contractility, sarcomere reorganisation, cell survival, metabolic adaptation, mitochondrial function and angiogenesis [58][15]. Structural or functional cardiac irregularities do not happen in this situation, and is usually not deemed a risk factor for heart failure [59].

2.1 Cardiac morphological changes

Pregnancy provides a unique model to study morphological modifications of the heart in a physiological situation of temporary preload and afterload alterations. In response to the demand to perfuse both the mother and the growing foetus, morphological changes are activated. These changes include increased Left ventricle (LV) wall thickness, LV mass and longitudinal and transverse chamber diameters [60]. Sphericity index also decreases from the first to the third trimester and return to normal status postpartum [60]. Most morphological changes that occur during pregnancy are reversed to normality postpartum [61].

An increase of 28% in LV wall thickness and 52% in LV wall mass above pre-pregnancy values were observed throughout pregnancy [17]. The increase in LV mass was found to be in excess of the increase in pregnant body size showing a true hypertrophic reaction with a rise in both left ventricular mass and left ventricle mass index [37][62].

The left atrial scopes increase steadily starting as early as 5 weeks of pregnancy peaking at 28–34 weeks' gestation [60][37]. Left atrial enlargement is possibly caused by an increase in preload as exhibited by the concurrent increase in SV and cardiac output during pregnancy [63][64].

LV end-diastolic dimension (LVEDD) increases substantially by nearly 10% in pregnancy, beginning as early as 12 weeks, peaking at 24–32 weeks and remaining unchanged thereafter until term [37]. Left ventricle end-systolic dimension (LVESD) was reported to increase by about 20% in pregnancy [62][65].

Conflicting reports in the cross-sectional area of the left ventricular outflow tract (CSA of LVOT) have been published [66]. Some reporting no change [67] whist several others reporting an increase [66][68][69]. The difference may be due to the incorrect geometrical assumptions of the LVOT being spherical [37].

Few studies have looked at the right ventricle (RV) size changes during pregnancy and have reported slightly increased RV area and volume when compared to non-pregnant groups [70][71].

2.2 Cardiac functional changes

2.2.1 LV systolic function

Physiological cardiac changes that take place during pregnancy enhance the heart's performance. Nevertheless, there have been some inconsistent reports on some parameters that determine heart function during pregnancy [60] [66] [72][73]. This variability may somewhat reflect disparities in methodology, the small study populations, and discrepancies in population characteristics such as maternal age and race.

Ejection fraction (EF), a measure of systolic function from M-mode echocardiography measurements was reduced during late pregnancy in several studies [66][73][74]. LV systolic function is resolved postpartum. The moderate reduction in cardiac function is mainly due to the increased chamber dimensions and the higher blood volume to be pumped in late pregnancy. However, some studies recorded no change in both EF and FS during the course of pregnancy [60][75].

Using speckle tracking echocardiography (STE), decline in left ventricular longitudinal global strain (LV longitudinal GS), a parameter of myocardial contraction was reported [66][76]. However, Naqvi et al [77] observed an increase in increase in LV radial strain rate (LVRSR) and longitudinal rate of deformation (LVLSR), particularly during first and second trimesters [74]. Savu et al [60], also reported a significant decrease in late pregnancy on LV

segmental longitudinal systolic deformation and deformation rate. This behaviour was true for all the 3 ventricular levels (basal, mid, and apical).

2.2.2 LV diastolic function

In gestation, there are only negligible changes in diastolic function and filling pressures [66]. The peak early and late diastolic mitral inflow (E wave and A wave) velocities increase resulting from raised preload and blood volume [74]. Nonetheless, the alteration in the A wave is greater than E wave; thus, a reduced E/A ratio is found in normal pregnancy. This may be instigated by the increased atrial contraction forced by increased left atrial filling pressures [74][78]. Correspondingly, the early and late diastolic myocardial velocity ratio (E'/A') also falls due to amplified atrial contractility [66][67].

Diastolic mechanical function based on strain analysis reported unchanged early diastolic global radial strain rate (GRSR), global circumferential strain rate (GCSR) and global longitudinal strain rate (GLSR) during pregnancy [75]. However, early diastolic GLSR time to peak (TTP) corrected for heart rate (HR) (GLSR TTP/HR) was found to be increased in pregnant women [75]. **Figure 3** illustrate some of the alterations of the maternal LV morphology and function.

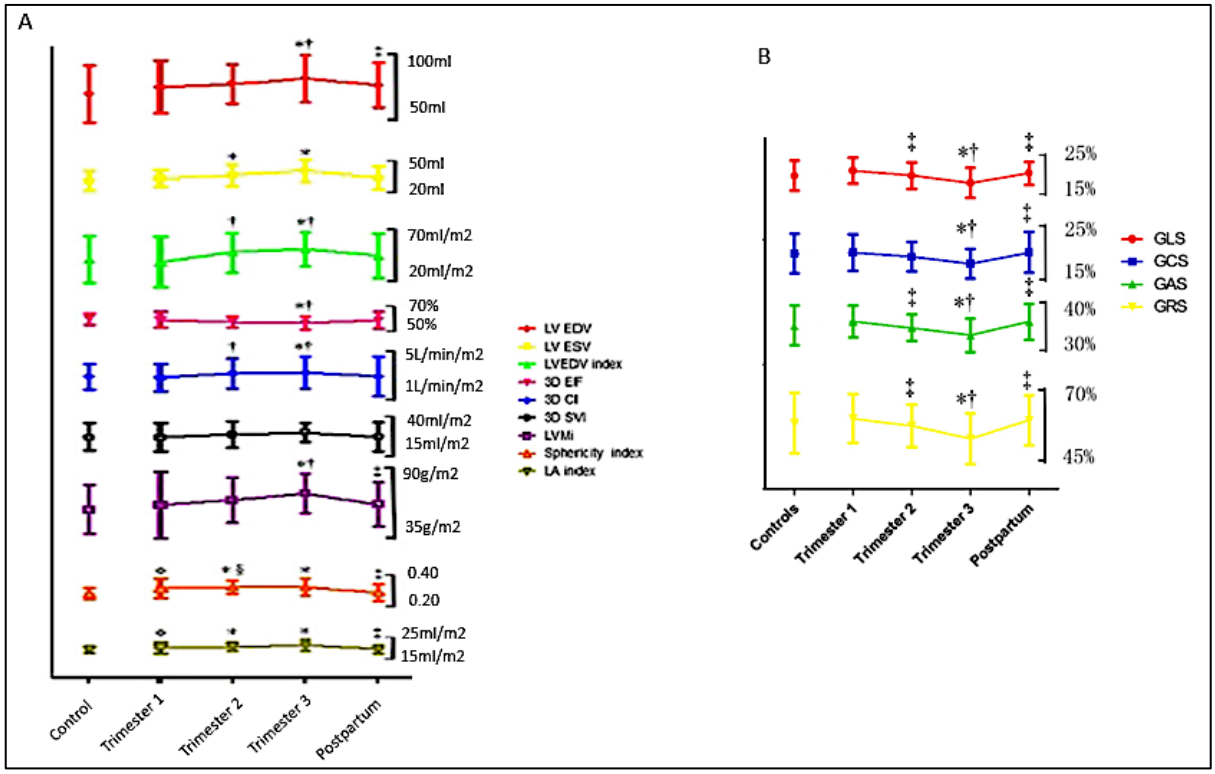

Figure 3: Illustrate some of the expected changes of the maternal LV morphology and function during pregnancy and postpartum by 3D speckle tracking echocardiography

***A**: LVEDV-left ventricular end-diastolic volume; LVESV-left ventricular end-systolic volume; LVEDVi-left ventricular end-diastolic volume index; EF-ejection fraction; CI-cardiac index; SVI-stroke volume index; LVMi-left ventricular mass index; LA index- left atrial volume index. **B**: GLS indicates global longitudinal strain; GCS, global circumferential strain; GAS, global area strain; GRS, global radial strain. *P < 0.05 vs. Controls; †P < 0.05 vs. Trimester 1; ‡P < 0.05 vs. Trimester 3; §P < 0.05 vs. Postpartum. The figure was adapted from Cong et al; 2015 [76].*

2.3 Measurement of heart function during pregnancy

The assessment of heart function is performed using various parameters: patient's family history, physical examination to ascertain the presence of clinical symptoms and signs, and blood tests.

2.3.1 History and clinical investigation

Cardiomyopathies, congenital heart disease, the Marfan syndrome and other varies disorders can be ascertained by collecting personal and family history [79]. Physical examinations including auscultation, BP and signs of dyspnoea are also crucial considering the physiological alterations that occur during pregnancy.

2.3.2 Electrocardiogram (ECG)

ECG recording can help to detect anomalies in the heart's rhythm and structure [80]. The bulk of pregnant patients have a normal ECG [81]. Conventional findings include transitory ST segment and T wave alterations, the presence of a Q wave and inverted T waves in lead III, an attenuated Q wave in lead AVF, and inverted T waves in leads V1, V2, and, seldomly, V3. ECG fluctuations can be connected to a gradual change in the position of the heart and may mimic left ventricular (LV) hypertrophy and other structural heart diseases [82].

2.3.3 Echocardiography

Echocardiography is, undoubtedly the most favoured investigative test for cardiovascular function in pregnant women. This is because of its non-invasiveness and accessibility with no risk of radiation to the mother and the fetus. Echocardiography gives detailed information about structural deformities and informs the pathophysiology of cardiac disease and its haemodynamic outcomes.

Table 1: Some echocardiographic changes during pregnancy. *(Adapted from Shuang et al, 2016 [74].*

Echocardiographic variables	**Changes during pregnancy**
Left ventricular dimension and volume	Increases
Left ventricular wall thickness and left ventricular mass	Increases
Left ventricular ejection fraction	Unchanged
Left ventricular fractional shortening	Unchanged
Left ventricular radial and longitudinal strain rate	Increases
Aortic root diameter	Mildly increases
Right ventricular dimension and volume	Increases
Right ventricular ejection fraction	Unchanged
Left atrial size and volume	Increases
Stroke volume (as measured using pulsed wave Doppler)	Increases
Mitral E wave velocity	Increases, then decreases
Mitral A wave velocity	Increases
Peak pulmonary artery systolic pressure estimated using tricuspid regurgitation jet	Unchanged

2.3.4 Magnetic resonance imaging (MRI) and computed tomography

MRI uses robust magnetic fields, magnetic field gradients, and radio waves to create images of the organs in the body. It is used as a secondary tool to diagnose complex heart diseases [83]. MRI is regarded as relatively safe specifically after the first trimester [84][85]. The use of gadolinium during MRI should be avoided as there is limited data on its long-term effects [86].

2.4 Physiological cardiac hypertrophy

During pregnancy, the heart and the discrete cardiomyocytes regularly undergo enlargement to counterbalance for increased cardiac output [87]. This increased cardiac mass is termed physiological hypertrophy. Pregnancy fosters eccentric hypertrophy, with no permanent effects on cardiac function [88]. It is characterized by a mild (10–20%) increase in cardiac mass and individual cardiomyocyte expansion in both length and width [89].

The cellular readjustment of the ventricular wall is also correlated with conserved or improved cardiac output but with significantly increased left ventricular volumes [90]. In accordance to the Laplace's law, individual cardiomyocytes increase in volume, and the heart develop hypertrophy to reduce ventricular wall tension and maintain function and efficiency in response to an increased workload [58][91]. Eccentric hypertrophy increases ventricular volume with a synchronized growth in wall and septal thickness [37]. **Figure 4** shows the morphology of eccentric hypertrophy in physiological remodeling.

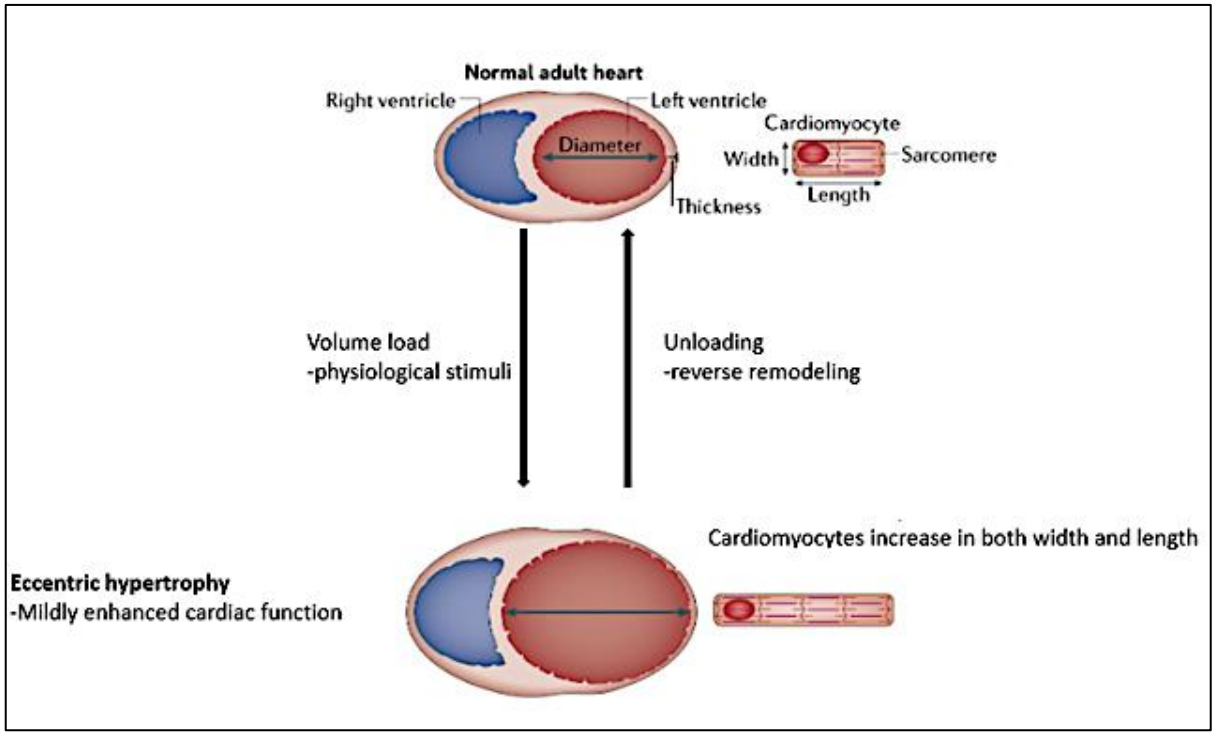

Figure 4: The morphology of eccentric cardiac hypertrophy.

Eccentric hypertrophy characterized by increased wall thickness and individual cardiomyocytes growth in both length and width. It occurs during pregnancy due to volume load and it is physiological and reversable when the load is removed. Figure was adapted from Maillet et al [92].

2.4.1 Cellular changes associated with cardiac hypertrophy

The heart is constituted of cardiomyocytes (muscle cells), non-myocytes (e.g., fibroblasts, endothelial cells, mast cells, vascular smooth muscle cells), and the surrounding extracellular matrix [93]. Cardiomyocytes, forms 85% of the heart mass, are the contracting cells of the heart, and they comprise of an organized series of sarcomeres [92]. Countering the altered physiological stress, cardiomyocytes increase in dimensions to meet with increased functional demand [94]. This increases the thickness of the walls but reduces interior dimensions of the ventricular chambers [94].

During cardiac remodeling, cardiomyocytes are capable of transducing mechanical stress from the surrounding environment to biochemical signals, a process referred to as "mechanotransduction" [49]. It was shown that stretching cultured cardiomyocytes speed up protein synthesis and specific gene expression without participation of neural or humoral factors [95]. One stretch receptor expressed in myocytes is the transient receptor potential channel (TRPC) [96]. Two subtypes of this receptor – TRPC1 and TRPC6 – are each activated

by stretching and are overexpressed in hypertrophy [97]. Integrins are another class of transmembrane protein that transmit stretch-related changes in the extracellular matrix through an intracytoplasmic tail [97].

Cardiomyocytes also integrate signals from extracellular matrix, the cell membrane, membrane-bound ion channels, the cytoskeleton, sarcomere, mitochondria and endoplasmic reticulum [59]. They also cross talk with other cells like endothelial cells, fibroblasts and inflammatory cells [98].

2.4.2 Molecular and biochemical signatures of physiological cardiac hypertrophy

Primary stimulants leading to the development and progression of cardiac hypertrophy are mechanical stress and neurohumoral stimulation [59]. Mechanical stress and neurohumoral stimulation also influence modulation of numerous cellular responses such as gene expression and protein synthesis [59]. To maintain physiological hypertrophy, it is also necessary to activate cell survival signaling, increase energy production and efficiency, increase angiogenesis proportional to the ventricular wall growth, activate antioxidant systems, and mitochondrial quality control [92][99].

The signaling pathways partaking in physiological cardiac hypertrophy during pregnancy are multifaceted and are different from the signaling pathways involved in pathological hypertrophy [88]. The key signaling proteins implicated in physiological cardiac hypertrophy includes p38 kinases, JNK, and AKT [99].

2.4.3 IGF-PI3K/AKT pathway

The insulin like growth factor (IGF)-phosphotidylinositide-3 kinase (PI3K)/AKT (p110a) pathway is a well characterized signaling cascades accountable for interceding physiological hypertrophy [100][101]. PI3K is a lipid kinase that releases inositol lipid products from the receptor tyrosine kinase (RTK) intracellular domain which in turn trigger intracellular signaling [100]. Activation of PI3K and its downstream serine-threonine kinase, AKT (or Protein Kinase B) play an important role in the cardioprotective effect of the tyrosine kinase receptor signaling pathway [102].

In adult dnPI3K transgenic mice, and in mice with cardiac-specific ablation of p110α subjected to a physiological stimulus (exercise) and a pathological stimulus (ascending aortic banding) showed significant hypertrophy in response to pressure overload. However, it showed an

attenuated hypertrophic response to swim training when compared with non-transgenic mice [100]. Constitutively active AKT1 mutant mice initially develop physiologic left ventricular hypertrophy, although pathologic conversion occurs over time [97]. This demonstrated that PI3K(p110α) is critical for physiological hypertrophy of the heart but not pathological hypertrophy.

Studies have also shown that inhibition of mammalian target of rapamycin (mTOR) with rapamycin can avert cardiac hypertrophy produced through AKT overexpression [102][103]. mTOR is a downstream effector of AKT, suggesting that AKT and its downstream molecules regulate development of cardiac hypertrophy [102][104].

2.4.4 JAK-STAT pathway

The glycoprotein 130/ janus associated kinase/signal transducers and activators of transcription (gp130/JAK/STAT) pathway is also prominent with physiological cardiac hypertrophy and/or protection [105][106]. The JAK/STAT pathway is stimulated by ligand binding to its receptor in the plasma membrane and the later homo- or heterodimerisation of the receptor [107]. In the heart, interleukin 6 (IL-6), IL-11, leukaemia inhibitory factor (LIF), oncostatin M, ciliary neurotrophic factor (CNTF) and cardiotrophin-like cytokine (CT-1) are the key cytokines that transduce their signals via glycoprotein 130 (gp130) largely to STAT 3 and STAT 5 [107]. Stimuli which trigger hypertrophic progression of cardiomyocytes such as mechanical stretch and pressure overload, myocardial infarction and angiotensin II (ANG II) treatment activate the JAK-STAT signaling in the heart [107].

Inhibition of STAT3 prompted regression of hypertrophy, implying that STAT3 is a major potential therapeutic target for cardiac hypertrophy [105]. In addition, over-expression of STAT 3 in mouse cardiomyocytes caused cardiac hypertrophy by increasing expression of hypertrophic genes and led to spontaneous concentric cardiac hypertrophy [105][108]. However, mice lacking STAT3 in cardiomyocytes (aMHC-Cretg/-; STAT3flox/flox,: (STAT3-KO)) developed normal pregnancy-induced hypertrophic after TAC caused doubts on the role of STAT3 in hypertrophy [108][109].

Studies in mice have also reported the cardioprotective effect of STAT 5 [106][110]. Available evidence indicates that STAT 5 interacts with p85, a regulatory subunit of PI3K, which then activate the PI3K/Akt signal pathway [111]. PI3K/Akt is crucially involved in compensatory cardiac adaptation [110].

2.4.5 Extracellular signal related kinases 1/2 (ERK1/2)

Extracellular signal related kinases 1/2 (ERK1/2) are also known as mitogen activated kinase 3/1 (MAPK3/1) are kinases activated by extracellular signals and growth factors which then translocate to the nucleus, phosphorylate targets, and initiate transcription [97]. Activation of ERK1/2 mediates both physiological and maladaptive processes in the heart. Overexpression of an active mutant ERK1 induces physiologic hypertrophy that is protective against ischemia reperfusion injury [97]. However, recently it was shown that loss of ERK1 and ERK2 from cardiomyocytes did not attenuate cardiac enlargement in response to TAC or exercise rather induced eccentric cardiomyocyte growth [112].

2.5 Angiogenic remodeling in normal pregnancy

Coronary angiogenesis play a vital role in maintaining cardiac vascularisation and perfusion during physiological remodeling [113]. Heart tissue enlargement during pregnancy must be accompanied by a corresponding expansion of the coronary vasculature to retain an adequate supply of oxygen and nutrients [34]. Hence, in pregnancy capillaries grow proportional to cardiomyocyte volume thus conserving the capillary density seen in non-hypertrophied hearts [34].

Vascular endothelial growth factor (VEGF) is the most important factor promoting angiogenic remodeling [114]. Maternal levels of total VEGF rise gradually throughout pregnancy [115][116]. VEGF begins blood vessel development by boosting vascular permeability and increasing endothelial cell proliferation [34]. Then angiopoietins subsequently further the remodeling, maturation and stabilisation of the originally undeveloped vasculature [117].

The placental growth factors (PGF, also called PlGF), are also important factors that influence angiogenesis [114]. The function of PIGF is less understood, however studies have reported a clear increase in free PIGF between 28 and 32 weeks of gestation [34][118].

2.6 Structural and extracellular matrix remodeling of the heart during pregnancy

The extracellular matrix (ECM) is an important structure which provides a supporting framework for cardiac function [26]. It is composed of predominantly collagen, which provides passive tension in stretched cardiac muscle, thereby influencing the end-diastolic volume of the heart [119]. Type I collagen (Col 1) accounts for approximately 85% to 90% of the collagenous matrix, whilst type III collagen (collagen 3) represents 5% to 11% of total the

myocardial collagens [120][121]. The cardiac ECM also contain fibronectin, glycosaminoglycans, and proteoglycans, and it acts as a reservoir for growth factors and proteases [122].

The ECM is rigorously controlled by balancing the synthesis and breakdown of component proteins [26][121]. Disruption of the ECM network structure compromise the structural integrity and function of the heart [123]. Again, excess production and build-up of ECM structural proteins, or fibrosis, results in augmented stiffness of the myocardium and affects ventricular contraction and relaxation, causing distorted architecture and function of the heart.

Studies assessing ECM remodeling by histological analysis in pregnant mice and rats showed no presence of interstitial fibrosis [61][88]. However, other studies have noticed the development of fibrosis during late pregnancy [124]. Limon-Miranda et al, 2014 revealed that Col I expression in left ventricles subsided during pregnancy whilst Col III increased [119]. The fibrosis observed could be the result from a compensatory effect in response to the increase in blood volume present in the pregnancy to improve the diastolic function. Col III forms finer bundles of more reticulate fibre that are more elastic and more malleable than col 1 matrix [125].

Matrix metalloproteinases (MMPs) and Tissue Inhibitor of Metalloproteinases (TIMPs) have important roles in ECM remodeling. MMPs families function to degrade ECM anchoring proteins such as integrins, collagens and fibronectins [88]. TIMPs inhibit MMPs activity is inhibited by TIMPs [126]. TIMPs activity vary by targets for instance TIMP1 is less active at inhibiting membrane-type MMPs including MMP14, 15, and 16, while both TIMP1 and TIMP3 interact with MMP9 [121].

ECM related genes are also the most significantly up-regulated group of genes in late pregnancy and immediate postpartum [26]. Parrot et al 2018 [121], observed low levels of TIMP 2–4 mRNA in the postpartum period [26][121]. In another study, MMP-1, MMP-2, and MMP-9 expression was depressed in the left ventricle of pregnant rats, while in the postpartum the MMP-1 and MMP-9 expression was similar to non-pregnant group [124][127]. The downregulation of MMPs suggest that they take part in the cardiac remodeling of the ECM during the pregnancy.

2.7 Regression of cardiac changes postpartum

Cardiac hypertrophy is rapidly reversed following pregnancy, and this is influenced by reduced preload [54][128]. **Table 2** summarizes the regression time of some of the changes that occur to the maternal cardiovascular system after labour. CO is known to rise by 60-80% immediately after delivery due autotransfusion from contracting uterus as well as decreased vena caval compression [1][15]. By 24 hrs postpartum cardiac output yields to pre-labour values and by 2 weeks postpartum it returns to pre-pregnant levels [129].

There is a loss of approximately 1000 ml of blood after delivery which is usually recovered over a few days due to transfer of fluids from the cellular compartments [15]. Normal plasma volume is established by 6-8 weeks.

Table 2: Regression period of cardiac changes that occur during pregnancy

Cardiac changes during pregnancy	**Regression period to pre-pregnant level**
Hemodynamic changes	
Cardiac output	6 weeks
Systemic vascular resistance	2 weeks
Blood volume	6-8 weeks
Heart rate	12 weeks
LV geometry	
LV mass	13 weeks [130]; > 6months [66]
LVIDd (mm)	1 month [65]; 6 months [66]; > 13 weeks [130]
LVIDs (mm)	6 months
LVEDV (ml)	6 months
LVESV (ml)	6 months
LV IVSd (cm)	6 months
LV PWd (cm)	6 months
LV function	
LVEF	6 months
LVGS	6 months

Cardiac mass, ventricular geometry, ventricular volumes, and ventricular function may continue for up to a year post-delivery despite the removal of the volume load [62][66]. However, most follow-up studies in normal pregnancy were conducted from 6 months after delivery [66][131][132]. A few studies that were conducted between 1 month and 3 months postpartum reported that LV mass, interventricular septum thickness and LV posterior wall thickness did not revert to normal level in this period [65][130].

Data on signaling implicated in the regression of physiological hypertrophy is also limited. Nevertheless, the VEGF-VEGF receptor-1 signaling pathway, activation of protein kinase G 1(PKG-1) pathway, and regulation of hypoxia inducible factor-1 (HIF-1) transcriptional activity have been detected during the regression of pathological cardiac hypertrophy [133][134][135].

VEDF-VEGF receptor 1 activation is linked to cyclic GMP-dependent protein kinase-1 (PKG-1) signaling pathways, and inhibition of cyclic GMP degradation leads to regression of pathological cardiac hypertrophy [133][136][137].

Section 3: Peripartum Cardiomyopathy (PPCM)

3.1 The epidemiology of cardiovascular disease in pregnancy

Pregnancy induced stress is often well tolerated in healthy mothers [138][139]. However, cardiovascular snags may occur in some women who did not have any preceding adverse cardiac history before pregnancy [88][138][140]. This could be exacerbation and unmasking of underlying conditions due to progressively increasing demand on the cardiovascular system or the development of completely new condition [141].

Cardiac disease account for up to 15% of maternal death in pregnant and postpartum women [142]. According to the World Health Organisation (WHO), maternal mortality in developed economies is around 12 per 100 000 live births (0.012%) and 239 per 100 000 live births (0.2%) in emerging economies, with large disparities both between and within countries [79][142][143][144].

Worldwide, hypertensive illnesses occur in 6–8% of all pregnancies and are the most common cardiovascular events during pregnancy [145].

Data from South Africa shows that heart disease affects at least 0.6 per cent of pregnant women attending antenatal care [146]. Rheumatic valvular disease dominates in Sub Saharan

Africa and other low to medium income countries, making 56–89% of all cardiovascular diseases in pregnancy. Peripartum cardiomyopathy (PPCM) contributing up to 34% of all the non-obstetric deaths in Africa [147]. Congenital heart disease (CHD) is less prevalent representing just 9–19% [139]. The low prevalence in congenital heart disease in pregnant women in emerging countries might be because many children with CHD will not get to reproductive age [148]. In Africa, a total of 18 cardiac operations are done per 1 million people which is way below the global mean number of cases that stands at 169 per million [139].

3.2 Definition of PPCM

PPCM is the occurrence of heart failure (HF) indications in the nineth month of gestation or in the first five months postpartum without prior history of HF before the last month of pregnancy [149][150]. The ejection fraction (EF) in PPCM women goes below 45% [151]. The symptoms of PPCM such as breathlessness, exercise intolerance, cough and shortness of breath may mimic common symptoms in normal pregnancy making it a difficult condition to diagnose [152]. An exhaustive assessment is necessary to exclude other potential cardiac and non-cardiac explanations for the patient's clinical presentation. The requirements for diagnosis of PPCM include clinical signs of heart failure and an echocardiographic left ventricular ejection fraction (LVEF) of ≤ 45%, ECG, and magnetic resolution imaging (MRI) [153]. Laboratory measurements of NT-proBNP, and right ventricular (RV) dysfunction may be measured as a predictor of outcome [45] [154].

3.3 Incidence of PPCM

The epidemiology of PPCM is sparse, however it occurs globally [155]. Most data from Africa originated from Nigeria and South Africa [155]. Other well studied countries include Haiti and USA. Lately, large cohort studies have been conducted in Germany [156], Japan [157], and Turkey [158]. However, reports from other European countries, the Middle East, Asia, and Australia remain scarce [155]. Systematic population estimates of the incidence of PPCM are lacking for a variety of reasons, including under-diagnosis, misdiagnosis, and lack of a systematic reporting mechanism [155].

The incidence rate in South Africa is 1 in 1000 live births [152]. Projected incidence in the United States ranges from 1 in 1000 to 1 in 4000 pregnancies [159]. Other well-described global hotspots, includes Nigeria and Haiti, where incidence rates range as high as 1 in 100 to

1 in 300 [160]. Although data from other parts of the world is still unknown, PPCM appears to be popular and carry a worse prognosis in women of African origin [150].

3.4 Aetiology of PPCM

The cause of PPCM is still unknown, although several hypotheses including viral myocarditis, fetal micro chimerism, malnutrition, the hemodynamic stress of pregnancy, autoimmune processes, inflammatory-factors, and low selenium levels have been associated [152][161] [162][163].

Unbalanced oxidative is another key player in the pathogenesis of PPCM. In normal pregnancy balance is maintained between reactive oxygen species (ROS) and total antioxidant capacity [164]. Oxidative stress level is elevated in PPCM patients and in PPCM animal models [165]. Augmented oxidative stress cause activation of cathepsin D, a peptidase which cuts 23kDa prolactin into the 16 kDa fragment. Matrix metalloproteinases (MMPs) may also cleave prolactin into the same vasoinhibins [166]. The cleaved prolactin form is angiostatic, apoptotic and impairs cardiomyocyte function [167][168].

Oxidative-stress-Cathepsin D-16kDa prolactin hypothesis provides the closest potential disease-specific pathophysiological mechanism and has led to the development of bromocriptine a therapeutic drug that block prolactin [167]. The raised level of 16-kDa PRL measured in PPCM patients is linked to low activation of STAT3 and the peroxisome proliferator-activated receptor gamma coactivator 1-alpha (PGC-1α) [169]. Studies shows that STAT3 facilitates cardioprotection form oxidative stress in part by upregulating antioxidant enzymes such as manganese sodium dismutase (MnSOD) [170]. MnSOD a powerful ROS scavenging enzyme located in mitochondria [170][171].

Increase level of 16kDa prolactin was also found to stimulate the release of micro-RNA 146a (miR-146a)–loaded exosomes from endothelial cell [172]. MicroRNA-146 inhibits production and movement of endothelial cells [172]. They are angiostatic and the also cause metabolic dysfunction in cardiomyocytes [172][161]. Furthermore, studies also revealed that 16kDa-PRL offsets vasorelaxation and angiogenesis via inhibition of the Ca^{2+}-related instigation of endothelial nitric oxide synthase (eNOS) [173][174].

Peroxisome proliferator-activated receptor gamma coactivator (PGC-1α) similarly augment angiogenic imbalance in PPCM by increasing the secretion of anti-angiogenic soluble fms-like

tyrosine kinase-1 (sFlt1) during pregnancy [175][152]. Another study also showed that higher serum relaxin-2 concentrations momentarily after birth are associated with better myocardial improvement after 2 months in PPCM patients who were diagnosed between 0 and 11 days postpartum [176]. Relaxin-2 is a hormone secreted in the first phase of pregnancy and acts as a pro-angiogenic and vasodilator.

Inflammation and autoimmune reactions are also potential factors that could induce and drive PPCM [177][173]. This inflammatory process is either cellular or molecular non-cellular or both [178]. Raised levels of circulating cytokines including interleukin-6 (IL-6), tumour necrosis factor-a (TNFa), C-reactive protein (CRP), and interferon gamma (IFNc) were also found in PPCM patients [174][178].

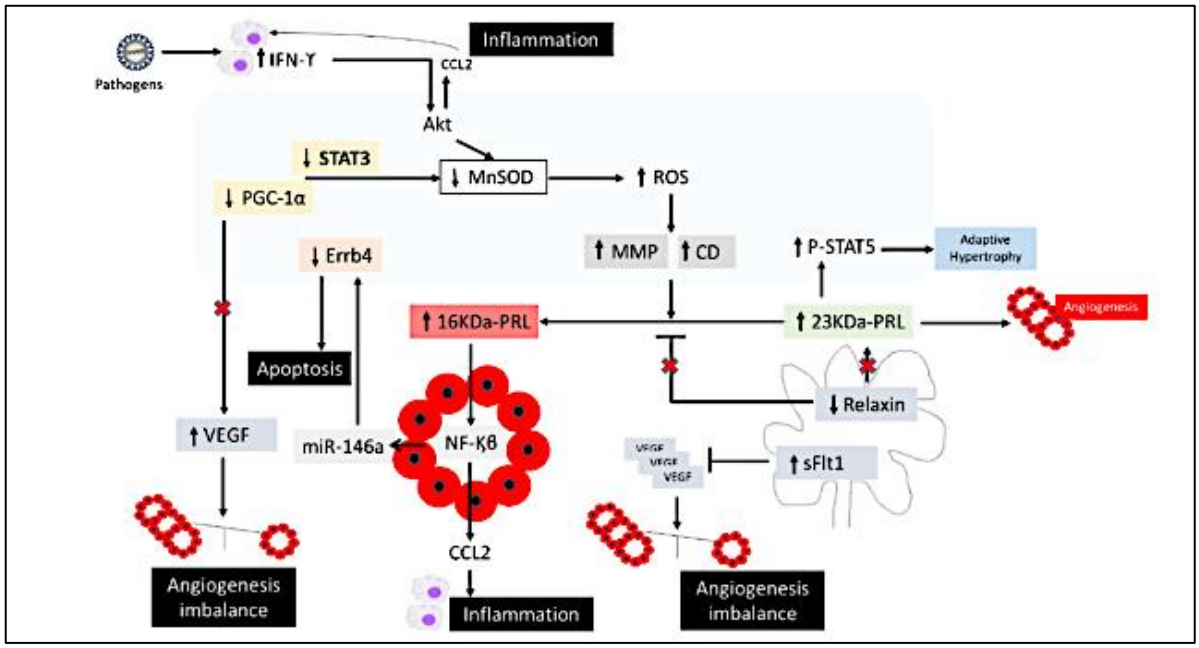

Figure 5: Suggested pathophysiological mechanisms causing PPCM *[161].*

Figure 5 summaries the role of inflammation, apoptosis and angiogenic imbalance in the pathophysiology of PPCM. The 16KDa fragment that result from cleavage of the 23kDa prolactin contributes to amplified expression of miR-146a and chemokine ligand 2 (CCL2). miR-146a induce cardiomyocyte apoptosis by inhibiting endothelial cell proliferation and survival whilst augmented CCL2 induces cardiac inflammation [161]. The angiogenic imbalance is also worsened by increased sFlt1 and decreased vascular endothelial growth VEGF and relaxin levels.

3.5 Cardiac remodeling in PPCM

Contrast with normal pregnancy remodeling, pathological remodeling is a maladaptive development. It is characterized by continuing ventricular dilatation, myocardial hypertrophy, fibrosis, and weakening of cardiac performance [179]. The devastating spiral of maladaptive changes often culminate to heart failure, arrhythmias, and death [180]. The initial structural changes of the heart is an adaptative effort to maintain normal cardiac function [181][182]. However, with prolonged stress, gradual and irreversible dysfunctional state of the heart may develop [183][184].

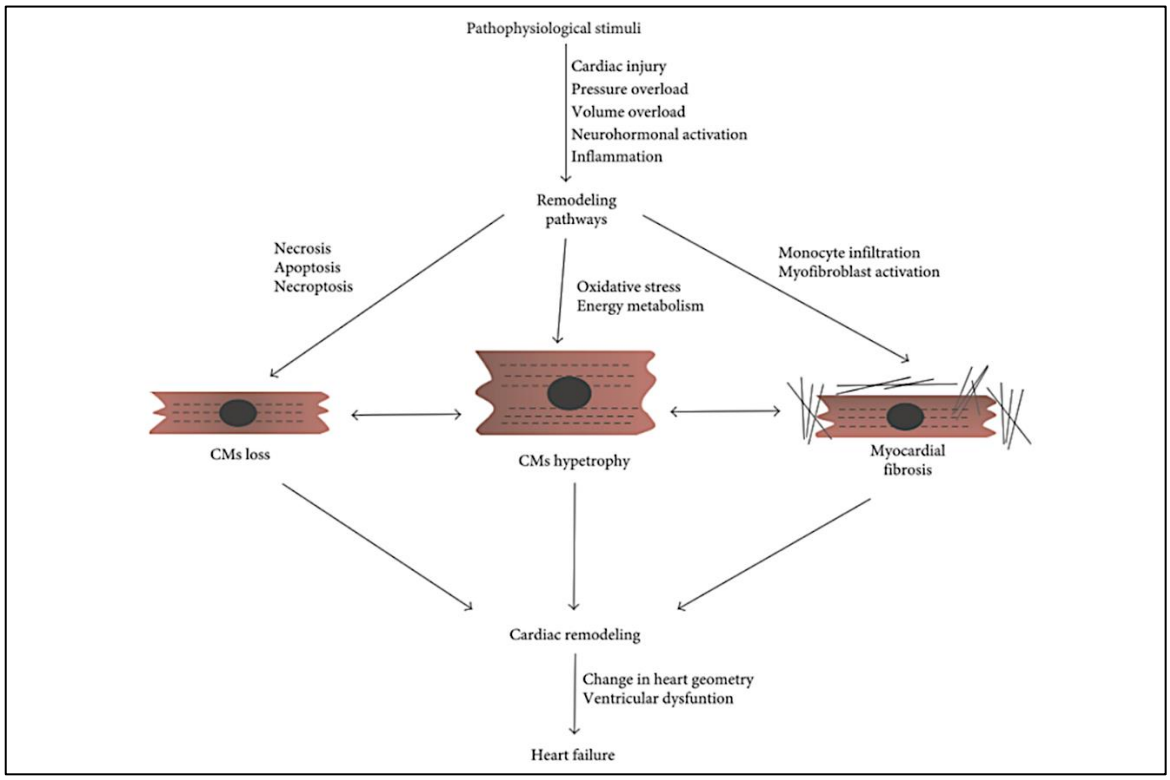

Figure 6: Schematic overview of the main events that contribute to cardiac remodeling in PPCM.
Figure adapted from Schirone et al, 2017 [183]. Increase in oxidative stress, inflammation and cell death which causes fibrosis and cardiac hypertrophy are the main even in cardiac remodeling in PPCM.

At cellular level, myocyte loss through necrosis, necroptosis, apoptosis, or autophagy, and fibrosis occurring through fibroblast proliferation characterize pathological remodeling [183][185][186]. Furthermore, changes in the expression of proteins implicated in excitation-contraction coupling (ECC), and variations in the energetic and metabolic situation of the myocyte also influences remodeling [187].

ECC process tightly controls calcium influx and uptake [188]. Impaired calcium uptake facilitated by proteins such as sarco/endoplasmic reticulum Ca^{2+}-ATPase (SERCA)-2a, and unrestrained calcium efflux through ryanodine receptors (RyRs) have been reported in PPCM hearts [94][189][190].

Again, activation of G-protein coupled receptor (GPCR) participates in cardiomyocyte remodeling and survival [191]. Mechanical stretch encourages the release of α and ß adrenergic receptor agonist (α and ßARs), angiotensin (AT)-II and endothelin-1, which contributes to the activation of GPCR signaling through Gαq subunits [192]. Overexpression of the Gαq subunit promotes PPCM [173][193].

3.5.1 Remodeling at myofilament level in PPCM

An analysis of cardiac biopsies acquired from PPCM patients showed increased compliant titin, reduced phosphorylation of titin at Ser4010, and impaired myofilament length-dependent activation [194]. The same study also reported that myofilaments from PPCM patients' hearts have a reduced cyclic AMP- protein kinase A (cAMP-PKA) activation and presents an increase in calcium $(Ca)^{2+}$-sensitivity [173][194].

3.5.2 Pathological eccentric hypertrophy in PPCM

Pathological eccentric hypertrophy seen in PPCM is different from the eccentric hypertrophy observed in normal pregnant physiological hypertrophy [189]. In pathological eccentric hypertrophy the chamber size increases whilst wall thickness does not increase proportionally in response to increased hemodynamic load [195]. The eccentric geometry inflicts a distinct mechanical drawback that is associated with reduced LV systolic function and operation [191]. However, in some cases little or no LV enlargement is observed despite a reduced ejection fraction whereas others display substantial LV enlargement [189][195].

Pathological eccentric hypertrophy in PPCM also differs from normal physiological hypertrophy in pregnancy on the induction of fetal gene program and the possibility of developing fibrosis [189][61].

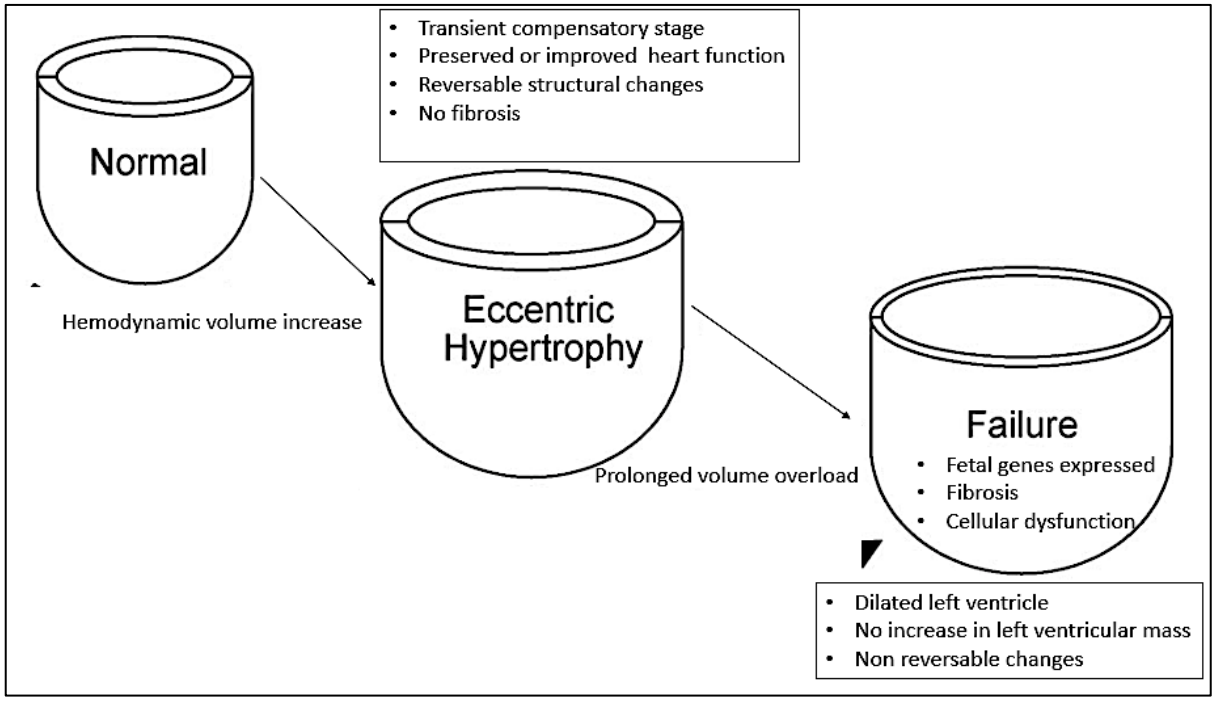

Figure 7: Morphology of eccentric hypertrophy leading to heart failure in PPCM.

Adapted from Kehat et al, 2010 [184]. Pathological increase in volume load usually results in a left ventricle with enlarged diameter but no wall thickness. In the presents of PPCM invoking stimuli the remodeling can progress to dilation and compromised function with fetal gene expression.

3.5.3 Signaling of pathological hypertrophy

Signaling via G-protein-coupled receptors (GPCR) stimulated by catecholamines, angiotensin II, and endothellin-1, are connected to pathological hypertrophy. Similarly, transgenic mice with cardiac-restricted overexpression of Gαq subunit fosters a form of PPCM that is coupled with hypertrophy and high cardiomyocyte apoptosis [192]. Peripartum hypertrophy is also a feature that is observed in STAT3-KO mice stirred with β1-adrenergic receptor (β-AR) agonists [193][173].

A good example of the activated pathways is the calcineurin-nuclear factor of activated T cells (NFAT) signaling axis. It is facilitated by the calcium/calmodulin-activated serine-threonine phosphatase, calcineurin (PP2B) [196]. The calcineurin/nuclear factor of activated T cells (NFAT) and NF-kB pathway was implicated as a key controller of cardiomyocyte hypertrophy both in vitro and in vivo [197]. PP2B conveys signals to the nucleus via the dephosphorylation and translocation of nuclear factor of activated T cell (NFAT) transcription factors [196]. The mechanical and neurohormonal stimuli activates Ca^{2+}- calmodulin (Cam) binding which controls the dephosphorylation of NFAT by means of PP2B [197]. The dephosphorylated NFAT

in turn triggers hypertrophy related transcriptional factors such as GATA-4 [197]. Ultimately, activated NFAT stimulates transcription of pathological hypertrophy-associated genes, including α-actin, endothelin-1, atrial natriuretic factor (ANF), and β-myosin heavy chain [97][198].

Another pathway that contributes to pathological cardiac hypertrophy in a similar manner is the mitogen-activated protein kinases (MAPK) c-Jun N-terminal kinase (JNK). **Figure 8** illustrate some of the signaling pathways that takes part in pathological hypertrophy.

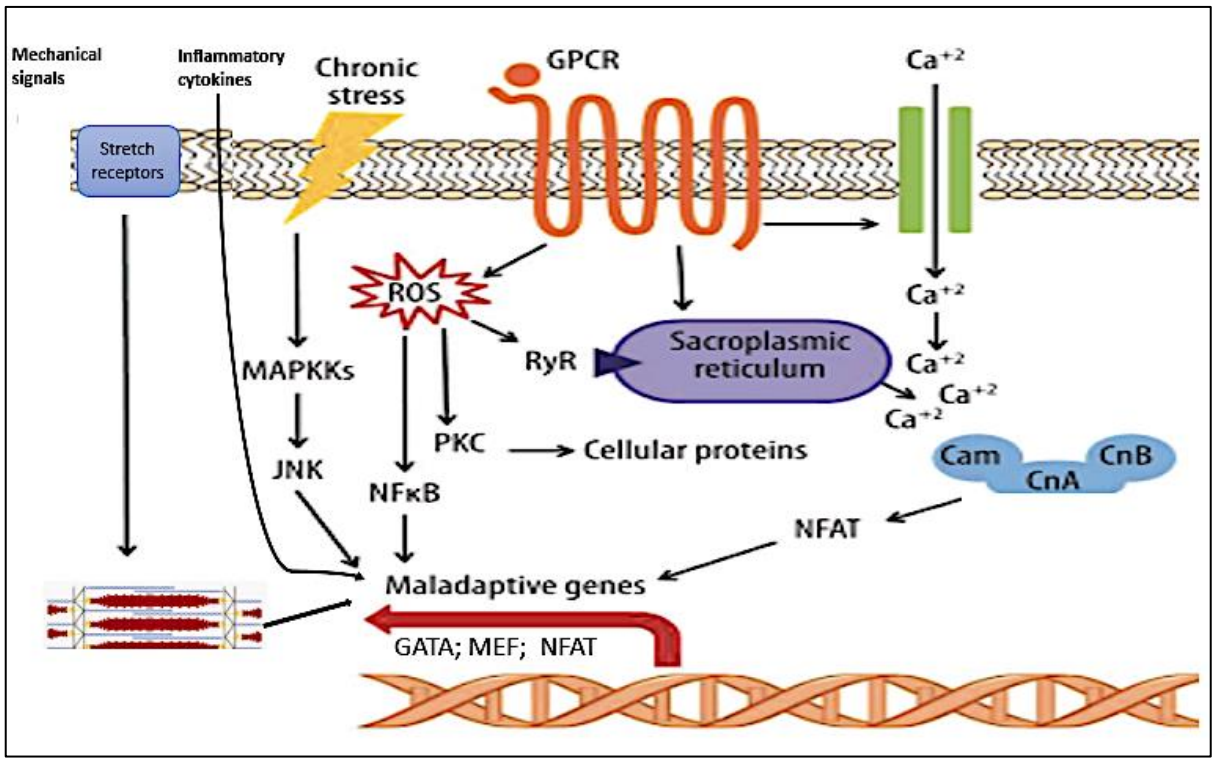

Figure 8: Diagrammatic representation of main intracellular signaling pathways regulating cardiac hypertrophy in PPCM.

The diagram was adapted from Samak et al, 2016 [49]. Neurohumoral and mechanical signals sensed by membrane bound receptors activate downstream mechanism. The transcription factor NFAT, responsible for cardiac hypertrophy, is positively regulated through calmodulin/calcineurin. The receptors signal through G proteins directly control downstream signaling effectors such as kinases and phosphatases. Calcineurin is a key transducing phosphatase. These signals culminate in altered transcription that includes the reinduction of the fetal gene program and hypertrophy.

In rodents, switching to the fetal gene expression profile is a typical feature of pathological cardiac hypertrophy. The fetal gene program includes up-regulation of cardiac myosin heavy chain-beta (β-MHC) instead of the adult predominant alpha isoform (α-MHC), skeletal alpha actin (SKA), and atrial natriuretic factor (ANF) genes [199][200]. GATA4 and myocyte enhancer

factor-2 (MEF2) transcription factors mediate the induction of a set of the fetal genes [97][200].

Additionally, cardiomyocytes also go through substrate switch. This is a change from the preferred fatty acid oxidation to carbohydrate-dependent energetic machinery turning on metabolic genes [49].

3.6 Cardiac fibrosis and Inflammation in PPCM

In PPCM, eccentric hypertrophy heart, LV remodeling is potentially accompanied by a typical loss of collagen fibrils around individual myocytes [201]. This may be attributed to augmented ECM proteolytic activity that is likely to reduce ECM content and thereby facilitating the overall ventricular dilatory process [202]. The remodeling of the PPCM heart is not completely understood and the recommendation to not use gadolinium in pregnant women has limited the use of magnetic resonance imaging (MRI) to assess fibrosis in PPCM patients.

Several studies have assessed circulating factors of cardiac fibrosis such as procollagen type-I N-terminal propeptide (PINP) and procollagen type-III N-terminal propeptide (PIIINP) in the diagnosis and prognosis of cardiac diseases [203][204][205]. Galectin-3 (Gal3) and soluble ST2 (sST2) and osteopontin (OPN) have also known to be contemporary markers of cardiac inflammation and fibrosis [206][207][208]. Azibani et al, found that high baseline galectin-3, soluble ST2, and OPN levels were associated with poor outcome in PPCM patients [203].

A cause effect connection between MMP proteolytic activity and LV dilation with a volume overload stimulus have also been published [209][210]. For example, a robust expression and activation of MMPs have been clearly identified in dilated cardiomyopathies [209][210][211]. In a rapid pacing model of inducing dilated cardiomyopathy, MMPs were induced early prior to significant changes in the cardiomyocytes [210]. In another study, TIMP-3 deficiency led to dilated cardiomyopathy [212].

The myofibroblasts also respond to proinflammatory cytokines like tumour necrosis factor [TNF]-a, interleukin [IL]-1, and IL-6 [213]. Sustained inflammatory cell infiltration is often observed in myocardial biopsy specimens collected from PPCM [214]. Studies have also shown that myocardial IL-1b, [TNF]-a, TGF-b1 and IL-4 induction may indirectly induce myocardial Col remodeling by the upregulation of MMPs and downregulation of TIMPs [215][216][217].

Section 4: Role of pregnancy hormones on the maternal cardiovascular system

This section is available as a research publication in **Clinical Research in Cardiology Journal.**

Kodogo V, Feriel Azibani ·, Sliwa K Role of pregnancy hormones and hormonal interaction on the maternal cardiovascular system: a literature review. https://doi.org/10.1007/s00392-019-01441-x

Clinical Research in Cardiology (2019) 108:831–846
https://doi.org/10.1007/s00392-019-01441-x

REVIEW

Role of pregnancy hormones and hormonal interaction on the maternal cardiovascular system: a literature review

Vitaris Kodogo[1] · Feriel Azibani[1] · Karen Sliwa[1]

Received: 21 November 2018 / Accepted: 4 February 2019 / Published online: 26 February 2019
© Springer-Verlag GmbH Germany, part of Springer Nature 2019

Abstract
Hormones have a vital duty in the conservation of physiological cardiovascular function during pregnancy. Alterations in oestrogen, progesterone and prolactin levels are associated with changes in the cardiovascular system to support the growing foetus and counteract pregnancy stresses. Pregnancy hormones are, however, also linked to numerous pathophysiological outcomes on the cardiovascular system. The expression and effects of the three main pregnancy hormones (oestrogen, prolactin and progesterone) vary depending on the gestation period. However, the reaction of a target cell also depends on the abundance of hormone receptors and impacts put forth by other hormones. Hormonal interaction may be synergistic, antagonistic or permissive. It is crucial to explore the cross talk of pregnancy hormones during gestation, as this may have a greater impact on the overall changes to the cardiovascular system.

Keywords Pregnancy · Hormones · Physiology of pregnancy · Prolactin · PPCM

Introduction

Pregnancy is accompanied by significant changes in the hormonal milieu [1]. Hormones play a major role in molecular and physical changes that are observed in maternal cardiovascular adaptations during pregnancy [2]. When well regulated, hormones maintain a physiological adaptation to the cardiovascular system [3]. However, hormonal imbalance can also trigger pathological changes that may be fatal to the maternal cardiovascular system [4, 5]. It is also important to consider hormonal interactions which may alter the individual hormone's impact. This literature review aims to explore the benefits and risks of individual pregnancy hormones, as well as their cross talks and interactions. A few reports have outlined the presence of hormonal interaction; however, the impact of these interactions on the cardiovascular system is not clear.

✉ Karen Sliwa
Karen.Sliwa-Hahnle@uct.ac.za

[1] Hatter Institute for Cardiovascular Research in Africa, Faculty of Health Sciences, University of Cape Town, 4th floor Chris Barnard Building, Observatory, Cape Town 7935, South Africa

Physiological changes of the cardiovascular system during pregnancy

Alterations in the cardiovascular system in pregnancy begin early in the first trimester (Table 1) in that, by 8 weeks, the cardiac output would have increased by 20% [2]. The initial change is probably peripheral vasodilatation, which leads to falling systemic vascular resistance (SVR) [6]. Heart rate rises as a compensatory response to falling SVR [6], it surges throughout gestation by 10–20 bpm, peaks in the last 3 months [3] and then yields to preconception levels within 10 days postpartum [7].

A recent meta-analysis study on cardiac output and haemodynamic changes during pregnancy confirmed that cardiac output also upturns during pregnancy, reaching its peak in the early third trimester [8]. Unlike heart rate, cardiac output follows a non-linear array of adaptation. Initially, it is alleged to be facilitated by increases in stroke volume, whereas, later, the increase is linked to heart rate [9, 10]. Stroke volume escalates gradually up to the second trimester and then stabilises or decreases late in the third trimester [11]. It then returns to non-pregnant values soon after delivery [2].

Table 1 Physiological changes of the cardiovascular system during pregnancy

Physiological Condition	During gestation			Postpartum	
	1st trimester	2nd trimester	3rd trimester	Early (0–2 months)	Late (2–6 months)
Vascular resistance	↓	↓	↓	↓	↓
Heart rate	↑	↑	↑	Remains high as in pregnancy	↑
Cardiac output	↑	↑	Minimal increases	↑	↑
Myocardial contractility	↓ [12] no difference [13]. ↑ [14]	↑ [14]	↑	↑	↑
Left ventricular volume	↑	↑	↑	↑	↑
Left atrial volume	↑	↑	↑	↑	↑
Left ventricular mass	↑	↑	↑	↑	↑
Ejection fraction	↑ [15]	No change[16] ↑ [17]	No change[16] ↑ [17]	↑	↑

Hemodynamic changes

The maternal cardiovascular system goes through progressive adaptations during pregnancy to support the mother and the growing foetus. These changes include increased circulating blood volume [12], reduced vascular resistance [13] and increased cardiac output [14]. Table 1 summarises some of the hemodynamic and physical changes in the cardiovascular system during pregnancy and postpartum.

Hemodynamic changes during pregnancy also cause blood pressure (BP) instabilities [15]. There are disparities on the normal alterations in uncomplicated pregnancies. However, in several studies where the National High Blood Pressure Education Program Working Group on High Blood Pressure in Pregnancy (NHBPEPWG) recommendations [16] were used to measure BP, systolic blood pressure (SBP) remained unchanged, whilst diastolic blood pressure (DBP) and mean atrial pressure (MAP) dropped up to 26–28 weeks [7, 17]. Thereafter, DBP and MAP rose towards term [7, 17].

Conflicting results have been reported on cardiac contractility during the first trimester of pregnancy. George et al. reported enhanced intrinsic contractility [13], whilst other studies have reported no change [3, 18], or decreased contractility [14] in the same phase of pregnancy.

Studies also reported either no change, or a significant increase, in the cross-sectional area of left ventricular outflow tract [3, 9]. The left atrial enlarges slowly, beginning at 5 weeks, and plateauing at 28–34 weeks [19, 20]. However, ventricular ejection fraction seems stable during the course of pregnancy [3].

Structural and extracellular matrix remodelling

Structural modifications within the heart reflect increased volume load related to pregnancy and cause dilatation of the valve ring and foster myocardial thickness (cardiac hypertrophy) [20]. Heart hypertrophy is either physiological and adaptive, or pathological, which is maladaptive [21]. Cardiac hypertrophy induced by pregnancy is a temporary revocable development of increased left-side chambers and myocyte dimension [1]. However, postpartum resolution of the ventricular hypertrophy seems to take longer (approximately > 6 weeks after birth) than the rest of the prepartum changes [9].

Pregnancy-induced cardiovascular complications

Pregnancy hemodynamic and hormonal changes are usually well tolerated in healthy mothers [22]. However, cardiovascular complications may develop in some women who did not have any preceding adverse cardiac history before pregnancy [23, 24]. Approximately, 1% of pregnant women are estimated to acquire cardiac disease during pregnancy, which can have a significant effect on both maternal and foetal outcomes [25–27]. These events, even if they are rare, could be fatal. Some of the complications include pathological cardiac hypertrophy [28], pregnancy-induced hypertensive disorder [23, 24], peripartum cardiomyopathy (PPCM) and several metabolic complications [10, 29].

South Africa recorded a constant increase in institutional maternal mortality rate (iMMR) for cardiovascular diseases, from 3.73 per 100,000 in 2005–2007 to 6 per 100,000 in 2011–2013 [30, 31]. iMMR due to cardiac disease in maternity in Africa is mostly dominated by PPCM (34%) and rheumatic heart disease (25.3%) [30]. In the United States, overall cardiovascular disease contributes to approximately 33% of maternal deaths during pregnancy [27].

Pathological cardiac hypertrophy

A pathological stimulus caused by pressure overload gives rise to concentric hypertrophy characterised by thick walls and dense myocardium [28, 32]. However, volume overload results in eccentric hypertrophy due to an increase in diastolic wall stress [32]. Eccentric hypertrophy is identified by large dilated ventricles and a relatively thin myocardium wall [32, 33]. These events can lead to cardiomyopathies and heart failure.

Gestational hypertension and pre-eclampsia/eclampsia

Pregnancy-induced hypertension (PIH) is the occurrence of new hypertension after 20 weeks gestation, in the absence of proteinuria or pre-eclampsia (PE) [34]. PE is identified when a woman with gestational hypertension also has elevated protein excretion in urine. Eclampsia is a severe complication of PE which is often accompanied with seizures [24].

PIH is deemed to be caused by many factors such as cardiovascular maladaptation, vasoconstriction, genetic predisposition, immunologic intolerance between feto-placental and maternal tissue, platelet activation and vascular endothelial dysfunction [34]. The presence of metabolic aspects, hyperlipidaemia and insulin resistance are also linked with PE [35].

Peripartum cardiomyopathy

PPCM is a disease identified by the occurrence of systolic heart failure in the ninth month of pregnancy, or in the first 5 months post-delivery in previously healthy women [36]. The pathophysiology of PPCM is still largely unknown, although numerous hypotheses including viral myocarditis, foetal microchimerism, malnutrition, hemodynamic stress of pregnancy, autoimmune processes, inflammatory factors, and low selenium levels have been implicated [37, 38].

A shift in the angiogenic balance toward an antiangiogenic environment has emerged as the strongest driving factor of PPCM [36, 39]. Findings in 2007 by Hilfiker-Kleiner et al. have demonstrated that PPCM is triggered by the swiftly shifting hormonal milieu of late gestation, leading to vasculopathy in susceptible women [40]. The antiangiogenic prolactin (16 kD) and sFLT1 are the major contributors [40].

The 16-kDa prolactin fragment is produced by digestion of the full-length prolactin (23 kDa) with proteolytic enzymes such as cathepsin D and matrix metalloproteinases (MMP) [40]. The increase of 16-kDa PRL level observed in PPCM patients has been associated with low activation of the signal transducer and activator of transcription 3 (STAT3) and the peroxisome proliferator-activated receptor gamma coactivator 1-alpha (PGC-1α) [41]. Reduced level of STAT 3 and PGC1-α further increases the activity of MMP and cathepsin D [38]. 16-kDa PRL also directly impairs endothelial function and triggers the release of micro-RNA 146a, which in turn has detrimental effects on cardiomyocytes [42].

Diagnosis of PPCM

Presenting symptoms in PPCM patients are highly variable but may include fatigue, dyspnea, orthopnea, peripheral edema, palpitations, chest pain, decreased exercise tolerance, and abdominal discomfort due to passive congestion of the liver [43, 44]. Most of these symptoms overlap with normal physiological symptoms of pregnancy hence the diagnosis is based on suspicion.

PPCM is considered to be a diagnosis of exclusion [37], a thorough evaluation is necessary to eliminate other potential cardiac and non-cardiac explanations for the patient's clinical presentation. The requirements for diagnosis of PPCM include clinical signs of heart failure and an echocardiographic left ventricular ejection fraction (LVEF) of $\leq 45\%$, ECG, and magnetic resolution imaging (MRI).

Laboratory measurements of NT-proBNP and right ventricular (RV) dysfunction may be measured as a predictor of outcome [37]. A recent study by Haghikia et al. confirmed the use of RV dysfunction to predict adverse outcome in PPCM [45]. Reduced RVEF at initial presentation in this study was associated with a lower rate of full cardiac recovery [45].

Management of PPCM

Management is targeted, as with other cardiomyopathies, on managing volume status, neutralising neurohormonal maladaptive responses, and preventing complications [46]. Patients presenting with acute severe heart failure symptoms require prompt treatment in an intensive care unit. However, because of the high rate of recovery in PPCM, early implantation of a permanent implantable cardioverter defibrillator should be avoided, and wearable cardiac defibrillators are often used instead [46, 47].

If PPCM presents during pregnancy diuretics to reduce preload and treat edema, vasodilators (hydralazine) to

increase cardiac output and stroke volume, and decrease vascular resistance, as well as beta-blockers are often administered [37, 48]. However, dehydration-induced hypoperfusion and lower foetal birth weight should be monitored in patients under treatment.

For PPCM that present postpartum neurohormonal blockade with angiotensin-converting enzyme inhibition, angiotensin receptor blockers, and mineralo-corticoid receptor blockers are considered as first-line heart failure medication according to standard heart failure guidelines [47, 48]. Recent reports have found that the use of bromocriptine, a drug inhibiting prolactin may be beneficial in patients with acute-onset PPCM [45]. All patients receiving bromocriptine should receive standard heart failure therapy with at least prophylactic anticoagulation.

Thromboembolism is often a complication in PPCM patients due to pregnant women having increased levels of coagulation factors VII, VIII, and X, and plasma fibrinogen during late pregnancy and up to 4–6 weeks postpartum [49]. A depressed LV function and hypercoagulable state cause a higher incidence (17%) of LV thrombus [49]. The American Heart Association, American College of Cardiology guidelines and European Society of Cardiology all support the use of anticoagulation resulting from a hypercoagulable state during pregnancy in patients with PPCM and severe LV dysfunction (LVEF < 30%) [49]. Another recent study investigating pregnancy outcome after exposure to the oral anticoagulant rivaroxaban in women at suspected risk for thromboembolic events gave reassurance to those women, who were inadvertently exposed to rivaroxaban in early pregnancy [50].

Sudden cardiac death has been reported in PPCM patients with sustained ventricular arrhythmias. A recent study underpins the elevated risk for ventricular tachyarrhythmias in patients with newly diagnosed PPCM and reduced LVEF [51]. Patients with sustained ventricular arrhythmias or history of sudden cardiac death in the acute setting may be candidates for a wearable cardioverter/defibrillator (WCD) [37, 51]. The use of implantable cardiac defibrillator (ICD) is another alternative; however, this option should be weighed as often PPCM patients recover cardiac function in 6 months [37].

Pregnancy-induced metabolic complications

Gestational diabetes mellitus (GDM) or hyperglycemia during pregnancy may lead to cardiovascular disease [24]. GDM is a form of Type 2 diabetic mellitus (T2DM), characterised by glucose intolerance of different levels established for the first time during pregnancy [52]. GDM possesses subsequent cardiovascular risks similar to those which build up in the non-pregnant female population once T2DM develops [52]. Studies have shown that diabetic patients have a two- to fourfold susceptibility to coronary artery disease (CAD) and myocardial infarction (MI) [53, 54]. Hence, a systematic dissection of the metabolic transformations arising during pregnancy, and in the subsequent years, provides an exceptional opportunity to find new biomarkers for better long-term outcomes, mainly to decrease cardiovascular risk [52].

Persistence of weight gain after pregnancy

Pregnancy is the only conventional physiological condition whereby the body gains more than 20% weight within 9 months [55]. Lactation increases the maternal ability to restore normal weight [55]. However, it can be hindered by lifestyle factors such as limited exercise, diet and inadequate sleep [55]. Kew et al. noted that an adverse cardiometabolic profile commences early in the first year if weight is not lost between 3 and 12 months after delivery [56].

Hormonal changes during pregnancy

Modifications of maternal endocrine and metabolic homeostasis are key for a successful pregnancy [57]. The hypothalamus, pituitary gland and the placenta add to the endocrine adaptations to pregnancy by producing numerous hormones [58]. Well-studied hormones that have a direct impact to the cardiovascular system include oestrogen, prolactin and progesterone. The levels are very dynamic during gestation and postpartum, and are critical in conserving the cardiovascular adaptations. Figure 1 is a schematic diagram which shows the changes of female hormones during pregnancy.

Oestrogen and progesterone levels increase steadily during pregnancy, attain their peak in the last trimester and drop soon after labour—as illustrated in Fig. 1. Oestrogen and progesterone are both produced in the corpus luteum during the first 10 weeks of gestation and, soon after implantation, the placenta takes over [59, 60]. In the third trimester, progesterone levels range from 100 to 200 ng/ml and the placenta secretes about 250 mg/day [60]. However, the placenta lacks the required enzymes to manufacture oestrogens from cholesterol or progesterone. To bypass this shortfall, dehydroisoandrosterone sulfate (DHA) from the foetal adrenal is processed to estradiol-17β by the trophoblasts.

Prolactin is secreted by the anterior pituitary gland in response to suckling stimulus of young mammals. The prolactin concentration increases during pregnancy so that, by the end of gestation, levels are 10–20 times higher than non-pregnant levels [60]. The increase in prolactin is most likely induced by increased estradiol concentrations during pregnancy [61]. However, its actions are antagonised by the presence of progesterone [62]. Following reduction of progesterone and oestrogen levels at parturition, copious

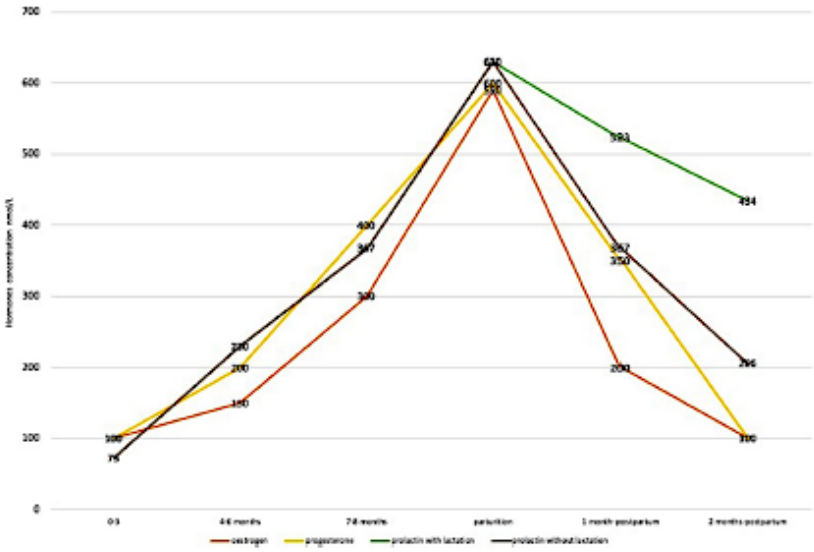

Fig. 1 Changes of hormones level during pregnancy and postpartum. Pregnancy hormones increase gradually from day 1 of pregnancy to birth. After birth most of the hormones start to revert back to normal levels. However, if there is lactation, prolactin levels remains high due to periodic stimulation

milk secretion begins [62]. Postpartum, throughout lactation, women respond with a dramatic elevation of prolactin levels during the suckling stimulation [63]. However, if the woman does not breastfeed, prolactin returns to normal levels within 2–3 weeks after delivery (Fig. 1).

Oestrogen

Oestrogens are a group of steroid hormones that are secreted by the ovaries and the placenta during pregnancy [64]. However, oestrogens can also be secreted by other non-reproductive tissues such as the liver, heart, muscle, bone and brain [65].

E2 is the predominant form and is involved in numerous physiological processes. E1 is secreted mainly after menopause and E3 is secreted by the placenta during pregnancy.

There are three major types of oestrogens known as estradiol, estrone, and estriol [66]. Estrone and estradiol are synthesised by the aromatisation of androstenedione and testosterone, respectively and estriol is synthesised from estrone [66]. E2 is the highly potent oestrogen secreted during the premenopausal period, whereas E1 is important after menopause, when it is synthesised from adrenal dehydroepiandrosterone in the adipose tissue [65]. E3 is the least abundant and it is formed by the placenta from E1 through 16α-hydroxylation [65].

When oestrogens are secreted into the blood stream, they affect numerous target cells which express oestrogen receptors. Several cells such as the endothelium, epithelium, muscle, bone, cartilage, hematopoietic cells, neurons and glia have oestrogen receptors. However, oestrogens can also operate in the paracrine and autocrine systems.

Physiological function of oestrogens on the cardiovascular system

Oestrogens have pleiotropic effects on the cardiovascular system. It controls vascular function [67, 68], inflammatory response [69], metabolism [10], insulin sensitivity [10], cardiac myocyte survival [70], mitochondrial function [71], development of hypertrophy [72] and ultimately cardioprotection [73, 74].

Oestrogen and endothelial function Vasculature provides sufficient perfusion of the maternal–foetal interface which is critical during pregnancy [75]. Oestrogens help to maintain efficient vascular adaptations during pregnancy [68].

In a rat model, new production of oestrogen during decidualisation assisted in angiogenesis at the implantation site and helped in maintaining early pregnancy [76]. As gestation progresses, oestrogens exert profound multifaceted protective effects on the vasculature [77]. Oestrogen has a direct effect on the endothelium and vascular smooth muscle, through both rapid signalling pathways and genomic mechanisms [78]. Cellular and animal studies have suggested generation of nitric oxide (NO) and prostacyclins, as potential benefits of oestrogen on the endothelium-mediating vasorelaxation, promoting endothelial repair and regeneration, with anti-inflammatory and antioxidant effects [79–83].

Oestrogen and cardiac hypertrophy Cardiac hypertrophy during pregnancy is influenced by adjustments in the signalling pathways, extracellular matrix and the levels of hormones [23]. Oestrogen can slow the development of hypertrophy by modulating several pathways of cardiac

hypertrophy [84–86]. The alleged molecular mechanisms involve calcineurin degradation [87], mammalian target of rapamycin signalling [88], control of phosphorylated p38 mitogen-activated protein kinase (MAPK) pathways [86] and regulation of cardiomyocyte histone deacetylases [89].

However, oestrogen was also found to exert pro- and anti-hypertrophic effects in vitro, dependent of its concentration [90]. A hypertrophic effect was observed at lower concentration and an anti-hypertrophic effect at higher concentration [90]. The hypertrophic effect of E2 is facilitated by raised ERK activation [85]. The mechanisms underlying the anti-hypertrophic effect of higher concentrations indicate its inhibitory effect on calcineurin via stimulation of myocyte-enriched calcineurin-interacting protein 1 [84, 91].

Oestrogen and cardiac oxidative stress E2 also improves the defence against oxidative stress in endothelial cells and cardiomyocytes [92, 93]. Often oxidative stress correlates to cardiomyocyte apoptosis and cardiac contractility [70, 94]. Several signalling pathways have been implicated to the E2 inhibition of myocyte apoptosis [95]. These consist of inhibition of NF-kB [96], stimulation of phosphoinositide-3 kinase/Akt signalling [97], prevention of apoptosis signal-regulating kinase 1 (ASK1) activity [98] and promotion of p38β activity, which cause inhibition of p53 and, later, improvement of mitochondrial redox response [99].

Oestrogens also defend against apoptosis of endothelial cells (ECs) [100, 101]. Dose-dependent treatment with E2 resulted in receptor-mediated inhibition of TNF-α-induced endothelial cell apoptosis [100]. This also preserved endothelial integrity and maintained functionality after noxious stimuli [100].

Mechanism of oestrogen function

Genomic oestrogen mechanism The mechanism of oestrogen action can be grouped into two classes—the genomic or classical pathway and the rapid non-genomic pathway (Fig. 3). The classical pathway of oestrogen action is dependent on two oestrogen receptors (ERs), ERα and ERβ, which act as transcription factors [72, 95, 102]. These two receptors are primarily found in the cytoplasm and they migrate into the nucleus after binding to E2 [103, 104]. In humans, ERα is encoded by *ESR1* gene whilst *ESR2* encodes ERβ [102].

ERs are members of the nuclear receptor superfamily [105]. They positively regulate gene expression by binding to target gene oestrogen response elements (EREs), changing the binding of other transcription factors and gathering co-activators to the transcriptosome [105]. Figure 2 illustrates the classical hormone/receptor paradigm. This involves ER monomers in the cytosol that make protein complexes with chaperone heat-shock proteins (HSP) [102]. When the ER–HSP complex binds with E2, the HSP dissociate leaves only ER–E2 monomers [102]. These ER–E2 monomers then dimerize, forming mainly homodimers [102]. However, ERα/ERβ heterodimers have also been detected [106]. ER dimers can bind directly to DNA via oestrogen response elements (ERE) in the promoter of target genes, or indirectly, through protein–protein tethering [105, 107]. This regulates a host of gene transcriptions, depending on the cell type, the presence of transcriptional cofactors, the type and concentration of the ligand, and the type of ER dimer formed [69].

Non-genomic oestrogen mechanism Nevertheless, numerous experimental studies also indicate the existence of a non-classical mechanism of steroid action. G-protein oestrogen receptor (GPER) is the main mediator of the rapid effects of oestrogens via non-classical receptor systems [69, 108, 109]. The localization of GPER has been the subject of controversy. Some authors have described it as associated with plasma membrane, while others suggested the endoplasmic reticulum [108, 110].

GPER also plays a part in regulating physiological vascular and myocardial functions [111, 112]. It is expressed in both endothelial and smooth muscle cells in the entire cardiovascular system [111]. Activation of GPER by oestrogens stimulates a number of signalling cascades, including mitogen-activated protein (MAP) kinase family members (e.g., extracellular signal-related kinase 1/2; ERK 1/2), activation of phosphatidylinositol-3-kinase (PI3K), generation of cAMP, and calcium mobilisation [111, 113].

Progesterone

High amounts of progesterone are secreted by the corpus luteum and small amounts by the adrenal glands [110, 114]. During human pregnancy, initial supply of progesterone is from the corpus luteum and then, after the 8th week, the production shifts to the placenta [60]. The placenta uses cholesterol as the initial substrate to manufacture progesterone [115]. Most of the produced progesterone enters the maternal circulation, but minute quantities diffuse across the placenta into the foetal circulation.

Physiological function of progesterone on the cardiovascular system

Progesterone induces a number of physiologic and protective effects on the cardiovascular system, such as an increase in blood volume [116], vasodilation [117] and cardiomyocytes protection against apoptosis [118].

Progesterone induces vasodilation Progesterone promotes vasodilation due to its effect on the function of eNOS by both genomic and non-genomic mechanisms

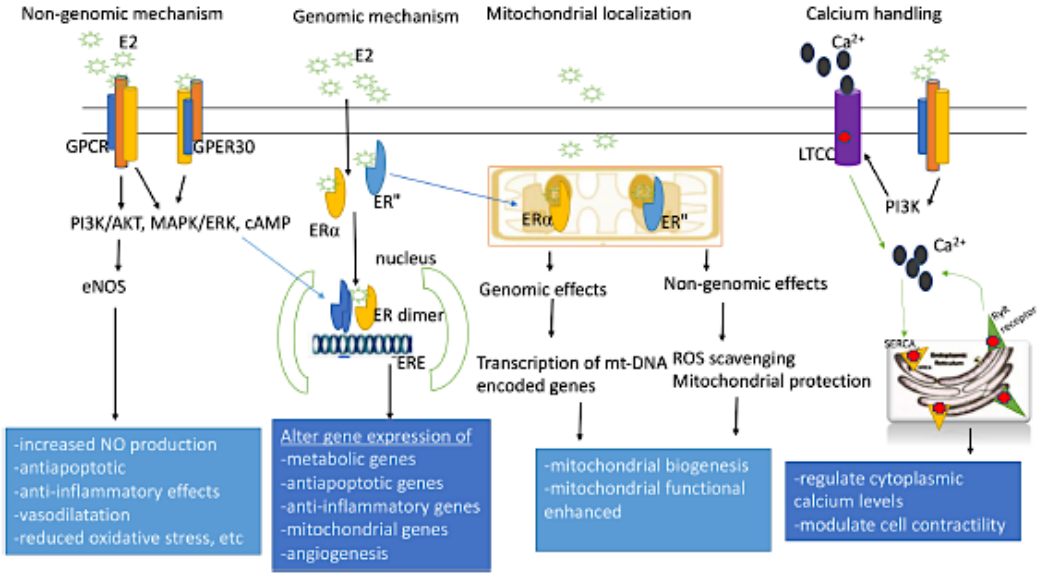

Fig. 2 Genomic and non-genomic effects of oestrogen on cardiac cells. Increase in phosphoinositide/AKT (PI3K/AKT) in the non-genomic signalling increases endothelial nitric oxide synthase (eNOS). Endothelial nitric oxide (eNO) relapses in blood vessels. Oestrogen inhibits cardiac fibrosis by increasing cyclic adenosine monophosphate/PKA (cAMP/PKA) block endothelin 1 (ET1) and transforming growth factor (TGFβ)-dependent cardiac hypertrophy and fibrosis. Genomic response also activates eNOS gene expression and numerous other genes involved during myocardial remodelling. Oestrogen has been shown to increase the electron transport chain activity and prevent the production of reactive oxygen species (ROS) in the mitochondria. It modulates the mitochondrial function through both genomic and non-genomic mechanisms. Oestrogen also modulates cell contractility by regulating calcium ion levels in the cytosol through non-genomic mechanism. Oestrogen binds directly to proteins such as the L-type calcium channels (LTCC), ryanodine receptor (RyR) or the SERCA. Oestrogen can also modulate cell contractility indirectly by producing PI3K which modulates LTCC. ● Mark proteins that directly bind oestrogen and modulate calcium handling

[119, 120]. Progesterone activates PI3K/Akt which then phosphorylates eNOS at serine 1177 (Ser1177-P-eNOS) [121, 122]. An increase of eNOS causes augmented NO production which changes the vascular tone and increases blood flow [123]. It also help in the balancing of the profound changes in electrolyte during physiological pregnancy [124].

Progesterone protects against apoptosis Progesterone was also found to protect cardiomyocytes from apoptotic cell death [118, 125]. In experimental studies using doxorubicin (Dox) to induce apoptosis, progesterone inhibited apoptosis in a dose- and time-dependent manner [118, 125]. Progesterone induces the expression of anti-apoptotic gene *Bcl-xL* [118]. Progesterone also induces transcription of several other genes such as *metallothionein I* [118]. Metallothionein I is an antioxidant metal-binding protein and also has cytoprotective effects [118].

Pathophysiological effect of progesterone during pregnancy

Several studies have shown that elevated levels of progesterone are associated with increased pathological effects in both men and women [126, 127]. The normal range of

Table 2 Reference ranges for progesterone in women at different stages of life

Life category	Reference range (ng/mL)
Early stage of menstrual cycle	< 1
Middle stage of menstrual cycle	5–20
Postmenopausal stage	< 1
Pregnancy	
First trimester	11.2–90
Second trimester	25.6–89.4
Third trimester	42.5–48.4

progesterone which varies greatly in women at different stages of life is summarised in Table 2.

High progesterone levels may promote upregulation of angiotensin I (Ang I) mRNA [128]. Subsequently, Ang I is cleaved by the ACE (angiotensin-converting enzyme) generating Ang II. ACE/Ang II causes vasoconstriction, inflammation, fibrosis, cellular growth and fluid retention [128]. This was also proved in an animal model study involving progesterone treatment, which demonstrated that high levels of progesterone are associated with a rapid decrease in vasodilation and blood pressure [124].

Increased serum progesterone levels have also been associated with increases in CD36 (cluster of differentiation 36) levels [129]. CD36 is a receptor for uptake of oxidised LDL (oxLDL) by monocytes/macrophages. This plays a prominent part in the formation of atherosclerotic lesions [129].

Progesterone also has a robust non-genomic effect on cardiac ion channels [130]. Exposure to small amounts of progesterone (100–1000 nM) decreases action potential duration (APD) and affects ventricular muscle contraction [126]. Progesterone attenuates and slows cardiomyocyte contraction, with calcium transients in males but not in females [126]. Additionally, progesterone (from 10-7M to 10-5M) has been shown to reduce Ca^{2+} uptake in the isolated papillary muscle of rabbit and guinea pig hearts [127].

Mechanisms of progesterone

The effects of progesterone are mediated by genomic (nuclear) and non-genomic (extranuclear) receptor mechanisms (Fig. 3) [131]. Progesterone is a lipophilic molecule which, during the genomic mechanism, diffuses into the cytoplasm where it interacts with two specific nuclear progesterone receptors (PRs), namely PR-A and PR-B. During physiological conditions, PR-A and PR-B are equally expressed in cardiomyocytes and other cells [131]. However, a third type, PR-C, is more abundant in myometrial tissue [132].

Upon binding to progesterone both isoforms of nuclear PR change shape. The receptors then homo- or hetero-dimerize and bind to hormone response elements (HRE) in the promoter regions of target genes [122]. In addition, PRs also act together with co-activators, co-repressors and transcription factors [133].

Progesterone also applies rapid non-classical effects on various signalling pathways, independent of transcriptional or genomic regulation [134]. This non-genomic mechanism is facilitated by membrane-bound PR (mPR) [135]. New data presented show that mPRα, mPRβ and mPRγ are also present in human endothelial and smooth muscle vascular cells [136]. Non-genomic effect of progesterone involves the rapid activation of MAPK signalling and intracellular Ca^{2+} increase [137]. Direct instant progesterone actions were

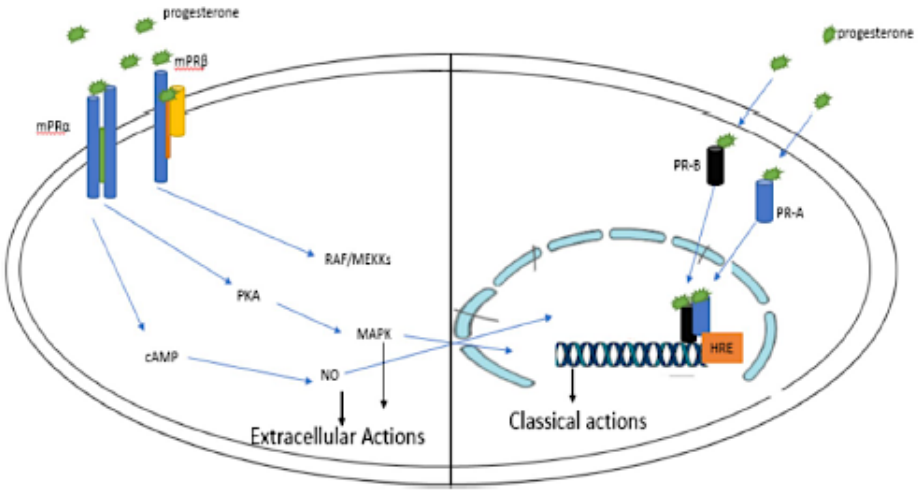

Fig. 3 Classical and non-genomic mechanism of progesterone. Progesterone activates the non-genomic pathway through membrane-bound receptors (mPRα, mPRβ and mPRγ). This rapid pathway elicits the activation of cyclic adenosine monophosphate (cAMP) and mitogenic-activated protein kinase (MAPK) pathways which, through other downstream pathways, produce the extranuclear actions of progesterone. The non-genomic and genomic pathways can also be overlapping with MAPK and nitric oxide (NO), influencing the expression of other genes. The genomic mechanism is facilitated by PR-A and PR-B which receive progesterone in the cytosol. The receptors dimerise and enter the nucleus

reported in humans and mammalian vascular smooth muscle cells causing a rapid influx of calcium [136].

Prolactin

Prolactin (PRL), also known as luteotropic hormone, is mainly involved in milk production in mammals [138]. During pregnancy, prolactin concentration increases after 6 weeks and reaches the highest level in late pregnancy [139]. The most abundant form of prolactin is the 23-kDa PRL which is secreted by the pituitary gland. However, the 23-kDa PRL can be spliced into smaller variants [140, 141].

Physiological function of prolactin

Prolactin is a multifunctional hormone whose receptors are expressed in almost all organs of the human body which, in turn, enables it to influence multiple physiological processes, including endocrine and cardiovascular properties [142, 143]. The major isoform, 23-kDa prolactin has proangiogenic activity and reportedly stimulates endothelial cell (EC) proliferation [138]. The first study to demonstrate that prolactin can stimulate the angiogenic process was conducted in bovine pulmonary artery endothelial cells, using rhodamine-labelled prolactin. The investigations observed specific prolactin uptake, indicating the presence of a prolactin receptor [144]. When the same endothelial cells were mechanically wounded and treated straight way with high prolactin doses between 62.5 and 1000 ng/mL, the cells differentiated and had reduced f-actin staining in comparison with controls that were not treated with prolactin [144].

An analytical study in rats also suggested that increased plasma prolactin can protect rat cardiomyocytes against intermittent hypoxia via phosphorylated Janus activator kinase (p-JAK2) and phosphorylated signal transducer activator of transcription factor 5 (p-STAT5) pathways for cell multiplication [143]. The same study also outlined that prolactin also protects cardiomyocytes by activating survival pathways such as PI3Kα/AKT and MAPK pathways through insulin-like growth factor 1 (IGF-1) [143].

Prolactin was also found to induce vasodilation in a study involving rat aortic rings [145]. This effect is mediated via increased NO production through the phosphorylation [145].

Pathophysiological effect of prolactin during pregnancy

Serum prolactin concentrations are associated with an adverse cardiovascular risk profile [146, 147]. A population-based study of (sample size 3929) men and women who were followed for 10 years observed a positive association of serum prolactin concentration and cardiovascular disease mortality [147]. Additionally, studies in the acute phase of coronary syndromes, ischemic strokes and transient ischemic attacks also reported elevated plasma prolactin [148]. The pathophysiology of prolactin is attributed to vasoinhibins rather than the full-length (23 kDa) prolactin [149–151].

Role of vasoinhibins in the pathophysiology of prolactin Vasoinhibins are smaller versions of prolactin resulting from proteolytic cleavage by cathepsin D or matrix metalloproteases [151]. All vasoinhibins contain the N-terminal region of prolactin and can interfere with angiogenesis by hindering endothelial cell migration, proliferation, differentiation and survival [151]. Vasoinhibins are sometimes known as the 16K-PRL.

Evidence showed that the 16K-PRL inhibits vascular endothelium growth factor (VEGF)-induced NO synthase (NOS) activity in endothelial cells which may mediate the antiangiogenic properties [152]. VEGF quickens endothelial cell proliferation via activation of the MAPK signalling cascade. Martine et al. [153] also proved the inhibition of the downstream kinases, Raf-1 and MAPK by 16K-PRL. Obstruction of eNOS activation can also lead to inhibition of vasodilation [152].

16K-PRL also induce cell apoptosis in vascular endothelial cells [153, 154]. The induced apoptosis is linked to rapid instigation of caspases 1 and 3 [154]. In bovine adrenal cortex capillary endothelial cells, Tabruyn et al. also noted the involvement of nuclear factor kappa B (NF-κB) in the activation of the caspase cascade by 16K-PRL [154].

In a study involving guinea pigs, 16K-PRL injected directly into a vein caused coronary and iliac artery constriction [155, 156]. Another study in rats' isolated arteries also confirmed the vasoconstriction action of prolactin [145]. However, evidence of vasoconstrictive action of prolactin in clinical studies is still controversial [157].

Recent data showed that 16K-PRL is implicated in the pathogenesis of PPCM (PPCM) [40]. Due to increased oxidative stress, the full-length 23-kDa prolactin is cleaved into the antiangiogenic, proinflammatory, and proapoptotic 16K-PRL [36]. The 16K-PRL will then directly impair endothelial function and trigger the release of micro-RNA 146a, which, in turn, has detrimental effects on cardiomyocytes [42]. The miR-146a internalised into cardiomyocytes will then suppress the neuregulin/ErbB pathway, thereby promoting cardiomyocyte apoptosis leading to heart failure [42, 158, 159].

Mechanisms of action of prolactin

The PRL activities are facilitated by the prolactin receptor (PRLR), which belongs to the cytokine receptor class 1 superfamily [157]. The classical PRLR is expressed in various tissues including the heart [157, 160]. There are three other isoforms of PRLR derived from proteolytic digestion of the full-length PRLR [157]. Abundant isoforms of PRLR

are: the full-length activating receptor-long form (LF), intermediate (IF) and short form (SF). However, a soluble isoform known as the PRLR-binding protein also exists [160].

JAK2-STAT cascade is the predominant pathway employed by PRL, although it can engage in other different second messenger cascades of signal transduction [157, 161]. Figure 4 summarises the mechanism of action of PRL. Ligand-mediated instigation of PRL-R causes tyrosine phosphorylation of numerous cellular proteins, including the receptor itself [157]. These activated isoforms bind to the STAT proteins which also become activated and form dimers which then migrate to the nucleus, where they regulate genes such as β-casein, β-lactoglobulin, interferon-regulatory factor-1 and others [157].

Interaction of the pregnancy hormones in the cardiovascular system

Hormones, apart from interacting with cells and cell receptors, also interact with each other. Hormone–hormone interaction could be synergistic, antagonistic or permissive. Both oestrogen and progesterone exert several effects of on the vascular function. They both stimulate vasodilation via promoting eNOS expression and NO-mediated relaxation [162–164]. Migliaccio et al. showed a physical interaction of the progesterone with the ER, which is an association necessary for progesterone to stimulate a signal transduction pathway, the MAPK pathway [165].

However, oestrogen and progesterone interaction, and cross talk could also be antagonistic [163]. In animal studies, medroxyprogesterone acetate counteracts the positive outcomes of oestrogens on endothelial function and coronary artery plaque size [166, 167]. Adams et al. demonstrated that the atherosclerosis extent of surgically postmenopausal cynomolgus monkeys, fed atherogenic diets and treated with hormones for 30 months, improved by 72% when treated with oral conjugated equine oestrogens (CEE) [166]. However, when treated with CEE plus medroxyprogesterone acetate (MPA) or MPA alone the atherosclerosis extent matched that of untreated controls [166].

In another study, progesterone hinders the ability of oestrogen to stimulate NO production in porcine arteries [155]. The same study also found that oestrogen can block progesterone-induced endothelial dysfunction and superoxide anion production [155]. This was again confirmed in ovariectomised mice where the vasoprotective effect of oestrogen on antioxidant enzyme expression and activity was prevented by co-injecting progesterone, resulting in added NADPH oxidase activity and reactive oxygen species (ROS) [167]. Surprisingly, clinical observational studies that evaluated treatment with oestrogen combined with progesterone in hormone replacement therapy (HRT) found comparable protective effects from combined oestrogen and progesterone

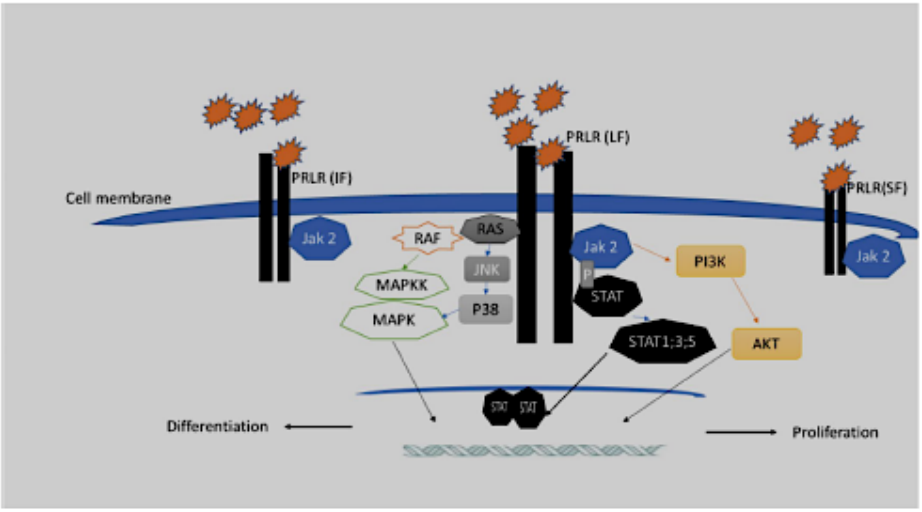

Fig. 4 Mechanism of prolactin action. The prolactin mechanism is facilitated by one of the three receptors; small, intermediate or full length. Prolactin involves several transduction pathways. However, the most dominant pathway is the Janus-activated kinase 2-signal transduction activation of transcription factor (Jak 2-Stat pathway). Other pathways such as the protein kinase (AKT) and mitogenic-activated protein kinase (MAPK) are also activated which, together with transcription factors, modulate several genes for cell differentiation and proliferation

just as that of oestrogen alone on the risk of coronary heart disease [168, 169].

The interaction of prolactin with other pregnancy hormones has not been thoroughly exploited. Interestingly, Malinari et al. found that treatment of porcine aortic endothelial cells with prolactin led to low levels of NO secretion and of the phosphorylation of ERK, Akt, and p38 [156]. Hence, prolactin may have antagonistic vasoconstrictive effects on both oestrogen and progesterone.

Conclusions

Hormones play an important role in maintaining physiological cardiovascular system during pregnancy. Hormonal concentration, availability of receptors and receptor concentration determine the extent of hormone impact. In addition to the individual effects of each hormone, hormones also interact with each other. It is crucial to study the interaction of hormones during pregnancy for a better understanding on cardiovascular diseases related to pregnancy. However, studies investigating the interaction of pregnancy hormones and its effects on the cardiovascular system are limited.

Acknowledgements This research could not have been conducted without the funding support towards running costs of the Hatter Institute for Cardiovascular Research in Africa from the University of Cape Town, the Medical Research Council South Africa (Grant ID 488000), The National Research Foundation South Africa (Grant ID 105867), and the Maurice Hatter Foundation and The Letten Foundation.

References

1. Chung E, Leinwand LA (2014) Pregnancy as a cardiac stress model. Cardiovasc Res 101:561–570. https://doi.org/10.1093/cvr/cvu013
2. Soma-pillay P, Nelson-piercy C, Tolppanen H, Mebazaa A (2016) Physiological changes in pregnancy. Cardiovasc J AFRICA 27:89–94. https://doi.org/10.5830/CVJA-2016-021
3. Sanghavi M, Rutherford JD (2014) Cardiovascular physiology of pregnancy. Circ AHA 10:1003–1008. https://doi.org/10.1161/CIRCULATIONAHA.114.009029
4. Osol G, Ko NL, Mandalà M (2017) Altered endothelial nitric oxide signaling as a paradigm for maternal vascular maladaptation in preeclampsia. Curr Hypertens Rep 19:1–12. https://doi.org/10.1007/s11906-017-0774-6
5. Dos Santos RL, Da Silva FB, Ribeiro RF, Stefanon I (2014) Sex hormones in the cardiovascular system. Horm Mol Biol Clin Investig 18:89–103. https://doi.org/10.1515/hmbci-2013-0048
6. Carlin A (2008) Physiological changes of pregnancy and monitoring. Res Clin Obstet Gynaecol 22:801–823. https://doi.org/10.1016/j.bpobgyn.2008.06.005
7. Melchiorre K, Sharma R, Thilaganathan B (2012) Cardiac structure and function in normal pregnancy. Curr Opin Obstet Gynecol 24:413–421. https://doi.org/10.1097/GCO.0b013e328359826f
8. Meah VL, Cockcroft JR, Backx K et al (2016) Cardiac output and related haemodynamics during pregnancy: a series of meta-analyses. Heart 102:518–526. https://doi.org/10.1136/heartjnl-2015-308476
9. Halla ME, Eric M, George JPG (2011) The heart during pregnancy. Rev Esp Cardiol 64:1045–1050. https://doi.org/10.1016/j.recesp.2011.07.009.The
10. Liu LX, Arany Z (2014) Maternal cardiac metabolism in pregnancy. Cardiovasc Res 101:545–553. https://doi.org/10.1093/cvr/cvu009
11. Sanghavi M, Rutherford JD (2014) Cardiovascular physiology of pregnancy. Circulation 130:1003–1008. https://doi.org/10.1161/CIRCULATIONAHA.114.009029
12. Melchiorre K, Sharma R, Khalil A, Thilaganathan B (2016) Maternal cardiovascular function in normal pregnancy: evidence of maladaptation to chronic volume overload. Hypertension 67:754–762. https://doi.org/10.1161/HYPERTENSIONAHA.115.06667
13. Gilson GJ, Samaan S, Crawford MH et al (1997) Changes in hemodynamics, ventricular remodeling, and ventricular contractility during normal pregnancy: a longitudinal study. Obstet Gynecol 89:957–962. https://doi.org/10.1016/S0029-7844(97)85765-1
14. Estensen ME, Beitnes JO, Grindheim G et al (2013) Altered maternal left ventricular contractility and function during normal pregnancy. Ultrasound Obstet Gynecol 41:659–666. https://doi.org/10.1002/uog.12296
15. Rebelo F, Farias DR, Mendes RH, Schlüsselal MM, Kac G (2015) Blood pressure variation throughout pregnancy according to early gestational BMI: A Brazilian Cohort. Arq Bras Cardiol 104:284–291. https://doi.org/10.5935/abc.20150007
16. National High Blood Pressure Education Program Working Group (1990) Report on high blood pressure in pregnancy. Am J Obstet Gynecol 183:1691–1712. https://doi.org/10.1067/mob.2000.107928
17. Gifford R, August P, Cunningham G et al (2000) National High Blood Pressure Education Working Group report on high blood pressure in pregnancy. Natl Institutes Heal NIH Publ no 00-3029, pp 3–5
18. Geva T, Mauer MB, Striker L et al (1997) Effects of physiologic load of pregnancy on left ventricular contractility and remodeling. Am Heart J 133:53–59. https://doi.org/10.1016/S0002-8703(97)70247-3
19. Mesa A, Jessurun C, Hernandez A et al (1999) Left ventricular diastolic function in normal human pregnancy. Circulation 1:511–517
20. Hunter S, Robson SC (1992) Adaptation of the maternal heart in pregnancy. Heart 68:540–543. https://doi.org/10.1136/hrt.68.12.540
21. Sampaolesi M, Van Calsteren K (2017) Physiological and pathological gestational cardiac hypertrophy: what can we learn from rodents? Cardiovasc Res 113:1533–1535. https://doi.org/10.1093/cvr/cvx192
22. Sliwa K, Böhm M (2014) Incidence and prevalence of pregnancy-related heart disease. Cardiovasc Res 101:554–560. https://doi.org/10.1093/cvr/cvu012
23. Li J, Umar S, Amjedi M et al (2012) New frontiers in heart hypertrophy during pregnancy. Am J Cardiovasc Dis 2:192–207
24. Gongora MC, Wenger NK (2015) Cardiovascular complications of pregnancy. Int J Mol Sci 16:23905–23928. https://doi.org/10.3390/ijms161023905
25. Siu SC, Sermer M, Colman JM et al (2001) Clinical investigation and reports prospective multicenter study of pregnancy outcomes in women with heart disease. Circulation 104:515–521. https://doi.org/10.1161/hc3001.093437
26. Elkayam U (2018) How to predict pregnancy risk in an individual woman with heart disease. J Am Coll Cardiol 71:2431–2433. https://doi.org/10.1016/j.jacc.2018.03.492

4.1 Heart derived hormones during pregnancy

The heart can also synthesize and secrete hormones with paracrine or endocrine function [218]. The hormones are synthesized and secreted from specific heart cells and their circulatory levels are highly controlled in response to modified internal cardiac function or external cardiac demand. Know heart-derived hormones include growth differentiation-15 (GDF-15), myostatin and atrial natriuretic peptide (ANP), brain (or B-type) natriuretic peptide (BNP) [219][220].

4.1.1 Growth/differentiation factor-15 expression in the heart

Growth/differentiation factor-15 (GDF-15, is a distance member of the transforming growth factor β superfamily (TGF-β) [221]. GDF-15 is also known as macrophage inhibitory cytokine 1 (MIC-1) non-steroidal anti-inflammatory drug-inducible gene (NAG)-1, placental transforming growth factor-beta (pTGFB), prostate-derived factor (PDF), and placental bone morphogenetic protein (PLAB) [222][223]. It is a 25-kD disulfide-linked dimeric protein cleavage from a 62-kD intracellular protein by a furin like protease [224]. Furin also known as the proprotein convertase subtilisin/kexin (PCSK)-3, PCSK5, and PCSK6 cleave pro- GDF-15, generating mature GDF-15 dimer [218][225].

GDF-15 is available at high levels in the blood of pregnant women, it is highly expressed in the placenta but its role in pregnancy remains unknown [226].

Heart expression of GDF-15 is low under physiological state, but its expression can be prompted in response to reactive oxygen species, proinflammatory cytokines, simulated ischemia, and mechanical stretch [221][227][228]. Plasma GDF-15 concentration is associated with cardiovascular diseases such as heart failure, coronary artery disease, and atrial fibrillation [225][229][230]. Marked elevation in GDF-15 level is associated with worsening heart failure severity [231]. However, GDF-15 has limited usefulness as an independent prognosis marker because the concentration is also related to cardiovascular risk factors, like age, diabetes, and current smoking and low HDL-cholesterol levels [232][233].

4.1.2 Cardioprotective functions of GDF-15

Accumulating evidence, at the molecular and cellular level suggests that GDF-15 contributes substantially to cardioprotection through multiple signaling pathways [234][235]. **Figure 9** summarizes the crucial involvement of GDF-15 in distinct cardioprotective signaling cascades.

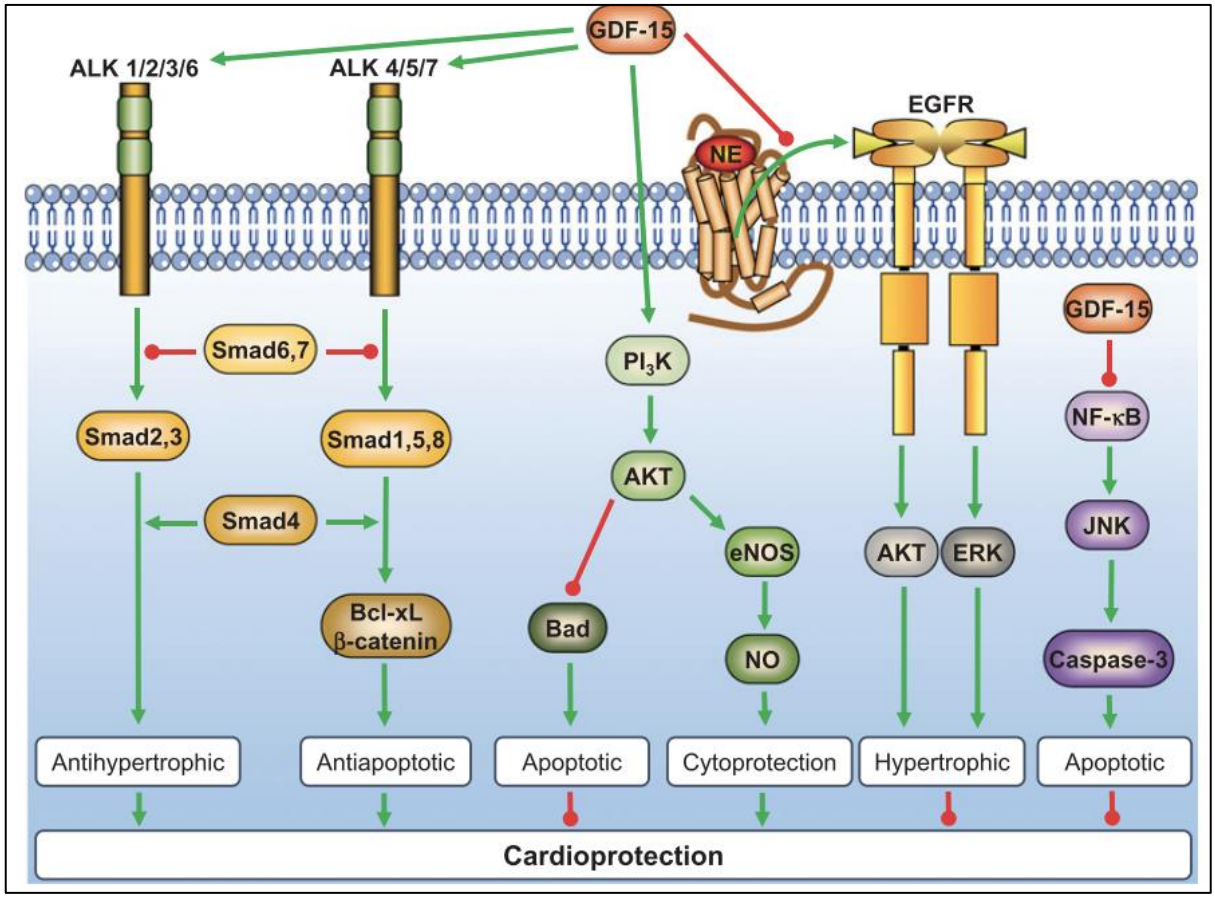

Figure 9: Distinct cardioprotective signaling modulated by GDF-15 [236]

ALK: ALK type 1 receptors; AKT: serine/ threonine kinase (protein kinase B); Bcl-xL: B-cell lymphoma-extra-large; EGFR: epidermal growth factor receptor; eNOS: endothelial nitric oxide synthase; ERK: extracellular signal-regulated kinases; GDF-15: growth differentiation factor-15; JNK: Jun-N-terminal kinase; NF-jB: nuclear factor kappa B; PI3K: phosphoinositide 3-kinase

GDF-15 has antihypertrophic and antiapoptotic functions activated through ALK type 1 receptors that phosphorylate several SMAD members [237]. GDF-15 can also hinder the transactivation of epidermal growth factor receptor (EGFR), therefore inhibiting the hypertrophic actions of both AKT and ERK in cardiomyocytes [236]. Li et al. also showed that increased GDF-15 protects endothelial cells against high glucose induced cellular injury by activating PI3K/AKT/eNOS signaling pathway and attenuating NF-KB/JNK activation [237]. Nevertheless, the antihypertrophic effect of GDF-15 has been contradicted in a study by Heger et al, 2010 who found that GDF-15 enhances hypertrophic growth that is mediated through PI3K and ERK and the transcription factor R-SMAD1 [238].

CHAPTER 2

JUSTIFICATION AND OBJECTIVES

1.1 Justification

Cardiac diseases including heart failure, account for up to 15% of maternal death and remain a major cause of morbidity and mortality in pregnant and postpartum women [79][142][143][144]. World Health Organisation (WHO) current efforts aim to pinpoint heart failure at its earliest preclinical stages in order to start treatment and prevent deterioration before the symptoms escalate.

During pregnancy, it can be more challenging to diagnose cardiovascular diseases as most indicators of cardiovascular diseases mimic physiological changes that occur during pregnancy. Understanding the physiological cardiovascular changes will help to establish precisely timed changes and identify deviations from regular patterns caused by maternal cardiovascular maladaptation. This will help in early diagnosis and prognosis assessment of cardiovascular diseases during pregnancy.

1.2 Main Objective

The main objective of this study was to assess the functional, structural and molecular cardiovascular changes that occur during physiological pregnancy with the goal to delineate possible mechanisms involved in the lack of reverse cardiac remodeling observed in peripartum cardiomyopathy (PPCM).

1.3 Specific Objectives

- To delineate functional, morphological and structural cardiovascular changes that occur during gestation and postpartum in healthy pregnant wild type mice(C57/BL6) (chapter 4).
- To explore potential signaling pathways that regulates physiological cardiac hypertrophy during pregnancy in mice (chapter 4).
- To identify a set of proteins from mice hearts that can track pregnancy induced cardiovascular remodeling and the recovery process (chapter 4).
- To assess the potential involvement of maternal hormones in the regulation of cardiac hypertrophy invitro (chapter 5).

- To delineate cardiovascular functional and morphological changes that occur during gestation and postpartum in healthy pregnant mothers (chapter 6).
- To assess the differences in expression of GDF-15 in peripartum cardiomyopathy (PPCM) patients and matched healthy controls (chapter 6).

1.4 Possible benefits

Our primary target was to reveal pathways in the heart that are modified during pregnancy and the postpartum period to expand our insights on cardiac remodeling that occur during these physiological states. Broadly, our findings will provide a molecular signature for physiological remodeling in response to volume load induced by pregnancy. Various forms of remodeling associated with chronic hemodynamic load can be compared against these finding to pinpoint areas of deviation. In addition, elucidating the pathways that mediates reverse remodeling postpartum will provide a basis for understanding the heart's adaption to load removal. If these pathways could be controlled, either alone or in conjunction with mechanical unloading, it might help in optimising myocardial recovery in HF.

CHAPTER 3

MATERIALS AND METHODS

Section 1: Morphological and functional cardiac changes during pregnancy and postpartum in wild type mice (C57/Bl6)

1.1 Animal ethics

Animal ethics was approved by the University of Cape Town Faculty of Health Sciences Animal Ethics Committee (**Appendix 1**). All experiments were conducted after proper training and authorisation of researchers by the South African Veterinary Service (SAVC). Animals were bred by the University of Cape Town Animal Breeding Unit under specific pathogen free (SPF 1) environment and the experiments were conducted in a biosafety level 1 (BSL 1) environment.

1.2 Experimental protocol

A total of 63 wild type virgin dams (C57/BL6 strain) aged between 10-14 weeks were used in this study. The mice were mated overnight. Copulatory plugs were then confirmed in the morning after mating. **Figure 10** summarizes the sampling time points.

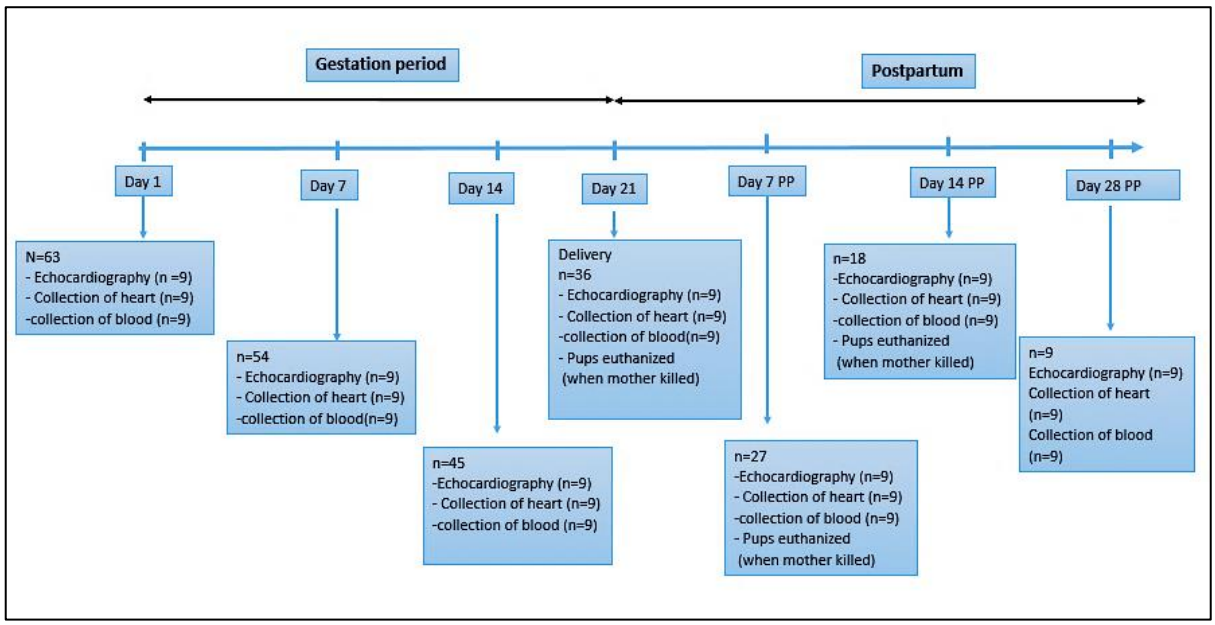

Figure 10: Experimental protocol for the assessment of cardiovascular changes during pregnant mice

A total of 63 virgin mice were used in this study. Aged 12-14 weeks. Nine mice were euthanized per time point. Day 1 is the day after mating night, Day 7 corresponds to 7 days after mating, Day 14: 14 days after mating, Day 21 is on the day of giving birth, Day 7 pp is 7 days after

giving birth, Day 14 pp: 14 days after giving birth and Day 28 pp- 28 days after giving birth. The hearts and blood samples were collected after echocardiography for further measurements.

Mice with confirmed copulatory plugs that were echoed to assess left ventricular structure and function and were euthanized the morning after mating formed Day 1 group. Day 1 group was used as the control group for all measurements. The other mice could carry their pregnancy until giving birth on Day 21. Some were also allowed to nurse their pups postpartum for up to 28 days.

The time points for sampling were Day 1, Day 7, Day 14, Day 21, Day 7 postpartum (Day 7 pp), Day 14 postpartum (Day 14 pp) and Day 28 postpartum (Day 28 pp). Nine mice were euthanized at each time point. Day 21 was the day of parturition.

After echocardiography, about 800µl of blood were collected directly from the heart (cardiac puncture) using a 25-gauge needle [239]. The blood was centrifuged, and the serum was used to measure hormone levels. The hearts were then harvested, trimmed of all connective tissue and weighed. The collected hearts were used for histology, protein expression and mRNA expression measurements.

1.3 Transthoracic Echocardiography in pregnant mice

1.3.1 Animal preparation

Mice were weighed to collect body weight before induction of anaesthesia with volatile inhalant isoflurane. The anaesthetic was inducted at 4% isoflurane in medical grade oxygen at a flow rate of 1L/minute in induction chamber for 4 minutes [240]. The depth of anaesthesia was assessed by pinching between the toes of the mice' left foot. If the mice does not respond it means it has lost its righting reflex. This entails that the mice do not get stressed with the echocardiograph process [241]. The anaesthetized mice were then transferred to a heating pad and placed in supine position. The heating pad helps to maintain the animal's body temperature at around 37^{o}C to preserve physiological function of the body system. The heating pad also have electrocardiograph probes which helps to monitor the mice electrocardiogram.

A nose cone supplying 1.5-2% isoflurane at 1L/minute oxygen flow rate was connected for maintenance of anaesthesia during echocardiography [240]. This ensures that the mice do

not wake up during the procedure. A rectal probe was inserted to monitor body temperature and heart rate during the procedure. The heart rate was maintained higher than 450 bpm.

The mice chests were shaved using pre-warmed depilating gel. The gel was cleaned with water and dried with a sponge gauze before putting the echocardiography gel. The echocardiography gel ensures proper contact between the mice and probe without pressing on the animal chest.

1.4 Cardiac structure and function measurements by conventional echocardiography

Cardiac structure and function of the mice were assessed using the Vivo 2100 platform imaging software V.1.6.0 (Visual sonic, Toronto Canada). An ultra-frequency probe which emits 550 MHz of ultrasound waves was used to acquire the images. The probe was placed in contact with the gel avoiding compressing the animal chest.

Imaging was done according to the Vivo Sonic imaging guidelines [242]. **Figure 11** illustrate the sequence in which the images were acquired, the different modes and views.

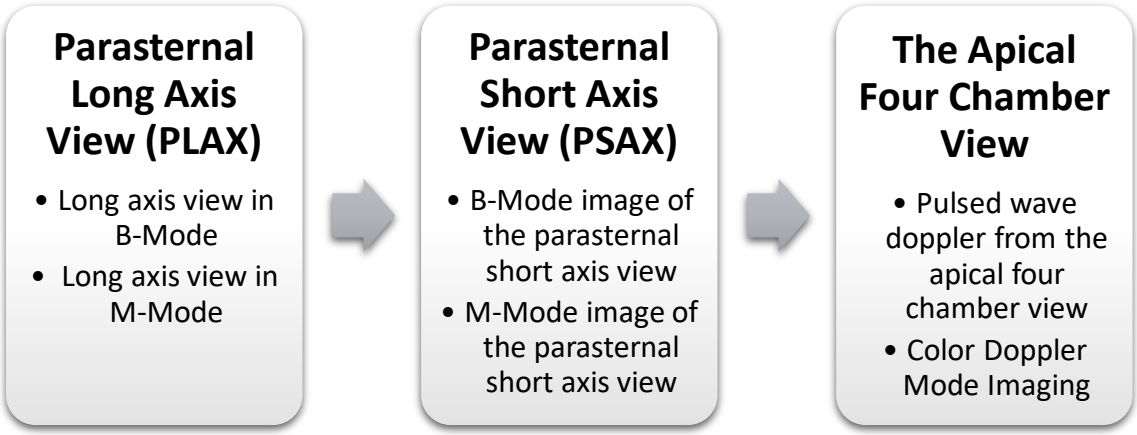

Figure 11: Echocardiography imaging guidelines outline

2D images were acquired in bright mode (B-mode) and motion mode (M-mode). The images were acquired in three views: parasternal long axis (PLAX), short axis (SAX) and the apical four chamber view (Api 4).

Bright mode (B-mode) imaging was used to acquire 2 dimensional (2D) images of an area of interest in grayscale. The images allowed for identification of anatomical structures and structure sizes were measured by the software. Motion mode (M-mode) imaging was used to acquire images in one dimension over time. Ultrasound beam was placed over an area for a time and the movement of that area was displayed in the spectrum. Pulsed-Wave (PW)

Doppler Mode imaging was used to analyse blood flow across the mitral valve and the system generates a PW Doppler spectrum which provided the information necessary to make velocity, acceleration and time measurements with the software. PW Doppler mode was used in combination with Colour Doppler which gave information on the direction of blood flow. The software assigned blue for the blood flowing away and red for blood flowing towards the probe.

1.4.1 Image acquisition procedure

Parasternal long axis (PLAX) view was acquired by placing the transducer over the left third or fourth intercostal space and orienting its notch toward the animal's right shoulder. To obtain the parasternal short axis view (PSAX) the probe was rotated 90^{o} clockwise from the PLAX position so that the transducer's notch was directed toward the animal's left shoulder. In order to obtain the Apical 4 chamber view (Api 4) the transducer was placed at the cardiac apex and oriented toward the animal's right scapula such that the transducer's notch faces the animal's left axilla. **Figure 12** shows representative images acquired in B-mode and M-mode images in different views.

For M-mode imaging the cursor was placed at the mid-papillary level and perpendicular to the interventricular septum and posterior wall of the LV. This was done for consistence, and to minimize variability. Again, the order of imaging and timing of imaging was maintained.

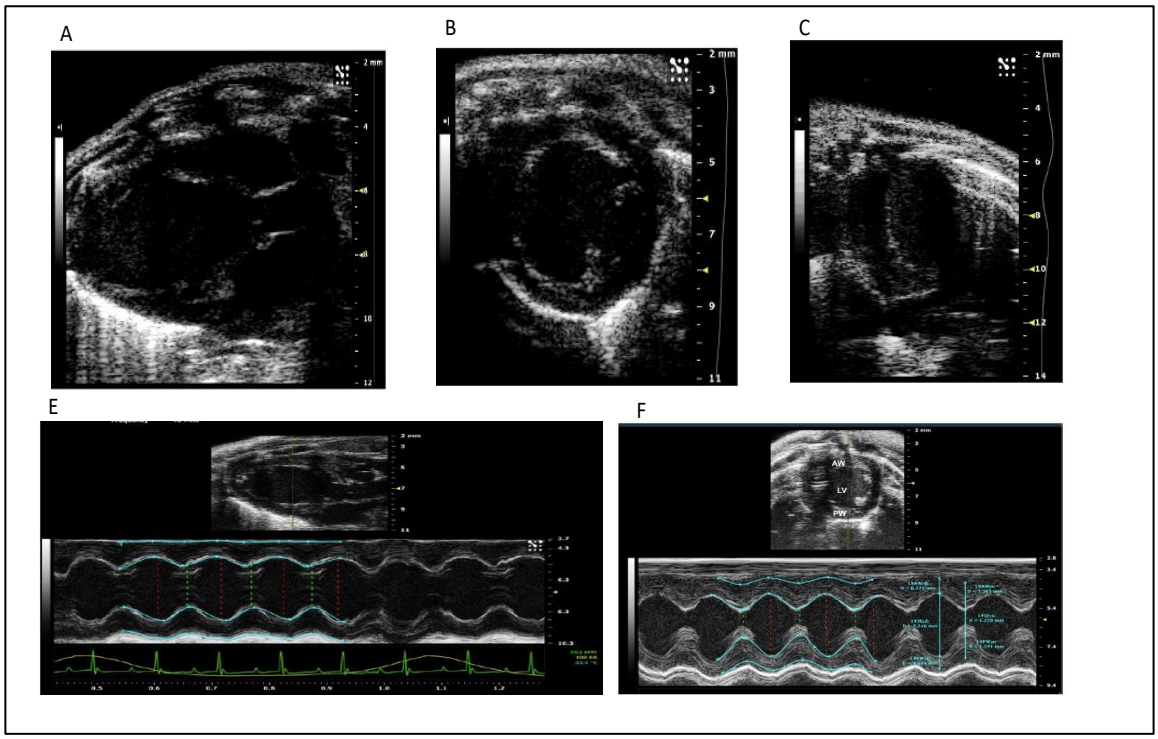

Figure 12: Representation of echocardiography images in B-mode and M-mode

A-C: Bright mode (B-mode) images in parasternal long axis (PLAX), short axis (SAX) and apical 4 chamber (API 4) views respectively. E- F: Motion mode (M-mode) images of PLAX and SAX. apical 4 chamber adapted from Visual sonic manual booklet [242].

Mitral valve flow measurements in Colour and PW doppler were used to assess for LV diastolic dysfunction. PW doppler allows determination of blood flow velocity profile from the mitral valve using 2-D image guidance. Transmitral flow velocity profiles include isovolumic contraction and relaxation times, ratio of early (E)-to-late (atrial, A) ventricular filling velocities (E/A), and deceleration of E wave [243]. **Figure 13** shows PW and Colour doppler images.

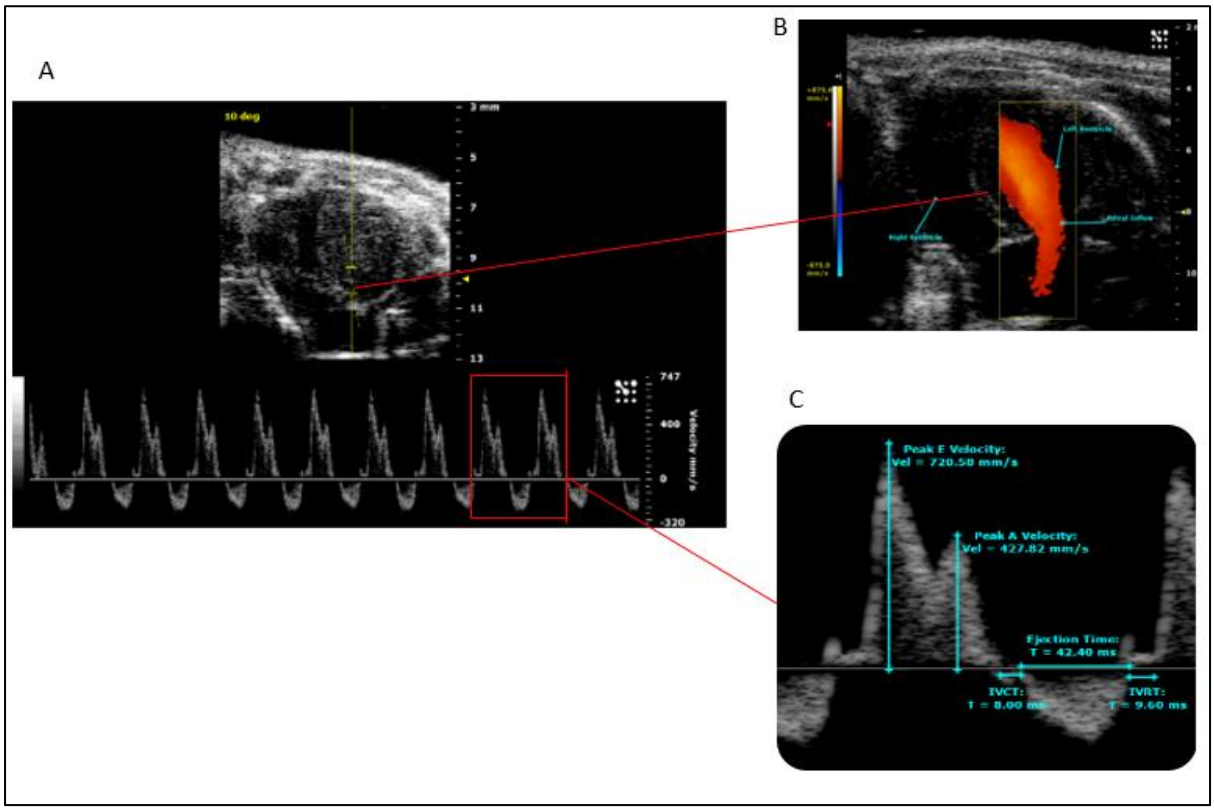

Figure 13: Pulse wave (PW) and Colour doppler images

A: Apical 4 chamber view in B-mode with sample volume directed under the mitral valve. B: Colour doppler image capturing transmitral flow direction. C: PW doppler mode waveform of mitral valve flow. Image was adapted from Visual sonic imaging guideline [242].

The E-wave represented the peak velocity blood flow from left ventricular relaxation in early diastole and A-wave represented peak velocity flow in late diastole caused by atrial contraction. The E/A ratio is a marker of diastolic function of the left ventricle. In a healthy heart the value of E/A should be greater than 1 meaning E velocity is greater than A velocity. A decrease in the E/A ratio is a strong indicator of diastolic dysfunction [243].

Isovolumic relaxation time (IVRT), was estimated as the time between the closure of the aortic valve and the opening of the mitral valve, whilst isovolumetric contraction time (IVCT) was estimated as the time between the closure of the mitral valve and the opening of the aortic valve. Diastolic dysfunction is associated with prolonged IVRT and IVCT [243].

Another parameter derived from transmitral PW doppler measurement was the deceleration times of the E wave. Again, prolonged deceleration time is linked to diastolic dysfunction [243][244].

1.4.2 Visible anatomy, available measurements and calculations

Visible anatomy in B-mode includes left ventricle (LV), right ventricle, left atrium, LV anterior wall, LV posterior wall, intraventricular septum, aorta, pulmonary artery, aortic valve, mitral valve, pulmonary veins and papillary muscles. However, this depends on the angle at which the probe is held.

Analysis of M-mode images were done with the Vevo lab software version 3.2.0 (Visual sonic, Canada). Left ventricular (LV) anterior wall thickness (LVAW), LV internal diameter (LVID) and LV posterior wall thicknesses (LVPW) in systole and diastole (LVAWs, LWAVd, LVIDs, LVIDd, LVPWs & LVPWd were measured. Measurements were taken at end systolic and end diastolic points. **Table 3** summarizes the anatomy and measurements of interest.

Table 3: Possible anatomy and measurements obtained from the conventional echocardiography

View	Mode	Visible anatomy	Available measurements
Parasternal Long Axis (PLAX) View	PLAX B-mode	• Left ventricle (LV) • LV Anterior wall • LV Posterior wall	• Diastolic and systolic volumes • Ejection fraction • Fractional shortening • Cardiac output • Stroke volume
	PLAX M-mode		LV anterior wall thickness in diastole and systole (LVAWd, LVAWs) LV internal diameter in diastole and systole (LVIDd, LVIDs) LV posterior wall thickness in diastole and systole (LVPWd, LVPWs) Intraventricular septum thickness in diastole and systole (IVSd, IVSs
Parasternal Short Axis (PSAX)	PSAX M-Mode	• Left ventricle Anterior wall Intraventricular septum • Papillary muscles	LV anterior wall thickness in diastole and systole (LVAWd, LVAWs) LV internal diameter in diastole and systole (LVIDd, LVIDs) LV posterior wall thickness in diastole and systole (LVPWd, LVPWs) Intraventricular septum thickness in diastole and systole (IVSd, IVSs)

Apical Four Chamber View	PW Doppler	• Left ventricle • Right ventricle • Mitral valve • Left atria Right atria • Tricuspid valve	• Mitral isovolumic relaxation and contract times (IVRT, IVCT) • Mitral velocity time integral (VTI) • Mitral deceleration time (MV Decel) • Peak early and atrial filling (Peak E, Peak A) • Aortic ejection time (AET)

Some of the functional and structural cardiac parameters were derived from the conventional measurements. For global LV systolic function, ejection fraction (EF) and fractional shortening (FS) are the most commonly used derived parameters [243]. EF (%) is a measurement, expressed as a percentage, of how much blood the left ventricle pumps out with each contraction. FS (%) is calculated by measuring the percentage change in left ventricular diameter during systole. Both parameters are derived from LV dimensions measured in M-mode [245]. EF (%) was calculated according to the formula: EF (%) = $[(LVID_d^3 – LVID_s^3)/ LVID_d^3]x100$ and FS (%) = $[(LVID_d – LVID_s)/ LVID_d]x100$ [245].

LV mass is also a derived parameter and was calculated by the formula: LVmass (mg) = $1.05[(IVS+LVID+LVPW)^3- LVID^3)$ [245]. **Table 4** shows the typical values in mice. However, these values may vary according to animal strain, size, sex and health [242].

Table 4: Typical values of mice, adapted from the Vevo 2100 imaging system guidelines [242].

Value	**Mice**
Ejection fraction	55-85%
Fractional Shortening	30-50%
Left Ventricle mass	65-90mg
Stroke volume	40-70 ul
Cardiac output	20-35mL/minute

Figure 14: Researcher working on the Vivo 2100 echocardiography machine at the HATTER Institute of Cardiovascular Research in Africa

Section 2: Molecular changes during pregnancy and postpartum in wild type mice (C57/Bl6)

2.1 Euthanasia and tissue sampling

Mice were euthanized with a high toxic dose intraperitoneal injection (IP) of sodium pentobarbitone (200mg/kg body mass) (Kyron Laboratories (PTY) LTD, Benrose, South Africa). The drug was diluted in saline solution. Once deeply anaesthetized, about 800µl of blood was drawn by cardiac puncture (directly from the heart). The chests were then opened to expose the heart. Whilst the heart was still beating, saturated solution of potassium chloride (1M KCl) was then injected into the heart muscle until the heart was arrested at diastole. The hearts were then excised, trimmed of connective tissue and weighed. Lung weight and tibia length were also recorded.

The apex of the hearts was cut and divided into four equal parts then immediately snap frozen in liquid nitrogen. The other sections of the hearts which contain the base were fixed in 4% paraformaldehyde (weight per volume) in phosphate buffer saline 1X for at least two days before transferring them to 70% ethanol until processing for histology.

2.2 Serum preparation and enzyme-linked immunosorbent assay (ELISA) determination of hormones level

To obtain serum mouse blood was collected in sterile empty tubes without anticoagulant. The blood was left to stand for more than 30 minutes, then centrifuged at 8000rpm for 5 minutes. The serum was then pipetted out with a sterile Pasteur pipette into a new 1.5 tube and stored at -80^{o}C until the day of experiments.

Progesterone and oestrogen levels in pregnant and postpartum mice were measured using progesterone Elisa kit (Enzo cat #ADI-900-011) and 17β-estradiol Elisa kit (Enzo cat #ADI-900-011) according to the manufacturer's instructions. Plates were read by Modulus microplate reader at 450nm wavelength. The results were calculated by first calculating the average net Optical Density (OD) bound for each standard and sample by subtracting the average non-specific binding OD (NSB OD) from the average OD bound (average net OD=average OD-NSB OD). Secondly the binding of each pair of standard wells was calculated as a percentage of the maximum binding wells (B0) (percent Bound=net OD/Net B0 OD X 100)

2.3 Analysis workflow of cardiac tissue and blood samples

Snap frozen hearts sections were transferred from liquid nitrogen into -80°C freezer. The samples were stored without thawing until protein and RNA extraction. **Figure 15** summarizes the experiments that were conducted to further characterize the molecular changes that occur during pregnancy and postpartum at specific time points.

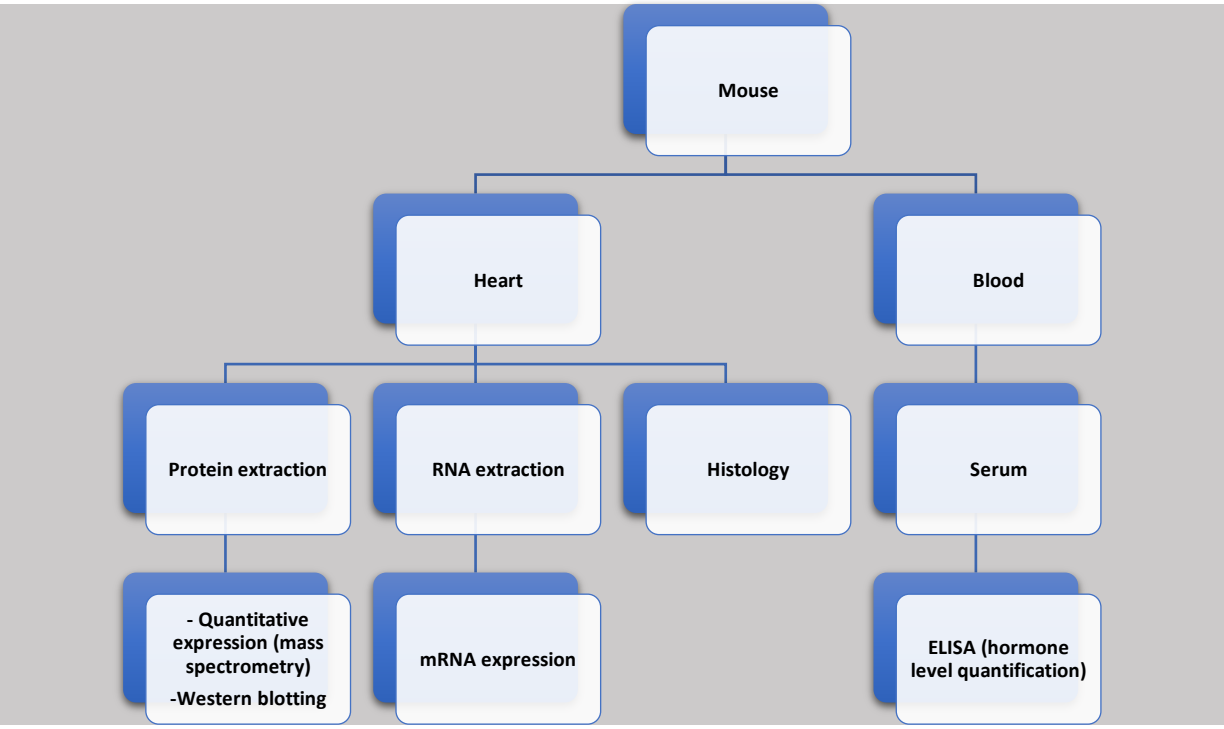

Figure 15: Analysis workflow of cardiac tissue and blood samples

After echocardiography assessment, mice hearts and blood were collected. The hearts were cut into two cross-sections. The apex for protein and RNA extraction, and the base for histology. The blood was collected for serum preparation which was used to quantify the hormones quantification by ELISA (enzyme linked immunoassay).

2.4 Protein extraction

Approximately 20 mg of snap frozen hearts tissue were pulverized by hammering the tissue rapped on aluminium foil and frozen in liquid nitrogen. The powdered hearts tissue were then added into vials containing 100µl of X1 RIPA buffer (50mM Tris HCl pH 7.4, 150 mM NaCl, 0.5% (w/v) Sodium Deoxycholate, 1.0 mM EDTA, 0.1% (w/v) SDS). Immediately, 1µl of protease inhibitor cocktail (10µg/ml leupeptin and 10µg/ml aprotinin at a concentration of 10µg per 10 ml) (Roche, SA) was added. The mixtures were then vortexed and sonicated for 1minute pulsating for 10 seconds after every 10 seconds until a homogenous mix was achieved. To digest DNA, 1µl of benzonase endonuclease was added. The samples were then incubated for

1 hour at 4^{o}C with vortexing after every 15 minutes before centrifuging at 13000 rpm for 20 minutes.

2.5 Protein concentration determination

The determination of protein concentration for Western blots by was done either by the Lowry Method (**Appendix 2**). Bicinchoninic acid (BCA) assay was used to confirm protein concentration before mass spectrometry according to standard operation procedure in (**Appendix 3**). To summarize the Lowry method, 1 ml of dH_2O was added to each 15 ml Eppendorf, followed by either different volumes of BSA to make the standard curve or 5µl of the protein samples. Then 1ml of solution A (equal volumes of CTC reagents, 10% SDS and 0.002% NaOH) was added. The mixtures were vortexed and incubated for 10 minutes at room temperature. Then 0.5ml of solution B were mixed in equal volumes to form solution A. 0.5ml of solution B (0.2% Folin) was then added before another incubation for 30 minutes. The samples were then loaded into a 96 well plate and absorbance was measured at 750nm wavelength (Modulus Microplate reader, Agilent, USA).

Section 3: Discovery mass spectrometry by Q-exactive Liquid Chromatograph Mass spectrometry (LC MS/MS)

Figure 16 provides an overview of the fundamental steps in label-free quantitative proteomics. These includes: (i) sample preparation including protein extraction, reduction, alkylation, and digestion; (ii) sample separation by liquid chromatography (LC or LC/LC) and analysis by MS/MS; (iii) data analysis including peptide/protein identification, quantification, and statistical analysis [246].

To acquire data on the mass spectrometer data dependent acquisition (DDA) mode was employed. In DDA mode, the mass spectrometer selects the most intense peptide ions in the first stage of tandem mass spectrometry, and then they are fragmented and analysed in a second stage of tandem mass spectrometry [247]. The relative quantification by peak intensity method was used. It has been observed that signal intensity from electrospray ionisation (ESI) correlates with ion concentration [246][248].

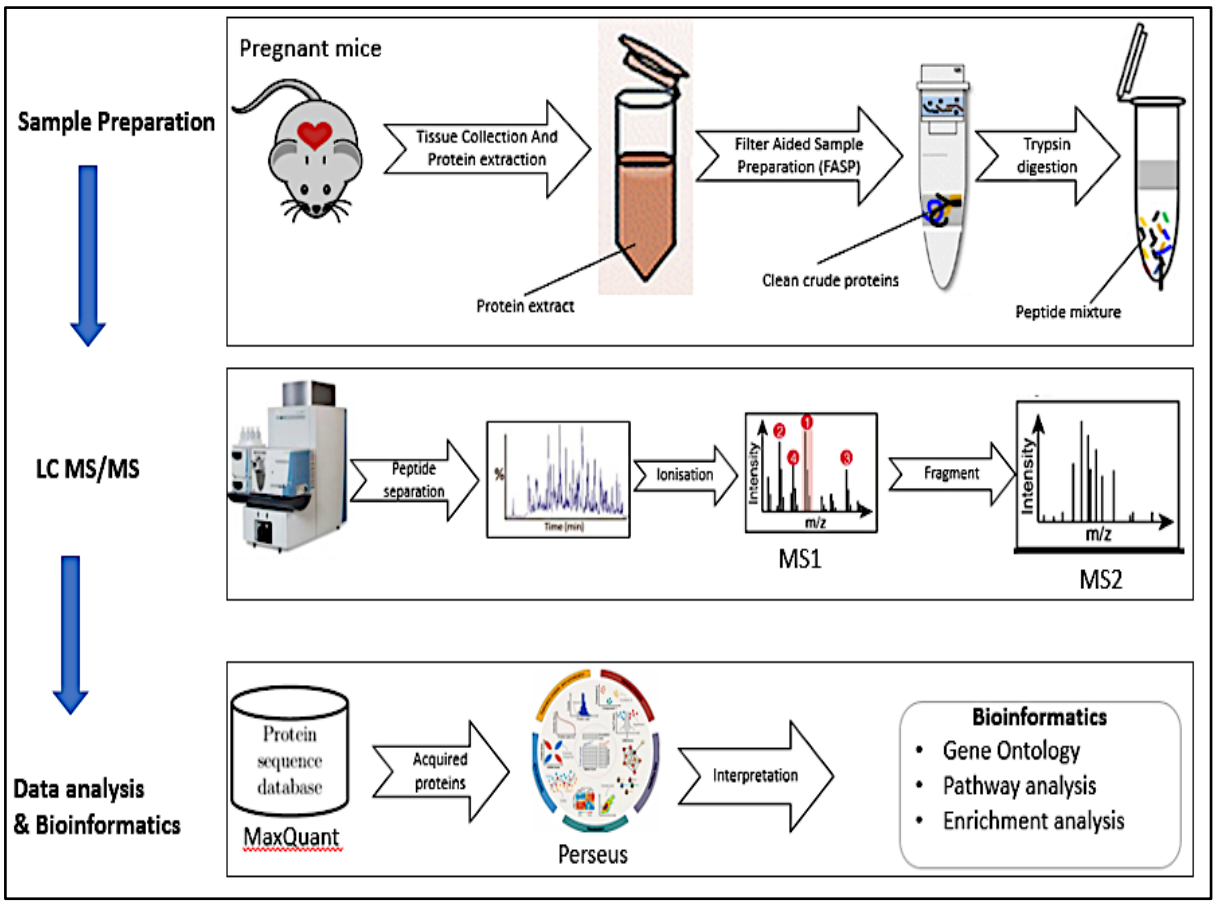

Figure 16: MS-based bottom-up proteomic experiment workflow

Initially the heart was extracted from the mouse heart, pulverized and lysed to obtain protein extract. The extract was reduced and alkylated before digested by trypsin. The digested peptides were then separated by LC and then analysed by a Q-exactive mass analyser. Protein search was done using MaxQuant, Statistics and Data visualisation was conducted by Perseus software. Bioinformatic was performed by Panther, String bd and Expression 2 Kinases softwares.

3.1 Sample Preparation (FASP) of tryptic digests

The purpose of FASP is to generate tryptic peptides from crude lysates for LC-MS analysis. It involves the reduction of cysteine bonds using dithiothreitol (DTT), denaturation of proteins using urea (UA), alkylation of cysteine residues with iodoacetamide (IAA), and digestion of proteins using trypsin.

For each sample, 100 µg of total proteins were incubated at 95°C for 3 minutes in the presence of 0.1M dithiothreitol (DTT) to reduce cysteine bonds. The reduce peptides were then loaded into molecular weight cut-off (MWCO) (UFC503096 - 30K FASP filters 500ul (Amicon Ultra centrifugal filter units 30 KDa pore size, 96 PK). Capacity of 0.2-200µg of peptides. Then goes through a stage of denaturation by AU and alkylation by IAA.

The proteins were eventually digested by trypsin (Trypsin-ultra, Mass Spectrometry Grade. New England Biolabs), at a final concentration of 0.5µg/µl for 12 hrs at 37^{o}C. **Appendix 4** outlines the SOP for FASP.

3.2 C18 desalting of tryptic peptides

The purpose of this process is to remove salts and dissolving the peptides in a buffer suitable for direct MS. Inhouse C18 stage tips were prepared using 200µl pipette tips and C18 SPE extraction disks (Empore Octadecyl C18 Extraction disks 2215, 20 PK, 47mm, Supelco, Sigma-Aldrich). The stage tips were activated by 80% acetonitrile (ACN), 0.1% formic acid (FA), equilibrated with 2% ACN, 0.1% FA and then eluted with 60% ACN, 0.1% FA in glass inserts. The samples were dried up in a speedVac concentrator and stored at -20^{o}C until the day of use.

3.3 LC MS/MS analysis

Samples were resuspended in 2% ACN, 0.1% FA to a final concentration of 200 ng/µl immediately prior to LC MS/MS analysis. Samples were separated by UHPLC inline on a Thermo Dionex Ultimate 3000 instrument prior to mass spectrometry. An autosampler injected 600ng of peptide for each sample onto an in-house packed 2cm C18 trap (100 µm ID, packed with Phenomenex Luna 100 Å hollow core beads) and washed at a flow rate of 5µl/minute with loading solvent A (2% ACN, 0.1% formic acid). The trap was switched in-line to an in-house packed 30cm analytical column (75 µm ID, packed with Phenomenex Aeiris peptide C18 3.6µm solid core beads) and the peptides were separated from 6% solvent B (100% ACN, 0.1% formic acid) in solvent A (100% water, 0.1% formic acid) to 30% B over 30 minutes at a flow rate of 0.4µl/minute. Peptides eluted directly into a Thermo QExactive hybrid orbitrap mass spectrometer.

The QExactive acquired spectra in data dependent (Top10) mode, with an MS1 resolution of 70 000 and an MS2 resolution of 17 500. MS1 scans were acquired with an AGC target of 3e6 or an IT of 250ms. MS2 scans were acquired with an AGC target of 1e6 or an IT of 80ms. Dynamic exclusion was set to 30 seconds, approximately half the average chromatographic peak width.

3.4 Data processing

Raw data were analysed using MaxQuant version 1.6.17.0 with default settings for the QExactive instrument. Match between runs was off and (label free quantification) LFQ was used for protein-level label free quantitative comparison.

3.5 Statistical analysis

Data were analysed using Perseus version 1.6.14.0. Briefly, raw LFQ data were filtered to remove reverse hit and contaminants, as well as proteins only identified by site. Data were median normalized, log2 transformed and valid values were filtered so that a minimum of 70% of each experimental group had valid (non-0) values. Groups were compared by One-way Anova, with a p value < 0.05 considered statistically significant. Post-hoc multiple testing correction (FDR) was applied. Significant proteins were then analysed using String-db 11 [249] to determine functional associations between the significant proteins, and enrichment analysis was performed to determine if any GO category/term or KEGG pathway was enriched. Identified, gene lists were fed into the transcription factor inference module of X2K using the tool and database ChIP-seq/chip Enrichment Analysis (ChEA) to obtain a list of transcription factors that are the likely upstream regulators of the identified differentially expressed gene set [250][251].

Section 4: Western Blotting

4.1 Sample preparation

80µg of protein lysates were then prepared for western blot by mixing with 1x sample buffer (0.125 M Tris, pH 6.8, 4% SDS, 20% glycerol) containing 4% β-mercaptoethanol. The samples were boiled on a heating block for 5 minutes at 95^{o}C. The samples were then centrifuged for 5 minutes at > 8000rpm to bring all the drops down before loading.

4.2 Sodium dodecyl sulfate–polyacrylamide gel electrophoresis (SDS-PAGE)

Western blot resolving and stacking gels were prepared and run according to the procedure in **Appendix 5. Appendix 6** provides information on loading of samples and western blot buffers.

4.3 Transfer/ Blotting to membrane

The resolved proteins were transferred from the gel to polyvinylidene fluoride (PVDF) membranes (Millipore). The membranes were initially activated by methanol for 5 minutes and then transferred to transfer buffer for 15 minutes before making the sandwich. Transfer was done at 0.02A overnight.

The membranes were then placed in methanol for 30 seconds and air dried. Before probing with the antibodies, the membranes were incubated for 2 minutes in Ponceau S Staining Solution (0.1% (w/v) Ponceau S in 5%(v/v) acetic acid).

4.4 Specific binding of proteins

Membranes were blocked in 5% fat free milk – 1x PBS for 60 minutes before probing with primary antibodies (1^{o} Ab) which were diluted with wash buffer (TBS + tween 20) to a ratio of 1: 1000. Incubation with 1^{o} Ab was done overnight at 4^{o}C. The membranes were then washed before incubation with specific secondary antibodies (2^{o} Ab). The blots were developed using Western Blot Chemiluminescence Reagent Plus (PerkinElmer, Boston, MA).

Table 5: Western Blot antibodies and dilutions

Antibody	Dilution	Supplier
AKT 1	1:1000	(Cat#CST2920S) Cell signalling
p-AKT^{ser473}	1:1000	(Cat# CST9018S) Cell signalling
Stat 5	1:1000	(Cat#CST94205S) Cell signalling
p-Stat 5^{Tyr694}	1:1000	(Cat# CST4322S) Cell signalling
Stat 3	1:1000	(Cat#MA1-13042) Invitrogen
p-Stat 3^{Tyr705}	1:1000	(Cat#9135) Cell signalling
GAPDH	1:1000	(Cat# AM4300) Invitrogen

Section 5: RNA isolation and quantification

Total RNA was extracted from the heart tissue using the Qiagen fibrous tissue RNA extraction kit (Qiagen, USA Cat 74704) according to manufacturer's instruction. **Figure 17** summarizes the workflow. In brief, the mice heart tissues were pulverized in liquid nitrogen, added to the lysis buffer which contained 14.3 M β-mercaptoethanol (β-ME) and homogenized. Proteins in the lysate were then digested with proteinase K enzyme at 55°C. The RNA was then washed and eluted.

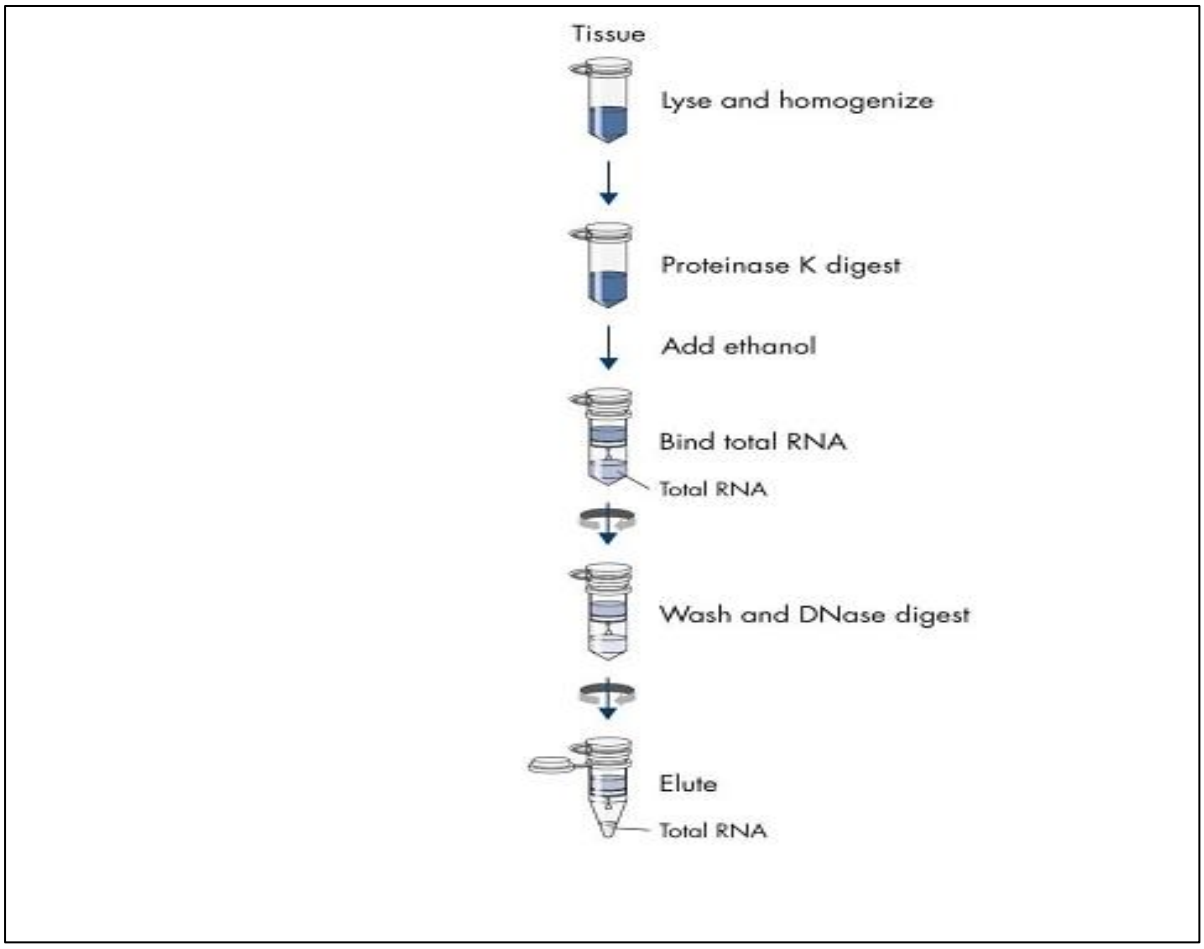

Figure 17: Total RNA extraction from fibrous tissue workflow

(Adapted from RNeasy Fibrous Tissue Mini Handbook)

RNA concentration was determined using the Nano drop (Thermo Scientific, 2000c spectrophotometer). The RNA was immediately stored at -80°C until synthesis of complementary DNA (cDNA).

cDNA was synthesized using FG RNA to cDNA kit (Applied Biosystems by Thermofisher Scientific, Life Technologies, Foster City, CA 94404, USA). Reverse transcription (RT) was

carried out at 42°C for 30 minutes followed by incubation at 95°C for 5 minutes. Amplification was carried out under the temperature profile: 94°C for 30 s; 55°C for 30 s; and 72°C for 1 minute. After 35 cycles, final amplification was carried out for 7 minutes. The concentration of cDNA was determined before diluting the cDNA to a concentration of 10ng /µl.

The resulting cDNA was analysed by quantitative real-time PCR (qPCR) using Rotor Gene 6000 (Corbett Research, United Kingdom). The FG, Syber green PCR Master Mix (Applied biosystems, Cat 4367659) was used according to the **Table 6.** Ten nanograms of each cDNA were used for qPCR to determine the level of expression of different genes.

Table 6: Reverse Transcription-PCR using FG, Syber green PCR Master Mix

Reagent	**Volume**
FG, Syber green PCR master mix	12.5 µl
qPCR primer assay	1 µl
RNAse-free water	10.5 µl
Total volume per reaction	24 µl

Table 7: qPCR Primers

Gene	**Forward primer**	**Reverse primer**
β-MHC	ATCAAGGGAAAGCAGGAAGC	CCTTGTCTACAGGTGCATCA
ANP	TGCCGGTAGAAGATGAGGTC	CGGTGACTCTCCACCACTTA
BNP	CAGAAGCTGCTGGAGCTGATAAG	TGTAGGGCCTTGGTCCTTTG
GDF-15	ATACTCAGTCCAGAGGTGAGAT	ATGCAGGCGTGCTTTGATCTG
Collagen 1	AAGACATCCCTGAAGTCAGC	CCTATGACTTCTGCGTCTGG
Collagen 3	ACAGCAGTCCAATGTAGATG	GAGCAGGTGTAGAAGGCTG
GAPDH	ACCACAGTCCATGCCATCAC	TCCACCACCCTGTTGCTGTA

Glyceraldehyde 3-phosphate dehydrogenase (GAPDH) was used as an endogenous control. No reverse transcriptase and no template controls were used to monitor for any

contaminating amplification. The $2^{-\Delta\Delta Ct}$ was used for both statistical analysis and data presentation (Livak & Schmittgen, 2001)[252].

Section 6: Histological changes during pregnancy and postpartum in wild type mice (C57/BL6)

6.1 Tissue processing

The fixed hearts were placed into embedding cassettes for tissue processing. The tissue processing procedure was divided into 3 steps: dehydration with a series of alcohols, clearing with xylene and infiltration with paraffin wax. Dehydration with a series of different alcohol concentrations removes all the water in the tissue. Due to alcohol not mixing with water, the clearing step replaces the alcohol with xylene, which can mix and be replaced with paraffin wax during the infiltration steps. Infiltration with paraffin wax allows for further preservation and easy sectioning into microscopically thin sections once embedded. The tissue was processed with an automated processor (Leica TP120 Tissue Processor) and Paraplast wax (Sigma-Aldrich, A6330-4LB, SA) was used for infiltration. The processing protocol is indicated in **Appendix 7**.

6.2 Sectioning

Two hrs prior to sectioning, the tissue blocks were placed in a freezer to cool and harden the wax. This improves sectioning. The tissue blocks were then trimmed and sectioned using a Leica RM 2125 RT microtome to obtain uniform 5µm sections. The sections were placed briefly in 70% ethanol and then into water at a temperature of approximately 40°C. This allows the tissue to stretch out before being mounted onto a glass slide. Tissue sections were then picked up from the water bath with a glass slide at an angle, to prevent the formation of bubbles between the tissue and the glass slide, which interfere with staining.

6.3 Haematoxylin and eosin staining

The standard H&E staining method does not stain specific structures or differentiate between different cells within tissue but allows for the visualisation of all the cells that make up a tissue. Haematoxylin and eosin are two different dyes; haematoxylin being basic and staining acidic components of a cells, while eosin is acidic and stains basic cellular components. When animal cells are stained with H&E, the nucleus of the cell is stained blue by haematoxylin and the cytoplasm is stained pink by eosin. Sections stained with H&E allow for the evaluation of

gross morphological characterisation of tissue. In some cases, different cell types may be apparent if some cells stain lighter than others.

Slides were placed on a hot surface (65^{o}C) for 2 minutes to melt the wax off the tissue. H&E staining was conducted following the procedure in **Appendix 8**. Imaging of the H&E was captured by Carl Zeiss upright microscope at X20 and X40 magnification.

6.4 Pico sirus red staining for collagen determination

Sections were dewaxed by washing 2X in xylene for 2 minutes each. Followed by dehydration in a series of ethanol 100% and 50% for three minutes. The sections were then rehydrated by washing 3X in deionized water before staining. Staining was done with 0.1% Sirius red in picric acid (Sigma Aldrich, South Africa) for one hour. Rinsing of stained slides was done in 0.5% (2.5ml acetic acid in 500ml water)- for two minutes thrice. The slides were then washed in a series of alcohol 95% alcohol, then 100% alcohol 2 minutes each to ensure proper dehydration before fixation. Fixation was done by washing the slides in xylene twice for 2 minutes each. Coverslips were then mounted with Eukitt mounting medium (O.Kindler, Germany).

Five focus fields were examined with a Nikon Eclipse 90i microscope using a X20 objective. Images were captured with the NIS-Elements Basic Research software (Nikon, Instech Co. Ltd, Japan) and quantified with the Image J version 1.52K software (NIH, USA). Cardiac interstitial fibrosis was expressed as percentage collagen deposition per total area sectioned.

Section 7: Cell culture

7.1 Maintenance of H9C2 cell line

H9C2 cardiomyocytes is a well-studied murine cell line derived from embryonic myocardium rat hearts. These cells were cultured in DMEM containing 10% fetal bovine serum (FBS), 100 units/l penicillin and streptomycin (1% pen/strep), for 48 hrs before passaging. Cells were incubated in a humidified atmosphere of 95% air and 5% CO_2 at 37°C up until 60-70% confluence. Treatments were conducted to cells at passage 18-23. All the treatments were done in triplicates and the experiments were repeated three times.

7.2 Cell treatment

Cells were grown on coverslips in 12 well plates to 60–70% confluency. 12 hrs prior to treatments, the cells were serum deprived by changing FBS concentration from 10% to 2%. Treatments included control, 50µM isoproterenol, 30nM of 17β-estradiol (E2), 30nM of progesterone and cotreatment with a combination of the drugs for 24 hrs. The coverslips were then fixed with 4% paraformaldehyde for 10 minutes following a thorough wash with 1% sterile phosphate buffered saline (PBS). This was followed by immunofluorescence staining for cell morphology measurements.

7.3 Actin immunofluorescence staining

H9C2 cells fixed with 4% paraformaldehyde were permeabilized with 0.5% Triton X-100 for 10 minutes, washed with 1% PBS and blocked with 5% BSA in PBS for 1h. Staining was done using phalloidin-Alexa-conjugated antibody (Alexa 488) for 1h in the dark. The antibody was diluted in 5% BSA in the ratio (1:500). After incubation with phalloidin the coverslips were washed with 1X PBS with agitation for 5 minutes each wash. The coverslips were then mounted on glass slides using Vectashield mounting media which also contain Dapi for nuclear staining.

7.4 Imaging and cell morphology measurements

Nine random fields were captured with a Zeiss Axiovert Fluorescence Microscope (AxioVision version 4.8.2) at X20 magnification. Dapi, phalloidin and merged images were saved for morphology measurements with Image J version 1.52K (NIH, USA). The cells' length and width were measured and analysed separately.

Section 8: Peripartum cardiomyopathy patients and Human Healthy Controls

8.1 Study design and patient enrolment

This study was approved by the Human Research Ethics Committee of the University of Cape Town, Cape Town, SA (R033/ 2013) and complies with the Declaration of Helsinki. All patients and controls gave written informed consent before study entry. Thirty-nine PPCM patients and 63 healthy control (HC) pregnant mothers were enrolled consecutively at Groote Schuur Hospital (University of Cape Town, SA). The HCs were recruited from the second trimester, third trimester and at 3 time points postpartum (1-4 weeks; 1-3 months and 4-6 months).

Inclusion criteria for the PPCM patients were age >16 and < 40, symptoms of congestive heart failure that developed in the last month of pregnancy or during the first 5 months post-partum without other identifiable cause for heart failure and left ventricular ejection fraction (LVEF) <45% measured by transthoracic echocardiography. Clinical assessment and evaluation of the New York Heart Association Functional Classification (NYHA FC) of each patient was done by experienced physicians.

HC in the same age group were recruited if the participants had no signs of heart failure and have ejection fraction >50% assessed by echocardiography.

8.2 Human echocardiography

Two-dimensional targeted M-mode echocardiography with doppler colour flow mapping was performed using a Hewlett Packard Sonos 5500 (Philips, Bothell, WA, USA) echocardiograph attached to a 2.5 or 3.5 MHz transducer. All studies were performed and interpreted by the same operator who was unaware of the other parameters investigated. LV dimensions were measured according to the American Society of Echocardiography Guidelines [253]. Measurements of LV dimensions and function were determined on an average of >3 beats.

CHAPTER 4

Assessment of cardiovascular changes that occur in healthy pregnant wild type mice (C57/BL6) during gestation and postpartum

1.1 Introduction

Model systems of heart disease and physiology have provided important insights of the pathogenesis, progression, and mechanisms underlying cardiovascular disease. However, skepticism about inability of animal models of pregnancy to recapitulate human cardiac phenotypes have been voiced [254][255][256]. Whilst none of the animal models exactly mirrors human pregnancy [257][258], mice and rats are by far the most popular models. Mice and rats offer practical advantages including relatively low costs, an easy maintenance, a long tradition in scientific research and the hemotrichorial labyrinth placenta type [254]. Cardiac performance and anatomical changes in mouse and rat models can also be easily monitored by ultrasound echocardiography with rigor and reproducibility.

Regardless of several reports on maternal cardiovascular adaptions during pregnancy, there are contradictory lines of evidence about maternal hemodynamics, heart structural changes and left ventricular (LV) performance [259][260]. Data reported on the enlargement of chamber size, LV wall thickness and mass are inconsistent [60][261][262]. Debateable results were also published on myocardial systolic function parameters, including ejection fraction (EF) and fractional shortening with studies reporting either increase, decrease or constant change [72][263][264].

Increased volume load and hormonal changes that occur during pregnancy induce complex cardiovascular modifications including cardiac hypertrophy [265][266]. Cardiac hypertrophy that occur during uncomplicated pregnancy is an important adaptive response to increased heart workload and holds a key role in cardiac remodeling [60][267][26]. Physiological hypertrophy induced by pregnancy is characterized by increase in cardiac mass and cardiomyocyte dimension, normal or enhanced contractile function coupled with normal architecture and organization of cardiac structure [59][88].

Pregnancy hormones holds a vital role in the maintenance of physiological cardiovascular function [268][269][270]. Invitro and animal studies supports the anti-hypertrophic effect of oestrogen [188][271][272]. Studies have also shown the role of increased levels of progesterone in inducing cardiac hypertrophy in early pregnancy via the activation of calcineurin [26][267].

The heart also express natriuretic hormones and peptide growth factors/cytokines such as growth differentiation-15 (GDF-15) which may function as an endogenous regulator of cardiac hypertrophy [273][234]. The fetal gene program is one of the most consistent markers of pathological cardiac hypertrophy, and genes within this group include brain natriuretic peptide (BNP), atrial natriuretic peptide (ANP), β-myosin heavy chain (β-MHC) [274][275][276][277].

The phosphatidylinositol-3-kinase (PI3K)-Akt- ERK1/2-ribosomal protein S6 kinase (p70S6K) pathway and janise activated kinases- signal transducer and activator of transcription (JAK/STAT) are some of the key pathways involved in pregnancy induced cardiac hypertrophy [278][279][108][107]. However, limited number of studies have investigated the molecular changes involved in the postpartum phase.

The pathogenesis of PPCM is closely tied to the cardiac modifications that accompany normal pregnancies [189]. It is of clinical importance therefore to understand the structural, molecular and functional cardiovascular changes that occur during pregnancy

We assessed the morphological, functional and histological changes of the heart induced by physiological pregnancy in healthy wild type mice (C57/Bl6). We also evaluated fibrosis and investigated the signaling pathways involved in regulation of physiological hypertrophy during pregnancy and postpartum in healthy mice. Furthermore, we employed proteomics method to describe the molecular cardiovascular changes that takes place during pregnancy and the reversal postpartum.

1.2 Material and Methods

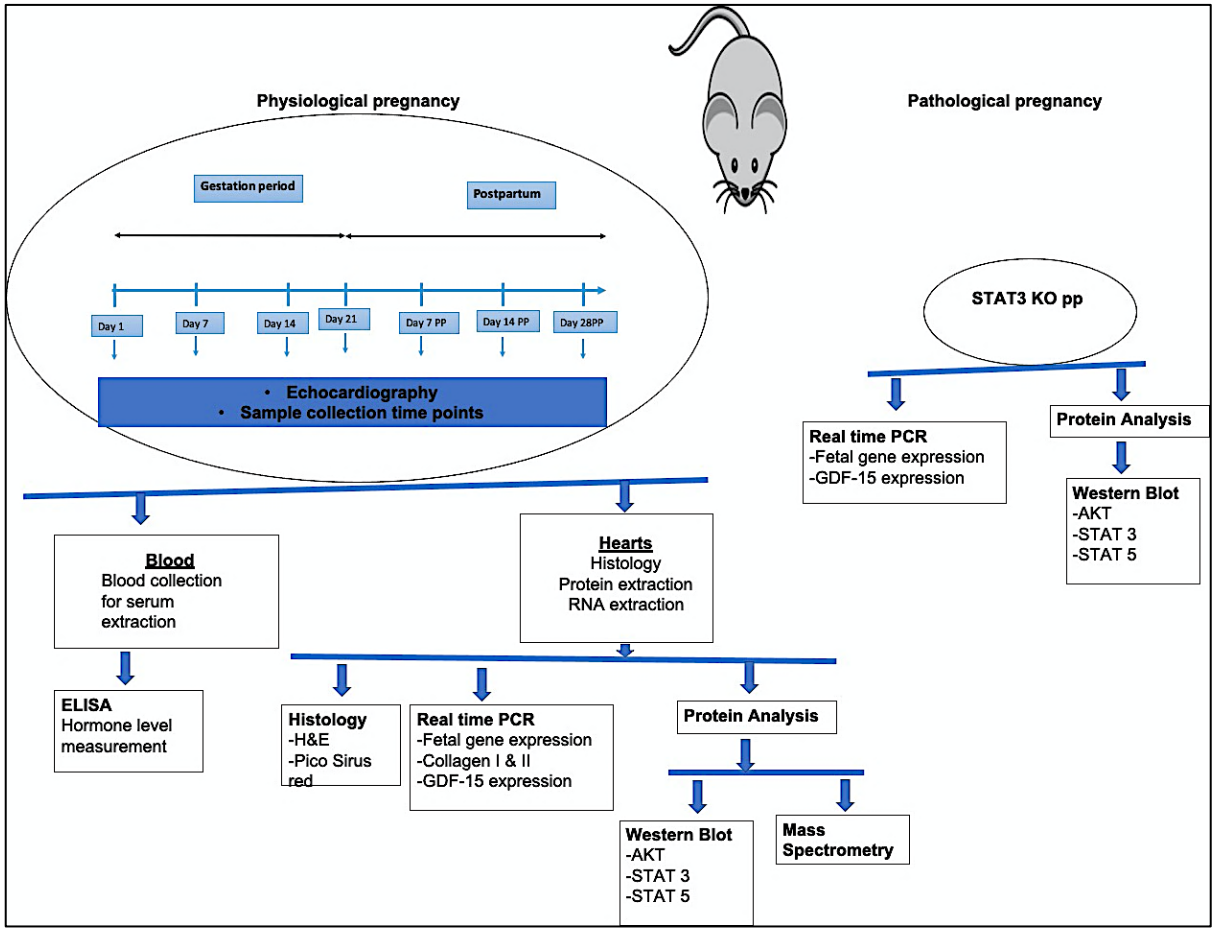

Figure 18: Experimental protocol for assessment of cardiovascular structure, morphology, function and molecular changes in pregnant mice

Echocardiography measurements were performed on the day of sacrifice. Hearts were harvested for histology, protein extraction and RNA extraction. Blood samples were collected for hormone level determination. STAT3 KO mice were included as a pathological group. Sample size was greater than 6 mice per group. Real time PCR and western blots were repeated 3 times.

1.3 Data Analysis and Statistics

Descriptive data are shown as means ± standard error (SE). Independent ANOVA was used to compare data between pregnant groups. Tukey post hoc was used to correct for multiple comparison. Statistical analysis and graphs were plotted using Graphpad Prism version 8.4.2 (San Diego, California). $P < 0.05$ was considered to indicate statistical significance.

1.4 Results

1.4.1 Echocardiograph left ventricular morphology and functional measurements in pregnant mice

Table 8: Left ventricular morphology and functional measurements in pregnant mice

Parameters	Gestation			Parturition	Postpartum		
	Day1 n= 8	Day 7 n= 8	Day 14 n = 9	Day 21 n = 9	Day 7pp n = 8	Day 14pp n = 8	Day 28pp n = 6
Stroke volume (SV) ul± SE	29.87± 1.36	30.95± 2.56	38.2± 2.43*	30.44± 2.98	37.96± 2.49*	37.99± 2.08*	45.75± 3.58**
BW(g)± SE	23.40± 0.66	27.00± 1.07	32.60± 1.28****	26.30± 1.01	30.50± 1.10***	30.70± 1.36***	30.50± 1.61***
HW (mg)± SE	103.97± 6.16	106.55± 9.43	113.47± 6.17	112.51± 3.67	132.95± 7.91*	134.78 ± 5.66**	121.63± 6.43
LV mass (mg) ±SE	61.34± 1.56	67.46± 6.33	87.92± 3.74*	68.46± 4.61	90.26± 10.16*	89.16± 5.46*	97.58± 7.81*
LW/TL	7.62± 0.32	8.87± 0.69	8.69± 0.31	8.96± 0.43	8.69± 0.69	9.51± 0.79	9.49± 0.77
LVAW (mm)±SE							
Diastole	0.78± 0.05	0.87± 0.05	0.84± 0.06	0.84± 0.06	0.87± 0.07	0.91± 0.04	0.88± 0.06
Systole	1.26± 0.14	1.32± 0.07	1.27± 0.08	1.31± 0.09	1.27± 0.12	1.40± 0.04	1.39± 0.10
LVPW (mm)± SE							
Diastole	0.70± 0.03	0.67± 0.04	0.78± 0.03	0.70± 0.05	0.78 ± 0.06	0.76 ± 0.05	0.81± 0.06
Systole	1.09± 0.06	1.08± 0.05	1.04± 0.09	1.11± 0.07	1.19± 0.13	1.17± 0.10	1.30 ± 0.08

Parameters	Gestation			Parturition	Postpartum		
	Day1 n= 8	Day 7 n= 8	Day 14 n = 9	Day 21 n = 9	Day 7pp n = 8	Day 14pp n = 8	Day 28pp n = 6
LVID (mm)±SE Diastole	3.40± 0.13	3.36± 0.16	3.72± 0.06**	3.28± 0.11	3.71± 0.14**	3.74± 0.12**	3.92± 0.17**
Systole	2.02± 0.13	2.28± 0.16	2.48± 0.06	1.98± 0.11	2.38± 0.14	2.55± 0.12	2.35± 0.17
LVEDV (ul)± SE	46.70± 3.93	47.40± 5.11	59.0± 2.34*	44.20± 3.54	59.50± 5.28	60.40± 4.55	61.30± 4.35
LVESV (ul)± SE	17.50± 2.94	17.70± 2.55	21.90± 1.36	13.70 ± 1.97	22.80± 4.08	23.70± 3.96	21.90± 5.50
LVID/LVPW Diastole	0.51± 0.05	0.52± 0.05	0.46± 0.03	0.51± 0.04	0.46± 0.05	0.44± 0.02	0.46± 0.03
EF % ±SE	67.60± 6.16	63.50± 2.16	62.50± 2.58	68.90± 3.51	62.60± 4.28	62.30± 4.82	68.80± 5.59
FS % ±SE	38.40± 5.58	33.70± 1.46	33.40± 1.92	38.30 ± 2.88	34.00± 3.34	33.80± 3.44	38.90± 4.41
E/A	1.50± 0.08	1.64± 0.11	1.41± 0.08	1.43± 0.05	1.46± 0.08	1.59± 0.17	1.54± 0.12
IVRT	17.55± 0.62	15.90± 1.24	16.90± 0.88	18.92± 1.44	17.49± 1.33	18.21± 0.96	20.85± 0.61
DT	16.16± 1.45	17.74± 2.68	17.64± 1.02	17.45± 0.85	17.19± 1.08	17.60± 1.82	19.04± 2.84

*Values are expressed as means ± SE. Mice were divided into 7 groups: Day 1_ non-pregnant; Day 7_7 days pregnant; Day 14_ 14 days pregnant; Day 21_parturition day; Day 7pp_7 days after parturition; Day 14pp_14 days after parturition; Day 28pp_28 days after parturition. Data were analysed by one-way ANOVA with Tukey's post hoc test. **** -p< 0.0001; ***-p<0.001; **-p<0.01; *-p<0.05 compared to Day 1. BW-body weight; HW-heart weight; TL-tibia length; LW-lung weight; LV- left ventricle; AW-anterior wall; PW-posterior wall; ID-internal diameter; EF-ejection fraction; FS-fractional shortening, E/A-transmitral E wave/A wave ratio; IVRT-isovolumetric relaxation time; DT-Mitral E wave deceleration time. The number of pups ranged between 3-10 pups. Embryos of pregnant mice were not counted.*

Body weight (BW) increased rapidly during pregnancy peaking at Day 14. BW was also higher in the postpartum mice compared to Day 1. Heart weight (HW) increased significantly in the

first two weeks postpartum (Day 7pp and Day 14pp) but not during pregnancy. LV mass increased by approximately 23.9% from Day 1 to Day 14 and this was sustained postpartum. Left ventricular end diastolic volume (LVEDV) increased gradually during pregnancy and was sustained postpartum ($p<0.01$). However, there was a significant decrease in LVEDV on Day 21 when compared to Day 14 ($p< 0.05$) and Day 7 pp ($p< 0.05$). No changes were observed on left ventricular anterior wall at diastole (LVAWd), left ventricular anterior wall at systole (LVAWs), left ventricular posterior wall at diastole (LVPWd) and left ventricular posterior wall at systole (LVPWs).

The assessed EF was normal throughout gestation and postpartum (>45%). However, a slight decrease in LVEF was observed on Day 14. Cardiac function seems to be slightly enhanced on the day of parturition. LV diastolic function was normal (E/A ratio> 1) throughout the study. No prolongation of isovolumetric relaxation (IVRT) and deceleration time was also maintained indicating that LV relaxation was not impaired.

1.4.2 Cardiac hypertrophy during pregnancy

Figure 19 shows heart weight normalized by tibia length (HW/TL) which is used as a marker of cardiac hypertrophy. HW/TL was significantly increased from Day 14 of pregnancy (> 20% increase; $p=0.01$ compared to Day 1). The hypertrophy remained elevated until Day 14pp. Slightly lower HW/TL ratio was observed on Day 28pp when compared to the other postpartum groups.

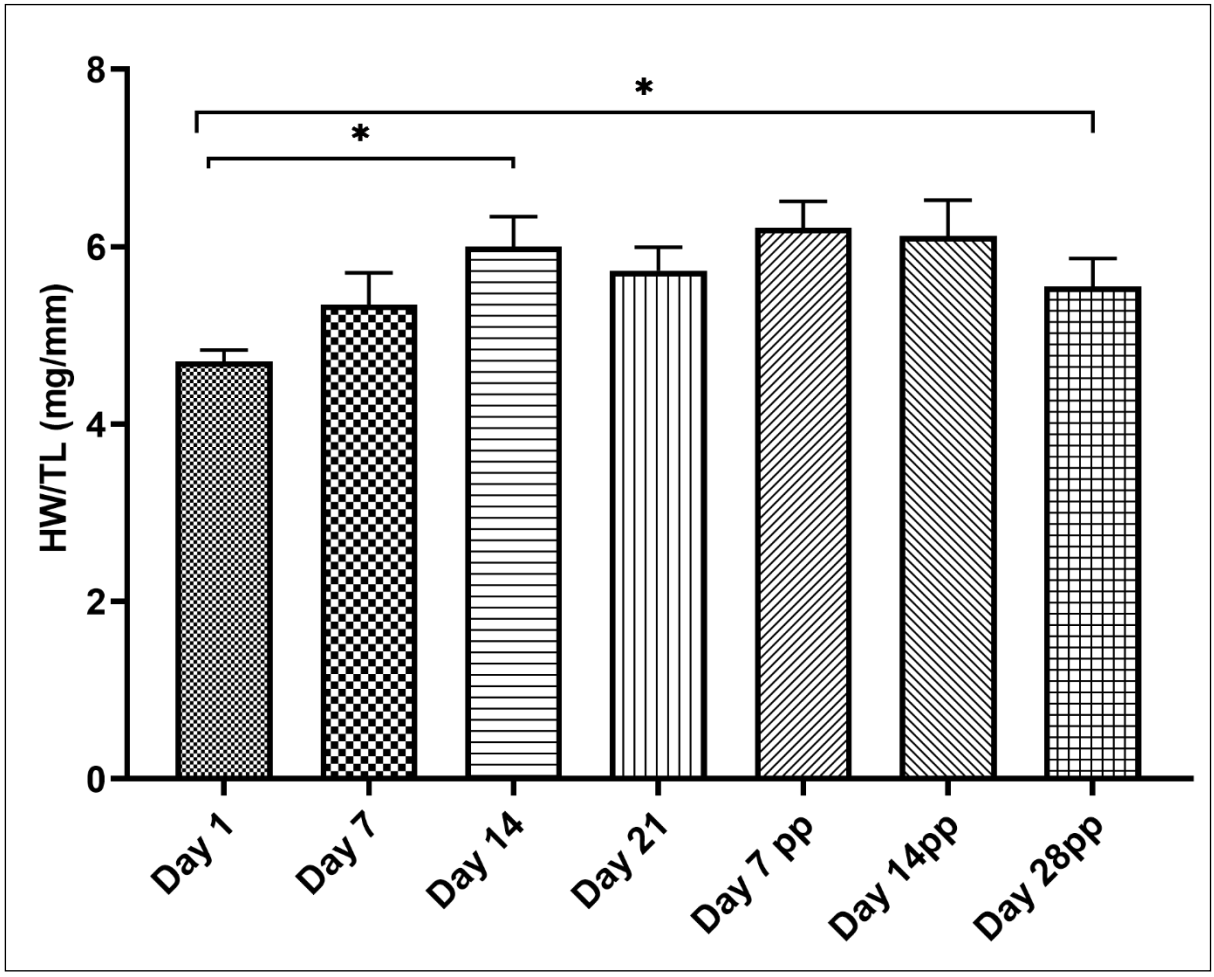

Figure 19: Heart weight (mg) to tibia length (mm) ratios for each group

*There was a significant increase in heart weight to tibia length (HW/TL) during pregnancy peak recorded at Day 14. This was maintained until 14 days after parturition. Until Day 28 postpartum the HW/TL had not reverted to non-pregnant level. n> 7 from Day 1-Day 14 pp and n=6 for Day 28 pp (pp-postpartum). *-P<0.05*

To confirm whether the pregnancy-induced cardiac hypertrophy was eccentric or concentric, we calculated relative wall thickness to ventricular diameter ratio (2x posterior wall/LV diameter at diastole) (**Table 8**). The relative wall thickness to ventricular diameter did not differ at any time point during pregnancy and postpartum. This indicate that the LV wall and chamber dimensional changes increased proportionally.

1.4.3 Hormone levels and the potential signaling pathways involved in the regulation of cardiac hypertrophy during pregnancy and postpartum in mice

Both progesterone and 17 β-oestradiol level increased rapidly during the gestation period peaking on Day 14. After parturition there was a steep decrease in both hormones, attaining

baseline level by Day 14 postpartum. From Day 7pp-Day 28pp, progesterone level was relatively constant and consistent among the mice (**Figure 20**).

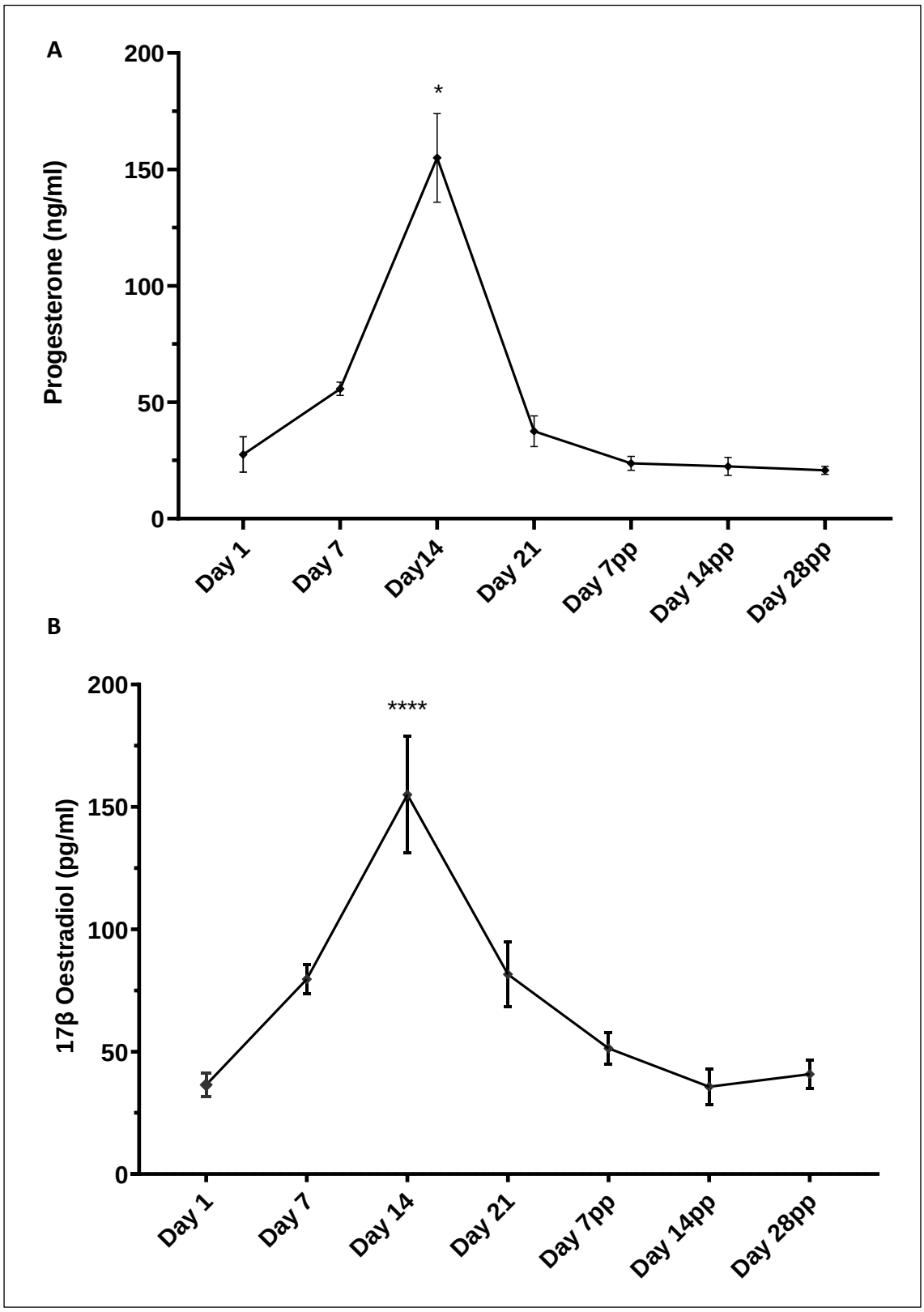

Figure 20: Oestrogen and progesterone level during pregnancy in mice

***A**: Serum progesterone levels increased gradually from Day 1 towards parturition. On the day of parturition there was an immediate drop to levels lower than 50ng/ml and continued to drop until Day 14 postpartum. **B**: The levels of oestrogen also followed a similar trend both*

*during pregnancy and postpartum. However, the drop was more gradual postpartum compared to progesterone graph. Four to seven serum samples were used per group. *-p<0.05; ***-p<0.001*

1.4.4 No cardiac fetal gene program induction during physiological pregnancy

No significant difference was observed in the expression of fetal genes (*ANP, BNP, β-MHC*) in physiological groups (**Figure 21-23**). However, mRNA expression of *BNP and β-MHC* was significantly raised in the STAT3 KO samples.

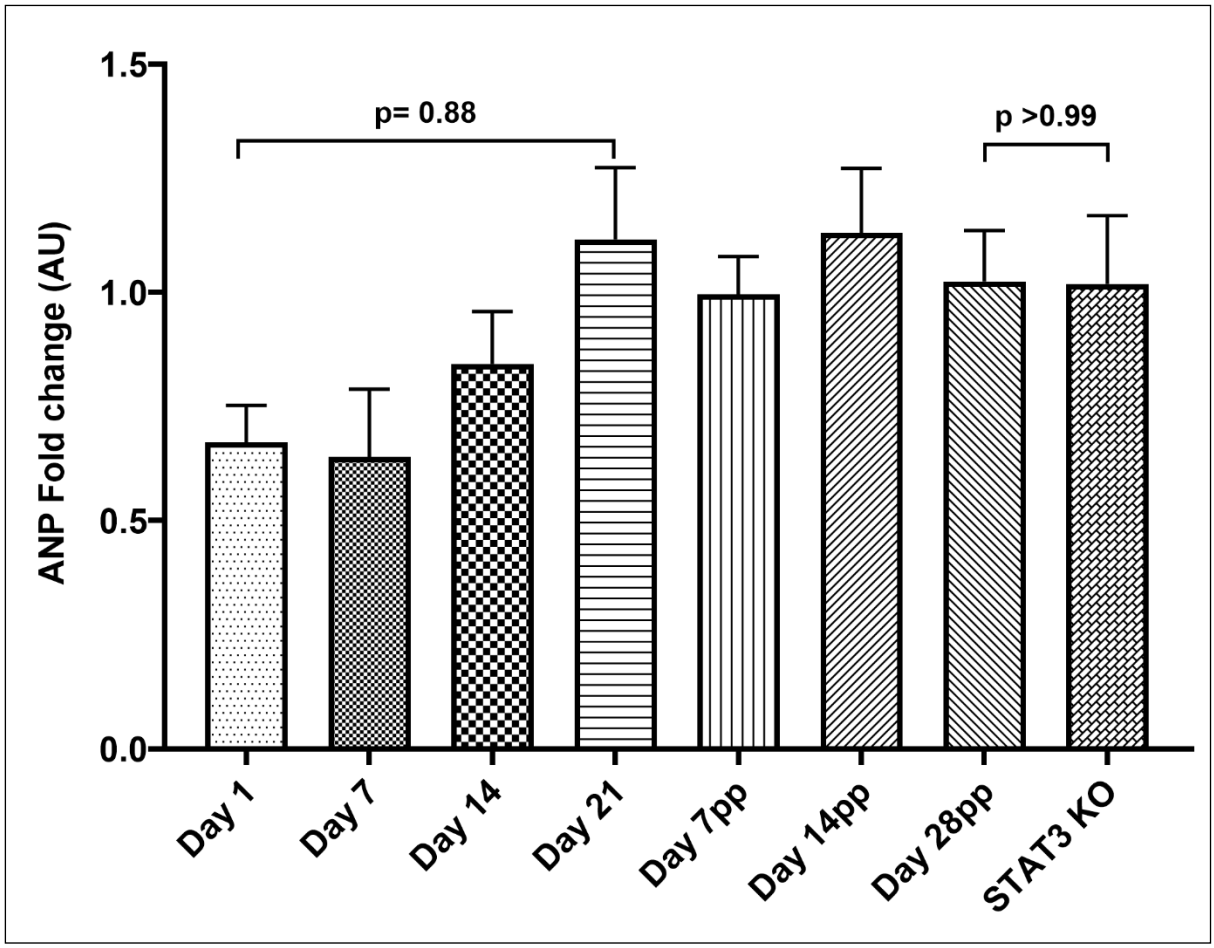

Figure 21: mRNA expression of Atrial Natriuretic Peptide gene in pregnant mice hearts

RT-qPCR was performed twice with 4–7 independent ventricular samples/group. Levels of the candidate gene was normalized to GAPDH. The bar graph displays fold change calculated using the Livak method $2^{-\Delta\Delta Ct}$ [252]*. Ct*-cycle threshold values; AU- arbitrary units. Ct values less than 15 and higher than 45 were considered invalid. ANP (Atrial Natriuretic Peptide).*

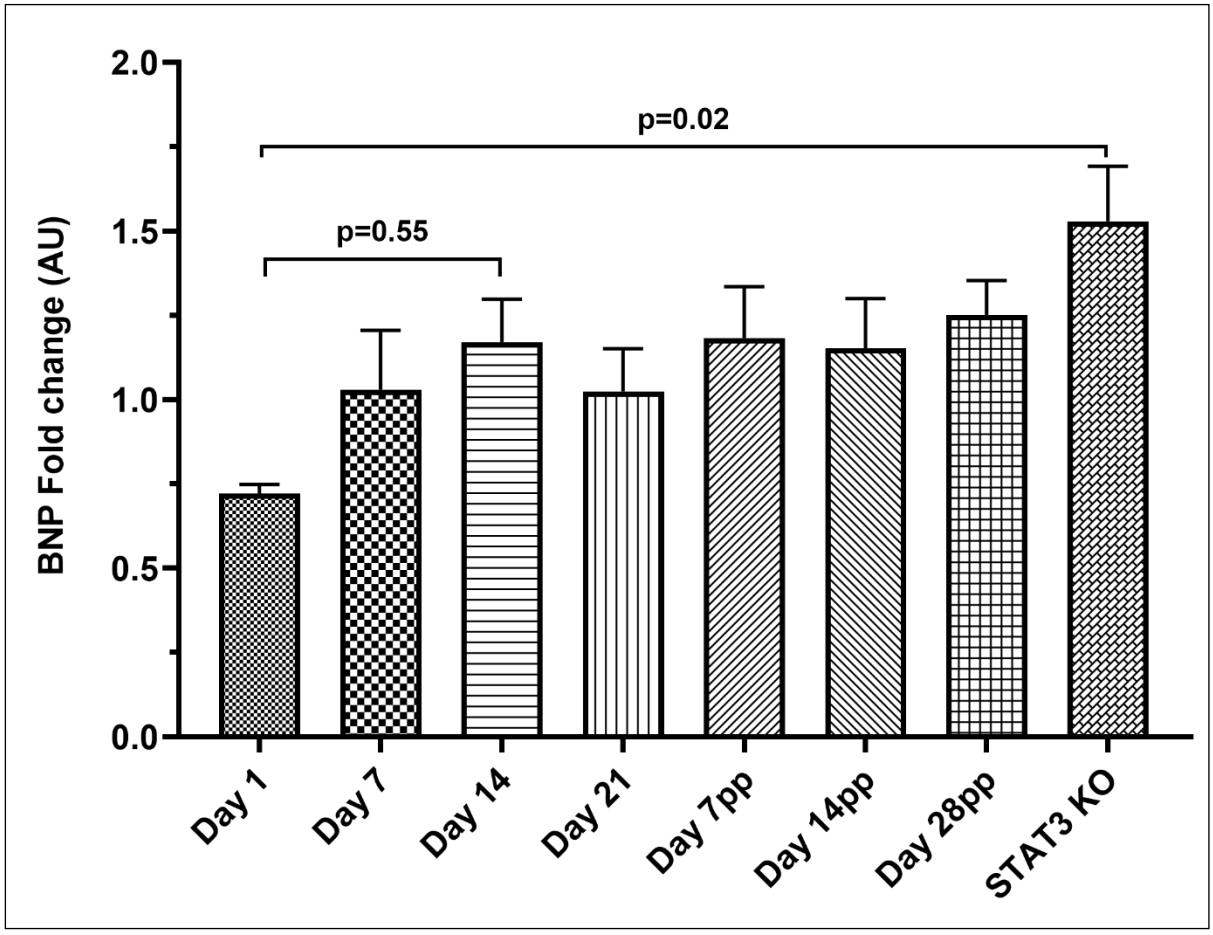

Figure 22: mRNA expression of Brain Natriuretic Peptide gene in pregnant mice hearts

RT-qPCR was performed twice with 4–7 independent ventricular samples/group. Levels of the candidate gene was normalized to GAPDH. The bar graph displays fold change calculated using the Livak method $2^{-\Delta\Delta Ct}$ [252]. *Ct*-cycle threshold values; AU- arbitrary units. Ct values less than 15 and higher than 45 were considered invalid. BNP (Brain Natriuretic Peptide).*

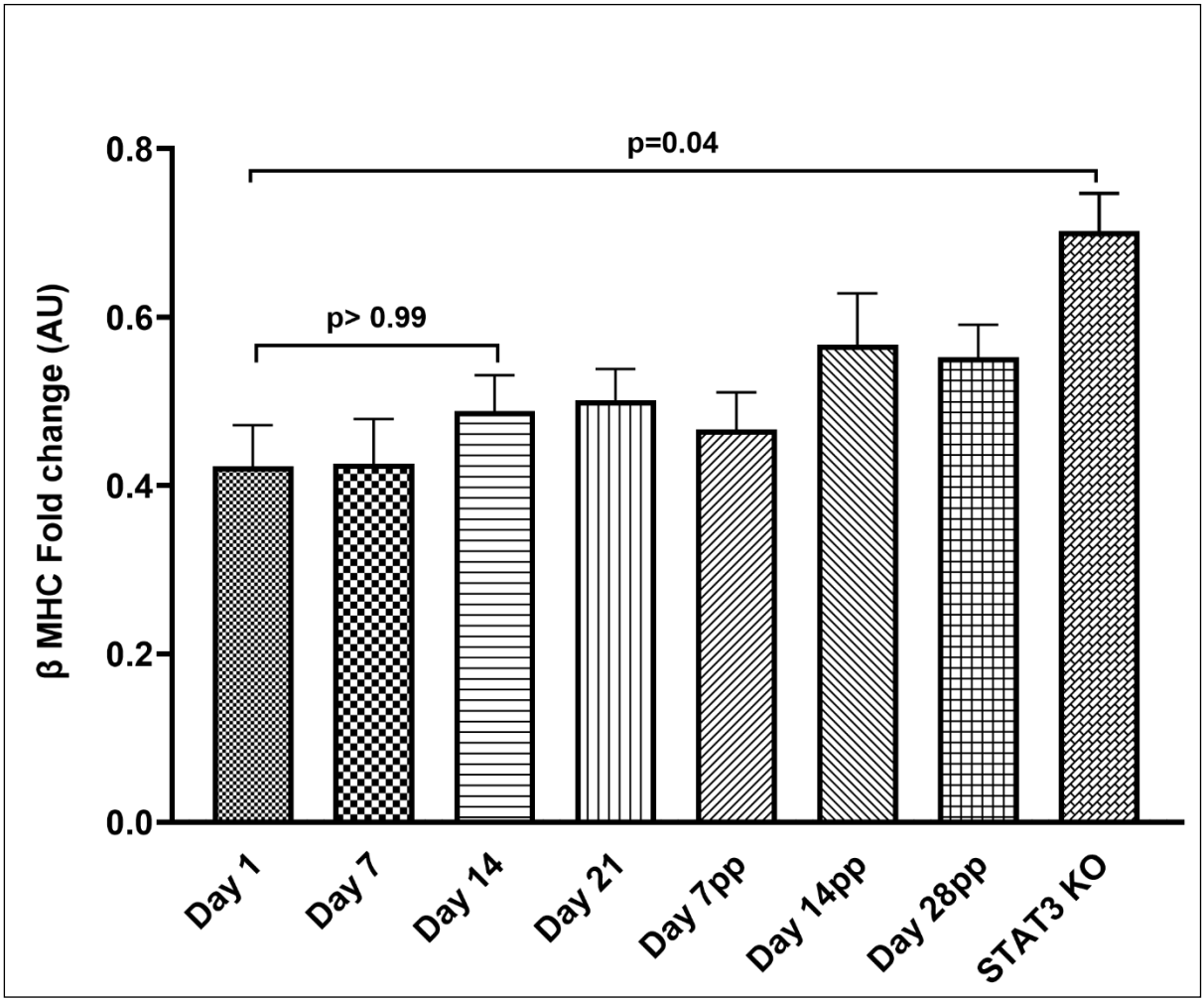

Figure 23: mRNA expression of b-myosin heavy chain gene in pregnant mice hearts

RT-qPCR was performed twice with 4–7 independent ventricular samples/group. Levels of the candidate gene was normalized to GAPDH. The bar graph displays fold change calculated using the Livak method $2^{-\Delta\Delta Ct}$ [252]. *Ct*-cycle threshold values; AU- arbitrary units. Ct values less than 15 and higher than 45 were considered invalid. β-myosin heavy chain.*

1.4.5 Potential signaling pathways involved in regulation of cardiac hypertrophy during pregnancy

Figure (24-26) shows the expression level of STAT3, STAT5, AKT and phosphorylation during pregnancy and postpartum

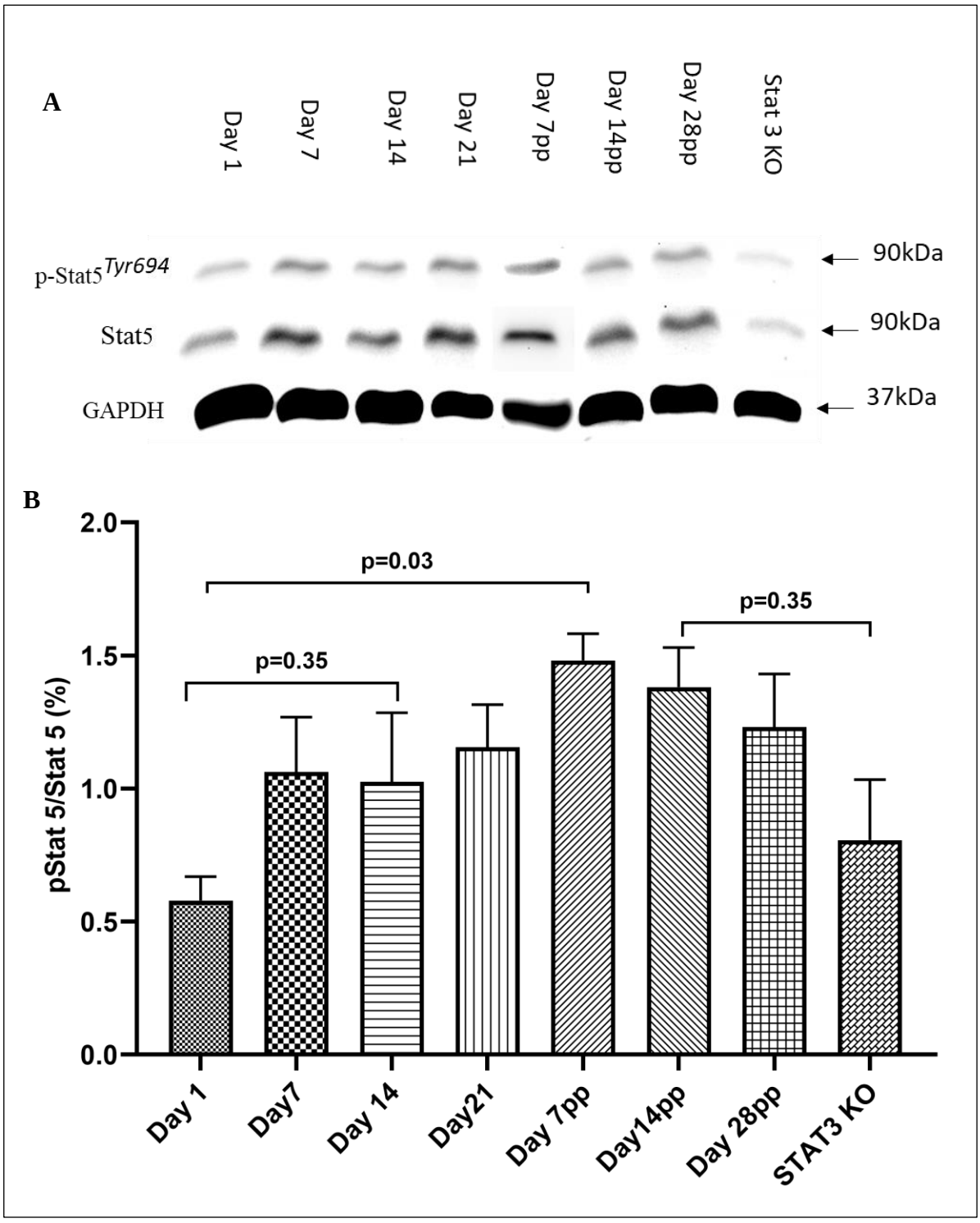

Figure 24: Expression of STAT5 during pregnancy and postpartum

Image shows representative blots per each protein and bar graphs shows the expression of STAT 3. Experiments were performed with at least 6 independent ventricles per group. Values are means ± SE. Data were analysed by one-way ANOVA with Tukey's post hoc test. p ≤ 0.05, was considered significantly different between groups. PP-postpartum

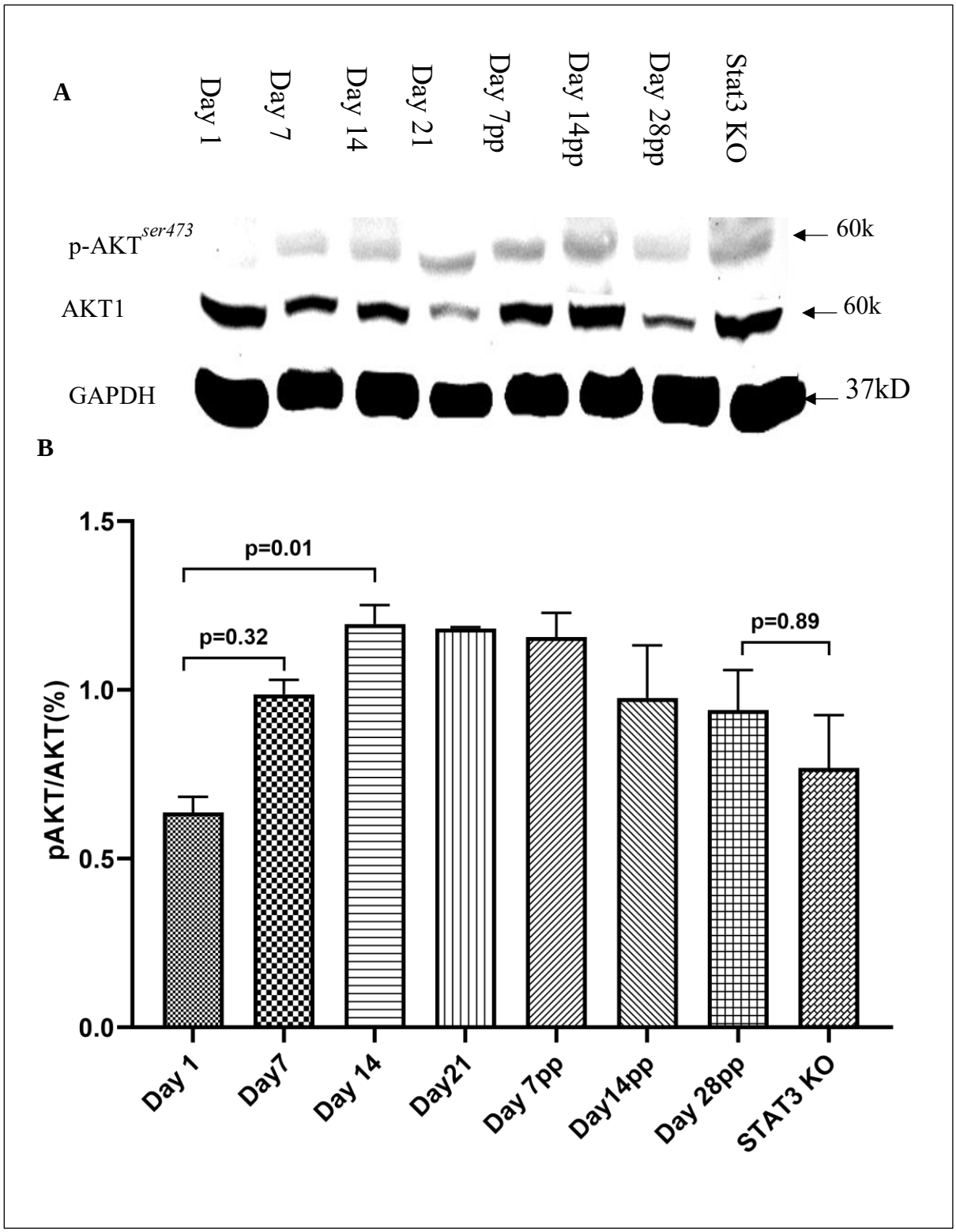

Figure 25: Expression of AKT during pregnancy and postpartum

Image shows representative blots per each protein and bar graphs shows the expression of AKT. Experiments were performed with at least 6 independent ventricles per group. Values are means ± SE. Data were analysed by one-way ANOVA with Tukey's post hoc test. $p \leq 0.05$, was considered significantly different between groups. PP-postpartum

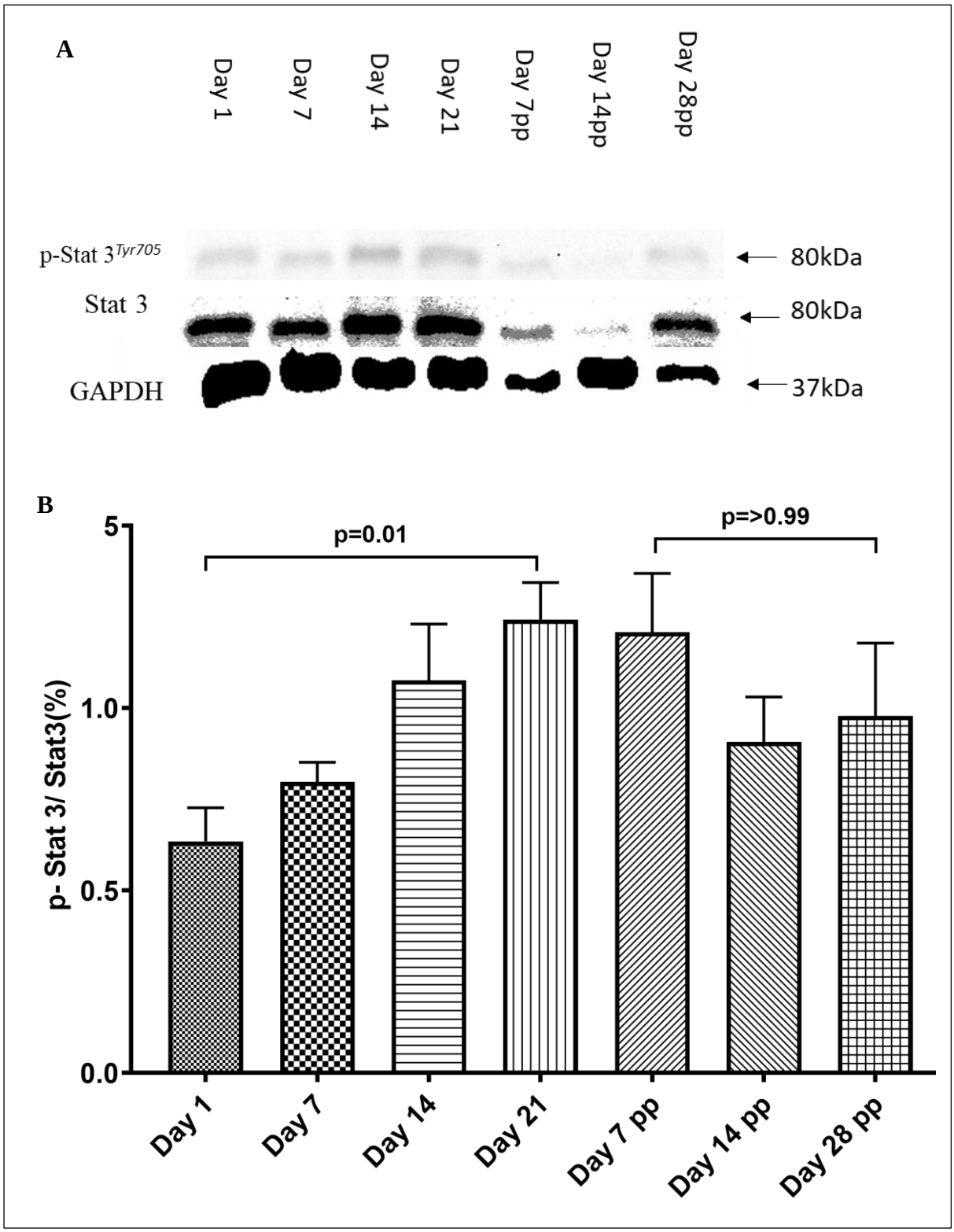

Figure 26: Expression of STAT 3 during pregnancy and postpartum

Image shows representative blots per each protein and bar graphs shows the expression of STAT 3. Experiments were performed with at least 6 independent ventricles per group. Values are means ± SE. Data were analysed by one-way ANOVA with Tukey's post hoc test. $p \leq 0.05$, was considered significantly different between groups. PP-postpartum

STAT 5 protein expression was significantly activated in the early postpartum phase (Day 7pp p=0.03). The expression gradually decreased on Day 14pp and Day 28pp. STAT 5 was not

activated in the pathological group (STAT3 KO). AKT expression also gradually increased during pregnancy, peaking at Day 14. AKT expression was then sustained until Day 7pp, before reverting to non-pregnant level. Again, no significant activation of AKT was observed in STAT3 KO. STAT 3 level did not change significantly during pregnancy and postpartum phase.

1.4.6 Histological and fibrotic changes during pregnancy and postpartum in wild type mice

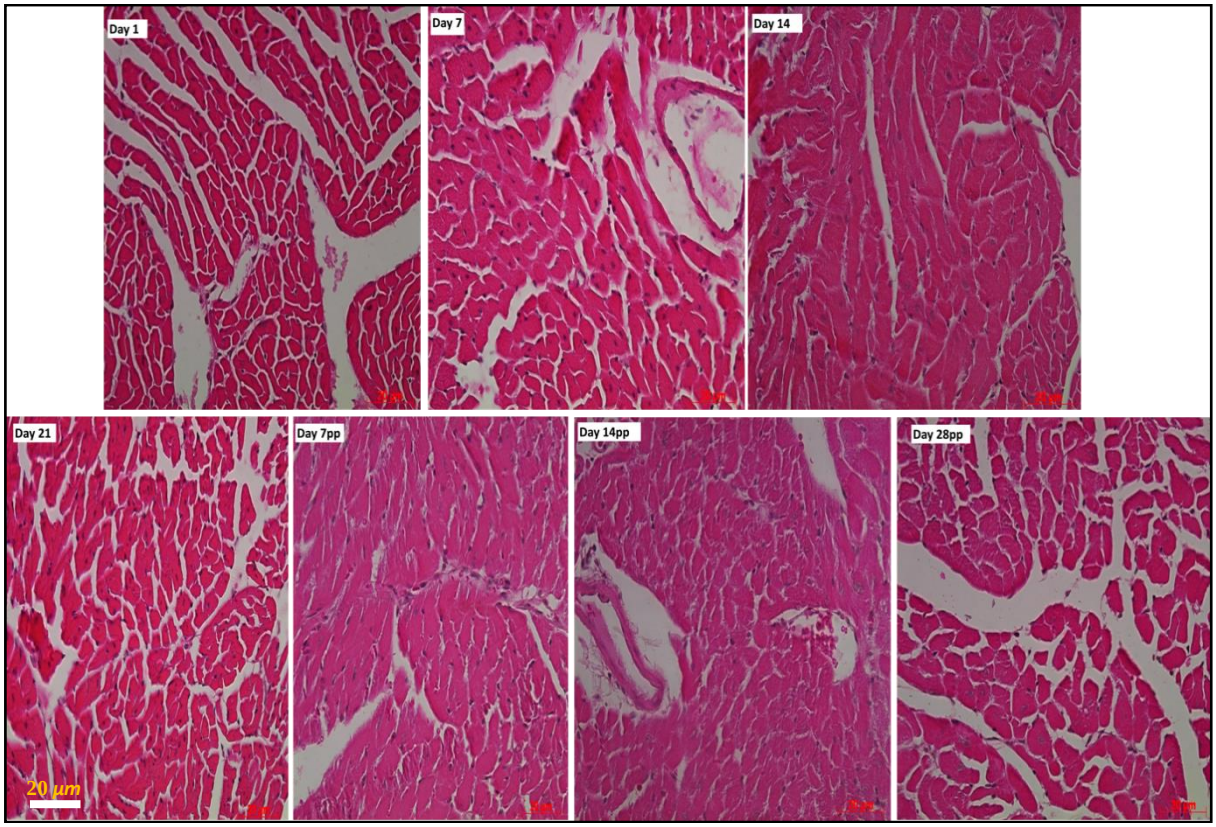

Figure 27: Representative image for hematoxylin-eosin H& E staining of pregnant mice hearts sections

Normal cell architecture with normal interstitial space and no evidence for associated intravascular and/or interstitial foreign body granulomas were observed (haematoxylin and eosin, magnification X40, scale 20 µm).

The ventricular myocardium of pregnant mice hearts showed normal architecture with normal interstitial space when stained by H&E. A limited number of central nucleated fibres were observed.

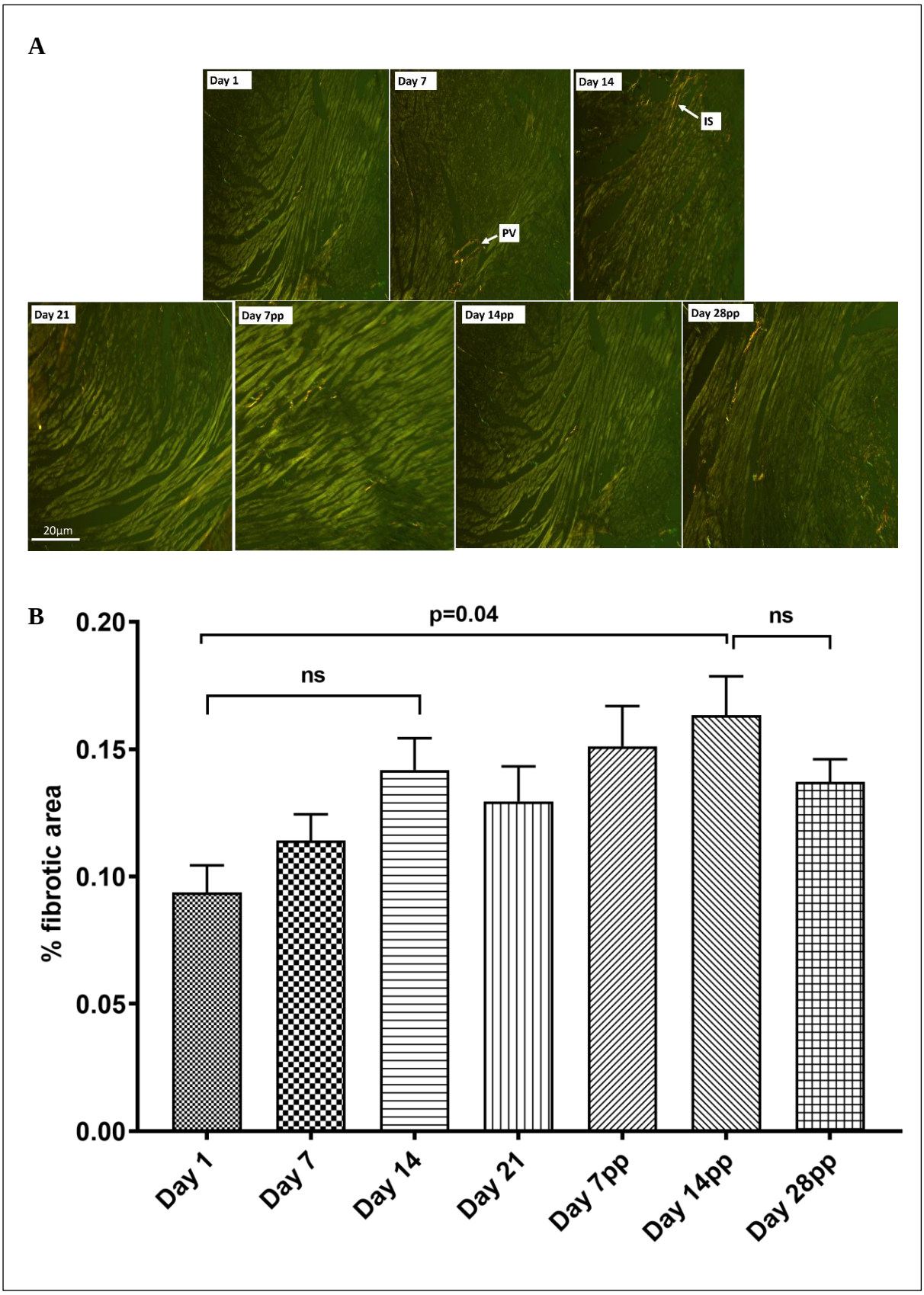

Figure 28: Heart histological illustrative sections and fibrotic quantification

A: Polarized microscopic views of myocardial collagen stained with *Pico sirus red. (20X magnification) orange birefringence staining indicates fibrotic tissue.* **B***: Fibrotic area quantification indicated that fibrosis was slightly induced in the postpartum period but not during gestation. PV-perivascular, IS-interstitial, PP-postpartum.*

Minimum but significantly different percentage area of interstitial fibrosis was observed in the postpartum phase (p=0.04) but not during pregnancy when compared to Day 1(**Figure 28B**). Signs of reversal were seen on Day 28pp. Perivascular fibrosis was not quantified.

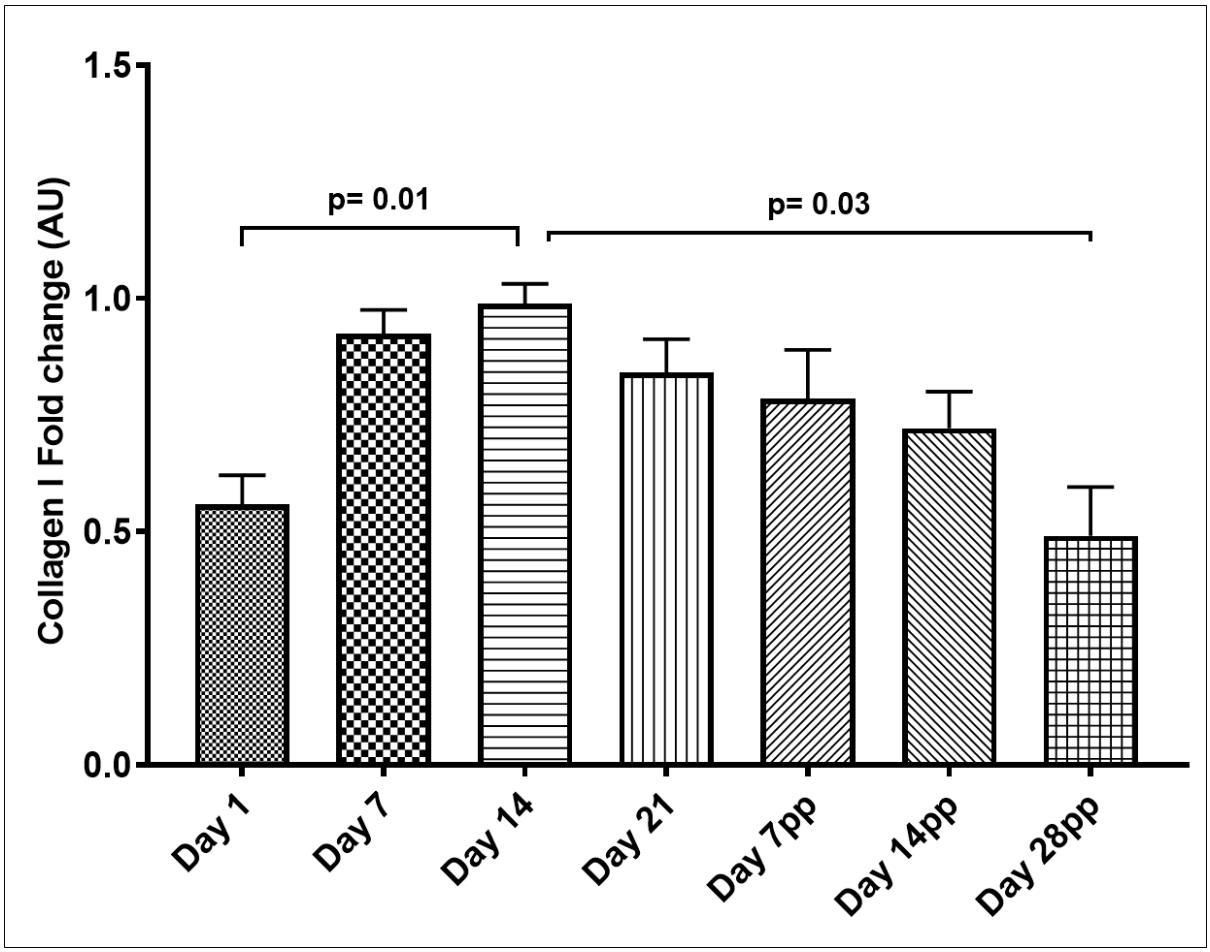

Figure 29*:* **Collagen type I mRNA expression in pregnant mice heart**

Collagen type 1 (Col I) mRNA expression. RT-qPCR was performed twice with 4−7 independent ventricular samples/group. Level of the candidate genes were normalized by GAPDH. The bar graph displays fold change calculated using the Livak method $2^{-\Delta\Delta Ct}$ [252]. *Ct*-cycle threshold values; AU- arbitrary units, PP- postpartum. Ct values less than 15 and higher than 45 were considered invalid.*

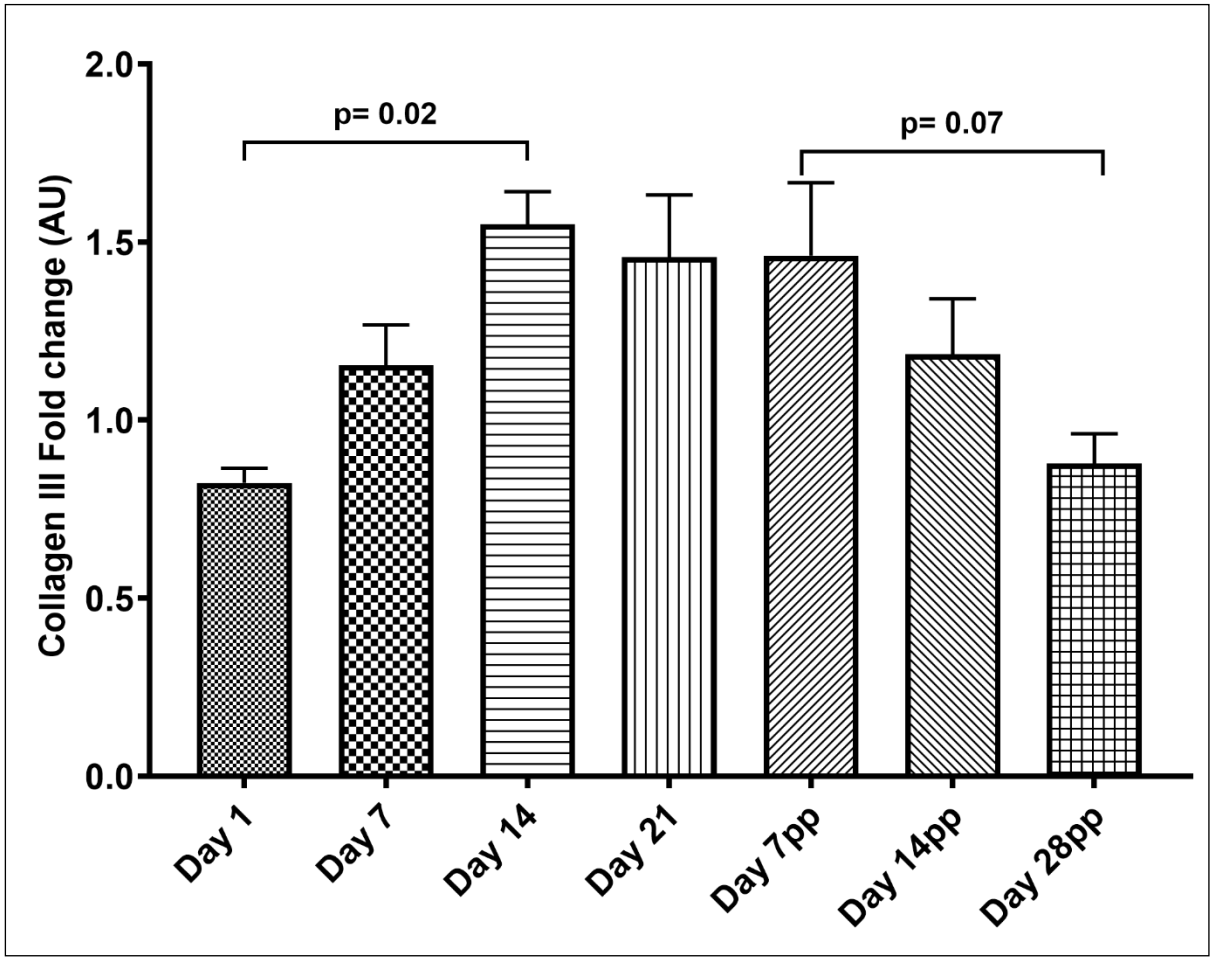

Figure 30: Collagen type III mRNA expression in pregnant mice

Collagen type 3 (Col III) mRNA expression. RT-qPCR was performed twice with 4–7 independent ventricular samples/group. Level of the candidate genes were normalized by GAPDH. The bar graph displays fold change calculated using the Livak method $2^{-\Delta\Delta Ct}$ [252]. *Ct*-cycle threshold values; AU- arbitrary units, PP- postpartum. Ct values less than 15 and higher than 45 were considered invalid.*

The mRNA levels of fibrotic indicators collagen type 1(Col I) (**Figure 29**) and collagen type 3 (Col III) (**Figure 30**) increased early in pregnancy and was sustained until early postpartum (Day 7pp). The expression gradually decreases from Day 14pp reverting to normal level of expression by Day 28pp.

1.4.7 Cardiac proteomic analysis of pregnant mice

We performed in-depth global protein expression profiling of pregnant mice hearts at different time points during pregnancy and postpartum. A total of 1190 proteins that contained 2 or more unique peptides were identified in all the samples.

There were similarities between timepoints in the specific proteins that were altered with only 14 proteins being significantly different across all groups compared to the control (Day 1). **Table 9** shows a list of 14 differentially expressed proteins. Corticosteroid-binding globulin

(Q06770), Transthyretin (P07309), Serine protease inhibitor A3C (P29621) and Beta-2-microglobulin (P01898), Dedicator of cytokinesis protein 2 (Q8C3J5) were the most differentially expressed proteins.

Table 9: List of overall differentially expressed proteins

Access No	Protein name	Biological process	P-value
Q06770	Corticosteroid-binding globulin	biological regulation; C21-steroid hormone metabolic process	<0.01
Q8C3J5	Dedicator of cytokinesis protein 2	acute inflammatory response;	0.01
P07309	Transthyretin	amine transport; cellular hormone metabolic process	0.02
P29621	Serine protease inhibitor A3C	Apoptosis; response to cytokine stimulus	0.02
P01898	Beta-2-microglobulin	anatomical structure development; antigen processing and presentation of endogenous peptide antigen via MHC class I	0.02
Q9QYR7	Acyl-coenzyme A thioesterase 1	acyl-CoA metabolic process	0.03
Q91Z83	Myosin-7	anatomical structure morphogenesis; regulation of the force of heart contraction	0.04
P61922	4-aminobutyrate aminotransferase, mitochondrial	negative regulation of blood pressure	0.04
Q05793	Basement membrane-specific heparan sulfate proteoglycan core protein	cardiac muscle tissue development; angiogenesis	0.04
A0A075B680	Immunoglobulin heavy variable 1-62-2	membrane invagination	0.04
P01756	Ig heavy chain V region AC38 205.12	antigen binding; immunoglobin	0.04

To get an overview of the expression of the significant proteins, a heat map was constructed (**Figure 31**). The heat map confirmed that the cardiac proteomes of postpartum mice were similar to the early pregnancy time points.

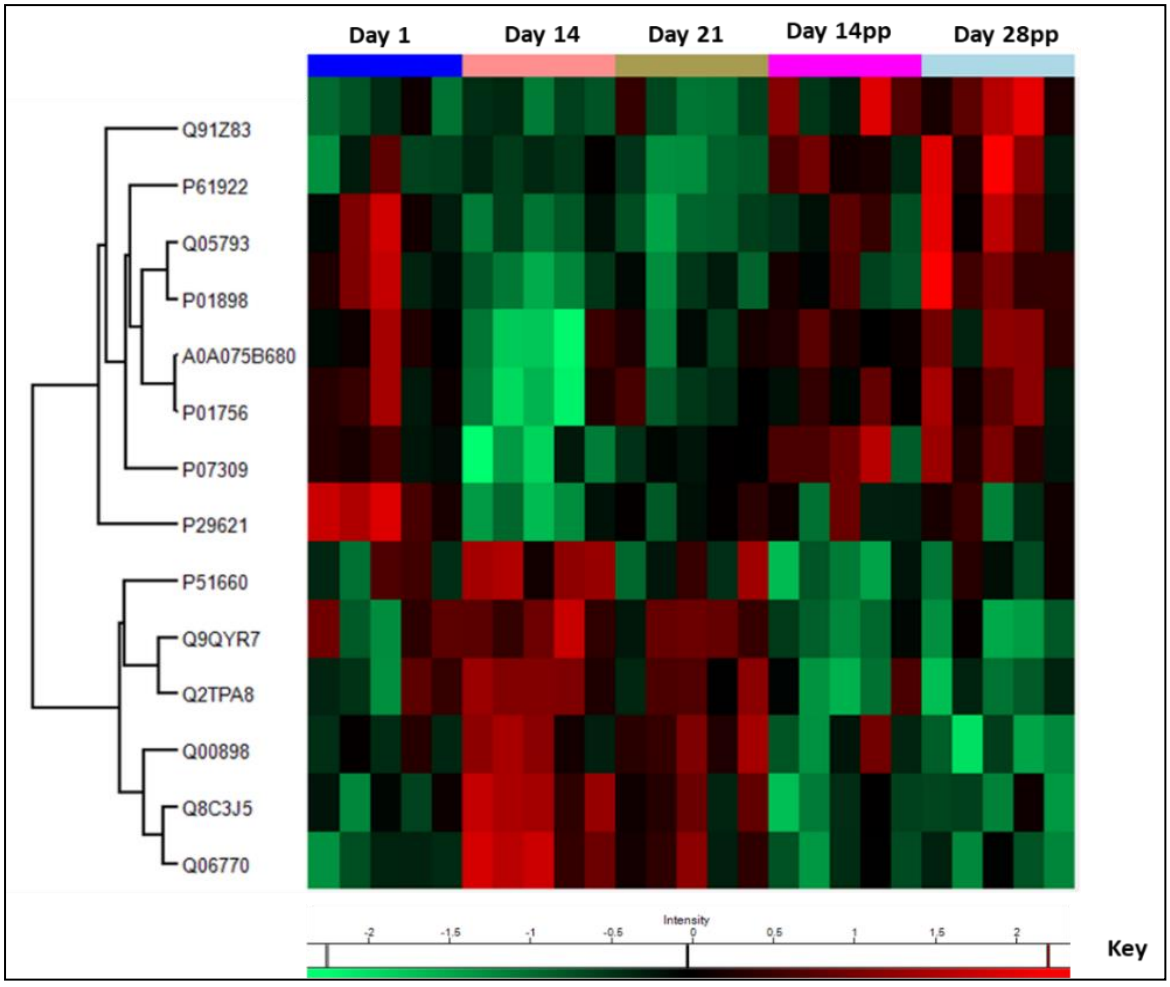

Figure 31: Heat map of hierarchical clustering of differentially abundant cardiac proteins at different pregnancy and postpartum time points

Colours represent relative abundance levels for each protein across time points based on z-scores. Green represent down-regulation whist red represent up-regulation. pp-postpartum

1.4.8 Comparison of protein expressions between late pregnancy and postpartum groups

The greatest proteomic response occurred in the late pregnancy (Day 14) and it was distinct from the postpartum groups (Day 14pp and Day 28pp). A total of 266 proteins were significantly changed between Day 14 and Day 14pp, whilst a total of 350 proteins were significantly changed between Day 14 and Day 28pp. Volcano plots on **Figure 32A& B** shows the differentially up and down regulated protein. Out of the 266 significant proteins between Day 14 and Day 14pp, 90 proteins were upregulated on Day 14pp, and 197 proteins were upregulated on Day 28pp.

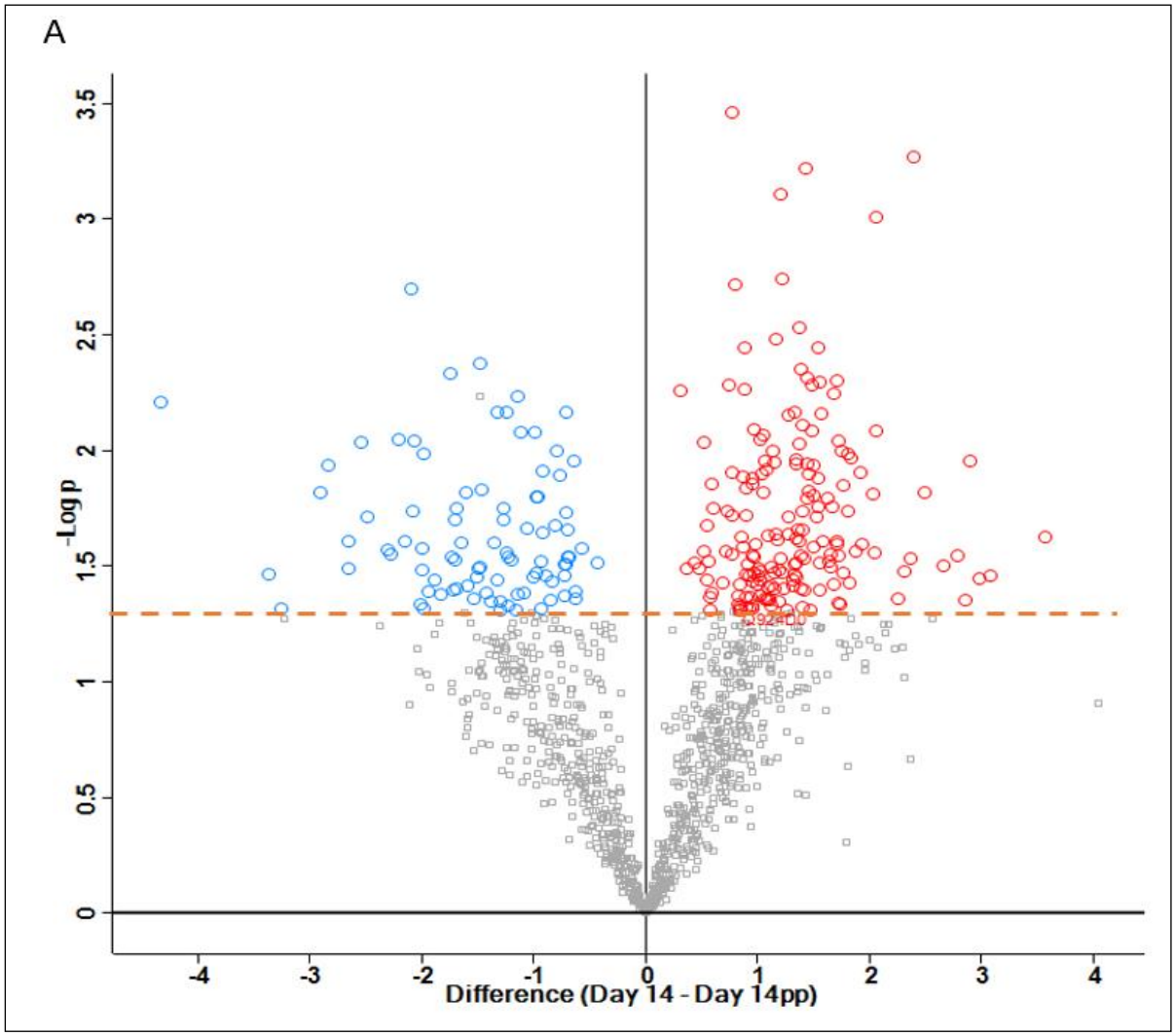
A
-Log p
3.5
3
2.5
2
1.5
1
0.5
0
-4
-3
-2
-1
0
1
2
3
4
Difference (Day 14 - Day 14pp)

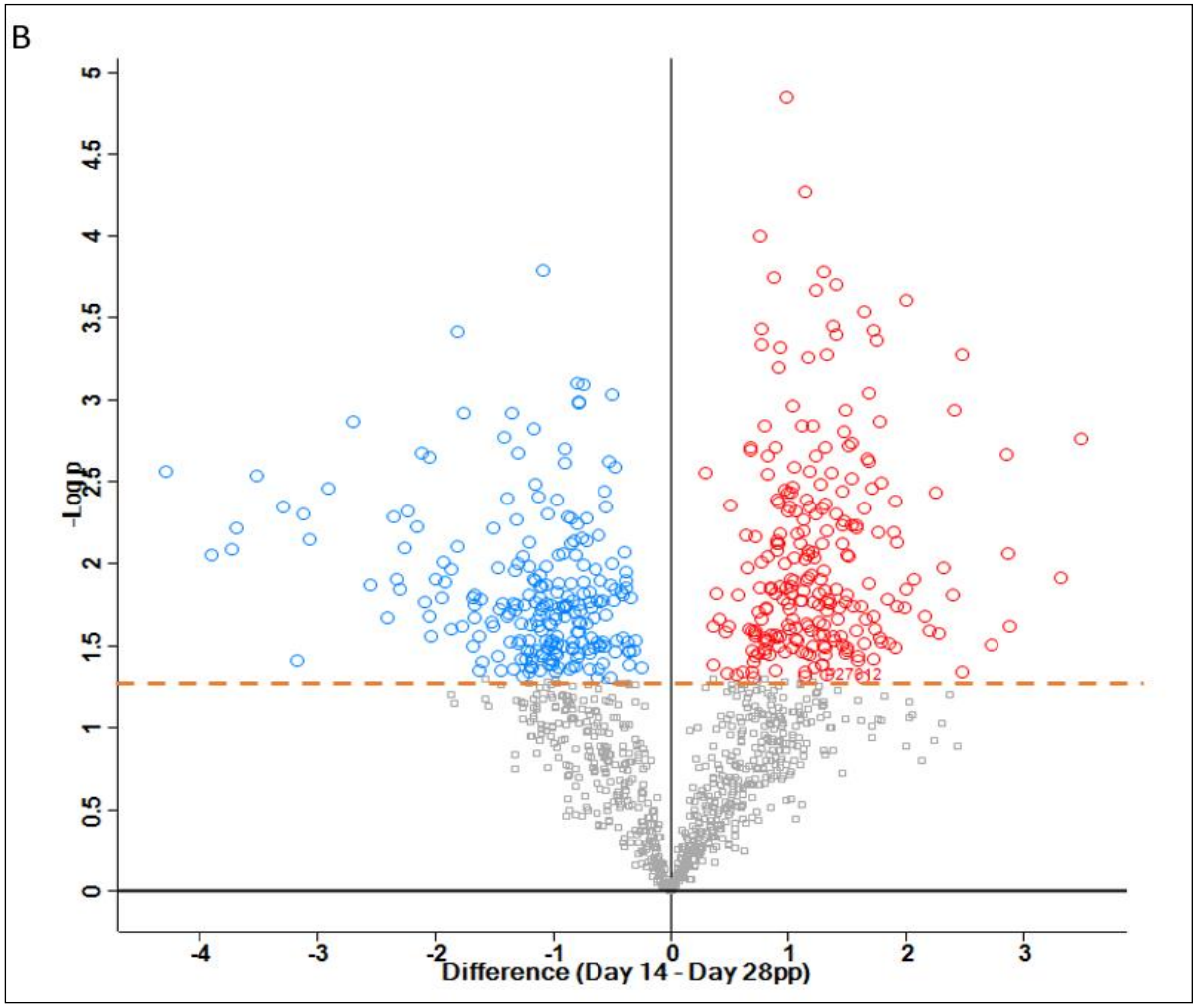

Figure 32: Volcano plots of differentially regulated proteins between groups.

***A**: Day 14 vs Day 14pp.* ***B**: Day 14vs Day 28pp. The plot constructed using −log10 (p value) against the mean difference. Proteins were graphed by fold change (Difference) and significance (-Log p) using a false discovery rate of 0.05 and an S0 of 0.1. Protein in red were considered significantly up, whilst blue were down regulated and grey were non significantly changed proteins using the Perseus software. Dashed horizontal line shows the p values cut-off.*

1.4.9 GO Annotation of differentially expressed proteins

The differentially expressed upregulated proteins on Day 14pp and on Day 28pp were analysed using the Gene Ontology database Panther (Protein ANalysis THrough Evolutionary Relationships). Enriched cellular localization, biological processes, and molecular function mapped by the proteomes were determined. **Figure 33A-C** summarizes the most statistically significant GO categories of the upregulated proteins on Day 14pp.

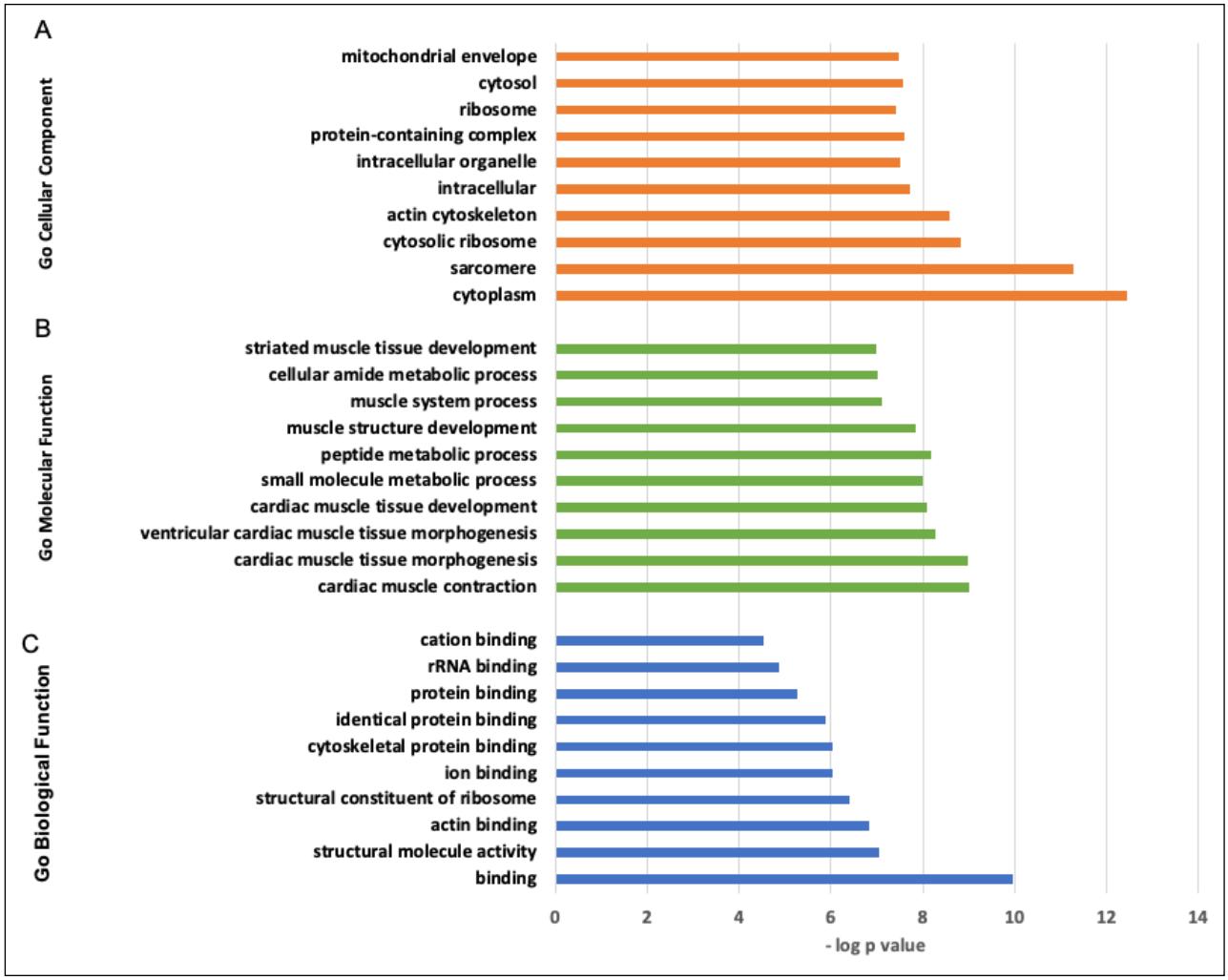

Figure 33: Gene Ontology classification of differentially up regulated proteins on Day 14pp

A: *Go Cellular Component (CC);* ***B****: Molecular Function (MF);* ***C****: Biological function category (BF). Graphs show the 10 most significant enriched Gene ontology (GO) categories of significantly upregulated proteins on Day 14pp.*

The enriched GO CC annotation of the upregulated proteins on Day 14pp suggested that cytoplasm, cytosolic ribosome, intracellular, protein-containing complex and cytosol were in the top 5 enriched categories. Most of the proteins upregulated on Day 14pp have binding properties or are involved in structural molecule activity. Moreover, gene ontology analysis based on the molecular function of upregulated proteins showed that cardiac muscle contraction, cardiac muscle tissue morphogenesis and development were part of the most enriched GO MF (**Figure 33B**).

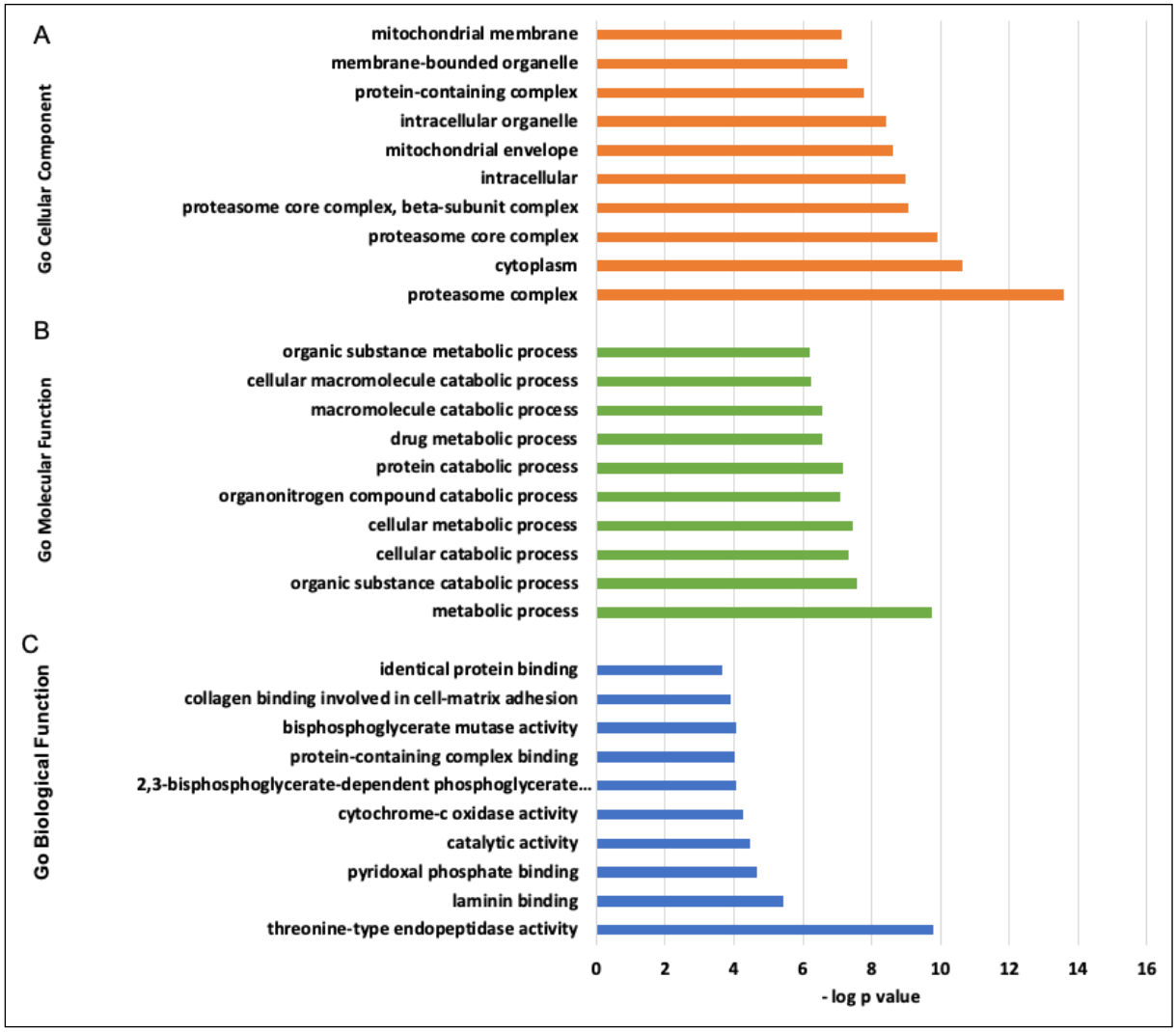

Figure 34: Gene Ontology classification of differentially up regulated proteins on Day 28pp

A: *Go Cellular Component (CC);* ***B****: Molecular Function (MF);* ***C****: Biological function category (BF). Graphs show the 10 most significant enriched Gene ontology (GO) categories of significantly upregulated proteins on Day 28pp.*

Proteasome complex, proteasome core complex, intracellular, intracellular organelle, and membrane bound organelle were in the top 5 enriched CC categories of upregulated proteins on Day 28pp. GO MF enrichment of upregulated proteins on Day 28pp suggested metabolic process, cellular catabolic process, organonitrogen compound catabolic process, drug metabolic process and cellular macromolecule catabolic process as the most enriched categories.

1.4.10 Protein-protein interaction analysis of proteins upregulated on Day 14pp and Day 28pp

To observe the interactions between upregulated proteins on Day 14 pp and Day 28pp we used String db (11.0) [249]. (**Figure 35 & Figure 36**) shows the known and predicted protein interactions on Day 14pp and Day 28pp respectively.

The interaction on Day 14pp indicate enrichment of cardiac contractile proteins, ribosomal proteins and additionally supported by the increase in cytochrome C oxidase.

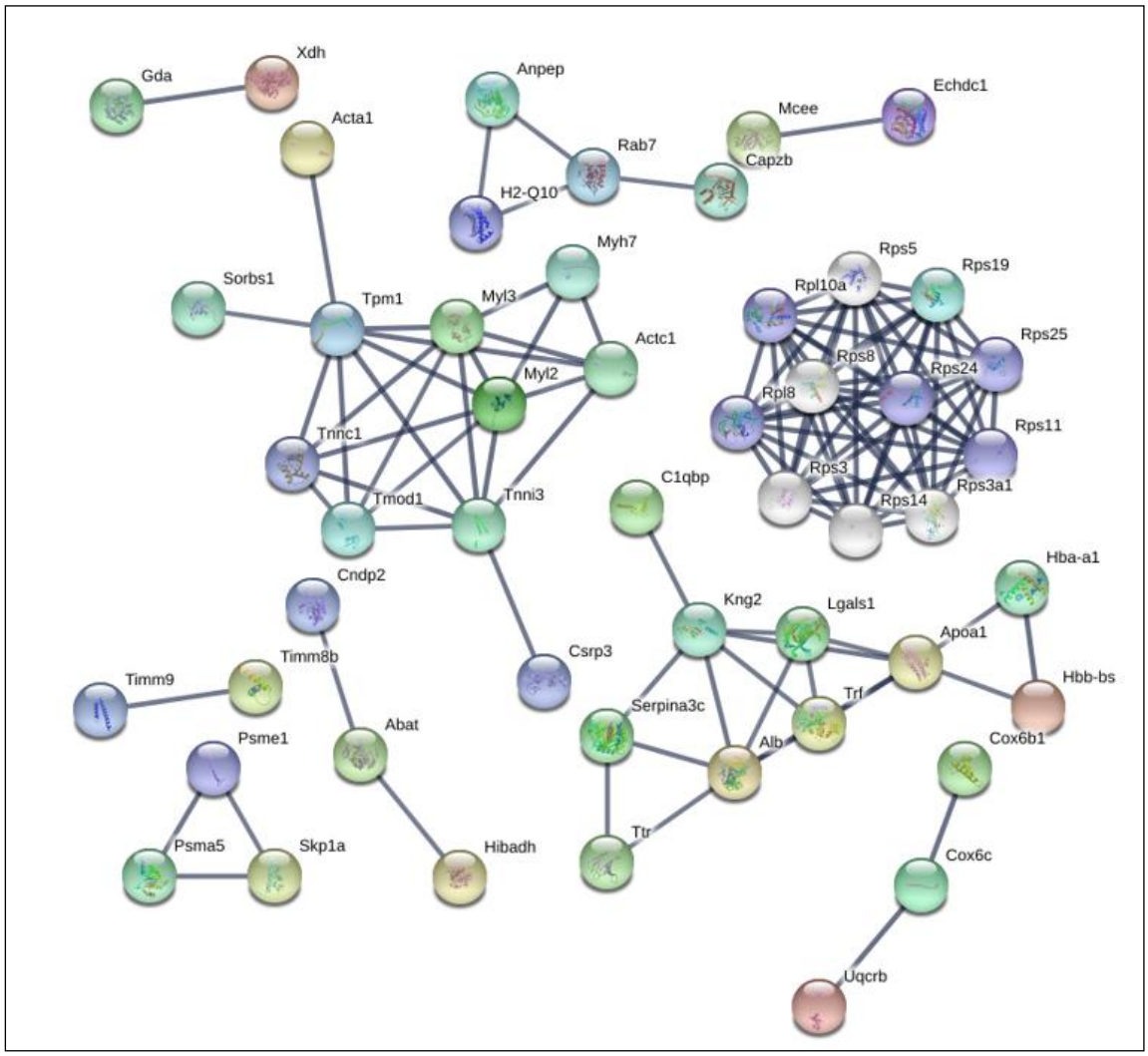

Figure 35: Protein-protein interaction (PPI) of upregulated proteins on Day 14pp

The confidence of prediction was set very high at 0.900. PPI enrichment p-value =4.8e-12. Maximum number of interactors was set at 5.

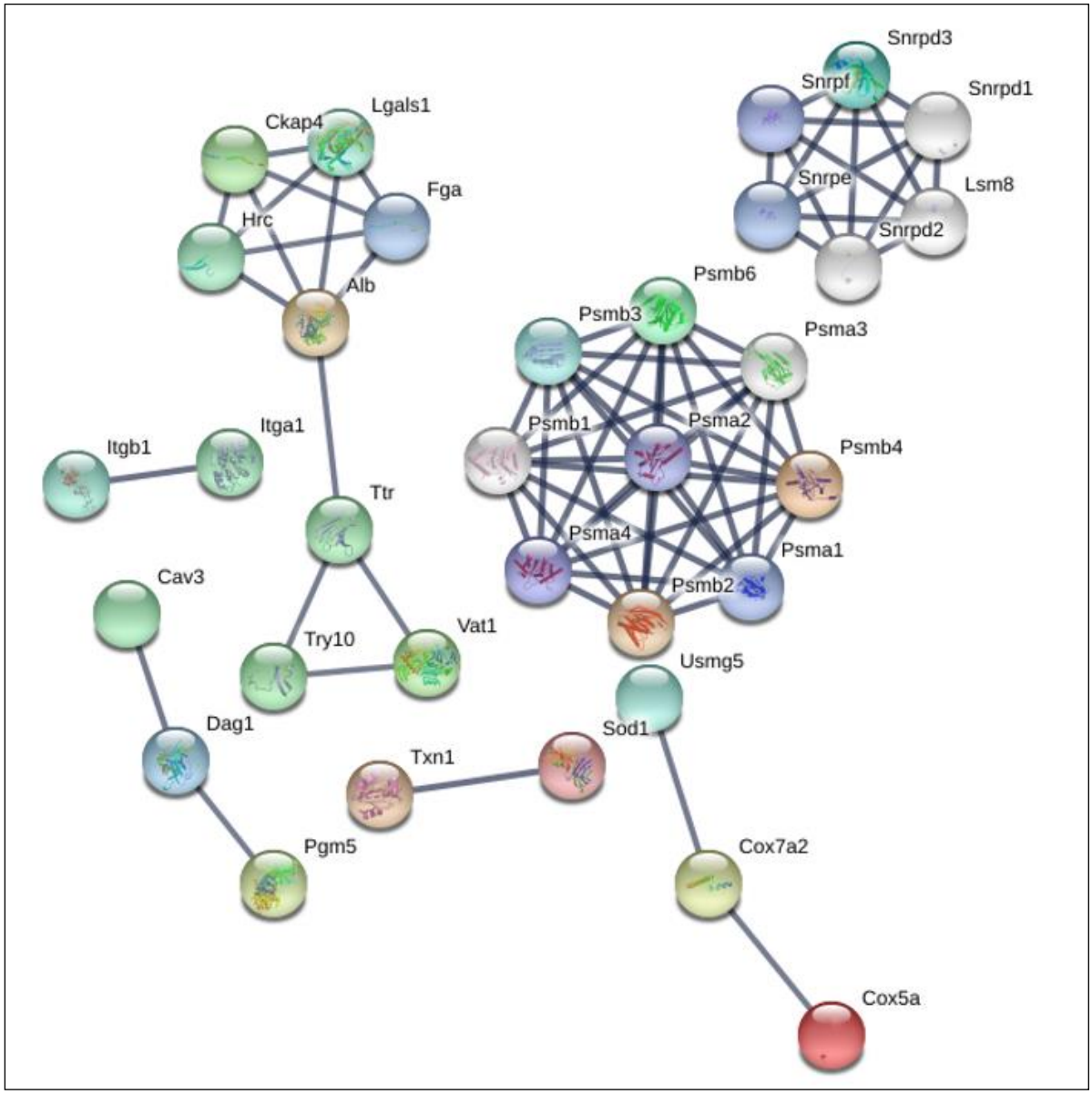

Figure 36: Protein-protein interaction (PPI) of upregulated proteins on Day 28pp

The confidence of prediction was set very high at 0.900. PPI enrichment p-value = < 1.0e-16. Maximum number of interactors was set at 5.

The interaction on Day 28pp indicate enrichment of proteasome subunits mainly component of the 20S core proteasome complex and small nuclear ribonucleoprotein, the building blocks of the spliceosome.

1.4.11 KEGG pathway analysis of differentially expressed proteins in the postpartum phase of pregnant mice

To explore the metabolic pathways of the significantly upregulated proteins, we investigated the enriched KEGG pathway analysis of the 90 proteins upregulated on Day 14pp and 197 proteins upregulated on Day 28pp. **Table 10** and **Table 11** shows a list the top 5 identified pathways on Day 14pp and Day 28pp.

Table 10: KEGG pathways enriched on Day 14pp

KEGG Pathways	Genes	p-value
Cardiac muscle contraction	Cox5a, Myl2, Cox6c, Uqcrb, Cox6b1, Myl3, Actc1, Tnni3, Myh7, Tpm1, Tnnc1	7.38E-14
Dilated cardiomyopathy (DCM)	Myl2, Myl3, Actc1, Tnni3, Myh7, Tpm1, Tnnc1	1.3E-07
Hypertrophic cardiomyopathy (HCM)	Myl2, Myl3, Actc1, Tnni3, Myh7, Tpm1, Tnnc1	9.55E-08
Ribosome	Rpl13, Rps11, Rpl8, Rps5, Rps9, Rplp1, Rps18, Rps19	1.08E-07
Adrenergic signaling in cardiomyocytes	Myl2, Myl3, Actc1, Tnni3, Myh7, Tpm1, Tnnc1	2.9E-06

Partial list of the enriched KEGG pathways and set of genes that contributed to the pathways. Cox-Cytochrome c oxidase, Myl-Myosin Light Chain, Uqcrb-Ubiquinol-cytochrome c reductase binding protein, Actc-Cardiac muscle alpha actin, Tpm1-Tropomyosin alpha-1 chain, Rpl-ribosomal protein L, Rps-ribosomal protein S, Rplp1-Ribosomal protein lateral stalk subunit P1

Table 11: KEGG pathways enriched on Day 28pp

KEGG Pathways	Genes	p-value
Proteasome	Psmb4, Psmb1, Psmd3, Psmd11, Psmb6, Psmc5, Psmd12, Psma6, Psmb2, Psmb3	7.23E-16
Dilated cardiomyopathy (DCM)	Itga1, Itgb1, Myh7, Dag1	1.5E-04
Hypertrophic cardiomyopathy (HCM)	Itga1, Itgb1, Myh7, Dag1	1.3E-04
Alzheimer's disease	Cox5a, Cox6c, Cox7a2, Rtn4, Snca	1.6E-04
ECM-receptor interaction	Col4a2, Itga1, Itgb1, Dag1	1.2E-04

Partial list of the enriched KEGG pathways and set of genes that contributed to the pathways. Psmb- Proteasome subunit beta, Psmd- 26S proteasome non-ATPase regulatory subunit, Psmc5- 26S protease regulatory subunit 8, Itga- Integrin subunit alpha, Dag1- dystroglycan, Rtn4- Reticulon, Snca- Alpha-synuclein, Col4a2- Collagen alpha-2(IV) chain.

Cardiac muscle contraction was the most significantly enriched pathways (p= 7.38E-14) on Day 14pp. We identified 11 proteins which contributed to this pathway which includes cytochrome c oxidase subunit 5a (Cox5a); myosin light chain 2 (Myl2); Cox6c; ubiquinol-cytochrome c reductase binding protein (Uqcrb); Cox6b1; Myl3; alpha cardiac actin (Actc1); cardiac troponin I (Tnni3); Myh7; tropomyosin alpha-1 (Tpm1) and troponin C1 (Tnnc1). Another important pathway involved Myl2; Myl3; Actc1; Tnni3; Myh7; Tpm1 and Tnnc1 which are proteins implicated in dilated cardiomyopathy (DCM) and hypertrophic cardiomyopathy (HCM).

The most significantly enriched pathway from upregulated proteins on Day 28pp was the proteasome (p= 7.23E-16). Ten important proteins contributed to this pathway proteasome

subunit beta type-4 (Psmb4); Psmb1; Psmd3; Psmd11; Psmb6; Psmc5; Psmd12; Psma6; Psmb2; Psmb3).

1.4. 12 Upstream regulatory analysis

To predict the upstream transcription factors which regulates the identified differentially expressed proteins, the list of proteins was input into the Expression 2 Kinases (X2K) software [251].

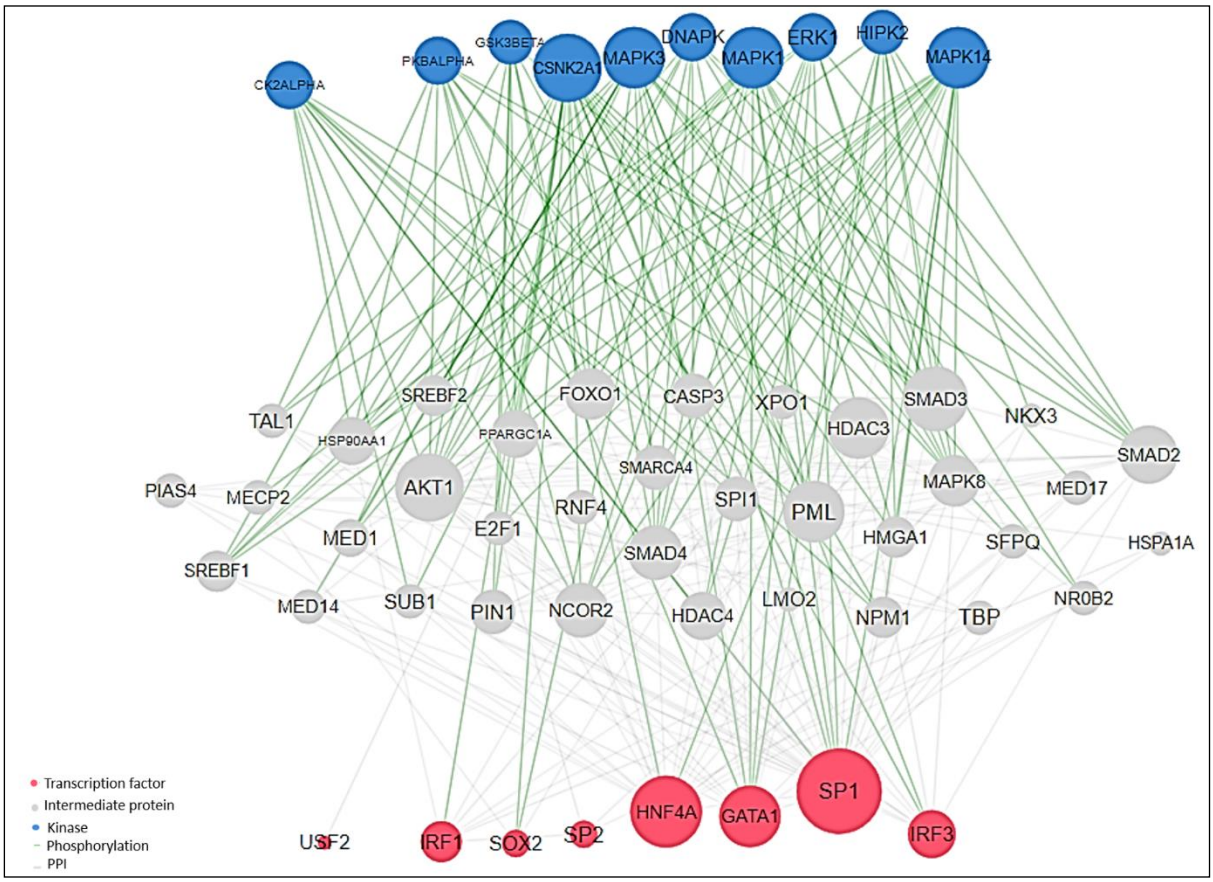

Figure 37: Inferred upstream regulatory network predicted to regulate the genes of upregulated proteins on Day 14pp.

Red nodes represent the top transcription factors predicted to regulate the expression of the input proteins list. Blue nodes represent the top predicted protein kinases known to phosphorylate the proteins within the expanded subnetwork. Green links represent kinase-substrate phosphorylation interactions between kinases and their substrates, while grey network edges represent physical protein-protein interactions. Transcription factor or kinase node size represents the rank according to the importance of the enriched proteins or target substrates respectively

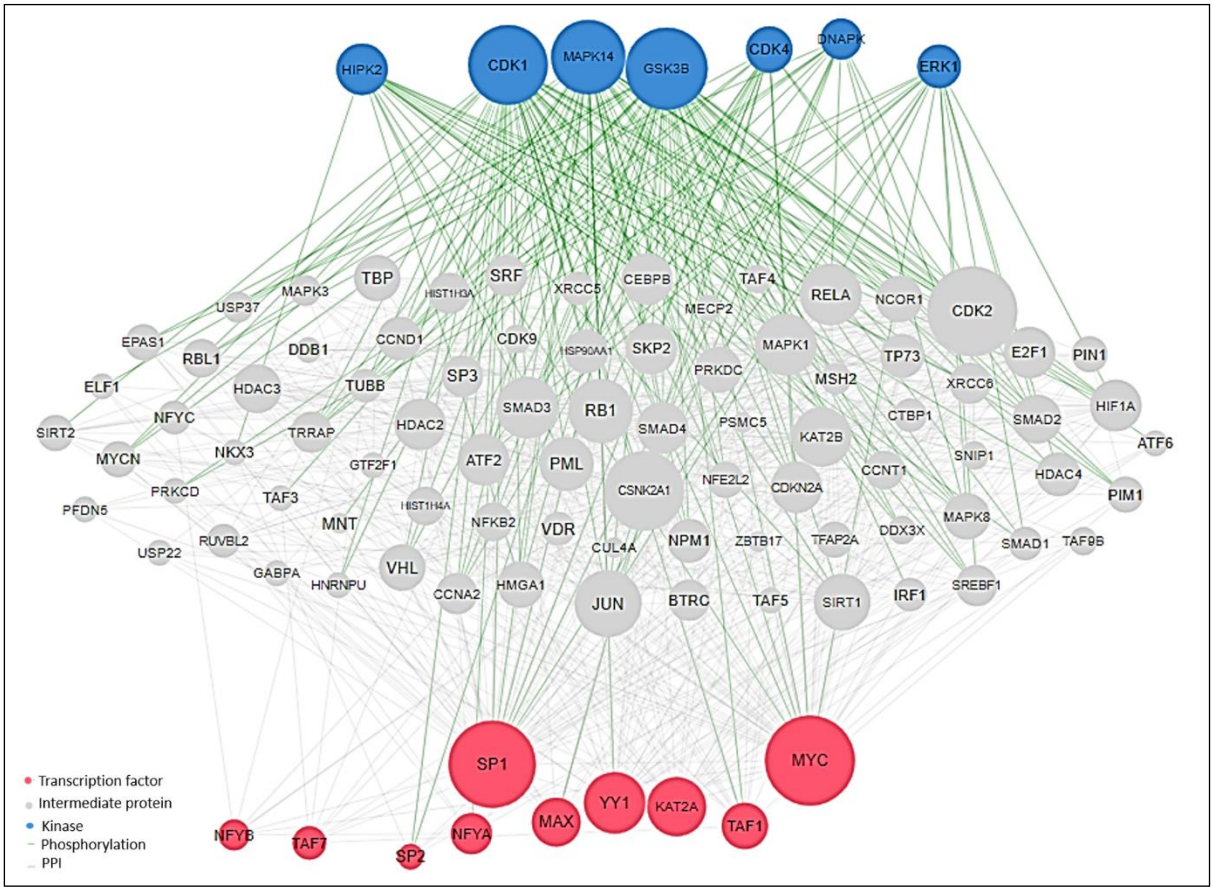

Figure 38: Inferred upstream regulatory network predicted to regulate the genes of upregulated proteins on Day 28pp.

Pink nodes represent the top transcription factors predicted to regulate the expression of the input gene list. Blue nodes represent the top predicted protein kinases known to phosphorylate the proteins within the expanded subnetwork. Green links represent kinase-substrate phosphorylation interactions between kinases and their substrates, while grey network edges represent physical protein-protein interactions. Transcription factor or kinase node size represents the rank according to the importance of the enriched proteins or target substrates respectively

Upstream regulatory network of proteins upregulated on Day 14pp (**Figure 38**) shows specificity protein 1 (SP1), hepatocyte nuclear factor 4 alpha (HNF4A), GATA binding protein 1 (GATA 1), interferon regulatory factor 3 (IRF3) and IRF1 as the top transcription factors that regulate proteins upregulated on Day 14 pp. The top predicted protein kinases known to phosphorylate the network includes CSNK2A1, MAPK1, MAPK3, MAPK14, ERK1 and HIPK2.

Figure 38 shows myelocytomatosis (MYC), yin yang 1 (YY1), specificity protein 1 (SP1) and histone acetyltransferase (KAT2A) as the top transcription factors that regulated proteins upregulated on Day 28pp.

mitogen-activated protein kinase 14 (MAPK14), cyclin-dependent kinase 1 (CDK1), glycogen synthase kinase 3 beta (GSK3B), ERK1 and HIPK2 were the top predicted protein kinases.

1.5 Discussion

1.5.1 Physiological cardiac functional and morphological changes associated with pregnancy in healthy mice

Echocardiography has been a technique of choice in assessing maternal heart adaptation during pregnancy due to its cost, availability and safety [280][281]. It has also been widely used in basic and translational research to study cardiac function in different models, including pregnant mice [282][283][284]. Despite several studies being published on cardiac changes during gestation, there is still controversy regarding parameters of assessing these changes [76][285].

Our study provides an assessment of the time course changes of LV dimensions and functions during normal pregnancy using conventional echocardiographic measurements in healthy pregnant mice.

1.5.1.1 LV dimension and volume changes in pregnant mice

Our findings substantiate the increase in blood volume during pregnancy. Increase in volume load leads to an increase in preload which manifests as an increase in LV volume and LV internal diameter [285][286][287]. An average increase of 25% in LVEDV ($p=0.003$) was reported in this study. LVEDV remained high throughout the postpartum period. Increased LVEDV has been observed in several human and mice study of normotensive pregnancy [3][11][12][37]. Data from our study also showed that LVEDV was sustained postpartum and had not resolved by Day 28pp. There is limited data on the exact time point when LVEDV is resolved postpartum. However, studies in human reported resolved preload changes after six months postpartum [66][76]. Umazume, et al [65], reported a progressive increase in LVEDV during pregnancy peaking at one week postpartum and the values remained high after one month postpartum.

LVESV did not change significantly in our study. However, the trend concurs with another study in pregnant goats [287]. Several studies in pregnant mothers have reported a decrease in LVESV [31][113][285][288]. The decrease in afterload is attributed to reduced systemic vascular resistance resulting in improved LV emptying in pregnant mothers [129][285]. In the contrary, a significant number of studies have also published an increase in LVESV

[66][289][290][291]. This discrepancy might be caused by the imperfectness of the methods used to estimate LV volumes, different quality of echocardiographic equipment and study population heterogeneity related to race or gestational age [290].

1.5.1.2 LV systolic and diastolic function

LVEF and LVFS markers of systolic function measured by convectional echocardiography were not altered in our normal pregnant mice model. LV function reports in pregnancy mice have been inconsistent with some studies reporting no significant changes [60][264][290][121], reduced functionality [76][292][61], or enhanced [261][293]. However, studies that tested isolated pregnancy heart under strict control of pre and afterload demonstrated improved systolic function [293][294]. The heart's ability to pump is enhanced in response to increased volume load during pregnancy, making it mechanically more efficient [295].

It is noteworthy mentioning that EF or FS have limitations in quantifying LV functionality in pregnancy since these parameters are highly depend on pre- and afterload [26]. Hence factors that affect preload and afterload previously described may also contribute to the inconsistency. Furthermore, the perception that normal LVEF equals normal systolic function and that abnormal LVEF equals abnormal function is not always the case. Studies in HF patients have found that over 50% of HF patients suffer from heart failure with preserved EF [296][297].

No significant changes in diastolic function were observed in our study. Like systolic function, conflicting data have also been published with regards to diastolic function during pregnancy. Some studies have published no change [75][261], whilst others have reported decrease in diastolic function [67][298]. A study that used tissue doppler imaging (TDI) which is an echocardiographic technique for assessing the diastolic function that is relatively independent of preload found that E/A ratio progressively reduced as pregnancy advanced [299].

Diastolic function is often not reported in pregnancy studies. Nevertheless, studies have suggested that diastolic dysfunction usually comes first before impairment of systolic function in most cardiovascular disease [298][300][301]. Hence, more accurate techniques such as TDI may be useful for monitoring maternal cardiac function in high- risk pregnancies to detect the early signs of cardiac failure and to prevent further deterioration with prompt interventions.

1.5.1.3 Cardiac hypertrophy in pregnant mice and postpartum

During pregnancy the heart develop cardiac hypertrophy through a complex process involving signaling pathways, cell structural changes and regulation by sex hormones [88][76][302]. Several studies have assessed cardiac anatomical changes in C57BL/6 mice during pregnancy and postpartum. In our study, we observed a maximum of 29.63 % increase in HW and a maximum of 59 % increase in LV mass. LV mass was high from late pregnancy (Day 14) and remained high for 2 weeks postpartum before reversal begins. HW progressively increase during pregnancy peaking in the postpartum period but not during pregnancy. Our finding is consistent with Parrott et al, 2018 [121] who reported significantly higher wet heart weight in the postpartum period but not in late pregnancy. Other studies also followed a similar pattern; however, they recorded the highest HW in late pregnancy between 17-20 days [61][303][304].

Slightly different results have also been reported on the regression of HW postpartum. Umar et al, 2012 reported that HW reverted to pre-pregnancy level in 7 days postpartum [61]. However, in our study HW remained high up to 14 days postpartum and signs of regression were only noticeable on Day 28pp. Similar findings were reported by Ventura et al, 2016 [304]. Human studies have reported sustained increased HW for varying periods between 3 months to 1 year [60][128].

Our study also confirmed that physiological pregnancy induced cardiac hypertrophy is eccentric and is a response to increased volume load [76][27]. Calculation of relative wall thickness (RWT) permits categorisation of an increase in LV mass as either concentric or eccentric hypertrophy [305]. RWT did not significantly change at all stages of pregnancy when compared to Day 1 group in our study. This indicated a properly regulated eccentric hypertrophy in pregnant mice with no signs of dilatation.

1.5.2 Potential signaling pathways involved in the regulation of cardiac hypertrophy during pregnancy and postpartum in mice

E2 and progesterone levels increased rapidly during pregnancy peaking in late pregnancy and suddenly dropped to non-pregnant level soon after parturition. Similar trends in hormone levels during pregnancy have been reported in previous studies [26][306]. Hormones are important in the regulation of physiological cardiovascular changes during pregnancy. The cardioprotective action of oestrogen has been well documented in many different experimental models of heart disease [307][308]. Progesterone has also been reported as an

important hormone required for pregnancy-induced cardiac hypertrophy in the early stages of pregnancy [302][309].

We subsequently assessed the expression of fetal gene program in physiological pregnancy groups and the pathological group. The transcript levels of *ANP, BNP and β-MHC* classical markers of pathological hypertrophy did not change significantly at all the stages of pregnancy and postpartum. However, significant increase in the expression of *BNP and β-MHC was* observed in the STAT3 KO. Other studies which quantified transcript levels of these classical markers of pathological cardiac hypertrophy supports the notion that cardiac hypertrophy due to pregnancy is physiological and does not trigger the fetal gene program [127][191].

We found that AKT expression and phosphorylation progressively increase during physiological pregnancy peaking in late pregnancy. However, the expression of AKT was reduced postpartum. This was in sync with other studies [191][306]. Conflicting results have been published especially in the late pregnancy phase with studies reporting increased phosphorylation [165], whilst others reporting reduced phosphorylation [99]. Chung et al, 2012, Lemmens et al, 2010 and others also demonstrated the importance of PI3K/AKT pathway in mediating pregnancy induced cardiac hypertrophy by looking at the downstream molecules [26][306].

Our speculation is that AKT expression could be induced by a combination of volume load and other factors such as pregnancy hormones milieu which are highly expressed during pregnancy and reduced in the postpartum phase. The activation of AKT with E2 has been described before [310][311].

STAT5 phosphorylation gradually increased during pregnancy, reaching significant level on Day 7pp. It then remained high until Day 28pp. A similar trend was also observed with STAT3. However, STAT3 phosphorylation was significant from Day 21 and remained high throughout the postpartum phase. Activation of the janise activated kinases- signal transducer and activator of transcription (JAK/STAT) has been reported to be protective to the heart in both physiological and pathological conditions [107][312]. We suggest that STAT3 and STAT5 pathways activation in the postpartum phase could be an adaptative response to maintain physiological cardiac hypertrophy. The ability of STAT3 to transduce hypertrophic signals through gp130 has been demonstrated in transgenic mice with cardiac-specific overexpression of the STAT3 gene (STAT3-TG)[313]. STAT 3-TG mice developed myocardial hypertrophy at 12 weeks of age [313]. Cardioprotective action of STAT5 has been observed in

remote ischemic preconditioning (RIPC) [314]. However, the role of STAT5 in the protection of experimental animals is still controversial [95][315].

In summary our study found that progesterone and oestrogen levels increase during pregnancy peaking in late pregnancy. The hormone levels drop immediately after parturition. Fetal gene expression is not triggered in pregnancy induced cardiac hypertrophy substantiating that pregnancy induces physiological cardiac hypertrophy. PI3K/AKT signalling pathway is activated during pregnancy and reduced in the postpartum phase. We hypothesis that PI3K/AKT signalling could be induced by pregnancy hormones which are in abundance during pregnancy and reduced postpartum. The JAK/STAT pathways are activated in the postpartum phase and could be responsible in modulating cardiac hypertrophy in the absence of AKT.

1.5.3 Histological and fibrotic changes during pregnancy and postpartum in wild type mice

Our histological analysis of pregnant mice hearts revealed that minimal interstitial fibrosis occurred in the early postpartum and reversed by Day 28pp. Our findings are in contrast with other studies which reported no presence of interstitial fibrosis in mice [61][88][316]. However, some studies in rats reported the presence of interstitial cardiac fibrosis in pregnancy [124][317].

Col I and Col III mRNA expression levels were upregulated during pregnancy and reverted to normal level postpartum. This was in synchrony with Limon-Miranda et al, 2014 [119]. However, Aljabri et al, 2011 reported that collagen isoforms gene expression in cardiac tissue did not change during pregnancy [317].

The presence of fibrosis in the early postpartum phase of pregnancy in our model could be due to prolonged volume load and hypertrophy observed until after 2 weeks postpartum. Virgen-Ortiz et al, 2009 also observed a heart with less ventricular rigidity during pregnancy [120]. This could be explained by the slightly higher Col III deposition than Col I observed in our study. Collier et al, 2012 recorded lower values of stiffness in Col III compared to Col I during single fibre deformation [318]. Nevertheless, Col III deposition was not too high to induce notable dilatation and diastolic dysfunction.

1.5.4 Cardiac proteomic analysis of pregnant mice

1.5.4.1 Overall, significantly changed proteins

The study identified only 14 proteins that were significantly changed across all time points. There were similarities in protein expression at different time points. This could be evidence that cardiac remodeling during pregnancy and postpartum is a continuous and reversable process.

Proteins involved in hormone metabolic process such as corticosteroid-binding globulin (CBG) and Transthyretin (TTR) were among the most significantly altered. CBG is synthesized in the adrenal gland and secreted into the bloodstream where it binds to glucocorticoids [319]. CBG was significantly upregulated during pregnancy and downregulated in the non-pregnant and postpartum groups in our study. Evidence from other studies suggest that CBG is a key determinant of progesterone concentrations in the maternal circulation during pregnancy [320]. TTR is also a carrier protein that transports thyroid hormones and retinol [321]. However, myocardial deposition of misfolded TTR has been implicated in different pathological diseases such as transthyretin amyloid cardiomyopathy (ATTR-CM) and hypertension and diabetes [322]. Our results showed that TTR was downregulated during pregnancy but upregulated in the early stages and postpartum.

Proteins involved in immune response and acute inflammation such as serine protease inhibitor A3C, immunoglobulin (Ig) heavy variable 1-62-2, Ig heavy chain V region AC38 205.12, Beta-2-microglobulin and dedicator of cytokinesis protein 2(Dock2) were also significantly changed. Studies have alluded on the importance of immune adaptation during pregnancy [323][324]. Dock 2 specifically regulates the migration, proliferation and activation of T cells and B cells by regulating cell skeleton restructuring [325]. Dock 2 also protects the cardiac cells from apoptosis and acute inflammation [326].

Another protein that was significantly altered was myosin-7. Myosin-7 is involved in cardiac anatomical structure, cardiac tissue development and regulation of cardiac contraction [327][328]. Our results showed that myosin-7 was upregulated only in the postpartum phase of pregnancy. This could indicate the presence of high stress on the cardiac muscle in the postpartum phase [328]. Another study also showed that cardiac myosin-7 expression could be triggered by unloading of the heart [329].

Basement membrane-specific heparan sulfate proteoglycan core protein also known as Perlecan (HSPG2) was upregulated in early pregnancy and postpartum. HSPG2 serves as an attachment substrate for cells and play essential roles in vascularization.

1.5.4.2 Cardiac hypertrophy and myofilaments in the early postpartum phase of pregnant mice

Observations from PPCM patients suggest that patients are protected throughout pregnancy and that the disease emerges mainly in the peripartum phase [152]. Evidence from our study suggest that the postpartum phase represents a state of increased proteostatic stress [330].

Functional annotation of the proteins upregulated on Day 14pp and Day 28pp shows a clear distinction of GO cellular component (GO CC), GO biological function (GO BF), and GO molecular function (GO MF). Most of the enriched GO CC from proteins upregulated on Day 14pp were sarcomere proteins, cytoplasmic proteins, actin cytoskeleton and ribosomal biogenesis complex. Increase in volume load, increases the left ventricular diastolic pressure and wall stress leading to addition of new sarcomeres in series, fiber elongation and chamber enlargement [331]. This progressive chamber enlargement will then lead to increased systolic wall stress, wall thickening and eccentric hypertrophy which normalizes the systolic stress.

Data from previous models of cardiac hypertrophy also confirm the upregulation of proteins involved in muscle contraction and myofilament movement such as Myl2, Tpm1, Tnnc1, Tnni3, Myl3, Myh7, Tmod1 and Actc1 [332][333]. In cardiac hypertrophy, the size of the cardiomyocyte increases, and there is heightened organisation of the sarcomere [334]. The sarcomere is the basic contractile unit of muscle fibre which is composed of the actin and myosin filaments [335]. According to the sliding filament theory, the active force for contraction of an individual sarcomere is an actin filament slide past the myosin filaments [335][336].

Cardiac hypertrophy in the early postpartum phase was also confirmed by echocardiography measurements conducted in this study (**Figure 19**). Similar findings were reported by Ventura et al, 2016 [304], whilst Umar et al, 2012 reported that hypertrophy reverted to pre-pregnancy level in 7 days postpartum [61]. Human studies have reported sustained increased HW in the postpartum period for varying periods between 3 months to 1 year [60][128].

Ribosome content and ribosomal biogenesis proteins such as Rps5, Rps19, Rps11 and Rps10 were also raised on Day 14pp. Growth of cardiac muscle cells during left ventricular hypertrophy (LVH) results from an increased accumulation of cellular protein due to an accelerated rate of protein synthesis [337]. It has been clearly demonstrated that ribosome biogenesis stimulates protein synthesis, thereby leading to cell growth [338][339]. Increased rates of protein synthesis in cardiac myocytes have been shown to correlate with an increase of activity of translation initiation factors and with a concomitant rise in the rate of translation initiation [339]. Specifically, during muscle hypertrophy, the amount of protein synthesis per unit RNA (translation efficiency) and the total ribosomal content (translation capacity) increase within muscle fibres [340].

Given that ribosome biogenesis represents the most energy consuming process in eukaryotic cells [341][342]. Mitochondrial components such as Cox 5a, Cox 6c and Cox 6b1 were also upregulated in the early postpartum phase. These are important enzymes necessary to maintain cardiac energy-production capacity of the overloaded hearts [343].

Taken together the proteome on Day 14pp indicated a stage involving increased protein synthesis, movement, and morphological changes that requires reorganisation of actin filaments.

1.5.4.3 Activation of Ubiquitin proteasome system (UPS) activation in the early postpartum phase of pregnant mice

Psme1, Psma5 and Skp1a were some of the other proteins that were upregulated on Day 14pp when compared to late pregnancy. Proteasomes are protein complexes which degrade unneeded or damaged proteins by proteolysis, a chemical reaction that breaks peptide bonds. Ubiquitin proteasome system (UPS) plays a critical role in cardiac structural remodeling by removing unwanted intracellular proteins and is involved in protein quality control [344][345].

Lorga et al, 2012 found that pregnancy is associated with decreased ubiquitin-proteasome proteolytic activity in pregnant mice and in cells [303]. Reduced level of ubiquitin-proteasome activity during pregnancy coincided with increased AKT expression. Studies have shown that ubiquitin protease specific-14 (USP14) a major deubiquitinating enzyme that regulates the UPS, is a substrate of AKT [346]. USP14 is a negative regulator of the UPS and can be activated

by AKT, we reasoned that AKT-mediated activation of USP14 might lead to inhibition of the UPS and generally enhance the stability of many important proteins during pregnancy [347].

Haghikia et al, 2012 also described a link between STAT3 and the UPS in mice [348]. Reduced STAT3 protein levels increased miR-199a expression which then subsequent down-regulation of ubiquitin conjugating enzyme E2I (Ube2i) and ubiquitin conjugating enzyme E2 G1 (Ube2g1) [348]. Phosphorylation of STAT3 (p-STAT3) was also found to stimulate proteolysis by activation of UPS in cancer cachexia study [349]. This also confirmed the important role of STAT3 as a factor controlling post-natal cardiac integrity.

Activation of UPS in the early postpartum phase together with cardiac hypertrophy seems counterintuitive. However, due to prolonged increase of workload, the heart reacts and increases in size, a reaction that represents an adaptive response to normalize wall stress and compensate for the increased hemodynamic load [350]. Increased cardiac wall stress from overload automatically creates an increase in protein synthesis [339]. Cellular stress also increase the production of denatured proteins, which must be degraded to avoid the activation of pro-apoptotic signals [339][351]. New evidence also suggests that UPS attends to the cell growth, favouring protein synthesis, subsequently evolving in left ventricular hypertrophy [352][353]. The suspected mechanism involve the degradation of repressors of hypertrophy, such as the inducible cyclic AMP early repressor (ICER) [354].

1.5.4.4 Proteomic expression driving cardiac reverse remodeling in the postpartum phase of pregnant mice

Several studies confirm the reversibility of physiological cardiac remodeling induced by pregnancy. However, the mechanisms of response to volume unloading have been studied less, probably because this condition is physiologically less relevant. However, the recent use of left ventricular assist system (LVAS) in clinical practice for patients with advanced heart failure have highlighted the importance of unloading response [329].

We observed a shift from hypertrophic and contraction proteins on Day 14pp to upregulation of proteasome complex proteins, endopeptidase activity proteins and spliceosome activity proteins on Day 28pp. We speculate that upregulation of UPS on Day 28pp could be a mechanism induced to stop and/or reverse the cardiac hypertrophy caused by pregnancy and early postpartum stress.

Protein turnover represents the balance between protein synthesis and degradation. The balance between protein synthesis and protein degradation determines if the heart will atrophy, hypertrophy, or neither [97]. It can be controlled quantitatively, for instance by an activation of protein synthesis during cardiac hypertrophy or by the activation of protein degradation during ventricular unloading [351]. Hypertrophy regression may occur if the protein turnover balance is in favor of protein degradation [351][355].

Proteasome-mediated proteolysis have been extensively characterized in skeletal muscle, in conditions of muscle wasting, atrophy, and cachexia [356][357]. In all types of atrophying muscle, the ubiquitin–proteasome system is activated, and it catalyses the degradation of the bulk of muscle proteins, especially myofibrillar components [358][359]. Previous studies in skeletal muscle atrophy have also shown that activation of the UPS is associated with an increase in mRNA levels of ubiquitin, ubiquitin conjugating enzymes, ubiquitin ligases, and components of the proteasome [355].

Whilst no study that directly assessed activation or impairment of the UPS in PPCM patients was found , evidence is rapidly mounting to link proteasome dysfunction with a multitude of cardiac diseases, including ischemia, reperfusion, atherosclerosis, hypertrophy, heart failure, and cardiomyopathies [345][360]. A consistent finding among all of the studies is the observation that polyubiquitinated proteins are increased in failing hearts compared with control hearts [345][361].

UPS have also been demonstrated to selectively degrade oxidatively damaged proteins [362][363]. It has been shown that various forms of oxidized proteins are degraded at faster rates than their native counterparts and inhibition of the proteasome stabilizes oxidized proteins in intact cells or in cell-free systems [363][364]. Accumulation of reactive oxidative species (ROS) forms the bases of a crucial pathway in PPCM pathogenesis. Elevated oxidative stress instigate the cleavage of hormone prolactin (PRL) by ROS-activated Cathepsin D into a smaller 16 kDa form which has detrimental effects on cardiomyocyte metabolism and the microvasculature [165][365].

In vitro and animal model studied by Haghikia el at, 2011, has also shown that knock-down of Ube2i and Ube2g1 impairs cardiomyocyte ultrastructure, suggesting a causal link between defective protein clearance and PPCM phenotypes [348]. This also further strengthens the suggestion that insufficient defence against oxidative stress plays an important role in PPCM pathogenesis.

1.5.4.5 Transcriptional regulatory network of physiological cardiac hypertrophy in the postpartum phase of pregnant mice

Our study identified several proteins upregulated on Day 14 and Day 28 postpartum. These proteins include mainly proteins involved in proteins synthesis, ribogenesis, energy metabolism, ubiquitin proteasome pathway, and signaling pathways. The question is how the pregnancy stress is perceived and converted into intracellular signals and how these signals change the transcriptional program that eventually leads to cardiac remodeling. We assume that cardiac transcription factors play a role in regulating the expression of cardiac proteins in the postpartum.

Transcription factors are nuclear proteins that bind promoter regulatory elements to activate or repress gene expression [366]. SP1, HNF4A, GATA1, IRF1 and IRF3 were the highly ranked transcription factors predicted to regulate the expression of proteins upregulated on Day 14pp. Day 14pp was a hypertrophic stage characterized by upregulation of protein synthesis, muscle contraction and myofilament and sarcomeric reorganization. Increasing evidence supports the involvement of SP1 in cardiac hypertrophy and muscle contraction [367][368][369]. Contradicting findings have been reported on whether SP1 is pro- or anti-hypertrophy. Wang et al, 2018 and Long et al, 2019 found that SP1 induces cardiac hypertrophy by upregulating the expression of long non-coding RNA (lncRNA) in angiotensin-II (AngII) induced cardiac hypertrophy model [370][371]. On the other hand, Dong et al, 2017 reported that SP1/SIRT1 signaling activated by flavonol (−)-epicatechin (EPI) blocked Ang II induced cardiac hypertrophy and the expression of fetal gene program [372]. SP1 has also been reported to be involved in protein synthesis through the activation of mammalian target of rapamycin (mTOR) signaling [373]. The actual role of SP1 in pregnancy heart need further investigations.

HNF4A, IRF1 and IRF3 have also been found to be regulators of cardiac hypertrophy in transverse aortic constriction (TAC) and Ang II model of cardiac hypertrophy both in vitro and in vivo [374]. IRF1 protein expression increases progressively during the early phase of hypertrophy development in TAC, and then dramatically decreases to below baseline levels during the later stage [374]. A similar trend has also been observed in patients with dilated and hypertrophic cardiomyopathy [374]. This could indicate that IRF1 may be involved in the compensatory stage of cardiac hypertrophy. In contrast, Lu et al, 2013 observed increased phosphorylation of IRF3 invivo model of chronic pressure overload invivo model[375].

YY1, NFYA, TAF1, NFYB, KAT2A and MAX were the highly ranked transcription factors that regulated proteins that were upregulated on Day 28pp. YY1 is a ubiquitous transcription factor that regulates expression of multiple genes. YYI is a transcription factor shown to act largely as a repressor of transcription of muscle genes [376][377]. Several studies have confirmed that YY1 protects the heart and cardiomyocytes from pathological cardiac hypertrophy and to provide valuable targets for the prevention of cardiac disease [378][379]. Tan et al, 2019 has also found that YY1 suppresses dilated cardiomyopathy and cardiac fibrosis by upregulating Bmp7 and downregulating Ctgf gene expression [380]. Another study also reported that YY1 prevents up-regulation of the fetal isoforms of gene expression in response to alpha- and beta-adrenergic stimulation by binding to and retaining in the nucleus class II histone deacetylases (HDACs) [378].

KAT2A, NFYA, NFYB and TAF 1 are also known repressors of cardiac hypertrophy [381][382][383]. We speculate that YY1 transcription factor in the late postpartum could be involved in the regulation and reversal of cardiac hypertrophy. However, further analysis is required to confirm the actual role and mechanism involved.

1.6 Conclusion

We conclude that pregnancy stress induced hemodynamic changes that led to cardiac remodeling in physiological pregnant mice. Some of the notable changes included increased SV and increased LVEDV. LVID also increased significantly from late pregnancy. Another striking observation was that pregnancy induced eccentric hypertrophy was sustained for a period over 2 weeks. Which was longer than previously reported.

We also conclude that AKT signaling could be the pathway involved in regulating physiological cardiac hypertrophy during the gestation period. The JAK/STAT takes over in the postpartum phase when AKT levels are low.

We also conclude that GDF-15 could be involved in the regulation of cardiac hypertrophy during pregnancy in mice. However, cardiac expression was significantly reduced in STAT3 KO mice.

Little but significant fibrosis occurred in the postpartum phase of pregnant mice which was reversed in late postpartum group.

We also conclude that they are similarities in the protein expressions at different time points during pregnancy and postpartum. However, there is an expression difference between the late pregnancy and postpartum groups. The proteins expressed on Day 14pp supported the

observation that cardiac hypertrophy is sustained for a long period postpartum. Protein expression on Day 28 pp showed the upregulation of the UPS. This could be involved in the reverse remodeling of cardiac hypertrophy and fibrosis. However, further studies are required to assess the actual role played by the UPS in the pregnancy heart and PPCM.

CHAPTER 5

Exploring the potential role of pregnancy hormones in the modulation of cardiac hypertrophy invitro

1.1 Introduction

During pregnancy the heart develops cardiac hypertrophy through a complex process involving signaling pathways, cell structural changes and regulation by sex hormones [88][76][302]. Cardiac hypertrophy is regarded as a compensation mechanism to overcome the increased workload when the stress or injury is transient. However, if the cardiac stress persists for a long time, the compensatory state can lead to maladaptive conditions.

Oestrogen and progesterone increase during pregnancy and could possibly play a role in the regulation of pregnancy induced cardiac hypertrophy. Animal studies support the antihypertrophic effect of oestrogen [271][272] and the prohypertrophic effect of progesterone [26][267]. Although studies have provided valuable information on the effect of oestrogen on cardiac hypertrophy, it is important to consider that most studies were performed in pathological conditions or independent of the other important pregnancy hormones like progesterone.

The heart also expresses genes of peptide growth factors/cytokines such growth differentiation 15 (GDF-15) in response to cardiac hypertrophy [234][384][385][386]. GDF-15, is synthesized as a prohormone and processed to become active hormones [385][387]. GDF 15 has been found to be a useful biomarker of response to treatment and prognosis in cardiovascular diseases [384][235].

β-adrenergic receptors (βARs) are the members of G-protein coupled receptors (GPCRs) family that are traditionally activated by the catecholamine hormone epinephrine and neurotransmitter norepinephrine [388][389]. βAR signalling promotes hypertrophy and apoptosis of cardiomyocytes [389]. Isoproterenol (Iso) is a synthetic β-adrenoceptor agonist which has been used to establish models of cardiac hypertrophy invivo and invitro [388].

In the present study we carried out a systematic invitro analysis on H9C2 cell line to understand the role of 17β-estradiol (E2) in combination with progesterone on the regulation of physiological and pathological cardiac hypertrophy. We also assessed the involvement of pregnancy hormones in the expression of GDF-15.

1.2 Materials and Methods

The study was conducted with adherent H9C2 cell line created from rat embryonic cardiomyocytes (ATCC, Manassas, VA, USA). Treatments were conducted between passages 18-23 on coverslips in 12 well plates grown to 60–70% confluency. All the treatments were done in triplicates and the experiments were repeated three times. Actin immunofluorescence staining was done using phalloidin-Alexa-conjugated antibody (Cat# A12379, Thermofisher Scientific) for cell morphology measurements. Nine random fields were captured per coverslip with a Zeiss Axiovert Fluorescence inverted microscope (AxioVision version 4.8.2) at X20 magnification.

Total RNA and proteins from H9C2 cells were extracted from cell pellets. The qPCR was performed with the Corbett Research Rotor Gene-6000 (Life Science, USA) using the Sybr green PCR master mix (Cat# 4367659; Applied biosystems). Primer sequences are listed in **Table 7.**

The proteins were detected with primary antibodies against the following proteins: *AKT, STAT 3, STAT5, p-AKT^{ser473}, p-STAT3^{Tyr705}, p-STAT5^{Tyr694} and Glyceraldehyde 3-phosphate dehydrogenase (GAPDH)* (for references and dilution refer to **Table 5**).

1.3 Statistics

Results are presented as mean± SEM unless otherwise stated. Statistical analysis was carried out using Graph Pad Prism 8.0. One-way ANOVA, and probability values were calculated by the Fisher method. A value of $p<0.05$ was accepted as statistically significant

1.4 Results

1.4.1 ISO induced hypertrophy in H9C2 cell line in a dose-dependent manner

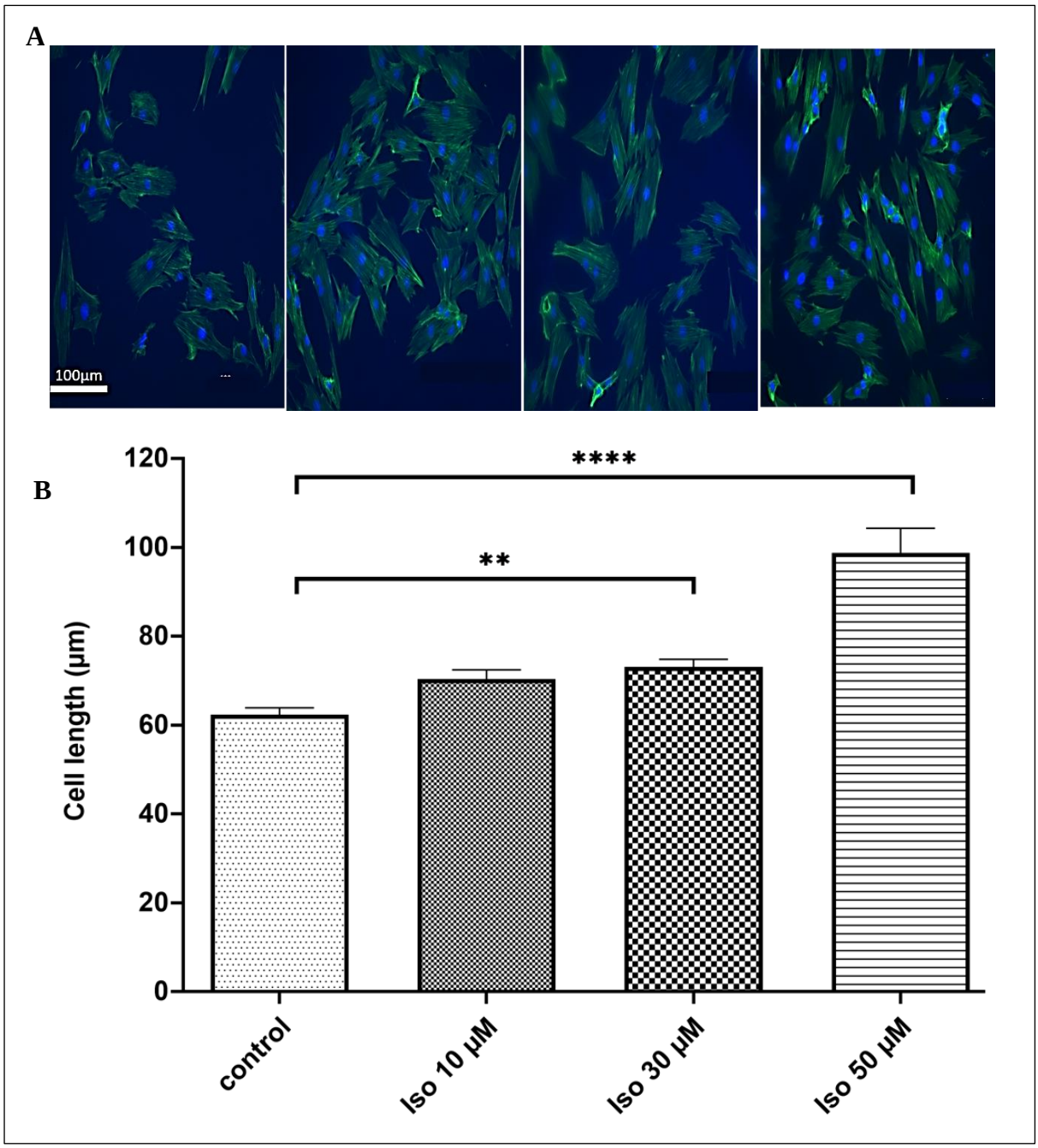

Figure 39: Isoproterenol induced cardiac hypertrophy in a dose depended manner

***A**: H9C2 cardiomyocytes were incubated in different doses of isoproterenol (Iso) for 24 hours followed by immunofluorescent staining for alpha-actin (green). Nuclei were stained with DAPI (blue). X20 magnification, Scale =100* µm*. Experiments were conducted in triplicate and were repeated 3 times. Nine random images were captured per each slide. **B**: Cell sizes were measured by Image J software. Data presented as means ± SEM, p< 0.05 was considered statistically significant difference. Iso-Isoproterenol*

We tested the hypertrophic model by treating the H9C2 cell line with increasing doses of isoproterenol (Iso) for 24 hours. **Figure 39** illustrates that Iso induces cardiac hypertrophy in a dose depended manner. 50µm Iso induced the highest increase of cell size and was selected for further treatments.

1.4. 2 Effect of oestrogen and progesterone on the regulation of cardiac hypertrophy invitro

Cardiomyocytes (H9C2) were treated with progesterone, 17β-oestradiol, or a combination of both progesterone and 17β-oestradiol to determine the effect of pregnancy hormones on hypertrophy. Oestrogen did not change the cells' size. However, progesterone alone significantly increased the cells' size. When combined 17β-oestradiol and progesterone no change in cell size was observed. 17β-oestradiol hindered the effect of progesterone.

17β-oestradiol and progesterone were then used in combination with Iso. 17β-oestradiol again hindered the effect of Iso to induced cell hypertrophy. However, progesterone did not change the effect of Iso on cardiomyocytes, neither augmented the increase in cell size. Combining progesterone, 17β-oestradiol and Iso again did not change the size of cardiomyocytes. **Figure 40A** shows treated H9C2 cells stained with phalloidin and emerged with Dapi stain.

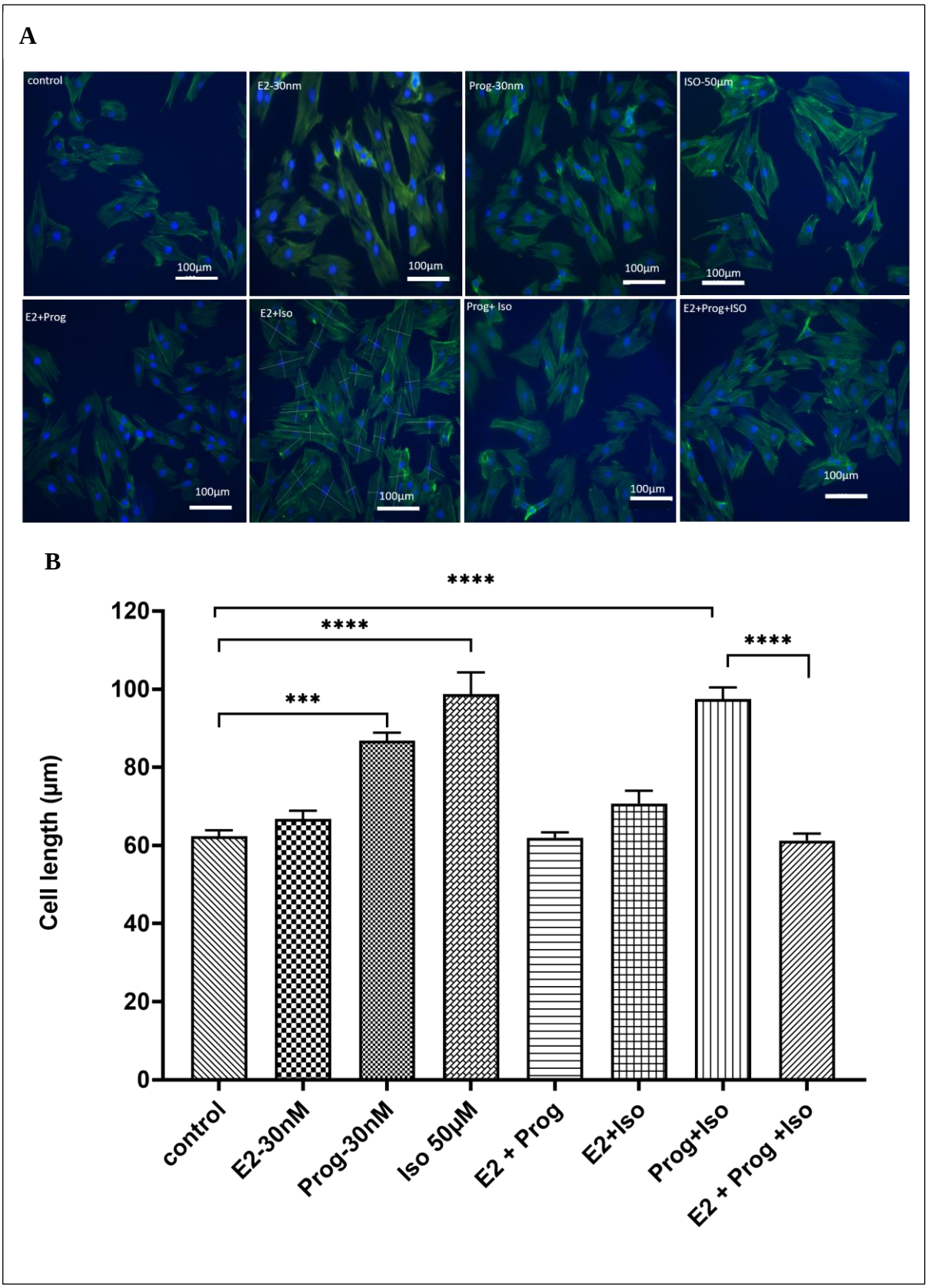

Figure 40: Effect of oestrogen and progesterone on H9C2 isolated cardiomyocytes

A: *representative fluorescent microscope images of H9C2 cardiomyocytes stained for alpha-actin (green). Nuclei were stained with DAPI (blue). X20 magnification, scale 100µm. Experiments were conducted in triplicate and were repeated 3 times. Nine random images were captured per each slide.* ***B:*** *Cell sizes were measured by Image J software. Nine random*

*images were captured per each slide and all visible complete cells were measured. Data presented as means ± SEM, p < 0.05 was considered statistically significant difference. ***=p <0.001; ****= p<0.0001*

1.4.3 Fetal gene program in response to hormones and isoproterenol treatment

Figure 41-43 shows the expression of fetal genes in cardiomyocytes in response to Iso and pregnancy hormones. Treatment combinations are as shown on the Figure X-axis. Oestrogen and progesterone did not induce fetal gene expression. However, Iso induced the expression of *BNP* and *β-MHC*. The expression of *BNP* and *β-MHC* induced by Iso was abrogated by oestrogen but not by progesterone. ANP expression was low in Iso treated cells. However, ANP expression increased in the presence of E2.

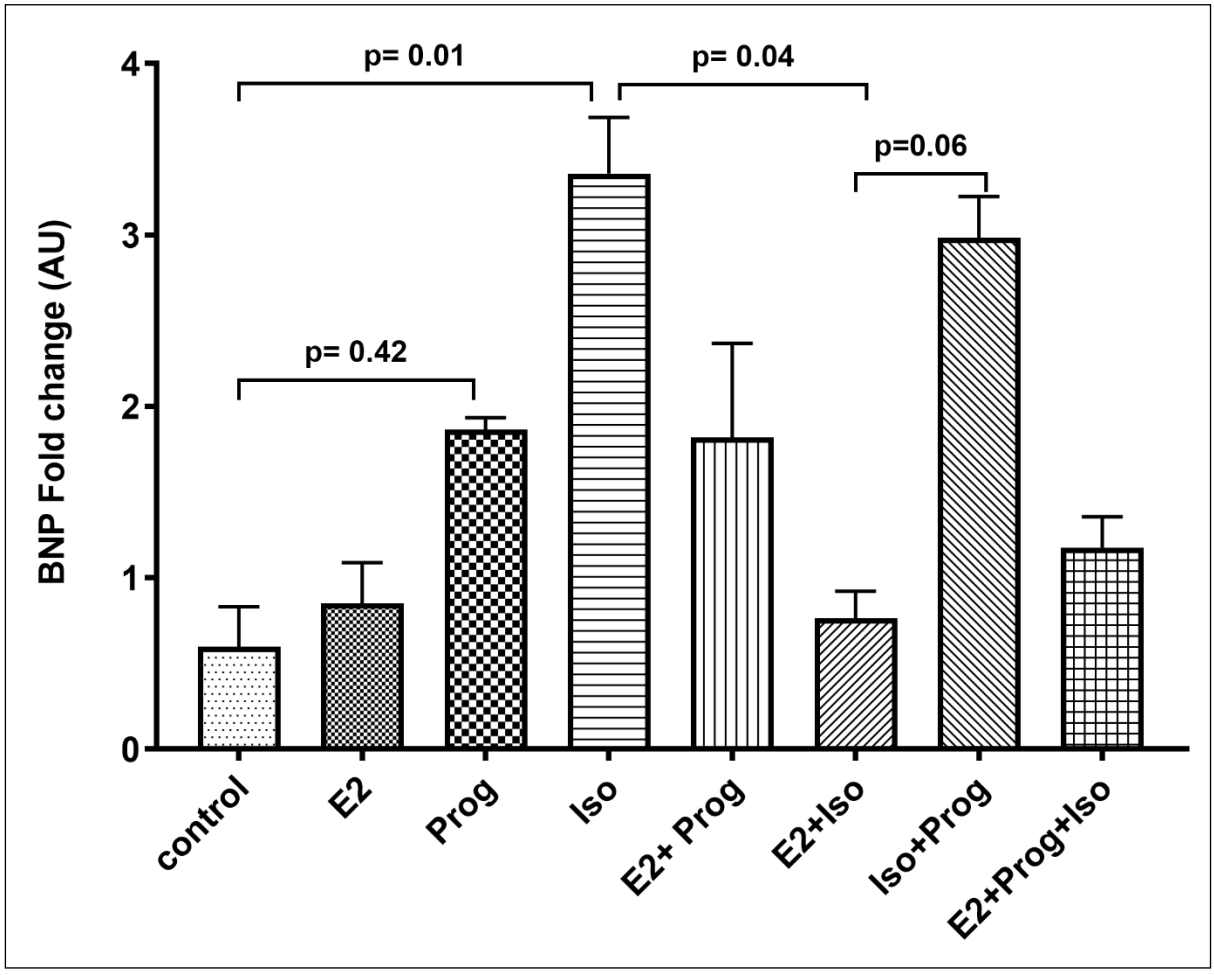

Figure 41: mRNA expression of Brain Natriuretic Peptide in H9C2 cells treated with hormones

Quantitative RT-PCR was performed in singlets and repeated 5 times. 30nM E2, 30nM Prog and 50µM Iso were used to treat H9C2 cells individually or cotreatment. Levels of all candidate genes were normalized by GAPDH. p < 0.05 was considered significantly different. The graphs display fold change calculated using the Livak method $2^{-\Delta\Delta CT}$ [252] *where CT-cycle threshold value. BNP- Brain Natriuretic Peptide.*

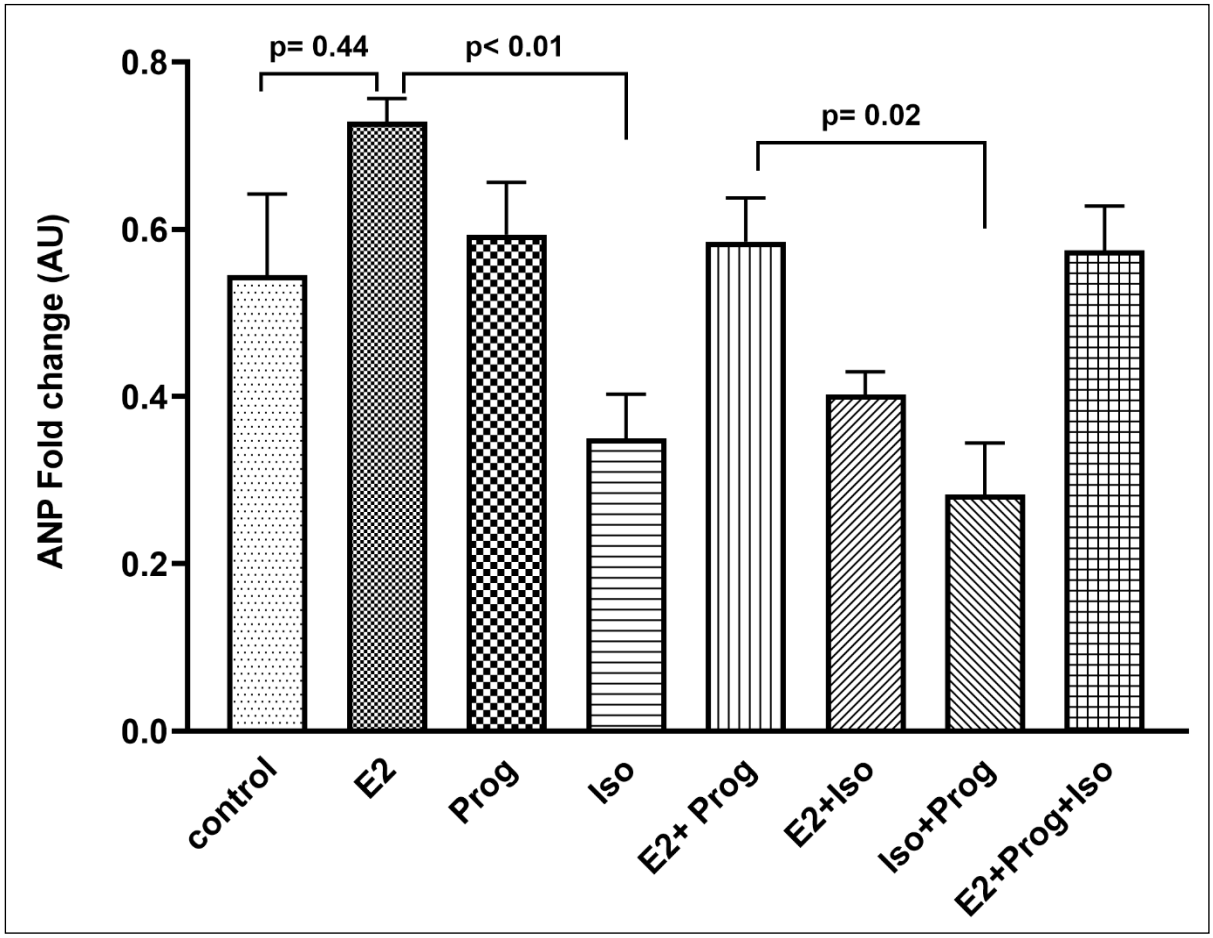

Figure 42: mRNA expression of *Atrial Natriuretic Peptide* in H9C2 cells treated with hormones

Quantitative RT-PCR was performed in singlets and repeated 5 times. 30nM E2, 30nM Prog and 50µM Iso were used to treat H9C2 cells individually or cotreatment. Levels of all candidate genes were normalized by GAPDH. p < 0.05 was considered significantly different. The graphs display fold change calculated using the Livak method $2^{-\Delta\Delta CT}$ [252] *where CT-cycle threshold value. ANP-Atrial Natriuretic Peptide.*

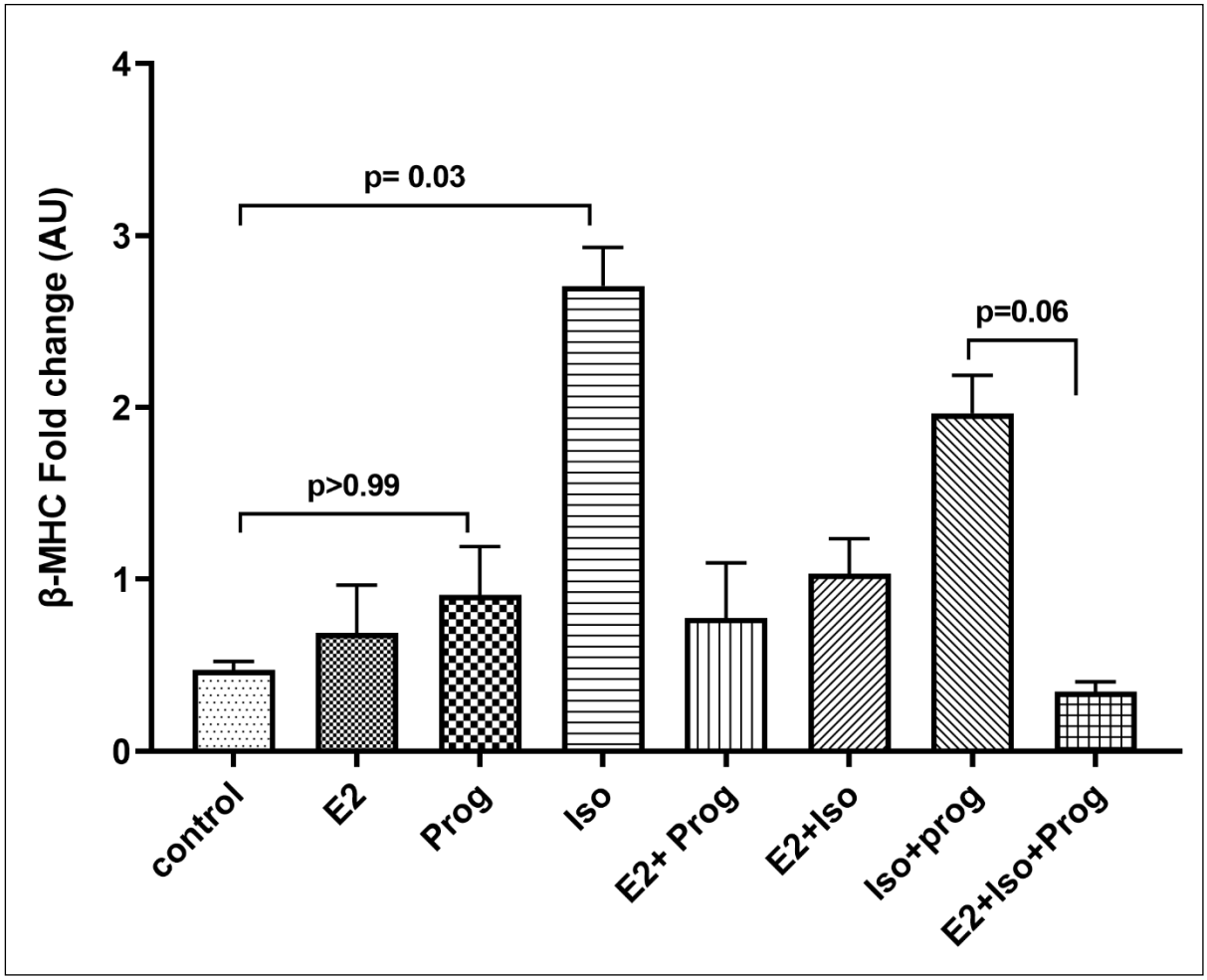

Figure 43: mRNA expression of beta myosin heavy chain in H9C2 cells treated with hormones

Quantitative RT-PCR was performed in singlets and repeated 5 times. 30nM E2, 30nM Prog and 50µM Iso were used to treat H9C2 cells individually or cotreatment. Levels of all candidate genes were normalized by GAPDH. p < 0.05 was considered significantly different. The graphs display fold change calculated using the Livak method 2^-ΔΔCT [252] *where CT-cycle threshold value. β-MHC- beta myosin heavy chain.*

1.4.4 Mechanisms employed by oestrogen in the regulation of physiological and pathological hypertrophy

To assess the mechanisms induced by the hormones. We measured the expression of AKT, STAT 5 and STAT 3 proteins. The level of AKT was significantly reduced by Iso when compared to E2 treatment. We did not find any significant difference in the expression of STAT 3 and STAT 5 in cells treated with either E2 or progesterone **(Figure 44&46).** When cells were cotreated with Iso and E2 the level of AKT remained unaltered. Progesterone did not show any effect on AKT expression either alone or combined with Iso.

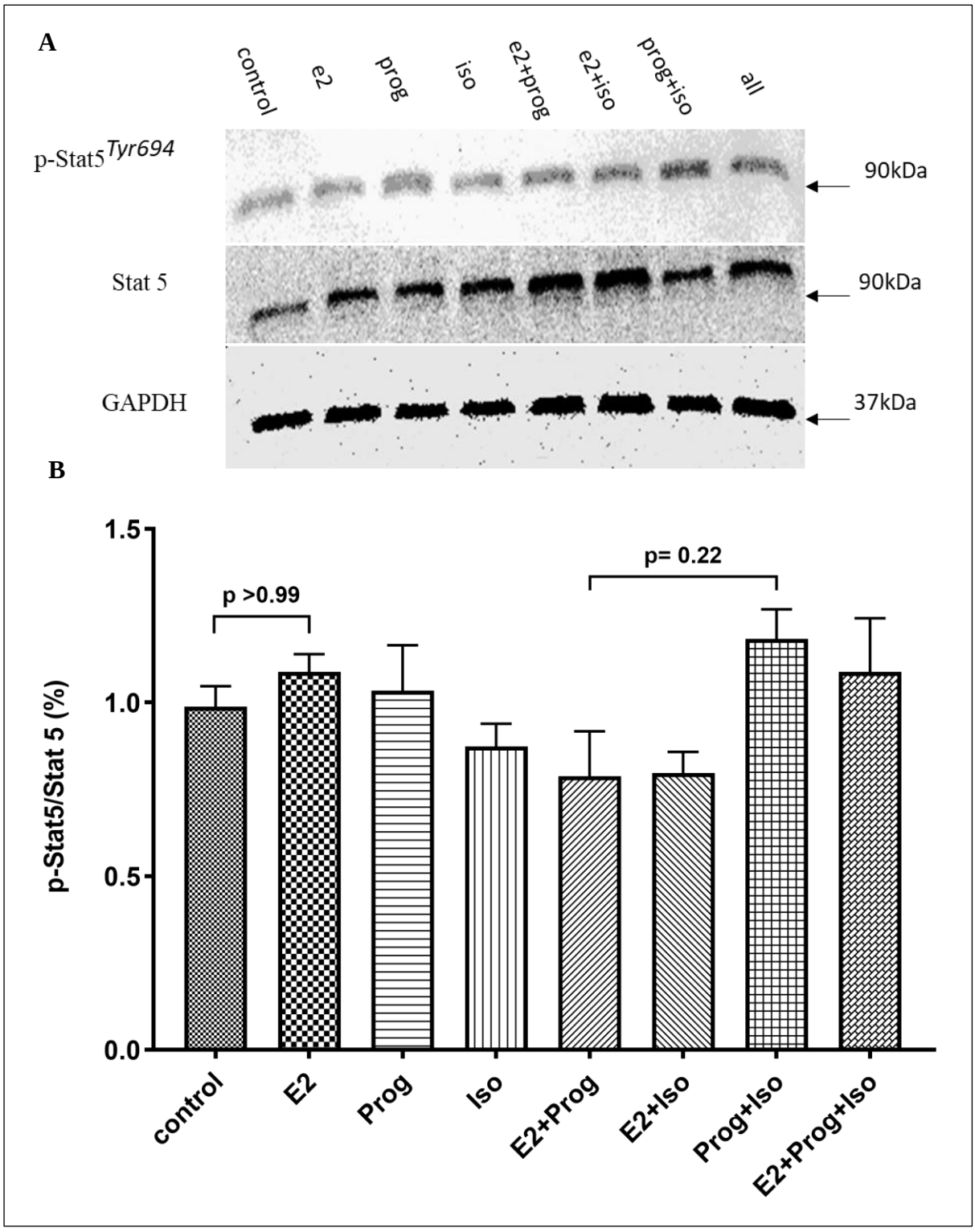

Figure 44: Expression and activation of STAT5 in oestrogen and progesterone treated H9C2 cells

***A**: Western blot analysis of the activation of STAT5 by 17 β oestradiol, progesterone and Iso.* ***B**: Bar represents percentage activation and representative blots are also shown per each protein. Experiments were conducted in duplicates and were repeated thrice.*

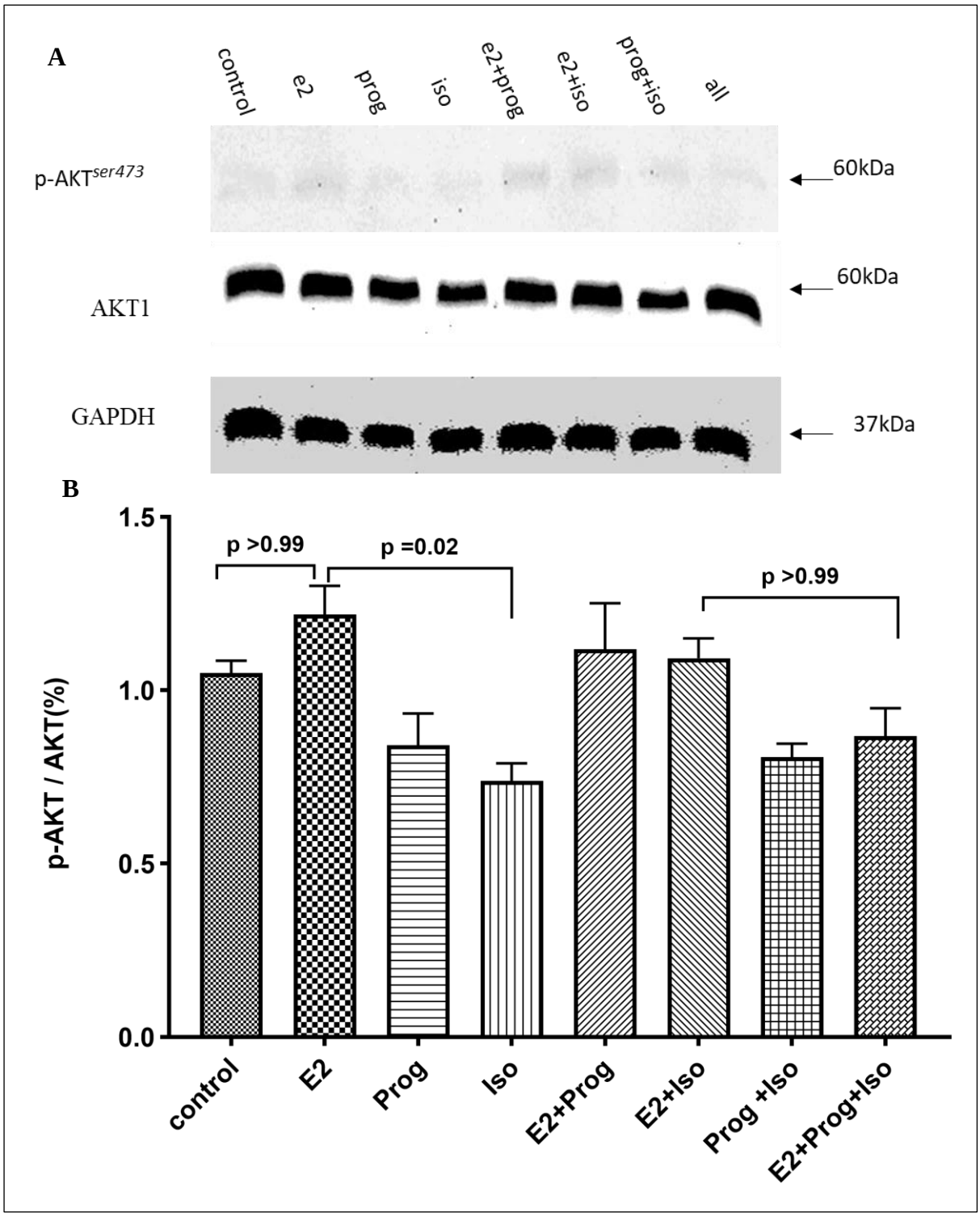

Figure 45: Expression and activation of AKT in oestrogen and progesterone treated H9C2 cells

***A**: Western blot analysis of the activation of AKT by 17 β oestradiol, progesterone and Iso.* ***B**: Bar represents percentage activation and representative blots are also shown per each protein. Experiments were conducted in duplicates and were repeated thrice*

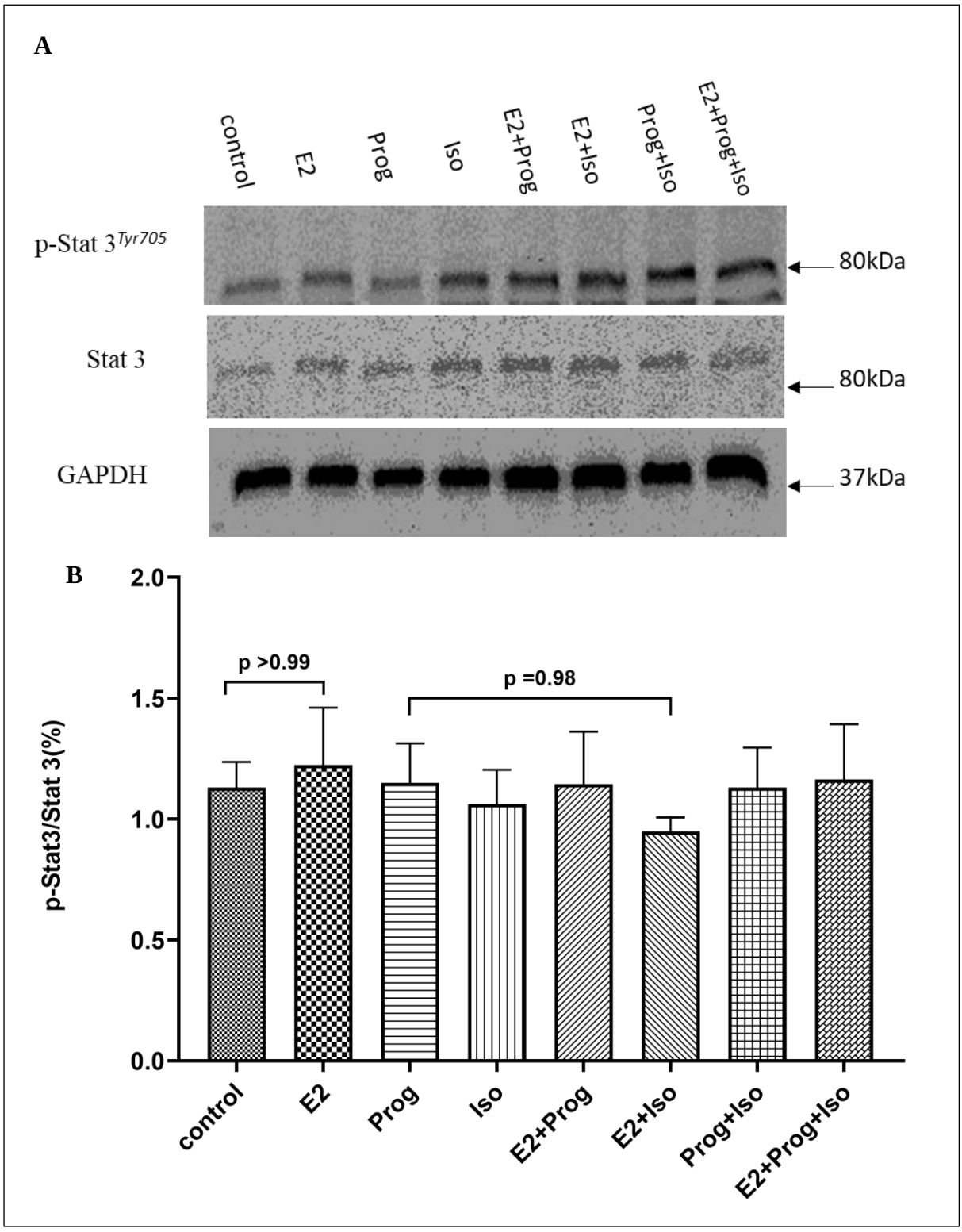

Figure 46: Expression and activation of STAT3 in oestrogen and progesterone treated H9C2 cells

***A**: Western blot analysis of the activation of STAT3 by 17 β estradiol, progesterone and Iso. **B**: Bar represents percentage activation and representative blots are also shown per each protein. Experiments were conducted in duplicates and were repeated thrice.*

1.4.5 Involvement of pregnancy hormones in modulating GDF-15 mRNA expression in H9C2 cell line

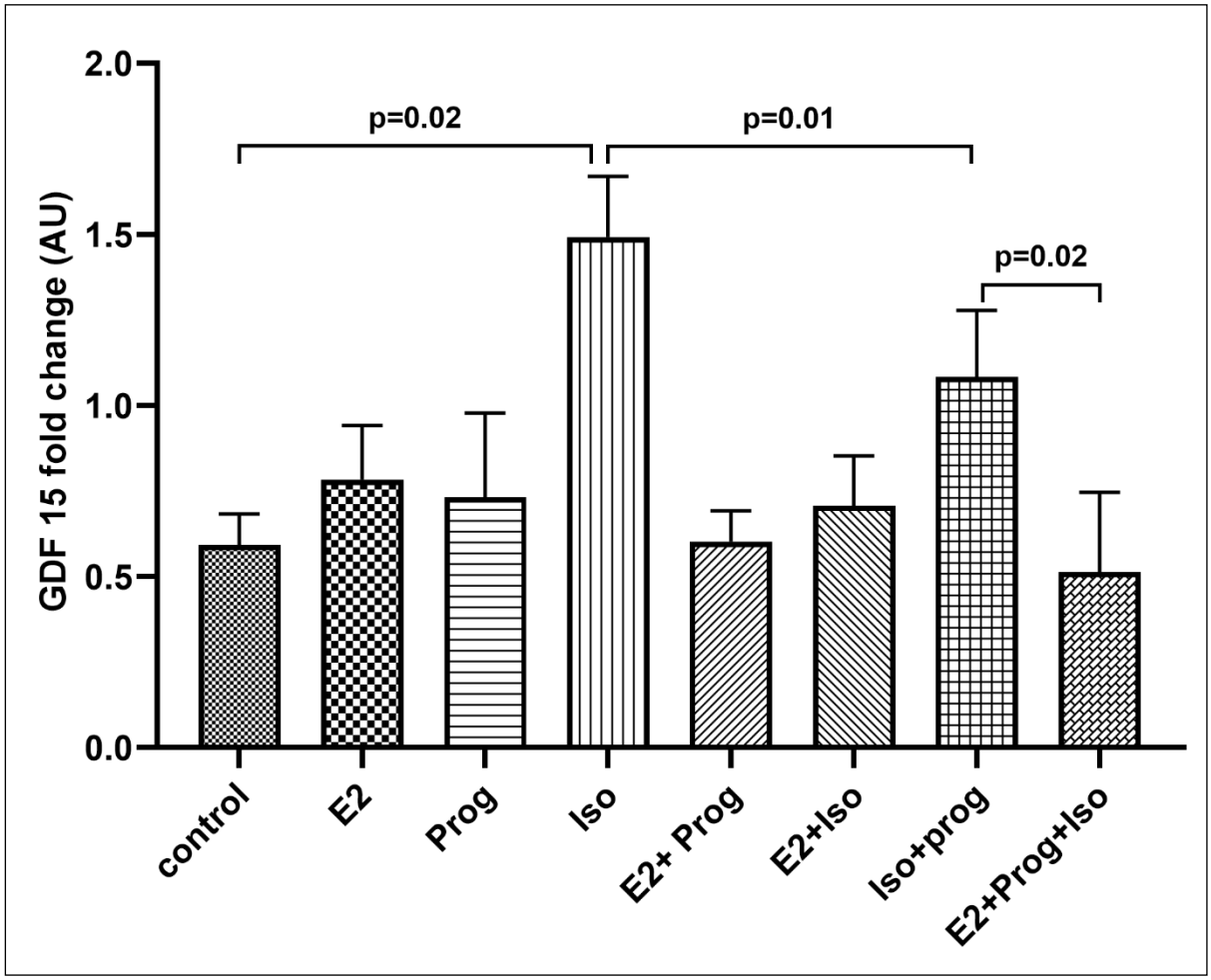

Figure 47: GDF-15 mRNA expression in H9C2 cells treated with pregnancy hormones

Quantitative RT-PCR was performed in singlets and repeated 5 times. 30nM E2, 30nM Prog and 50µM Iso were used to treat H9C2 cells individually or cotreatment. Levels of all candidate genes were normalized by GAPDH. p < 0.05 was considered significantly different. The graphs display fold change calculated using the Livak method $2^{-\Delta\Delta CT}$ [252] *where CT-cycle threshold value. GDF-15- growth differentiation 15.*

Iso also induced increased expression of GDF-15. The effect of Iso on GDF-15 mRNA expression was also hindered by cotreatment with E2. Single treatment with progesterone or E2 did not have any effect on the expression of GDF-15.

1.5 Discussion

1.5.1 Combined effect of progesterone and oestrogen on the regulation of cardiac hypertrophy in H9C2 cell line invitro

To explore the potential role of pregnancy hormones on the modulation of cardiac hypertrophy, we treated H9C2 cells with E2 and progesterone as single treatments and in combination. Our results showed that E2 did not induce cardiac hypertrophy whilst progesterone induced cardiac hypertrophy. Assessment of fetal gene expression on cardiomyocytes treated with progesterone indicated that progesterone induced physiological cardiac hypertrophy. Similar results were published by Chung et al, 2012 [390]. Previous studies showed that progesterone can cause cardiomyocytes hypertrophy by increasing proteins synthesis and activation of calcineurin [26][267][391]. Co-treatment of H9C2 cells with E2 and progesterone hindered the pro-hypertrophic effect of progesterone. These results showed that changes in pregnancy hormones may contribute to pregnancy-induced cardiac adaptation. Several studies support that pregnancy hormones play a vital role in maintenance of physiological cardiac remodeling [268][269][270].

We then demonstrated the effect of E2 and progesterone on Iso induced hypertrophy in cardiomyocytes (H9C2 cell line). Iso is commonly used to induce pathological hypertrophy in H9C2 cells. We attest that Iso induced increase in H9C2 cell size in a dose dependent manner. Iso treatment was also significantly associated with marked increase in hypertrophy markers BNP and *β-MHC* expression confirming pathological hypertrophy. Previous studies have also confirmed the activation of fetal gene program by Iso in cardiomyocytes [388][392].

We observed that E2 abrogated both Iso and progesterone induced hypertrophy in H9C2, marked by both reduction in cell size and suppression of the fetal gene expression. These findings have been reported by other studies, emphasising the anti-hypertrophic role of oestrogen [393][308][394]. We observed that the anti-hypertrophic effect of E2 was effective on both physiological and pathological hypertrophy.

AKT expression level was slightly reduced in cells treated with Iso and progesterone when compared to control. The activation of AKT was restored when Iso and progesterone were co-treated with E2. The activation of AKT with E2 has been described in previous [310][311].

We would like to speculate that E2 exerts its antihypertrophic effect through activation of PI3K/AKT signaling pathway. PI3K/AKT pathway seems to regulate both physiological and pathological hypertrophy. However, studies involving PI3K catalytic isoforms in mice indicate

that PI3K (p110γ) mediates pathological cardiac hypertrophy whilst PI3K (p110α) induces physiological cardiac hypertrophy [102][395][396]. Wende et al, 2015 also argue that long-term activation of the PI3K/AKT pathway in the adult heart may contribute to pathological left ventricular hypertrophy by reducing mitochondrial oxidative capacity [397]. It is not known whether E2 regulates the expression of both the isoforms and how the expression is regulated.

1.5.2 Involvement of pregnancy hormones in modulating GDF-15 expression

GDF-15 mRNA expression was significantly associated with E2 level during pregnancy in mice. We therefore speculated that E2 may be involved in the secretion of GDF-15 during pregnancy induced cardiac hypertrophy. We therefore quantified GDF-15 mRNA expression in cardiomyocytes treated with hormones and Iso to assess the involvement of E2 and progesterone in the modulation of cardiac expression of GDF-15.

We observed that Iso instead of E2 nor progesterone induced increase expression of GDF-15 mRNA. Our finding supports the notion that GDF-15 maybe a stress induced growth factor and its expression level is increased in response to either pathological stress or just biomechanical stress. Other experimental studies confirmed cardiomyocytes express GDF-15 in response to mechanical stretch, ischaemia, oxidative and nitrosative stress [228][398][227]. Frank et al, 2008 found that GDF-15 production is favoured in stretched cardiomyocytes [228].

1.6 Conclusion

We conclude that pregnancy hormones play a crucial role in the regulation of cardiac hypertrophy. Progesterone induces physiological cardiomyocytes hypertrophy without expression of fetal genes. However, E2 demonstrated to have antihypertrophic effect against both physiological and pathological hypertrophy. We speculate that E2 exerts its effect through activation of the PI3K/AKT signaling pathway. Hence, E2 could be playing 2 roles to the pregnancy heart, first to regulate physiological hypertrophy and protecting against pathological hypertrophy.

CHAPTER 6

Echocardiography assessments of healthy pregnant mothers and the expression of growth differentiation 15 (GDF-15) in Peripartum Cardiomyopathy (PPCM) patients

1.1 Introduction

Cardiovascular physiological changes that occur during pregnancy are usually well tolerated in many healthy women and resolve without causing any complications [15]. However, the changes may lead to decompensation in some previously healthy women with pre-existing co-morbidities or unmasking of pre- pregnancy disease. Cardiovascular disease in pregnancy is the leading cause of maternal mortality, affecting 1-4% of every pregnancy [399][280]. Approximately 1 in 1000 women in South Africa will have trouble remodeling the heart in late pregnancy or the postpartum period, where the heart remains dilated and becomes weak giving rise to PPCM [152]. The pathogenesis of PPCM is closely linked to the cardiovascular modifications that accompany normal pregnancies [189]. It is particularly important to understand cardiovascular physiological adaptations to pregnancy in order to elucidate the pathological disorders and to better anticipate complications.

Studies in PPCM described a proinflammatory response with a positive correlation between C-reactive protein levels and increased levels of TNF-alpha, Fas-Apo-1, IL-6 [400][401]. Several other studies have also reported enhanced oxidative stress in PPCM patients [402][165].

Experimental studies suggest that GDF-15 maybe cardioprotective, and that its expression reflects the onset of cardiac damage and its participation in the mitigation of damage [234][403][238]. Kempf et al, 2006, reported antiapoptotic action of GDF 15 in neonatal cardiomyocytes after stimulated ischemia [221]. Xu et al, 2006 also reported that transgenic mice overexpressing GDF-15 were partially resistant to pressure overload induced hypertrophy [234].

Nevertheless, GDF-15 can also play a causal role in the adverse cardiac remodeling depending on the microenvironment [404]. Circulating GDF 15 level is increasingly being found as positively correlated with left ventricular mass and wall thickness in hypertrophic cardiomyopathy, primary hypertension, and ischemic heart diseases [10][11]. The pro-hypertrophic mechanism of GDF-15 involves dysregulation of small mothers against decapentaplegic 1 (Smad 1) pathway through phosphoinositide 3-kinase (PI3K) and extra-cellular signal-regulated kinase (ERK) [238][405].

GDF 15 is also an inflammation-associated hormone. It is found to be induced by inflammation and positively correlates with inflammatory markers in numerous disease state such as lupus and sepsis [406][407][408]. Luan et al, 2019 demonstrated that GDF-15 promotes survival in inflammatory states through central induction of metabolic adaptation [409].

Given that the features of PPCM like heart failure, cardiac hypertrophy, inflammation and raised oxidative stress, also occur in other disease conditions reported to affect GDF-15 expression. We also aimed to assess the level of circulating GDF- 15 in PPCM patients and healthy mothers.

1.2 Materials and Methods

Sixty-three (63) healthy control (HC) pregnant mothers were enrolled consecutively at Groote Schuur Hospital (University of Cape Town, SA) from second trimester until 4-6 months postpartum. Clinical assessment and echocardiography of each patient was performed by experienced physicians.

Levels of GDF-15 were determined in 39 PPCM patients and time point matched healthy control using Quantikine® ELISA kit (R&D systems; United States) according to the manufacturer's instructions. All the samples were measured in duplicate and the analyses were performed in a blind setup.

1.3 Data Analysis and Statistics

Data was analysed using GraphPad Prism version 8.03 for Windows (La Jolla, California, USA). Continuous data are expressed as mean ± standard deviation or median (range) and categorical data as frequencies (%). Normality was assessed using D'Agostino and Pearson omnibus normality test. $\chi 2$ test and Fisher's exact test were used for discrete variables; un-paired t-test with Mann–Whitney U test were used for continuous variables. Independent ANOVA was used to compare data between pregnant groups. Tukey post hoc was used to correct for multiple comparison. $P < 0.05$ was considered to indicate statistical significance.

1.4 Results

1.4.1 Echocardiography assessment of healthy pregnant mothers

Table 12 summarizes the demographics and echocardiograph measurements of 63 HC participants at different time points during pregnancy and postpartum. The participants in

this study were aged between 21-35 years. Age and height did not differ between the groups. Majority of the participants 65% had previous 1/2 pregnancies, 23.8% had a family history of CVD, 11.1% had history of hypertension.

Table 12: Demographic characteristics and echocardiographic measurements of normal pregnant mothers

Characteristic N=63	Pregnancy		Postpartum(pp)		
	2nd Trimester n=11	3rd Trimester n=7	1-4 weeks pp n=8	1-3 months pp n= 15	4-6 months pp n=21
Age (mean±SD)	24.91±5.17	26.00±5.20	28.63±6.16	24.47±6.16	26.71±6.29
Height (mean±SD)	162.5±5.76	159.9±7.29	158.6±6.44	159.6±6.58	159.7±5.27
Weight (mean±SD)	66.45±8.88	77.14±11.50 *	67.00±13.49	64.67±9.28	74.81±14.27
SBP (mean±SD)	100.5±13.99	104.6±8.70	109.9±12.86	121.1±18.55*	121.0±17.43 **
DBP (mean±SD)	65.64±12.17	68.14±8.42	73.13±8.51	79.67±12.80*	79.14±12.14 *
Heart rate (HR) (mean±SD)	83.80±13.14	90.14±12.65	68.75±14.24##	70.73±7.60##	76.33±12.66
LVEF (mean±SD)	63.67±8.86	51.29±5.59*	60.75±8.23	57.67±8.58	54.76±8.91
LVEDD	45.63±5.53	45.57±6.71	45.88±8.32	47.00±6.57	44.67±7.32
LVESD	29.75±5.34	33.71±4.11	31.00±6.78	32.53±4.24	31.86±5.14
Left Atrial Size	26.64±5.12	27.00±3.61	27.50±4.57	26.07±3.49	27.52±4.42
Aortic root size (mean±SD)	22.10±5.67	22.71±3.55	23.50±2.73	24.40±3.20	26.67±3.47
Race n (%) African Coloured	7(64) 4(36)	5(71) 2(29)	2(25) 6 (75)	3(20) 12(80)	6(29) 15(71)
Family History of CVD n (%)	1(9)	1(14)	1(13)	4(27)	8(38)
Hypertension History n (%)	0(0)	1(14)	2(25)	1(7)	3(14)
Previous TB n (%)	0(0)	1(14)	0(0)	2(13)	0(0)
HIV status n (%) Positive	0(0)	1(13)	2(25)	2(13)	3(14)
Pregnancy n (%) 1-2 3-4 >4	8(80) 1(10) 1(10)	5(83) 1(17) 0(0)	3(33) 6(67) 0(0)	11(73) 4(67) 0(0)	14(70) 6(30) 1(0)

Continuous data were expressed as mean±SD or median and range, according to normality of distribution. Categorical variables are presented as frequencies (percentages) and compared using Fisher's exact tests. CVD, Cardiovascular disease; LVEF, left ventricular ejection fraction; LVEDD, Left Ventricular End Diastolic Diameter; LVESD, Left Ventricle End Systolic Diameter;

*SBP, Systolic Blood. **-p<0.01; *-p<0.05 compared to 2nd trimester, ## -p<0.01 compared to 3rd trimester*

Mean systolic blood pressure (SBP) increased progressively from 100.5mmHg in the 2nd trimester to 121 mmHg in the 1-3 months pp and 4-6 months pp groups. Diastolic blood pressure (DBP) also increased from 65.64mmHg in the 2nd trimester to 79.67 mmHg in the 1-3 months pp. There was no mid-trimester blood drop observed. Heart rate was also significantly reduced in the 1-4 weeks pp and 1-3 months pp groups relative to the 3rd trimester.

Left ventricular ejection fraction (LVEF) was also significantly reduced in the 3rd trimester compared to the 2nd trimester. No significant change was observed in the left ventricular end diastolic diameter (LVEDD), left ventricular end systolic diameter (LVESD) and left atrial size.

1.4.2 Clinical and demographic characteristics of PPCM patients

Clinical and demographic characteristics of all patients are summarized in **Table 13**. Mean age was 29.1 ±5.1 years; 64% were of African ethnicity whilst 33% were of mixed race and 1 patient was white.

HIV was reported in 28% of the patients whilst 3% reported previous history of tuberculosis (TB) and 8% also reported chronic hypertension. Most of the patients (64%) were in New York Heart Association Functional Classification (NYHA FC) III-IV at recruitment. Mean systolic blood pressure (SBP) and mean diastolic blood pressure (DBP) were 113±19 mmHg and 74±13 mmHg respectively. 97% of the patients presented postpartum and the median gestation period was 39 weeks ranging between 30-40 weeks. All patients had singlet pregnancy.

Table 13: Baseline Maternal Characteristics of 39 cohort patients

	All Patients (n=39)
Age at enrolment (years)	29.1± 5.1
Ethnicity, n (%)	
African or Black (n, %)	25(64)
Mixed race	13(33)
White	1(3)
General medical history, n (%)	
Chronic hypertension	3(8)
Hypercholesterolemia	0(0)
HIV	11(28)
Syphilis	0(0)
Tuberculosis	1(3)
Clinical history and presentation, n (%)	
Previously known CVD	5(13)
NYHA FC I-II	14(36)
NYHA FC III-IV	25(64)
SBP in mmHg	113±19
DBP I mmHg	74±13
Heart rate in beats per minute	101±16
BMI in kg/m^2	26±5
Obstetric history, n (%)	
Para (median, range)	2(0-6)
Nulliparous, n (%)	1(3)
Twin pregnancies	0(0)
Completed weeks of pregnancy (median, range)	39(30-40)
Caesarean delivery	10(26)
Echocardiogram	
LVEDD (mm)	59.6±7.3
LVESD (mm)	50.7±7.3
EF (%)	27.5±8.5

Continuous data were expressed as mean±SD or median and range, according to normality of distribution. Categorical variables are presented as frequencies (percentages) and compared using Fisher's exact tests. BMI, body mass index; CVD, Cardiovascular disease; EF, ejection fraction; LVEDD, Left Ventricular End Diastolic Diameter; LVESD, Left Ventricle End Systolic Diameter; NYHA FC, New York Heart Association Functional Class; SBP, Systolic Blood

1.4.3 Plasma circulation level of GDF-15 in PPCM patients and postpartum matched controls

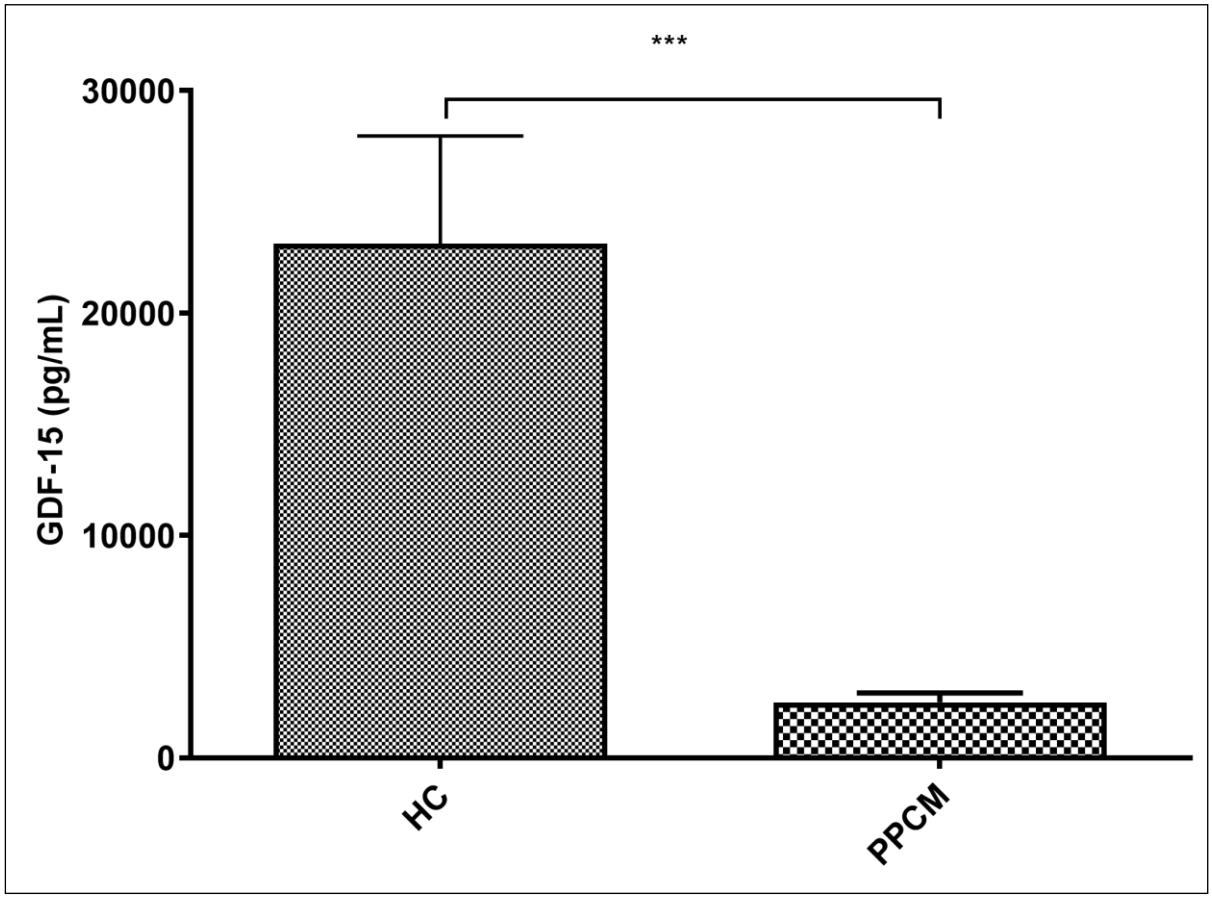

Figure 48: Circulating plasma levels of GDF-15 in PPCM patients and Healthy Controls

*Plasma levels was significantly reduced in PPCM patients (median of 1338 [235-11728]) when compared to postpartum healthy controls (median 15630 [718-59376]) (*** P<0.0001). HC- healthy controls; PPCM- peripartum cardiomyopathy*

The circulation level of GDF-15 was significantly reduced in PPCM patients when compared to age and time pregnant time point matched controls (**Figure 48**).

1.5 Discussion

1.5.1 Cardiac functional and morphological changes associated with pregnancy in healthy women

The present study examined hemodynamic, cardiac structural and systolic functional changes in healthy pregnant and postpartum mothers. The results showed slightly reduced SBP and DBP during pregnancy which subsequently recovered in the postpartum. No mid- trimester blood pressure drop was observed. The findings corroborated the known blood pressure patterns during pregnancy [410][411]. Although many studies have shown this similar pattern some studies have observed a drop in blood pressure in the 2$^{nd\ trimester}$ [36][412].

We also observed reduction in left ventricular systolic function in the 3rd trimester. The functional reduction was evidenced by reduction in LVEF. Similar findings were also reported by other studies [66][76]. However, others have also reported no significant change [132][413] and increased functionality [72]. Inconsistency in LVEF could be caused by the variations in ventricular loading conditions (preload and afterload) in pregnancy [26].

Another source of error encountered when using 2D methods to measure LVEF is that they are less accurate in patients with regional variation in systolic function, as the measurements can be obtained from a region of the LV cavity where the function is discordant from the overall ventricular function [363]. 2D echocardiography may also have reduced accuracy if the imaging planes used for the measurement are incorrect [363].

1.5.2 Reduced circulation level of growth differentiation factor 15 in peripartum cardiomyopathy

Serum GDF-15 concentration was reported to be elevated with increasing stage of heart failure and might have potential value in distinguishing stages of chronic heart failure (CHF) [414]. Additionally, it has been reported that GDF-15 can also provide prognostic information beyond established clinical and biochemical markers in patients with CHF [415].

However, our study found that GDF-15 level was significantly lower in PPCM patients when compared to healthy controls. This finding was intriguing as it contradicts the finding in other pathological cardiovascular conditions. The exact factors that cause reduction in circulatory GDF-15 in PPCM are largely unknown. There is also limited evidence of the relationship between circulating GDF-15 level and pregnancy related cardiovascular diseases.

A study by Chen et al, 2016 also reported reduced serum GDF-15 levels in the third trimester in women presenting with preeclampsia compared to their gestation-age-matched controls [416]. This finding contradicted finding by Marjono et al, 2002 who reported no significant difference in GDF-15 in pre-eclamptic compared to healthy pregnancy [417]. Sugulle et al, 2009 on the other hand observed higher concentration of GDF-15 in preeclampsia and diabetes patients compared to controls. Attributions to these differences need investigations in large studies with considering maternal age and ethnicities.

Circulating GDF-15 concentrations rise rapidly in maternal blood during early pregnancy, reaching the highest level in the third trimester [418][419]. The major source of the high maternal circulating GDF-15 in pregnancy is most likely the placenta, specifically secreted by

the villous trophoblast cells [420][421]. Additionally, increased iron absorption during pregnancy could also increase GDF-15 secretion [422][423].

GDF-15 display an array of properties that are cardioprotective including anti-hypertrophy, anti-inflammatory and anti-apoptotic that could benefit the heart during pregnancy stress [234][403][230]. At the molecular and cellular level, accumulating evidence suggests that GDF-15 contributes substantially to cardioprotection through the ALK type 1 receptors (ALK 1–7) which then phosphorylate several SMAD members [235][405]. Additionally, GDF-15 also activates the PI3K/AKT/eNOS pathway and inhibiting ROS-induced activation of the NF-jB/JNK cascade [424]. In view of this, we speculate that reduced GDF-15 in PPCM patients might contribute to the susceptibility of the maternal heart to PPCM and heart failure.

However, regarding that the study was cross sectional and had a small sample size which can undermine an association study and lead to false positive results, our findings that GDF-15 levels were reduced in PPCM patients may need to be confirmed in a large sample size.

1.6 Conclusion

We conclude that hemodynamic changes occur during physiological pregnancy evidenced by reduced SBP, DBP during pregnancy and increased HR in the late pregnancy. We also conclude that LV systolic function was reduced in the late pregnancy.
Serum GDF-15 was greatly reduced in PPCM patients when compared with healthy controls. Hence, GDF-15 can not be used as a cardiovascular marker to predict PPCM like with other HF conditions.

CHAPTER 7

Discussion

This study aimed to explore cardiovascular functional, structural and molecular changes that occur during pregnancy with the goal to delineate possible mechanisms involved in the lack of reverse cardiac remodeling observed in PPCM. We also wanted to explore the potential involvement of common pregnant hormones and other cardiac hormones in the regulation of cardiac hypertrophy.

Using ultrahigh frequency echocardiography, the study showed that considerable functional and morphological changes occur in wild type mice during pregnancy and postpartum. Hemodynamic changes were confirmed by the progressive increase in stroke volume and cardiac output. Stroke volume increased from as early as Day 7 of pregnancy. Increased stroke volume during pregnancy conforms with previous studies in different animals and humans [27][287][261]. Left ventricular end diastolic volume (LVEDV) a measure of preload significantly increased from late pregnancy and remained high throughout the postpartum period. Similar patterns have been observed in humans [60]. However, studies in humans reported resolved preload changes after six months postpartum [66][76]. Umazume, et al [65], reported a progressive increase in LVEDV during pregnancy peaking at one week postpartum and the values remained high after one month postpartum.

Moreover, the study also confirmed cardiovascular morphological changes during physiological pregnancy. Left ventricular mass (LV mass) and left ventricular internal diameter (LVID) increased significantly from late pregnancy and remained high throughout the postpartum period. Our findings were consistent with several other studies [61][121][303][304]. Cardiac morphological changes that occur during pregnancy are most likely inflicted by the hemodynamic changes.

Another important observation from the healthy pregnancy mouse model was the presence of eccentric hypertrophy which started in late pregnancy and remained high until Day 14 pp. Signs of regression of cardiac hypertrophy were only observed on Day 28pp. Nevertheless, the hypertrophy had not resolved to non-pregnant level by the last day of the study. Limited and contradicting data is available on when physiological hypertrophy revert to pre-pregnant state. Ventura et al, 2016 reported similar findings, where hypertrophy was sustained for more than 2 weeks after parturition in healthy mice [304]. However, slightly different results

were reported by Umar et al, 2012 who reported heart weight reverting to pre-pregnancy level in 7 days postpartum in mice [61]. There are also differences in reports from human studies which reported varying periods between 3 months to 1 year after giving birth [60][128].

Cardiac systolic functions remained normal (EF >50%) throughout the study and no significant change was observed at all the time points. Studies have reported conflicting findings on LV systolic function from no significant changes [60][121][264][290], reduced functionality [61][76][292], or enhanced [261][293]. It is noteworthy pointing out that EF and FS are highly depended on preload and afterload [26]. Hence, factors that affect preload and afterload in pregnancy may be contributing to the inconsistency. However, studies that tested isolated pregnancy heart under strict control of preload and afterload demonstrated improved systolic function [293][294]. The pregnant heart's ability to pump was enhanced, making it mechanically more efficient [295].

Histological analysis revealed the presence of slight perivascular and interstitial fibrosis which was reversed postpartum. This finding is in contrast with other studies in pregnant mice which reported no presence of interstitial fibrosis [61][88][316]. However, it was in sync with some studies in rats which reported interstitial cardiac fibrosis in pregnancy [124][317]. The fibrosis observed in our experiments could be a compensatory effect in response to the increase in blood volume present in the pregnancy [124].

We then explored the cardiac protein expression profiles to investigate the molecular changes that occur at different pregnant and postpartum time points. The results indicated that there were similarities in the proteomic profiles between time points. Only 14 proteins were significantly different across all groups. The significant proteins fall into proteins involved in hormone metabolic process, proteins involved in immune response and acute inflammation, proteins involved in cardiac anatomical structure, cardiac tissue development, regulation of cardiac contraction and proteins that play a role in vascularization.

However, the greatest proteomic response occurred in late pregnancy and the protein set was distinct from that expressed in the postpartum groups (Days 14pp and 28pp). Differential protein expression analysis showed upregulation of protein clusters involved in muscle contraction and myofilament movement like MYL2, ACTC1 and TNNC1 on Day 14pp. The observed cluster expression on Day 14pp confirmed the presence of cardiac hypertrophy

which was observed in other cardiac hypertrophy models [332][333]. This finding substantiates the prolongation of cardiac hypertrophy in the postpartum phase.

The expression on Day 28pp showed upregulation of ubiquitin proteasome system (UPS). The UPS is the major pathway for protein degradation in the heart to remove damaged and misfolded proteins [330][351]. Previous studies have reported that UPS is downregulated during pregnancy and restored to non-pregnant level within a week postpartum. Upregulation of UPS in late postpartum could be a mechanism for reversing cardiac hypertrophy during unloading. Activation of the UPS can prevent or reverse cardiac hypertrophy by enhancing degradation of superfluous proteins [351][425]. Razeghi et al, 2003 also reported that unloading of the heart results in atrophic remodeling associated with UPS [426]. Previous studies have also reported that dysfunction of the UPS is implicated in cardiac hypertrophy and congestive heart failure, induced by pressure overload [427][428]. In the contrary other studies have shown that proteasome inhibitors have beneficial effects on the prevention and/or reversal of cardiac hypertrophy [353][429]. Further studies are required to understand the actual role played by the UPS in the regulation of pregnancy induced cardiac hypertrophy.

Furthermore, we explored the potential signaling pathways involved in the regulation of cardiac hypertrophy during pregnancy in mice. Pregnancy-related cardiac hypertrophy was unable to trigger significant changes in the mRNA levels of classic markers of pathological hypertrophy (*ANP, BNP, β-MHC)* at any stage of normal pregnancy and postpartum. This supported that pregnancy induced cardiac hypertrophy was physiological. The physiological state of cardiac hypertrophy induced by pregnancy was also reported by other researchers [295][88]. Assessment of the fetal gene program in STAT3 KO mice clearly outlined the difference between physiological and pathological hypertrophy. Expression of fetal gene program in STAT3 KO mice but not in wild type mice was also reported by Hilfiker-Kleiner et al ,2007 [165].

We also assessed the cardiac mRNA expression of GDF-15 in healthy pregnant mice and STAT3 KO. GDF-15 mRNA expression was increased in late pregnancy and remained high for the first two weeks after parturition. Strikingly, the expression of GDF-15 was low in the STAT3 KO mice's hearts. To the best of our knowledge, this was the first study reporting cardiac specific GDF-15 expression in pregnant mice and postpartum.

Experimental studies have shown the myocardial protective effect of GDF-15 through its anti-apoptosis, anti-inflammation and anti-myocardial remodeling [430][431][225]. However, findings of its role in myocardial hypertrophy are contradictory. GDF-15 was found to inhibit myocardial hypertrophy through a Smad2/3 and Smad6/7 pathway in a pressure-induced hypertrophy model [221]. In contrary, Heger, et al 2010 reported enhanced hypertrophic growth of cardiomyocytes treated with GDF-15 [238]. Further investigations are required to ascertain the actual role of GDF-15 in modulation of pregnancy induced cardiac hypertrophy and the signalling pathways involved.

Our study also found significant activation of AKT in healthy mice cardiac tissue during pregnancy but not in the postpartum. Similar activation pattern of AKT in pregnant mice has been reported by other studies [191][306]. Chung et al, 2012, Lemmens et al, 2010 and others also demonstrated the importance of PI3K/AKT pathway in mediating pregnancy induced cardiac hypertrophy by looking at the downstream molecules [26][306]. However, conflicting results have also been published especially in the late pregnancy, with studies reporting increased AKT phosphorylation [165], whilst others reporting reduced AKT phosphorylation [99].

The JAK/STAT pathway was significantly activated in the postpartum phase but not during pregnancy. We speculate that JAK/STAT pathway mediate physiological cardiac hypertrophy in the postpartum phase when AKT expression has reduced. Previous studies agree that the JAK/STAT signaling pathway plays an important role in mediating cardiac hypertrophy in both physiological and pathological conditions [106][432]. However, prolonged activation of STAT3, is strongly implicated in the progression of cardiac hypertrophy to heart failure [105][313].

We also demonstrated in a cell culture model that E2 regulates cardiomyocytes hypertrophy. It exhibited anti-hypertrophic effects in both physiological and pathological conditions in our cell culture model. The antihypertrophic effect of E2 could also be mediated through PIK3/AKT signaling pathway [433][434]. The involvement of AKT in physiological cardiac hypertrophy has been described in other studies [435][436]. Progesterone, on the other hand induced physiological cardiomyocytes hypertrophy without the induction of fetal genes. Previous studies showed that progesterone can cause cardiomyocytes hypertrophy by increasing proteins synthesis and activation of calcineurin [26][267][391]. Taking this together, our results showed that changes in pregnancy hormones may control the

pregnancy-induced cardiac hypertrophy changes. Several studies also support that pregnancy hormones play a vital role in maintenance of physiological cardiac remodeling [268][269][270].

Further investigations in the cell culture showed that GDF-15 expression is neither regulated by oestrogen nor progesterone. However, the expression of GDF-15 was raised in isoproterenol treated cell which exhibited increase in cell size. We speculate that the expression of GDF-15 in pregnancy induced hypertrophy hearts could be a response to stretch of cardiac cells rather than hormonal effect. Frank et al, 2008 also confirmed that GDF-15 production is favoured in stretched cardiomyocytes [228]. However, further studies are required to explore the actual role and regulation of GDF-15 in pregnancy heart.

None of our hormone treatments in cell culture significantly altered the expression of either STAT3 or STAT5. However, research in other fields have published contradicting roles of E2 on STAT3 expression. Dziennis et al, 2007 published that E2 induce STAT3 in in experimental cerebral ischemia [437], whilst Yamamoto et al, reported that E2 suppresses STAT3 mediated gene expression in in breast cancer cells [438].

Eventually, we assessed cardiovascular changes in physiological pregnancy in healthy mothers. Our focus was to provide data on changes that occur in the postpartum period. We observed significant decrease in blood pressure during pregnancy which normalizes in the postpartum phase. Heart rate increased in late pregnancy and normalizes early postpartum. Although many studies have shown this similar patterns during pregnancy [410][411], some studies have observed a drop in blood pressure in the 2^{nd} trimester [36][412]. The causes of this discrepancy are not clear.

We also observed reduced systolic function in late pregnancy. Other studies corroborate this finding [76][66], whilst others have also reported no significant change [132][413] and increased functionality [72]. The main reason for this inconsistency is that LVEF is affected by variations in pre-load and after-load which are often affected by several factors during pregnancy.

We assessed plasma level of GDF-15 in PPCM patients and healthy controls. GDF-15 was significantly reduced in PPCM patients. This finding contradicts previous studies which proposed GDF-15 as a marker of heart failure. GDF-15 display an array of properties that are cardioprotective including anti-hypertrophy, anti-inflammatory and anti-apoptotic that could benefit the heart during pregnancy stress [234][403][230]. In view of this, we speculate that

reduced GDF-15 in PPCM patients might contribute to the susceptibility of the maternal heart to PPCM and heart failure. However, further studies that assess the actual role played by GDF-15 in cardiac remodeling during pregnancy should be conducted. More studies are also required to establish the mechanisms by which GDF-15 exert its antihypertrophic and prohypertrophic effects.

7.1 Summary Conclusions

Chapter 4: In this chapter we used ultra high frequency echocardiography to delineate functional and morphological cardiovascular changes that occur during pregnancy in healthy pregnant wild type mice. We conclude that pregnancy induces increased SV and preload from late pregnancy in mice. We also observed changes in structure and morphology of the heart which includes increased LVID, and eccentric hypertrophy. Hypertrophy that occurs during pregnancy is sustained for about 2 weeks in the postpartum and signs of reversal were observed after the 4^{th} week postpartum. LVSF did not change significantly at any time point.
Hereafter, we used western blotting analysis to explore the potential signaling mechanisms that maybe involved in the regulation of pregnancy induced cardiac hypertrophy. We concluded that AKT signaling might be used to regulate physiological hypertrophy during pregnancy whilst the JAK/STAT pathway regulates hypertrophy in the postpartum. We also observed an increase in GDF-15 expression in healthy pregnant mice and reduced expression in the STAT3 KO mice. The time points with increased expression of GDF-15 corresponded to the times points of significant cardiac hypertrophy.
We then used histological techniques to assess for any structural changes on the cardiac tissue. We observed slight increase in fibrotic tissue during pregnancy in mice and this was reversed postpartum.
Furthermore, we used proteomics technique to identify proteins that can track pregnancy induced cardiovascular remodeling. We identified 14 proteins that are involved in hormone metabolic, immune response and acute inflammation, cardiac anatomical structure, cardiac tissue development and vascularization to be overally changed during pregnancy and postpartum. Our study also corroborated that cardiac hypertrophy is sustained for a longer period than previously reported. We also found upregulation of the UPS in the late postpartum group which corresponds to the reversal of both cardiac hypertrophy and fibrosis.
Chapter 5: In this chapter we used a cell culture model to assess the potential involvement of pregnancy hormones in the regulation of cardiac hypertrophy. We concluded that E2 has

antihypertrophic properties which abrogated both physiological and pathological cardiac hypertrophy through the activation of AKT pathway. We also observed that progesterone induces physiological cardiomyocytes hypertrophy which does not trigger fetal gene expression. We also concluded that both progesterone and E2 might not be involved in the regulation of GDF-15 expression during pregnancy. However, we speculate that the expression might be caused by cardiomyocytes stretch due to hypertrophy.

Chapter 6: In this chapter we assessed cardiovascular functional and morphological changes that occur during gestation and postpartum in healthy pregnant mother. Our results showed that SBP and DBP increase gradually from 2nd trimester reaching normal level in the postpartum. The HR was significantly high in late pregnancy when compared to the postpartum period. LVEF was significantly reduced in the late pregnancy.

We also observed that the serum level of GDF-15 was significantly reduced in PPCM patients when compared to healthy controls. Bearing in mind of the cardioprotective role of GDF-15 we speculate that the reduced level of GDF-15 increases the susceptibility of the pregnancy heart to PPCM.

7.2 Ways Forward

The most distinct physical presentation of the normal pregnancy heart is the reversable eccentric cardiac hypertrophy. The key element to this phenotype is an adaptation of proteins' turnover, associated with myocyte elongation via serial addition of sarcomeres and extracellular matrix degradation. It has become clear that the UPS play major roles in protein turnover, and in protein quality control by removal of damaged, oxidised, and/or misfolded proteins. However, lack of knowledge on the precise underlying molecular mechanisms and involvement of UPS in pregnancy-induced hypertrophy impairs the understanding of the remodeling process.

Dysfunction of the UPS is also rapidly gaining recognition as a potentially important mechanism involved in the pathogenesis of several cardiac diseases, including PPCM [426]. The pathogenesis of PPCM is tied to the cardiovascular remodeling induced by volume load and other stress during pregnancy. Increased oxidative stress during late gestation and in the early postpartum period, and high levels of the nursing hormone prolactin(PRL) have been shown to be an important aetiology of PPCM [439]. This led to PPCM-specific treatment called the BOARD concept (Bromocriptine, Oral heart failure therapies, Anticoagulants, vasoRelaxing agents, and Diuretics) where, in addition to standard heart failure therapy, the

PRL blocker bromocriptine and anti-coagulation is added [365][402]. However, the use of bromocriptine faces ethical challenges since it prevents the mother from nursing and the baby from getting breast milk [439][440]. Posing a need for alternative druggable pathways that regulate oxidative stress.

Experimental studies have shown that UPS can regulate both oxidative stress and volume unloading which are both common in the postpartum phase of pregnancy [345]. In addition, evidence also support the role of UPS in regulation of sarcomere protein turnover and cardiomyocyte size and how this play a role in induction of the hypertrophic phenotype [441]. We hypothesis that the UPS contributes significantly to the pathogenesis of PPCM. Hence, understanding the role of UPS and its regulation in pregnancy may lead to early diagnosis and/or influence therapeutic strategies for prevention and treatment of PPCM and other pregnancy related pathological cardiovascular conditions. However, further investigations on the precise role and mechanisms of UPS in pregnancy induced cardiac remodeling are needed. This includes assessment of proteasome lytic activity of each subunit and substrates firstly in pregnant model animals and then in humans at different time points during pregnancy and postpartum.

It would also be interesting to investigate the role played by GDF-15 in the regulation of cardiac hypertrophy and establishing the mechanisms involved. It would be best if started in an isolated cell culture model using pure GDF-15 and blocking agents and/or small interfering RNA (siRNA) to establish the downstream signaling molecules involved. GDF-15 would then be administered in in vivo models of physiological or pathological hypertrophy to assess its therapeutic function.

REFERENCES

1. Talbot L, Maclennan K (2016) Physiology of pregnancy. Anaesth Intensive Care Med 17:341–345. https://doi.org/10.1016/j.mpaic.2016.04.010

2. Magon N, Kumar P (2012) Hormones in pregnancy. Niger Med J 53:179. https://doi.org/10.4103/0300-1652.107549

3. Costa MA (2016) The endocrine function of human placenta: An overview. Reprod Biomed Online 32:14–43. https://doi.org/10.1016/j.rbmo.2015.10.005

4. Li M, Song Y, Rawal S, et al (2020) Plasma Prolactin and Progesterone Levels and the Risk of Gestational Diabetes: A Prospective and Longitudinal Study in a Multiracial Cohort. Front Endocrinol (Lausanne) 11:1–10. https://doi.org/10.3389/fendo.2020.00083

5. Taylor R, S H, Burney RO (2015) Endocrinology of Pregnancy. In: Basic and Clinical endocrnology. In: De Groot LJ, Chrousos G, Dungan K, et al., editors. Endotext [Internet]. South Dartmouth (MA): MDText.com, pp 1–67

6. Holesh J, Lord M (2020) Physiology, Ovulation - StatPearls - NCBI Bookshelf

7. Ain KB, Refetoff S, Same DH, Murata Y (1988) Effect of estrogen on the synthesis and secretion of thyroxine-binding globulin by a human hepatoma cell line, hep G2. Mol Endocrinol 2:313–323. https://doi.org/10.1210/mend-2-4-313

8. Newbern D, Freemark M (2011) Placental hormones and the control of maternal metabolism and fetal growth. Curr Opin Endocrinol Diabetes Obes 18:409–416. https://doi.org/10.1097/MED.0b013e32834c800d

9. Sibiak R, Jankowski M, Gutaj P, et al (2020) Placental Lactogen as a Marker of Maternal Obesity, Diabetes, and Fetal Growth Abnormalities: Current Knowledge and Clinical Perspectives. J Clin Med 9:1142. https://doi.org/10.3390/jcm9041142

10. Ekinci EI, Torkamani N, Ramchand SK, et al (2017) Higher maternal serum prolactin levels are associated with reduced glucose tolerance during pregnancy. J Diabetes Investig 8:697–700. https://doi.org/10.1111/jdi.12634

11. LoMauro A, Aliverti A (2015) Respiratory physiology of pregnancy: Physiology masterclass. Breathe (Sheffield, England) 11:297–301.

https://doi.org/10.1183/20734735.008615

12. Hegewald MJ, Crapo RO (2011) Respiratory Physiology in Pregnancy. Clin Chest Med 32:1–13. https://doi.org/10.1016/j.ccm.2010.11.001

13. Charalambous S, Fotas A, Rizk DEE (2009) Urolithiasis in pregnancy. Int Urogynecol J 20:1133–1136. https://doi.org/10.1007/s00192-009-0920-z

14. Cheung KL, Lafayette RA (2013) Renal Physiology of Pregnancy. Adv Chronic Kidney Dis 20:209–214. https://doi.org/10.1053/j.ackd.2013.01.012

15. Soma-pillay P, Nelson-piercy C, Tolppanen H, Mebazaa A (2016) Physiological changes in pregnancy. Cardiovasc J AFRICA • 27:89–94. https://doi.org/10.5830/CVJA-2016-021

16. Aguree S, Gernand AD (2019) Plasma volume expansion across healthy pregnancy: A systematic review and meta-analysis of longitudinal studies. BMC Pregnancy Childbirth 19:1–11. https://doi.org/10.1186/s12884-019-2619-6

17. Sanghavi M, Rutherford JD (2014) Cardiovascular Physiology of Pregnancy. Circ AHA 10:1003–1008. https://doi.org/10.1161/CIRCULATIONAHA.114.009029

18. Talbot L, Maclennan K (2016) Physiology of pregnancy. Anaesth. Intensive Care Med.

19. de Haas S, Ghossein-Doha C, van Kuijk SMJ, et al (2017) Physiological adaptation of maternal plasma volume during pregnancy: a systematic review and meta-analysis. Ultrasound Obstet Gynecol 49:177–187. https://doi.org/10.1002/uog.17360

20. OSOFSKY HJ, WILLIAMS JA (1964) Changes in Blood Volume During Parturition and the Early Postpartum Period. Am J Obstet Gynecol 88:396–398. https://doi.org/10.1016/0002-9378(64)90441-7

21. Greenberg JA, Bell SJ, Guan Y, Yu Y (2011) Folic Acid Supplementation and Tube Defect Prevention. Rev Obstet Gynecol 4:52–59. https://doi.org/10.3909/riog0157

22. O'Malley EG, Cawley S, Kennedy RAK, et al (2018) Maternal anaemia and folate intake in early pregnancy. J Public Health (Oxf) 40:e296–e302. https://doi.org/10.1093/pubmed/fdy013

23. James AH (2015) Thrombosis in pregnancy and maternal outcomes. Birth Defects Res

Part C - Embryo Today Rev 105:159–166. https://doi.org/10.1002/bdrc.21106

24. Jessica A. Reese, Ph.D., Jennifer D. Peck, Ph.D., David R. Deschamps, M.D., Jennifer J. McIntosh, D.O., Eric J. Knudtson, M.D.*, Deirdra R. Terrell, Ph.D., Sara K. Vesely, Ph.D., and James N. George MDD (2018) Platelet Counts during Pregnancy. N Engl J Med 1:139–148. https://doi.org/10.1016/j.physbeh.2017.03.040

25. McCrae KR (2006) Thrombocytopenia in pregnancy. Thrombocytopenia 11:265–274. https://doi.org/10.5958/2394-2754.2016.00002.3

26. Chung E, Leinwand LA (2014) Pregnancy as a cardiac stress model. Cardiovasc Res 101:561–570. https://doi.org/10.1093/cvr/cvu013

27. Umar S, Nadadur R, Iorga A, et al (2012) Cardiac structural and hemodynamic changes associated with physiological heart hypertrophy of pregnancy are reversed postpartum. J Appl Physiol 113:1253–1259. https://doi.org/10.1152/japplphysiol.00549.2012

28. Zygmunt M, Herr F, Münstedt K, et al (2003) Angiogenesis and vasculogenesis in pregnancy. Eur J Obstet Gynecol Reprod Biol 110:10–18. https://doi.org/10.1016/S0301-2115(03)00168-4

29. Cébe-Suarez S, Zehnder-Fjällman A, Ballmer-Hofer K (2006) The role of VEGF receptors in angiogenesis; complex partnerships. Cell Mol Life Sci 63:601–615. https://doi.org/10.1007/s00018-005-5426-3

30. Conrad KP (2011) Maternal vasodilation in pregnancy: The emerging role of relaxin. Am J Physiol - Regul Integr Comp Physiol 301:. https://doi.org/10.1152/ajpregu.00156.2011

31. Duvekot JJ, Cheriex EC, Pieters FAA, et al (1993) Early pregnancy changes in hemodynamics and volume homeostasis are consecutive adjustments triggered by a primary fall in systemic vascular tone. Am J Obstet Gynecol. https://doi.org/10.1016/0002-9378(93)90405-8

32. Oung DAY, Ohnson ANNJ, Sorio FRO, et al (1998) Temporal relationships between hormonal and hemodynamic changes in early human pregnancy. 54:2056–2063. https://doi.org/10.1046/j.1523-1755.1998.00217.x

33. Carlin A (2008) Physiological changes of pregnancy and monitoring. Res Clin Obstet Gynaecol 22:801–823. https://doi.org/10.1016/j.bpobgyn.2008.06.005

34. Gogiraju R, Bochenek ML, Schäfer K (2019) Angiogenic Endothelial Cell Signaling in Cardiac Hypertrophy and Heart Failure. Front Cardiovasc Med 6:. https://doi.org/10.3389/fcvm.2019.00020

35. Timokhina E, Kuzmina T, Strizhakov A, et al (2019) Maternal Cardiac Function after Normal Delivery, Preeclampsia, and Eclampsia: A Prospective Study. J Pregnancy 2019:. https://doi.org/10.1155/2019/9795765

36. Rebelo F, Farias DR, Mendes RH, et al (2015) Blood Pressure Variation Throughout Pregnancy According to Early Gestational BMI: A Brazilian Cohort. Arq Bras Cardiol 284–291. https://doi.org/10.5935/abc.20150007

37. Melchiorre K, Sharma R, Thilaganathan B (2012) Cardiac structure and function in normal pregnancy. Curr Opin Obstet Gynecol 24:413–421. https://doi.org/10.1097/GCO.0b013e328359826f

38. Gifford R, August P, Cunningham G, et al (2000) National High Blood Pressure Education Working Group Report on High Blood Pressure in Pregnancy. Natl Institutes Heal NIH Publ no 00-3029 3–5

39. Loerup L, Pullon RM, Birks J, et al (2019) Trends of blood pressure and heart rate in normal pregnancies: A systematic review and meta-analysis. BMC Med 17:1–12. https://doi.org/10.1186/s12916-019-1399-1

40. Sacks FM, Willett WC, Smith A, et al (2000) Blood Pressure Patterns in Normal Pregnancy, Gestational Hypertension, and Preeclampsia. Hypertension 131–138. https://doi.org/10.1161/01.HYP.31.1.131

41. Finkelstein I, Bgeginski R, Tartaruga MP, et al (2006) Heart rate and blood pressure behavior throughout pregnancy, with training in water medium. Rev Bras Med do Esporte 12:336–339

42. Meah VL, Cockcroft JR, Backx K, et al (2016) Cardiac output and related haemodynamics during pregnancy: A series of meta-analyses. Heart 102:518–526. https://doi.org/10.1136/heartjnl-2015-308476

43. Michael E. Halla, Eric M. George JPG (2011) The Heart During Pregnanc. Rev Esp Cardiol 64:1045–1050. https://doi.org/10.1016/j.recesp.2011.07.009.The

44. Liu LX, Arany Z (2014) Maternal cardiac metabolism in pregnancy. Cardiovasc Res 101:545–553. https://doi.org/10.1093/cvr/cvu009

45. Sanghavi M, Rutherford JD (2014) Cardiovascular physiology of pregnancy. Circulation 130:1003–1008. https://doi.org/10.1161/CIRCULATIONAHA.114.009029

46. Azevedo PS, Polegato BF, Minicucci MF, et al (2016) Cardiac Remodeling: Concepts, Clinical Impact, Pathophysiological Mechanisms and Pharmacologic Treatment. Arq Bras Cardiol 106:62–9. https://doi.org/10.5935/abc.20160005

47. Schüttler D, Clauss S, Weckbach LT, Brunner S (2019) Molecular Mechanisms of Cardiac Remodeling and Regeneration in Physical Exercise. Cells 8:1128. https://doi.org/10.3390/cells8101128

48. Wu Q-Q, Xiao Y, Yuan Y, et al (2017) Mechanisms contributing to cardiac remodelling. Clin Sci 131:2319–2345. https://doi.org/10.1042/CS20171167

49. Samak M, Fatullayev J, Sabashnikov A, et al (2016) Cardiac Hypertrophy: An Introduction to Molecular and Cellular Basis. Med Sci Monit Basic Res 22:75–79. https://doi.org/10.12659/MSMBR.900437

50. Gilson GJ, Samaan S, Crawford MH, et al (1997) Changes in hemodynamics, ventricular remodeling, and ventricular contractility during normal pregnancy: A longitudinal study. Obstet Gynecol 89:957–962. https://doi.org/10.1016/S0029-7844(97)85765-1

51. Vega RB, Konhilas JP, Kelly DP, Leinwand LA (2017) Molecular Mechanisms Underlying Cardiac Adaptation to Exercise. Cell Metab 25:1012–1026. https://doi.org/10.1016/j.cmet.2017.04.025

52. Cohn JN, Ferrari R, Sharpe N (2000) Cardiac remodeling-concepts and clinical implications: A consensus paper from an International Forum on Cardiac Remodeling. J Am Coll Cardiol. https://doi.org/10.1016/S0735-1097(99)00630-0

53. Dorsa Pontes HB, Vieira Pontes JCD, Neto E de A, et al (2016) Cardiac remodelling: General aspects and mechanisms. Curr Res Cardiol 3:. https://doi.org/10.4172/2368-

0512.1000073

54. Mihl C, Dassen WRM, Kuipers H (2008) Cardiac remodelling: concentric versus eccentric hypertrophy in strength and endurance athletes. Neth Heart J 16:129–33. https://doi.org/10.1007/BF03086131

55. Wu Q-Q, Xiao Y, Yuan Y, et al (2017) Mechanisms contributing to cardiac remodelling. Clin Sci 131:2319–2345. https://doi.org/10.1042/cs20171167

56. Cohn JN, Ferrari R, Sharpe N (2000) Cardiac remodeling-concepts and clinical implications: A consensus paper from an International Forum on Cardiac Remodeling. J Am Coll Cardiol 35:569–582. https://doi.org/10.1016/S0735-1097(99)00630-0

57. Iemitsu M, Miyauchi T, Maeda S, et al (2001) Physiological and pathological cardiac hypertrophy induce different molecular phenotypes in the rat. Am J Physiol Integr Comp Physiol 281:R2029–R2036. https://doi.org/10.1152/ajpregu.2001.281.6.R2029

58. Nakamura M, Sadoshima J (2018) Mechanisms of physiological and pathological cardiac hypertrophy. Nat Rev Cardiol 15:387–407. https://doi.org/10.1038/s41569-018-0007-y

59. Shimizu I, Minamino T (2016) Journal of Molecular and Cellular Cardiology Physiological and pathological cardiac hypertrophy. J Mol Cell Cardiol 97:245–262. https://doi.org/10.1016/j.yjmcc.2016.06.001

60. Savu O, Jurcuţ R, Giuşcă S, et al (2012) Morphological and functional adaptation of the maternal heart during pregnancy. Circ Cardiovasc Imaging 5:289–297. https://doi.org/10.1161/CIRCIMAGING.111.970012

61. Umar S, Nadadur R, Iorga A, et al (2012) Cardiac structural and hemodynamic changes associated with physiological heart hypertrophy of pregnancy are reversed postpartum. J Appl Physiol 113:1253–1259. https://doi.org/10.1152/japplphysiol.00549.2012

62. Stewart RD, Nelson DB, Matulevicius SA, et al (2016) Cardiac magnetic resonance imaging to assess the impact of maternal habitus on cardiac remodeling during pregnancy. Am J Obstet Gynecol 214:640.e1-640.e6. https://doi.org/10.1016/j.ajog.2015.11.014

63. Borges VTM, Matsubara BB, Magalhães CG, et al (2011) Effect of physiological overload on pregnancy in women with mitral regurgitation. Clinics 66:47–50. https://doi.org/10.1590/S1807-59322011000100009

64. Yosefy C, Shenhav S, Feldman V, et al (2012) Left atrial function during pregnancy: A three-dimensional echocardiographic study. Echocardiography 29:1096–1101. https://doi.org/10.1111/j.1540-8175.2012.01745.x

65. Umazume T, Yamada T, Yamada S, et al (2018) Morphofunctional cardiac changes in pregnant women: Associations with biomarkers. Open Hear 5:. https://doi.org/10.1136/openhrt-2018-000850

66. Estensen ME, Beitnes JO, Grindheim G, et al (2013) Altered maternal left ventricular contractility and function during normal pregnancy. Ultrasound Obstet Gynecol 41:659–666. https://doi.org/10.1002/uog.12296

67. Mesa A, Jessurun C, Hernandez A, et al (1999) Left Ventricular Diastolic Function in Normal Human Pregnancy. Circulation 1:511–517

68. Jindal R, Bajwa SK, Bajwa SJS, Jindal R (2012) Pregnancy in cardiac disease: clinical, obstetric and anaesthetic concerns. Sri Lanka J Obstet Gynaecol 33:174. https://doi.org/10.4038/sljog.v33i4.4809

69. Shin J, Kim M, Lee J, et al (2016) Pregnancy in hypertrophic cardiomyopathy with severe left ventricular outflow tract obstruction. J Cardiovasc Ultrasound 24:158–162. https://doi.org/10.4250/jcu.2016.24.2.158

70. Tso GJ, Lee JM, Shaban NM, et al (2014) Normal echocardiographic measurements in uncomplicated pregnancy, a single center experience. J Cardiovasc Dis Res 5:3–8. https://doi.org/10.5530/jcdr.2014.2.2

71. Kelly ACO, Sharma G, Vaught AJ, Zakaria S (2019) The Use of Echocardiography and Advanced Cardiac Ultrasonography During Pregnancy. https://doi.org/10.1007/s11936-019-0785-5

72. Bamfo JEAK, Kametas NA, Nicolaides KH, Chambers JB (2007) Maternal left ventricular diastolic and systolic long-axis function during normal pregnancy. Eur J Echocardiogr 8:360–368. https://doi.org/10.1016/j.euje.2006.12.004

73. Eghbali M, Deva R, Alioua A, et al (2005) Molecular and functional signature of heart hypertrophy during pregnancy. Circ Res 96:1208–1216. https://doi.org/10.1161/01.RES.0000170652.71414.16

74. Liu S, Elkayam U, Naqvi TZ (2016) Echocardiography in Pregnancy: Part 1. Curr Cardiol Rep 18:. https://doi.org/10.1007/s11886-016-0760-7

75. Ando T, Kaur R, Holmes AA, et al (2015) Physiological adaptation of the left ventricle during the second and third trimesters of a healthy pregnancy: a speckle tracking echocardiography study. Am J Cardiovasc Dis 5:119–126

76. Cong J, Fan T, Yang X, et al (2015) Structural and functional changes in maternal left ventricle during pregnancy: A three-dimensional speckle-tracking echocardiography study. Cardiovasc Ultrasound 13:1–10. https://doi.org/10.1186/1476-7120-13-6

77. Rinaldi CA, Leclercq C, Kranig W, et al (2014) Improvement in acute contractility and hemodynamics with multipoint pacing via a left ventricular quadripolar pacing lead. J Interv Card Electrophysiol 40:75–80. https://doi.org/10.1007/s10840-014-9891-1

78. Mesa A, Jessurun C, Hernandez A, et al (1999) Left Ventricular Diastolic Function in Normal Human Pregnancy. Circulation 99:511–517

79. Regitz-Zagrosek V, Blomstrom Lundqvist C, Borghi C, et al (2011) ESC Guidelines on the management of cardiovascular diseases during pregnancy. Eur Heart J 32:3147–3197. https://doi.org/10.1093/eurheartj/ehr218

80. Akinwusi PO, Oboro VO, Adebayo RA, et al (2011) Cardiovascular and electrocardiographic changes in Nigerians with a normal pregnancy. Cardiovasc J Afr 22:71–75. https://doi.org/10.5830/CVJA-2010-043

81. M S (2014) Electrocradiographic Q RS Axis, Q Wave and T-wave Changes in 2 nd and 3 rd Trimester of Normal Pregnancy. J Clin Diagnostic Res. https://doi.org/10.7860/jcdr/2014/10037.4911

82. Chaudhary S, Saha CG, Sarkar D (2016) Electrocardiographic Changes During Pregnancy at Third Trimester: A Comparative Study. Med J Shree Birendra Hosp 14:41–46. https://doi.org/10.3126/mjsbh.v14i2.13367

83. Bekiesińska-Figatowska M, Romaniuk-Doroszewska A, Szkudlińska-Pawlak S, et al

(2017) Diagnostic imaging of pregnant women – The role of magnetic resonance imaging. Polish J Radiol 82:220–226. https://doi.org/10.12659/PJR.900071

84. Alorainy IA, Albadr FB, Abujamea AH (2006) Attitude towards MRI safety during pregnancy. Ann Saudi Med 26:306–309. https://doi.org/10.5144/0256-4947.2006.306

85. Ray JG, Vermeulen MJ, Bharatha A, et al (2016) Association between MRI exposure during pregnancy and fetal and childhood outcomes. JAMA - J Am Med Assoc 316:952–961. https://doi.org/10.1001/jama.2016.12126

86. Garcia-Bournissen F, Shrim A, Koren G (2006) Motherisk Update: Safety of gadolinium during pregnancy. Can Fam Physician 52:309–310

87. Thornburg KL, Jacobson SL, Giraud GD, Morton MJ (2000) Hemodynamic changes in pregnancy. Semin Perinatol 24:11–14. https://doi.org/10.1016/S0146-0005(00)80047-6

88. Li J, Umar S, Amjedi M, et al (2012) New frontiers in heart hypertrophy during pregnancy. Am J Cardiovasc Dis 2:192–207

89. Shimizu I, Minamino T (2016) Physiological and pathological cardiac hypertrophy. J Mol Cell Cardiol 97:245–262. https://doi.org/10.1016/j.yjmcc.2016.06.001

90. Carreño JE, Apablaza F, Ocaranza MP, Jalil JE (2006) Cardiac Hypertrophy: Molecular and Cellular Events. Rev Española Cardiol (English Ed 59:473–486. https://doi.org/10.1016/s1885-5857(06)60796-2

91. Hill JA, Olson EN (2008) Cardiac plasticity. N Engl J Med 358:1370. https://doi.org/10.1056/NEJMra072139

92. Maillet M, Berlo JH Van, Molkentin JD (2015) Molecular basis of physiological heart growth: fundamental concepts and new players Marjorie. 14:38–48. https://doi.org/10.1038/nrm3495.Molecular

93. Bernardo BC, Weeks KL, Pretorius L, McMullen JR (2010) Molecular distinction between physiological and pathological cardiac hypertrophy: Experimental findings and therapeutic strategies. Pharmacol Ther 128:191–227. https://doi.org/10.1016/j.pharmthera.2010.04.005

94. Harvey PA, Leinwand LA (2011) Cellular mechanisms of cardiomyopathy. J Cell Biol 194:355–365. https://doi.org/10.1083/jcb.201101100

95. Yamazaki T, Komuro I, Yazaki Y (1998) Signalling pathways for cardiac hypertrophy. Cell Signal 10:693–698. https://doi.org/10.1016/S0898-6568(98)00036-9

96. Falcón D, Galeano-Otero I, Calderón-Sánchez E, et al (2019) TRP channels: Current perspectives in the adverse cardiac remodeling. Front Physiol 10:. https://doi.org/10.3389/fphys.2019.00159

97. Stansfield WE, Ranek M, Pendse A, et al (2014) The Pathophysiology of Cardiac Hypertrophy and Heart Failure. In: Cellular and Molecular Pathobiology of Cardiovascular Disease. pp 51–78

98. Psarras S, Beis D, Nikouli S, et al (2019) Three in a Box: Understanding Cardiomyocyte, Fibroblast, and Innate Immune Cell Interactions to Orchestrate Cardiac Repair Processes. Front Cardiovasc Med 6:1–23. https://doi.org/10.3389/fcvm.2019.00032

99. Gonzalez AMD, Osorio JC, Manlhiot C, et al (2007) Hypertrophy signaling during peripartum cardiac remodeling. AJP Hear Circ Physiol 293:H3008–H3013. https://doi.org/10.1152/ajpheart.00401.2007

100. Bernardo BC, Weeks KL, Pretorius L, Mcmullen JR (2010) Pharmacology & Therapeutics Molecular distinction between physiological and pathological cardiac hypertrophy : Experimental fi ndings and therapeutic strategies. Pharmacol Ther 128:191–227. https://doi.org/10.1016/j.pharmthera.2010.04.005

101. Ellison GM, Waring CD, Vicinanza C, Torella D (2012) Physiological cardiac remodelling in response to endurance exercise training: Cellular and molecular mechanisms. Heart 98:5–10. https://doi.org/10.1136/heartjnl-2011-300639

102. Aoyagi T, Matsui T (2011) Phosphoinositide-3 Kinase Signaling in Cardiac Hypertrophy and Heart Failure. Curr Pharm Des 17:1818–1824. https://doi.org/10.2174/138161211796390976

103. Shioi T, McMullen JR, Tarnavski O, et al (2003) Rapamycin attenuates load-induced cardiac hypertrophy in mice. Circulation 107:1664–1670. https://doi.org/10.1161/01.CIR.0000057979.36322.88

104. Xu L, Brink M (2016) mTOR, cardiomyocytes and inflammation in cardiac hypertrophy. Biochim Biophys Acta - Mol Cell Res 1863:1894–1903. https://doi.org/10.1016/j.bbamcr.2016.01.003

105. Harhous Z, Booz GW, Ovize M, et al (2019) An Update on the Multifaceted Roles of STAT3 in the Heart. Front Cardiovasc Med 6:1–18. https://doi.org/10.3389/fcvm.2019.00150

106. Wagner MA, Siddiqui MAQ (2012) The JAK-STAT pathway in hypertrophic stress signaling and genomic stress response. Jak-Stat 1:131–141. https://doi.org/10.4161/jkst.20702

107. Kishore R, Verma SK (2012) Roles of STATs signaling in cardiovascular diseases. Jak-Stat 1:118–124. https://doi.org/10.4161/jkst.20115

108. Haghikia A, Stapel B, Hoch M, Hilfiker-Kleiner D (2011) STAT3 and cardiac remodeling. Heart Fail Rev 16:35–47. https://doi.org/10.1007/s10741-010-9170-x

109. Kurdi M, Zgheib C, Booz GW (2018) Recent Developments on the Crosstalk Between STAT3 and Inflammation in Heart Function and Disease. Front Immunol 9:3029. https://doi.org/10.3389/fimmu.2018.03029

110. Kimura A, Ishida Y, Furuta M, et al (2018) Protective Roles of Interferon-γ in Cardiac Hypertrophy Induced by Sustained Pressure Overload. J Am Heart Assoc 7:. https://doi.org/10.1161/JAHA.117.008145

111. Santos SCR, Lacronique V, Bouchaert I, et al (2001) Constitutively active STAT5 variants induce growth and survival of hematopoietic cells through a PI 3-kinase/Akt dependent pathway. Oncogene 20:2080–2090. https://doi.org/10.1038/sj.onc.1204308

112. Tham YK, Bernardo BC, Ooi JYY, et al (2015) Pathophysiology of cardiac hypertrophy and heart failure: signaling pathways and novel therapeutic targets. Arch Toxicol 89:1401–1438. https://doi.org/10.1007/s00204-015-1477-x

113. Hall ME, George EM, Granger JP (2011) The Heart During Pregnancy. Rev Española Cardiol (English Ed 64:1045–1050. https://doi.org/10.1016/j.rec.2011.07.008

114. Burton GJ, Charnock-Jones DS, Jauniaux E (2009) Regulation of vascular growth and

function in the human placenta. Reproduction 138:895–902. https://doi.org/10.1530/REP-09-0092

115. Eun SL, Oh MJ, Jae WJ, et al (2007) The levels of circulating vascular endothelial growth factor and soluble Flt-1 in pregnancies complicated by preeclampsia. J Korean Med Sci 22:94–98. https://doi.org/10.3346/jkms.2007.22.1.94

116. Wheeler T, Evans PW, Anthony FW, et al (1999) Relationship between maternal serum vascular endothelial growth factor concentration in early pregnancy and fetal and placental growth. Hum Reprod 14:1619–1623. https://doi.org/10.1093/humrep/14.6.1619

117. Thomas M, Augustin HG (2009) The role of the angiopoietins in vascular morphogenesis. Angiogenesis 12:125–137. https://doi.org/10.1007/s10456-009-9147-3

118. Mebazaa A, Seronde MF, Gayat E, et al (2017) Imbalanced angiogenesis in peripartum cardiomyopathy: Diagnostic value of placenta growth factor. Circ J 81:1654–1661. https://doi.org/10.1253/circj.CJ-16-1193

119. Limon-Miranda S, Salazar-Enriquez DG, Muñiz J, et al (2014) Pregnancy Differentially Regulates the Collagens Types i and III in Left Ventricle from Rat Heart. Biomed Res Int 2014:. https://doi.org/10.1155/2014/984785

120. Virgen-Ortiz A, Marin JL, Elizalde A, et al (2009) Passive mechanical properties of cardiac tissues in heart hypertrophy during pregnancy. J Physiol Sci 59:391–396. https://doi.org/10.1007/s12576-009-0047-5

121. Parrott ME, Aljrbi E, Biederman DL, et al (2018) Feature Article: Maternal cardiac messenger RNA expression of extracellular matrix proteins in mice during pregnancy and the postpartum period. Exp Biol Med 243:1220–1232. https://doi.org/10.1177/1535370218818457

122. Frangogiannis NG (2017) The extracellular matrix in myocardial injury, repair, and remodeling. J Clin Invest 127:1600–1612. https://doi.org/10.1172/JCI87491

123. D. F, A. T, J. L, Z. K (2012) Cardiac fibroblasts, fibrosis and extracellular matrix remodeling in heart disease. Fibrogenes Tissue Repair 5:1–13

124. Virgen-Ortiz A, Limón-Miranda S, Salazar-Enríquez DG, et al (2019) Matrix metalloproteinases system and types of fibrosis in rat heart during late pregnancy and postpartum. Med 55:1–8. https://doi.org/10.3390/medicina55050199

125. Bishop JE, Lindahl G (1999) Regulation of cardiovascular collagen synthesis by mechanical load. Cardiovasc Res 42:27–44. https://doi.org/10.1016/S0008-6363(99)00021-8

126. Bowers S, Banerjee I, Baudino T (2010) The Extracellular Matrix: At the Center of it All. J Mol Cell Cardiol 48:474–482. https://doi.org/10.1007/s11103-011-9767-z.Plastid

127. Chung E, Heimiller J, Leinwand LA (2012) Distinct cardiac transcriptional profiles defining pregnancy and exercise. PLoS One 7:. https://doi.org/10.1371/journal.pone.0042297

128. Clapp JF, Capeless E (1997) Cardiovascular function before, during, and after the first and subsequent pregnancies. Am J Cardiol 80:1469–1473. https://doi.org/10.1016/S0002-9149(97)00738-8

129. (2012) Physiologic Changes During Normal Pregnancy and Delivery. Cardiol Clin 30:317–329. https://doi.org/10.1016/J.CCL.2012.05.004

130. Simmons LA, Gillin AG, Jeremy RW (2002) Structural and functional changes in left ventricle during normotensive and preeclamptic pregnancy. Am J Physiol - Hear Circ Physiol 283:1627–1633. https://doi.org/10.1152/ajpheart.00966.2001

131. Castleman JS, Ganapathy R, Taki F, et al (2016) Echocardiographic Structure and Function in Hypertensive Disorders of Pregnancy: A Systematic Review. Circ Cardiovasc Imaging 9:e004888. https://doi.org/10.1161/CIRCIMAGING.116.004888

132. Adeyeye VO, Balogun MO, Adebayo RA, et al (2016) Echocardiographic Assessment of Cardiac Changes During Normal Pregnancy Among Nigerians. Clin Med Insights Cardiol 10:157–162. https://doi.org/10.4137/CMC.S40191.TYPE

133. Jianglong H, James YK (2012) Regression of Pathological Cardiac Hypertrophy: Signaling Pathways and Therapeutic Targets. Pharmacol Ther 135:337–354. https://doi.org/10.1038/jid.2014.371

134. Hou J, Kang YJ (2012) Regression of pathological cardiac hypertrophy: Signaling

pathways and therapeutic targets. Pharmacol Ther 135:337–354. https://doi.org/10.1016/j.pharmthera.2012.06.006

135. Zhou Z, Johnson WT, Kang YJ (2009) Regression of copper-deficient heart hypertrophy: reduction in the size of hypertrophic cardiomyocytes. J Nutr Biochem 20:621–628. https://doi.org/10.1016/j.jnutbio.2008.06.007

136. Shiojima I, Sato K, Izumiya Y, et al (2005) Disruption of coordinated cardiac hypertrophy and angiogenesis contributes to the transition to heart failure. J Clin Invest 115:2108–2118. https://doi.org/10.1172/JCI24682

137. Takimoto E, Champion HC, Li M, et al (2005) Chronic inhibition of cyclic GMP phosphodiesterase 5A prevents and reverses cardiac hypertrophy. Nat Med 11:214–222. https://doi.org/10.1038/nm1175

138. Franklin WJ, Benton MK, Parekh DR (2011) Cardiac disease in pregnancy. Texas Hear Inst J 38:151–153

139. Sliwa K, Böhm M (2014) Incidence and prevalence of pregnancy-related heart disease. Cardiovasc Res 101:554–560. https://doi.org/10.1093/cvr/cvu012

140. Gongora MC, Wenger NK (2015) Cardiovascular complications of pregnancy. Int J Mol Sci 16:23905–23928. https://doi.org/10.3390/ijms161023905

141. Amegah AK (2018) Tackling the Growing Burden of Cardiovascular Diseases in Sub-Saharan Africa: Need for Dietary Guidelines. Circulation 138:2449–2451. https://doi.org/10.1161/CIRCULATIONAHA.118.037367

142. Knight M, Bunch K, Tuffnell D, et al (2018) Mbrrace 2014-16

143. NYLIN G (1947) Heart disease and pregnancy. Cardiologia 11:151–174. https://doi.org/10.1159/000164827

144. Elkayam U, Goland S, Pieper PG, Silverside CK (2016) High-Risk Cardiac Disease in Pregnancy: Part I. J Am Coll Cardiol 68:396–410. https://doi.org/10.1016/j.jacc.2016.05.048

145. Regitz-Zagrosek V, Seeland U, Geibel-Zehender A, et al (2011) Cardiovascular diseases in pregnancy. Dtsch Arztebl Int 108:267–273. https://doi.org/10.3238/arztebl.2011.0267

146. Watkins DA, Sebitloane M, Engel ME, Mayosi BM (2012) The burden of antenatal heart disease in South Africa: A systematic review. BMC Cardiovasc Disord 12:23. https://doi.org/10.1186/1471-2261-12-23

147. Soma-Pillay P, Seabe J, Sliwa K (2016) The importance of cardiovascular pathology contributing to maternal death: Confidential Enquiry into Maternal Deaths in South Africa, 2011-2013. Cardiovasc J Afr 27:1–6. https://doi.org/10.5830/CVJA-2016-008

148. Zimmerman M, Sable C (2020) Congenital heart disease in low-and-middle-income countries: Focus on sub-Saharan Africa. Am J Med Genet Part C Semin Med Genet 184:36–46. https://doi.org/10.1002/ajmg.c.31769

149. Patel H, Madanieh R, Kosmas CE, et al (2015) Reversible cardiomyopathies. Clin Med Insights Cardiol 9:7–14. https://doi.org/10.4137/CMC.S19703

150. Blauwet L a., Sliwa K (2011) Peripartum cardiomyopathy. Obstet Med 4:44–52. https://doi.org/10.1258/om.2010.100054

151. Bauersachs J, Arrigo M, Hilfiker-Kleiner D, et al (2016) Current management of patients with severe acute peripartum cardiomyopathy: practical guidance from the Heart Failure Association of the European Society of Cardiology Study Group on peripartum cardiomyopathy. Eur J Heart Fail 18:1096–1105. https://doi.org/10.1002/ejhf.586

152. Hilfiker-Kleiner D, Sliwa K (2014) Pathophysiology and epidemiology of peripartum cardiomyopathy. Nat Rev Cardiol 11:364–70. https://doi.org/10.1038/nrcardio.2014.37

153. Bauersachs J, König T, van der Meer P, et al (2019) Pathophysiology, diagnosis and management of peripartum cardiomyopathy: a position statement from the Heart Failure Association of the European Society of Cardiology Study Group on peripartum cardiomyopathy. Eur J Heart Fail 21:827–843. https://doi.org/10.1002/ejhf.1493

154. Bello NA, Arany Z (2016) Molecular mechanisms of peripartum cardiomyopathy: A vascular/hormonal hypothesis. Trends Cardiovasc Med 25:499–504. https://doi.org/10.1016/j.tcm.2015.01.004.Molecular

155. Sliwa K, Mebazaa A, Hilfiker-Kleiner D, et al (2017) Clinical characteristics of patients

from the worldwide registry on peripartum cardiomyopathy (PPCM). Eur J Heart Fail 1–11. https://doi.org/10.1002/ejhf.780

156. Haghikia A, Podewski E, Berliner D, et al (2015) Rationale and design of a randomized, controlled multicentre clinical trial to evaluate the effect of bromocriptine on left ventricular function in women with peripartum cardiomyopathy. Clin Res Cardiol 104:911–917. https://doi.org/10.1007/s00392-015-0869-5

157. Kamiya C a., Kitakaze M, Ishibashi-Ueda H, et al (2011) Different Characteristics of Peripartum Cardiomyopathy Between Patients Complicated With and Without Hypertensive Disorders. Circ J 75:1975–1981. https://doi.org/10.1253/circj.CJ-10-1214

158. Biteker M, Ilhan E, Biteker G, et al (2012) Delayed recovery in peripartum cardiomyopathy: An indication for long-term follow-up and sustained therapy. Eur J Heart Fail 14:895–901. https://doi.org/10.1093/eurjhf/hfs070

159. Gunderson EP, Croen LA, Chiang V, et al (2011) Epidemiology of Peripartum Cardiomyopathy. Obstet Gynecol 118:583–591. https://doi.org/10.1097/AOG.0b013e318229e6de

160. Sliwa K, Mebazaa A, Hilfiker-Kleiner D, et al (2017) Clinical characteristics of patients from the worldwide registry on peripartum cardiomyopathy (PPCM): EURObservational Research Programme in conjunction with the Heart Failure Association of the European Society of Cardiology Study Group on PPCM. Eur J Heart Fail 19:1131–1141. https://doi.org/10.1002/ejhf.780

161. Azibani, Feriel. Sliwa K (2018) Peripartum Cardiomyopathy : An Update Peripartum Cardiomyopathy. COMORBIDITIES Hear Fail 10:

162. Yamac H, Bultmann I, Sliwa K, Hilfiker-Kleiner D (2010) Prolactin: a new therapeutic target in peripartum cardiomyopathy. Heart 96:1352–1357. https://doi.org/10.1136/hrt.2009.179218

163. Hilfiker-Kleiner D, Sliwa K, Drexler H (2008) Peripartum Cardiomyopathy: Recent Insights in its Pathophysiology. Trends Cardiovasc Med 18:173–179. https://doi.org/10.1016/j.tcm.2008.05.002

164. Toescu V, Nuttall SL, Martin U, et al (2002) Oxidative stress and normal pregnancy. Clin Endocrinol (Oxf) 57:609–613. https://doi.org/10.1046/j.1365-2265.2002.01638.x

165. Hilfiker-Kleiner D, Kaminski K, Podewski E, et al (2007) A Cathepsin D-Cleaved 16 kDa Form of Prolactin Mediates Postpartum Cardiomyopathy. Cell 128:589–600. https://doi.org/10.1016/j.cell.2006.12.036

166. Macotela Y, Aguilar MB, Guzmán-Morales J, et al (2006) Matrix metalloproteases from chondrocytes generate an antiangiogenic 16 kDa prolactin. J Cell Sci 119:1790–1800. https://doi.org/10.1242/jcs.02887

167. Hilfiker-Kleiner D, Kaminski K, Podewski E, et al (2007) A Cathepsin D-Cleaved 16 kDa Form of Prolactin Mediates Postpartum Cardiomyopathy. Cell 128:589–600. https://doi.org/10.1016/j.cell.2006.12.036

168. Arany Z (2018) Understanding Peripartum Cardiomyopathy. Annu Rev Med 69:1.1-1.12. https://doi.org/10.1146/annurev-med-041316

169. Patten IS, Rana S, Shahul S, et al (2012) Sup-Cardiac angiogenic imbalance leads to peripartum cardiomyopathy. Nature 485:333–8. https://doi.org/10.1038/nature11040

170. Negoro S, Kunisada K, Fujio Y, Funamoto M (2001) Activation of Signal Transducer and Activator of Hypoxia / Reoxygenation-Induced Oxidative Stress Through the Upregulation of Manganese Superoxide Dismutase. 979–981

171. Hilfiker-Kleiner D, Sliwa K, Drexler H (2008) Peripartum Cardiomyopathy: Recent Insights in its Pathophysiology. Trends Cardiovasc Med 18:173–179. https://doi.org/10.1016/j.tcm.2008.05.002

172. Halkein J, Tabruyn SP, Ricke-Hoch M, et al (2013) MicroRNA-146a is a therapeutic target and biomarker for peripartum cardiomyopathy. J Clin Invest 123:2143–2154. https://doi.org/10.1172/JCI64365

173. Ricke-hoch M, Pfeffer TJ, Hilfiker-kleiner D (2020) Peripartum cardiomyopathy : basic mechanisms and hope for new therapies. 520–531. https://doi.org/10.1093/cvr/cvz252

174. Sliwa K, Skudicky D, Candy G, et al (2002) The addition of pentoxifylline to

conventional therapy improves outcome in patients with peripartum cardiomyopathy. Eur J Heart Fail 4:305–309. https://doi.org/10.1016/S1388-9842(02)00008-9

175. Patten IS, Rana S, Shahul S, et al (2012) Cardiac angiogenic imbalance leads to peripartum cardiomyopathy. Nature 485:333–338. https://doi.org/10.1038/nature11040

176. Nonhoff J, Ricke-Hoch M, Mueller M, et al (2017) Serelaxin treatment promotes adaptive hypertrophy but does not prevent heart failure in experimental peripartum cardiomyopathy. Cardiovasc Res cvw245. https://doi.org/10.1093/cvr/cvw245

177. Haghikia A, Kaya Z, Schwab J, et al (2015) Evidence of autoantibodies against cardiac troponin I and sarcomeric myosin in peripartum cardiomyopathy. Basic Res Cardiol 110:1–9. https://doi.org/10.1007/s00395-015-0517-2

178. Ricke-hoch M, Bultmann I, Stapel B, et al (2014) Opposing roles of Akt and STAT3 in the protection of the maternal heart from peripartum stress. 587–596. https://doi.org/10.1093/cvr/cvu010

179. Nishida K, Otsu K (2016) Autophagy during cardiac remodeling. J Mol Cell Cardiol 95:11–18. https://doi.org/10.1016/j.yjmcc.2015.12.003

180. Kavazis AN (2015) Pathological vs. physiological cardiac hypertrophy. J Physiol 593:3767. https://doi.org/10.1113/JP271161

181. Dorn GW (2007) The fuzzy logic of physiological cardiac hypertrophy. Hypertension 49:962–970. https://doi.org/10.1161/HYPERTENSIONAHA.106.079426

182. Shimizu I, Minamino T (2016) Physiological and pathological cardiac hypertrophy. J Mol Cell Cardiol 97:245–262. https://doi.org/10.1016/j.yjmcc.2016.06.001

183. Schirone L, Forte M, Palmerio S, Frati G (2017) A Review of the Molecular Mechanisms Underlying the Development and Progression of Cardiac Remodeling Leonardo. Oxid Med Cell Longev 10:1–16

184. Kehat I, Molkentin JD (2010) Molecular pathways underlying cardiac remodeling during pathophysiological stimulation. Circulation 122:2727–2735. https://doi.org/10.1161/CIRCULATIONAHA.110.942268

185. Barallobre-barreiro J, Didangelos A, Schoendube FA, et al (2012) Proteomics Analysis of Cardiac Extracellular Matrix Remodeling in a Porcine Model of Ischemia / Reperfusion Injury. https://doi.org/10.1161/CIRCULATIONAHA.111.056952

186. Li L, Zhao Q, Kong W (2018) Extracellular matrix remodeling and cardiac fibrosis. Matrix Biol 68–69:490–506. https://doi.org/10.1016/j.matbio.2018.01.013

187. Kehat I, Molkentin JD (2010) Molecular pathways underlying cardiac remodeling during pathophysiological stimulation. Circulation 122:2727–2735. https://doi.org/10.1161/CIRCULATIONAHA.110.942268

188. Pai P, Velmurugan BK, Kuo C-H, et al (2017) 17beta-Estradiol and/or estrogen receptor alpha blocks isoproterenol-induced calcium accumulation and hypertrophy via GSK3beta/PP2A/NFAT3/ANP pathway. Mol Cell Biochem. https://doi.org/10.1007/s11010-017-3048-3

189. Bollen IAE, Van Deel ED, Kuster DWD, Van Der Velden J (2015) Peripartum cardiomyopathy and dilated cardiomyopathy: Different at heart. Front Physiol 6:1–9. https://doi.org/10.3389/fphys.2014.00531

190. Sag CM, Wagner S, Maier LS (2013) Role of oxidants on calcium and sodium movement in healthy and diseased cardiac myocytes. Free Radic Biol Med 63:338–349. https://doi.org/10.1016/j.freeradbiomed.2013.05.035

191. Eghbali M, Deva R, Alioua A, et al (2005) Molecular and functional signature of heart hypertrophy during pregnancy. Circ Res 96:1208–1216. https://doi.org/10.1161/01.RES.0000170652.71414.16

192. Hayakawa Y, Chandra M, Miao W, et al (2003) Inhibition of Cardiac Myocyte Apoptosis Improves Cardiac Function and Abolishes Mortality in the Peripartum Cardiomyopathy of Gαq Transgenic Mice. Circulation 108:3036–3041. https://doi.org/10.1161/01.CIR.0000101920.72665.58

193. Stapel B, Kohlhaas M, Ricke-Hoch M, et al (2017) Low STAT3 expression sensitizes to toxic effects of ??-adrenergic receptor stimulation in peripartum cardiomyopathy. Eur Heart J 38:349–361. https://doi.org/10.1093/eurheartj/ehw086

194. Bollen IAE, Ehler E, Fleischanderl K, et al (2017) Myo fi lament Remodeling and

Function Is More Impaired in Peripartum Cardiomyopathy Compared with Dilated Cardiomyopathy and Ischemic Heart Disease. 187:. https://doi.org/10.1016/j.ajpath.2017.08.022

195. Gaasch WH, Zile MR (2011) Left ventricular structural remodeling in health and disease: With special emphasis on volume, mass, and geometry. J Am Coll Cardiol 58:1733–1740. https://doi.org/10.1016/j.jacc.2011.07.022

196. Wilkins BJ, Dai YS, Bueno OF, et al (2004) Calcineurin/NFAT Coupling Participates in Pathological, but not Physiological, Cardiac Hypertrophy. Circ Res 94:110–118. https://doi.org/10.1161/01.RES.0000109415.17511.18

197. Rohini A, Agrawal N, Koyani CN, Singh R (2010) Molecular targets and regulators of cardiac hypertrophy. Pharmacol Res 61:269–280. https://doi.org/10.1016/j.phrs.2009.11.012

198. Chin ER, Olson EN, Richardson JA, et al (1998) A calcineurin-dependent transcriptional pathway controls skeletal muscle fiber type. Genes Dev 12:2499–2509. https://doi.org/10.1101/gad.12.16.2499

199. Cox EJ, Marsh SA (2014) A systematic review of fetal genes as biomarkers of cardiac hypertrophy in rodent models of diabetes. PLoS One 9:1–11. https://doi.org/10.1371/journal.pone.0092903

200. Lyons GE, Schiaffino S, Sassoon D, et al (1990) Developmental regulation of myosin gene expression in mouse cardiac muscle. J Cell Biol 111:2427–2436. https://doi.org/10.1083/jcb.111.6.2427

201. Fessler, Michael B.; Rudel, Lawrence L.; Brown M (2008) 基因的改变NIH Public Access. Bone 23:1–7. https://doi.org/10.1038/jid.2014.371

202. Solomonov I, Zehorai E, Talmi-Frank D, et al (2016) Distinct biological events generated by ECM proteolysis by two homologous collagenases. Proc Natl Acad Sci U S A 113:10884–10889. https://doi.org/10.1073/pnas.1519676113

203. Azibani F, Pfeffer TJ, Ricke-Hoch M, et al (2020) Outcome in German and South African peripartum cardiomyopathy cohorts associates with medical therapy and fibrosis markers. ESC Hear Fail 7:512–522. https://doi.org/10.1002/ehf2.12553

204. Schmidt A, Forne I, Imhof A (2014) Bioinformatic analysis of proteomics data. BMC Syst Biol 8:S3. https://doi.org/10.1186/1752-0509-8-S2-S3

205. Zannad F, Alla F, Dousset B, et al (2000) Limitation of excessive extracellular matrix turnover may contribute to survival benefit of spironolactone therapy in patients with congestive heart failure: Insights from the Randomized Aldactone Evaluation Study (RALES). Circulation 102:2700–2706. https://doi.org/10.1161/01.CIR.102.22.2700

206. Motiwala SR, Szymonifka J, Belcher A, et al (2013) Serial measurement of galectin-3 in patients with chronic heart failure: Results from the ProBNP Outpatient Tailored Chronic Heart Failure Therapy (PROTECT) study. Eur J Heart Fail 15:1157–1163. https://doi.org/10.1093/eurjhf/hft075

207. G. Michael Felker, MD, MS*, Mona Fiuzat, PharmD*, Vivian Thompson, MPH†, Linda K. Shaw, MS†, Megan L. Neely, PhD†, Kirkwood F. Adams, MD‡, David J. Whellan, MD§, Mark P. Donahue, MD, MHS*, Tariq Ahmad, MD, MPH*, Dalane W. Kitzman, MD|| ILP, MD¶ (2013) Soluble ST2 in Ambulatory Patients with Heart Failure: Association with Functional Capacity and Long-Term Outcomes. Circ Hear Fail 6:1172–1179. https://doi.org/10.1038/jid.2014.371

208. Oh K, Seo MW, Kim YW, Lee D-S (2015) Osteopontin Potentiates Pulmonary Inflammation and Fibrosis by Modulating IL-17/IFN-γ-secreting T-cell Ratios in Bleomycin-treated Mice. Immune Netw 15:142. https://doi.org/10.4110/in.2015.15.3.142

209. Tyagi SC (2000) Physiology and homeostasis of extracellular matrix: Cardiovascular adaptation and remodeling. Pathophysiology 7:177–182. https://doi.org/10.1016/S0928-4680(00)00046-8

210. Chancey AL, Brower GL, Peterson JT, Janicki JS (2002) Effects of matrix metalloproteinase inhibition on ventricular remodeling due to volume overload. Circulation 105:1983–1988. https://doi.org/10.1161/01.CIR.0000014686.73212.DA

211. King MK, Coker ML, Goldberg A, et al (2003) Selective matrix metalloproteinase inhibition with developing heart failure: Effects on left ventricular function and structure. Circ Res 92:177–185. https://doi.org/10.1161/01.RES.0000052312.41419.55

212. Fedak PWM, Smookler DS, Kassiri Z, et al (2004) TIMP-3 deficiency leads to dilated cardiomyopathy. Circulation 110:2401–2409. https://doi.org/10.1161/01.CIR.0000134959.83967.2D

213. Segura AM, Frazier OH, Buja LM (2014) Fibrosis and heart failure. Heart Fail Rev 19:173–185. https://doi.org/10.1007/s10741-012-9365-4

214. Ntusi NBA, Mayosi BM (2009) Aetiology and risk factors of peripartum cardiomyopathy: A systematic review. Int J Cardiol 131:168–179. https://doi.org/10.1016/j.ijcard.2008.06.054

215. Li J, Schwimmbeck PL, Tschope C, et al (2002) Collagen degradation in a murine myocarditis model: Relevance of matrix metalloproteinase in association with inflammatory induction. Cardiovasc Res 56:235–247. https://doi.org/10.1016/S0008-6363(02)00546-1

216. Sivasubramanian N, Coker ML, Kurrelmeyer KM, et al (2001) Left ventricular remodeling in transgenic mice with cardiac restricted overexpression of tumor necrosis factor. Circulation 104:826–831. https://doi.org/10.1161/hc3401.093154

217. Siwik DA, Chang DLF, Colucci WS (2000) Interleukin-1 β and tumor necrosis factor-α decrease collagen synthesis and increase matrix metalloproteinase activity in cardiac fibroblasts in vitro. Circ Res 86:1259–1265. https://doi.org/10.1161/01.RES.86.12.1259

218. Zhao J, Pei L (2020) Cardiac Endocrinology: Heart-Derived Hormones in Physiology and Disease. JACC Basic to Transl Sci 5:949–960. https://doi.org/10.1016/j.jacbts.2020.05.007

219. Garciá-Arias MR, Gómez-Acosta SA, Medina-Galindo J, et al (2020) Heart as an endocrine organ. Med Interna Mex 36:199–211. https://doi.org/10.24245/mim.v36i2.2911

220. Wang T, Liu J, McDonald C, et al (2017) GDF 15 is a heart-derived hormone that regulates body growth . EMBO Mol Med 9:1150–1164. https://doi.org/10.15252/emmm.201707604

221. Kempf T, Eden M, Strelau J, et al (2006) The transforming growth factor-β superfamily

member growth-differentiation factor-15 protects the heart from ischemia/reperfusion injury. Circ Res 98:351–360. https://doi.org/10.1161/01.RES.0000202805.73038.48

222. Bootcov MR, Bauskin AR, Valenzuela SM, et al (1997) MIC-1, a novel macrophage inhibitory cytokine, is a divergent member of the TGF-β superfamily. Proc Natl Acad Sci U S A 94:11514–11519. https://doi.org/10.1073/pnas.94.21.11514

223. Wischhusen J, Melero I, Fridman WH (2020) Growth/Differentiation Factor-15 (GDF-15): From Biomarker to Novel Targetable Immune Checkpoint. Front Immunol 11:. https://doi.org/10.3389/fimmu.2020.00951

224. Cleavage P (2018) Growth Differentiation Factor 15 Maturation Requires Proteolytic Cleavage by PCSK3, -5, and -6. 1–11

225. Xu X, Li Z, Gao W (2011) Growth differentiation factor 15 in cardiovascular diseases: From bench to bedside. Biomarkers 16:466–475. https://doi.org/10.3109/1354750X.2011.580006

226. Lawton LN, Bonaldo MDF, Jelenc PC, et al (1997) Identification of a novel member of the TGF-beta superfamily highly expressed in human placenta. Gene 203:17–26. https://doi.org/10.1016/S0378-1119(97)00485-X

227. Clerk A, Kemp TJ, Zoumpoulidou G, Sugden PH (2007) Cardiac myocyte gene expression profiling during H2O 2-induced apoptosis. Physiol Genomics 29:118–127. https://doi.org/10.1152/physiolgenomics.00168.2006

228. Frank D, Kuhn C, Brors B, et al (2008) Gene expression pattern in biomechanically stretched cardiomyocytes: Evidence for a stretch-specific gene program. Hypertension 51:309–318. https://doi.org/10.1161/HYPERTENSIONAHA.107.098046

229. Wang J, Wei L, Yang X, Zhong J (2019) Roles of Growth Differentiation Factor 15 in Atherosclerosis and Coronary Artery Disease. J Am Heart Assoc 8:e012826. https://doi.org/10.1161/JAHA.119.012826

230. George M, Jena A, Srivatsan V, et al (2016) GDF 15 - A Novel Biomarker in the Offing for Heart Failure. Curr Cardiol Rev 12:37–46. https://doi.org/10.2174/1573403x12666160111125304

231. Wollert KC, Kempf T, Wallentin L (2017) Growth differentiation factor 15 as a biomarker in cardiovascular disease. Clin Chem 63:140–151. https://doi.org/10.1373/clinchem.2016.255174

232. Lind L, Wallentin L, Kempf T, et al (2009) Growth-differentiation factor-15 is an independent marker of cardiovascular dysfunction and disease in the elderly: Results from the Prospective Investigation of the Vasculature in Uppsala Seniors (PIVUS) study. Eur Heart J 30:2346–2353. https://doi.org/10.1093/eurheartj/ehp261

233. Lori B. Daniels, MD, MAS*, Paul Clopton, MS*,†, Gail A. Laughlin, PhD‡, Alan S. Maisel, MD, FACC*,†, and Elizabeth Barrett-Connor M (2008) Growth-Differentiation Factor-15 is a Robust, Independent Predictor of 11-Year Mortality Risk in Community-Dwelling Older Adults: The Rancho Bernardo Study. Circulation 23:1–7. https://doi.org/10.1161/CIRCULATIONAHA.110.979740.Growth-Differentiation

234. Xu J, Kimball TR, Lorenz JN, et al (2006) GDF15/MIC-1 functions as a protective and antihypertrophic factor released from the myocardium in association with SMAD protein activation. Circ Res 98:342–350. https://doi.org/10.1161/01.RES.0000202804.84885.d0

235. Arkoumani M, Papadopoulou-Marketou N, Nicolaides NC, et al (2020) The clinical impact of growth differentiation factor-15 in heart disease: A 2019 update. Crit Rev Clin Lab Sci 57:114–125. https://doi.org/10.1080/10408363.2019.1678565

236. Adela R, Banerjee SK (2015) GDF-15 as a target and biomarker for diabetes and cardiovascular diseases: A translational prospective. J Diabetes Res 2015:. https://doi.org/10.1155/2015/490842

237. Li J, Yang L, Qin W, et al (2013) Adaptive Induction of Growth Differentiation Factor 15 Attenuates Endothelial Cell Apoptosis in Response to High Glucose Stimulus. PLoS One 8:1–8. https://doi.org/10.1371/journal.pone.0065549

238. Heger J, Schiegnitz E, Von Waldthausen D, et al (2010) Growth differentiation factor 15 acts anti-apoptotic and pro-hypertrophic in adult cardiomyocytes. J Cell Physiol 224:120–126. https://doi.org/10.1002/jcp.22102

239. Parasuraman S, Raveendran R, Kesavan R (2010) Blood sample collection in small laboratory animals. J Pharmacol Pharmacother 1:87–93.

https://doi.org/10.4103/0976-500X.72350

240. Valentim AM, Alves HC, Olsson IAS, Antunes LM (2008) The effects of depth of isoflurane anesthesia on the performance of mice in a simple spatial learning task. J Am Assoc Lab Anim Sci 47:16–19

241. Pachon RE, Scharf BA, Vatner DE, Vatner SF (2020) Best anesthetics for assessing left ventricular systolic function by echocardiography in mice. 308:1–13. https://doi.org/10.1152/ajpheart.00890.2014

242. 2100 KV I m a g i n g G u i d e G u i d e t o S m a l l A n i m a l E c h o c a r d i o g r a p h y u s i n g t h e V e v o ® 2 1 0 0 I m a g i n g S y s t e m. Imaging 0–25

243. Ram R, Mickelsen DM, Theodoropoulos C, Blaxall BC (2011) New approaches in small animal echocardiography: imaging the sounds of silence. AJP Hear Circ Physiol 301:H1765–H1780. https://doi.org/10.1152/ajpheart.00559.2011

244. Gibson DG, Francis DP (2003) Clinical assessment of left ventricular diastolic function. Heart 89:231–238. https://doi.org/10.1136/heart.89.2.231

245. Fisher P, Noyes H, Kemp S, Stevens R Systematic Method for Discovery of Candidate Genes Responsible. Methods Mol Biol 329–345. https://doi.org/10.1007/978-1-60761-247-6

246. Zhu W, Smith JW, Huang CM (2010) Mass spectrometry-based label-free quantitative proteomics. J Biomed Biotechnol 2010:. https://doi.org/10.1155/2010/840518

247. Meyer J (2019) Fast Proteome Identification and Quantification from Data-Dependent Acquisition–Tandem Mass Spectrometry (DDA MS/MS) Using Free Software Tools. Methods Protoc 2:8. https://doi.org/10.3390/mps2010008

248. Lengqvist J, Andrade J, Yang Y, et al (2009) Robustness and accuracy of high speed LC-MS separations for global peptide quantitation and biomarker discovery. J Chromatogr B Anal Technol Biomed Life Sci 877:1306–1316. https://doi.org/10.1016/j.jchromb.2009.02.052

249. Szklarczyk D, Gable AL, Lyon D, et al (2019) STRING v11: Protein-protein association networks with increased coverage, supporting functional discovery in genome-wide experimental datasets. Nucleic Acids Res 47:D607–D613.

https://doi.org/10.1093/nar/gky1131

250. Lachmann A, Xu H, Krishnan J, et al (2010) ChEA: Transcription factor regulation inferred from integrating genome-wide ChIP-X experiments. Bioinformatics 26:2438–2444. https://doi.org/10.1093/bioinformatics/btq466

251. Chen EY, Xu H, Gordonov S, et al (2012) Expression2Kinases: mRNA profiling linked to multiple upstream regulatory layers. Bioinformatics 28:105–111. https://doi.org/10.1093/bioinformatics/btr625

252. Livak KJ, Schmittgen TD (2001) Analysis of relative gene expression data using real-time quantitative PCR and the 2-ΔΔCT method. Methods 25:402–408. https://doi.org/10.1006/meth.2001.1262

253. Lang RM, Badano LP, Mor-Avi V, et al (2015) Recommendations for cardiac chamber quantification by echocardiography in adults: An update from the American society of echocardiography and the European association of cardiovascular imaging. Eur Heart J Cardiovasc Imaging 16:233–271. https://doi.org/10.1093/ehjci/jev014

254. Enders AC, Blankenship TN (1999) Comparative placental structure. Adv Drug Deliv Rev 38:3–15. https://doi.org/10.1016/S0169-409X(99)00003-4

255. Maria Dahl Andersen AKOA, Maria Dahl Andersen AKOA, Duvald CS, et al (2018) Animal Models of Fetal Medicine and Obstetrics. In: Intech. p 13

256. Doevendans PA, Daemen MJ, De Muinck ED, Smits JF (1998) Cardiovascular phenotyping in mice. Cardiovasc Res 39:34–49. https://doi.org/10.1016/S0008-6363(98)00073-X

257. Maria Dahl Andersen AKOA, Maria Dahl Andersen AKOA, Duvald CS, et al (2018) Animal Models of Fetal Medicine and Obstetrics. In: Intech. p 13

258. Camacho P, Fan H, Liu Z, He JQ (2016) Small mammalian animal models of heart disease. Am J Cardiovasc Dis 6:70–80

259. Lip GYH, Steeds RP (2016) Ventricular Structure and Function Echocardiographic Structure and Function in Hypertensive Disorders of Pregnancy A Systematic Review. 1–13. https://doi.org/10.1161/CIRCIMAGING.116.004888

260. Vasapollo B, Valensise H, Novelli GP, et al (2002) Abnormal maternal cardiac function

and morphology in pregnancies complicated by intrauterine fetal growth restriction. Ultrasound Obstet Gynecol 20:452–457. https://doi.org/10.1046/j.1469-0705.2002.00847.x

261. Desai DK, Moodley J, Naidoo DP (2004) Echocardiographic assessment of cardiovascular hemodynamics in normal pregnancy. Obstet Gynecol 104:20–29. https://doi.org/10.1097/01.AOG.0000128170.15161.1d

262. Naqvi TZ, Elkayam U (2012) Serial echocardiographic assessment of the human heart in normal pregnancy. Circ Cardiovasc Imaging 5:283–285. https://doi.org/10.1161/CIRCIMAGING.112.974808

263. Bamfo JEAK, Kametas NA, Nicolaides KH, Chambers JB (2007) Reference ranges for tissue Doppler measures of maternal systolic and diastolic left ventricular function. Ultrasound Obstet Gynecol 29:414–420. https://doi.org/10.1002/uog.3966

264. Vlahović-Stipac A, Stankić V, Popović ZB, et al (2010) Left ventricular function in gestational hypertension: Serial echocardiographic study. Am J Hypertens 23:85–91. https://doi.org/10.1038/ajh.2009.168

265. Melchiorre K, Sharma R, Khalil A, Thilaganathan B (2016) Maternal cardiovascular function in normal pregnancy: Evidence of maladaptation to chronic volume overload. Hypertension 67:754–762. https://doi.org/10.1161/HYPERTENSIONAHA.115.06667

266. Opie LH, Commerford PJ, Gersh BJ, Pfeffer MA (2006) Controversies in ventricular remodelling. Lancet

267. Sampaolesi M, Van Calsteren K (2017) Physiological and pathological gestational cardiac hypertrophy: what can we learn from rodents? Cardiovasc Res 113:1533–1535. https://doi.org/10.1093/cvr/cvx192

268. Lyrio R, Jr FR, Stefanon I (2014) Sex hormones in the cardiovascular system. 18:89–103. https://doi.org/10.1515/hmbci-2013-0048

269. Kodogo V, Azibani F, Sliwa K (2019) Role of pregnancy hormones and hormonal interaction on the maternal cardiovascular system: a literature review. Clin Res Cardiol 1–16. https://doi.org/10.1007/s00392-019-01441-x

270. Novella S, Pérez-Cremades D, Mompeón A, Hermenegildo C (2019) Mechanisms underlying the influence of oestrogen on cardiovascular physiology in women. J Physiol 597:4873–4886. https://doi.org/10.1113/JP278063

271. Holden P (2011) Characterization Of Pregnancy Induced Cardiac Hypertrophy In Rats. Online Theses Diss

272. Dworatzek E, Mahmoodzadeh S, Schubert C, et al (2014) Sex differences in exercise-induced physiological myocardial hypertrophy are modulated by oestrogen receptor beta. Cardiovasc Res 102:418–428. https://doi.org/10.1093/cvr/cvu065

273. Horio T, Nishikimi T, Yoshihara F, et al (2000) Inhibitory Regulation of Hypertrophy by Endogenous Atrial Natriuretic Peptide in Cultured Cardiac Myocytes. Hypertension 35:19. https://doi.org/10.1161/01.HYP.35.1.19

274. Mishra S, Ling H, Grimm M, Zhang T (2011) Cardiac Hypertrophy and Heart Failure Development Through Gq and CaM Kinase II Signaling. NIH-PA 56:598–603. https://doi.org/10.1097/FJC.0b013e3181e1d263.Cardiac

275. Kan C, Cao J, Hou J, et al (2019) Correlation of miR-21 and BNP with pregnancy-inducedhypertension complicated with heart failureand the diagnostic value. Exp Ther Med 3129–3135. https://doi.org/10.3892/etm.2019.7286

276. Barry SP, Davidson SM, Townsend PA (2008) Molecular regulation of cardiac hypertrophy. Int J Biochem Cell Biol 40:2023–2039. https://doi.org/10.1016/j.biocel.2008.02.020

277. Thum T, Galuppo P, Wolf C, et al (2007) MicroRNAs in the human heart: A clue to fetal gene reprogramming in heart failure. Circulation 116:258–267. https://doi.org/10.1161/CIRCULATIONAHA.107.687947

278. Chung E, Yeung F, Leinwand LA (2012) Akt and MAPK signaling mediate pregnancy-induced cardiac adaptation. J Appl Physiol 112:1564–1575. https://doi.org/10.1152/japplphysiol.00027.2012

279. Yeves AM, Villa-Abrille MC, Pérez NG, et al (2014) Physiological cardiac hypertrophy: Critical role of AKT in the prevention of NHE-1 hyperactivity. J Mol Cell Cardiol 76:186–195. https://doi.org/10.1016/j.yjmcc.2014.09.004

280. Regitz-Zagrosek V, Blomstrom Lundqvist C, Borghi C, et al (2018) 2018 ESC Guidelines on the management of cardiovascular diseases during pregnancy. Eur Heart J 32:3147–3197. https://doi.org/10.1093/eurheartj/ehr218

281. Narayanan M, Elkayam U, Naqvi TZ (2016) Echocardiography in Pregnancy: Part 2. Curr Cardiol Rep 18:1–12. https://doi.org/10.1007/s11886-016-0761-6

282. De Lucia C, Wallner M, Eaton DM, et al (2019) Echocardiographic Strain Analysis for the Early Detection of Left Ventricular Systolic/Diastolic Dysfunction and Dyssynchrony in a Mouse Model of Physiological Aging. Journals Gerontol - Ser A Biol Sci Med Sci 74:455–461. https://doi.org/10.1093/gerona/gly139

283. Schnelle M, Catibog N, Zhang M, et al (2018) Echocardiographic evaluation of diastolic function in mouse models of heart disease. J Mol Cell Cardiol 114:20–28. https://doi.org/10.1016/j.yjmcc.2017.10.006

284. Bhan A, Sirker A, Zhang J, et al (2014) High-frequency speckle tracking echocardiography in the assessment of left ventricular function and remodeling after murine myocardial infarction. Am J Physiol - Hear Circ Physiol 306:1371–1383. https://doi.org/10.1152/ajpheart.00553.2013

285. Sengupta SP, Bansal M, Hofstra L, et al (2017) Gestational changes in left ventricular myocardial contractile function: new insights from two-dimensional speckle tracking echocardiography. Int J Cardiovasc Imaging 33:69–82. https://doi.org/10.1007/s10554-016-0977-y

286. Katz R, Karliner JS, Resnik R (1978) Effects of a natural volume overload state (pregnancy) on left ventricular performance in normal human subjects. Circulation 58:434–441. https://doi.org/10.1161/01.CIR.58.3.434

287. Szaluś-Jordanow O, Czopowicz M, Witkowski L, et al (2018) Change of heart dimensions and function during pregnancy in goats. Res Vet Sci 118:351–356. https://doi.org/10.1016/j.rvsc.2018.03.005

288. Geva T, Mauer MB, Striker L, et al (1997) Effects of physiologic load of pregnancy on left ventricular contractility and remodeling. Am Heart J 133:53–59. https://doi.org/10.1016/S0002-8703(97)70247-3

289. Cong J, Fan T, Yang X, et al (2015) Structural and functional changes in maternal left ventricle during pregnancy: a three-dimensional speckle-tracking echocardiography study. Cardiovasc Ultrasound 13:6. https://doi.org/10.1186/1476-7120-13-6

290. Mieghem T Van, Imaging C (2012) Morphological and Functional Adaptation of the Maternal Heart During Pregnancy. Circ Cardiovasc Imaging is 10:. https://doi.org/10.1161/CIRCIMAGING.111.970012

291. Nii M, Ishida M, Dohi K, et al (2018) Myocardial tissue characterization and strain analysis in healthy pregnant women using cardiovascular magnetic resonance native T1 mapping and feature tracking technique. J Cardiovasc Magn Reson 20:4–13. https://doi.org/10.1186/s12968-018-0476-5

292. Khan SG, Melikian N, Mushemi-Blake S, et al (2016) Physiological reduction in left ventricular contractile function in healthy postpartum women: Potential overlap with peripartum cardiomyopathy. PLoS One 11:1–13. https://doi.org/10.1371/journal.pone.0147074

293. Li J, Umar S, Iorga A, et al (2012) Cardiac vulnerability to ischemia/reperfusion injury drastically increases in late pregnancy. Basic Res Cardiol 107:. https://doi.org/10.1007/s00395-012-0271-7

294. Buttrick PM, Schaible TF, Malhotra A, et al (1987) Effects of pregnancy on cardiac function and myosin enzymology in the rat. Am J Physiol - Hear Circ Physiol 252:. https://doi.org/10.1152/ajpheart.1987.252.4.h846

295. Eghbali M, Wang Y, Toro L, Stefani E (2006) Heart Hypertrophy During Pregnancy: A Better Functioning Heart? Trends Cardiovasc Med 16:285–291. https://doi.org/10.1016/j.tcm.2006.07.001

296. den Ruijter H, Pasterkamp G, Rutten FH, et al (2015) Heart failure with preserved ejection fraction in women: The dutch queen of hearts program. Netherlands Hear J 23:89–93. https://doi.org/10.1007/s12471-014-0613-1

297. Lam CSP, Donal E, Kraigher-Krainer E, Vasan RS (2011) Epidemiology and clinical course of heart failure with preserved ejection fraction. Eur J Heart Fail 13:18–28. https://doi.org/10.1093/eurjhf/hfq121

298. Fok WY, Chan LY, Wong JT, et al (2006) Left ventricular diastolic function during normal pregnancy: Assessment by spectral tissue Doppler imaging. Ultrasound Obstet Gynecol 28:789–793. https://doi.org/10.1002/uog.3849

299. Fok WY, Chan LY, Wong JT, et al (2006) Left ventricular diastolic function during normal pregnancy: Assessment by spectral tissue Doppler imaging. Ultrasound Obstet Gynecol 28:789–793. https://doi.org/10.1002/uog.3849

300. Zile MR, Brutsaert DL (2002) New concepts in diastolic dysfunction and diastolic heart failure: Part I: Diagnosis, prognosis, and measurements of diastolic function. Circulation 105:1387–1393. https://doi.org/10.1161/hc1102.105289

301. Galderisi M (2005) Diastolic dysfunction and diastolic heart failure: Diagnostic, prognostic and therapeutic aspects. Cardiovasc Ultrasound 3:1–14. https://doi.org/10.1186/1476-7120-3-9

302. Chung E, Yeung F, Leinwand LA (2013) Calcineurin activity is required for cardiac remodelling in pregnancy. 402–410. https://doi.org/10.1093/cvr/cvt208

303. Iorga A, Dewey S, Partow-Navid R, et al (2012) Pregnancy Is Associated with Decreased Cardiac Proteasome Activity and Oxidative Stress in Mice. PLoS One 7:1–9. https://doi.org/10.1371/journal.pone.0048601

304. Ventura NM, Li TY, Tse MY, et al (2015) Onset and regression of pregnancy-Induced cardiac alterations in gestationally hypertensive mice: The role of the natriuretic peptide system. Biol Reprod 93:1–8. https://doi.org/10.1095/biolreprod.115.132696

305. Chen H, Hwang H, McKee LAK, et al (2013) Temporal and morphological impact of pressure overload in transgenic FHC mice. Front Physiol 4 AUG:1–12. https://doi.org/10.3389/fphys.2013.00205

306. Chung E, Yeung F, Leinwand LA (2012) Akt and MAPK signaling mediate pregnancy-induced cardiac adaptation. 1564–1575. https://doi.org/10.1152/japplphysiol.00027.2012

307. Iorga A, Li J, Sharma S, et al (2016) Rescue of pressure overload-induced heart failure by estrogen therapy. J Am Heart Assoc 5:1–12. https://doi.org/10.1161/JAHA.115.002482

308. Lin K-H, Kuo W-W, Shibu M, et al (2017) E2/ER β Enhances Calcineurin Protein Degradation and PI3K/Akt/MDM2 Signal Transduction to Inhibit ISO-Induced Myocardial Cell Apoptosis. Int J Mol Sci 18:892. https://doi.org/10.3390/ijms18040892

309. Moshal KS, Zhang Z, Roder K, et al (2014) Progesterone modulates SERCA2a expression and function in rabbit cardiomyocytes. AJP Cell Physiol 307:C1050–C1057. https://doi.org/10.1152/ajpcell.00127.2014

310. Ricke-Hoch M, Bultmann I, Stapel B, et al (2014) Opposing roles of Akt and STAT3 in the protection of the maternal heart from peripartum stress. Cardiovasc Res 101:587–596. https://doi.org/10.1093/cvr/cvu010

311. Eghbali M, Deva R, Alioua A, et al (2005) Molecular and functional signature of heart hypertrophy during pregnancy. Circ Res 96:1208–1216. https://doi.org/10.1161/01.RES.0000170652.71414.16

312. Fischer P, Hilfiker-Kleiner D (2007) Survival pathways in hypertrophy and heart failure: The gp130-STAT3 axis. Basic Res Cardiol 102:393–411. https://doi.org/10.1007/s00395-007-0674-z

313. Kunisada K, Negoro S, Tone E, et al (2000) Signal transducer and activator of transcription 3 in the heart transduces not only a hypertrophic signal but a protective signal against doxorubicin-induced cardiomyopathy. Proc Natl Acad Sci U S A 97:315–319. https://doi.org/10.1073/pnas.97.1.315

314. Heusch G, Musiolik J, Kottenberg E, et al (2012) STAT5 activation and cardioprotection by remote ischemic preconditioning in humans. Circ Res 110:111–115. https://doi.org/10.1161/CIRCRESAHA.111.259556

315. Zouein FA, Altara R, Chen Q, et al (2015) Pivotal Importance of STAT3 in Protecting the Heart from Acute and Chronic Stress: New Advancement and Unresolved Issues. Front Cardiovasc Med 2:1–17. https://doi.org/10.3389/fcvm.2015.00036

316. Lemmens K, Doggen K, de Keulenaer GW (2011) Activation of the neuregulin/ErbB system during physiological ventricular remodeling in pregnancy. Am J Physiol - Hear Circ Physiol 300:931–942. https://doi.org/10.1152/ajpheart.00385.2010

317. Aljabri MB, Songstad NT, Lund T, et al (2011) Pregnancy protects against antiangiogenic and fibrogenic effects of angiotensin II in rat hearts. Acta Physiol 201:445–456. https://doi.org/10.1111/j.1748-1716.2010.02234.x

318. Collier P, Watson J, H van Es M, et al (2012) Getting to the heart of cardiac remodeling; how collagen subtypes may contribute to phenotype. J Mol Cell Cardiol 57:148–53

319. Gulfo J, Castel R, Ledda A, et al (2019) Corticosteroid-Binding Globulin is expressed in the adrenal gland and its absence impairs corticosterone synthesis and secretion in a sex-dependent manner. Sci Rep 9:1–10. https://doi.org/10.1038/s41598-019-50355-1

320. Lei JH, Yang X, Peng S, et al (2015) Impact of corticosteroid-binding globulin deficiency on pregnancy and neonatal sex. J Clin Endocrinol Metab 100:1819–1827. https://doi.org/10.1210/jc.2014-4254

321. Xiong T, Zhong C, Zhou X, et al (2017) Maternal circulating transthyretin level is longitudinally associated with increased risk of gestational diabetes mellitus: It is not just an indicator of nutritional status. Diabetes Care 40:e53–e54. https://doi.org/10.2337/dc16-2731

322. Ruberg F, Berk J (2012) Transthyretin (TTR) Cardiac Amyloidosis. Circulation 126:1286–1300. https://doi.org/10.1161/CIRCULATIONAHA.111.078915.Transthyretin

323. Aghaeepour N, Ganio EA, Mcilwain D, et al (2017) An immune clock of human pregnancy. Sci Immunol 2:1–12. https://doi.org/10.1126/sciimmunol.aan2946

324. Orefice R (2020) Immunology and the immunological response to pregnancy. Best Pract Res Clin Obstet Gynaecol 1–11. https://doi.org/10.1016/j.bpobgyn.2020.07.013

325. Chen Y, Meng F, Wang B, et al (2018) Dock2 in the development of inflammation and cancer. Eur J Immunol 48:915–922. https://doi.org/10.1002/eji.201747157

326. Nishikimi A, Uruno T, Duan X, et al (2012) Blockade of inflammatory responses by a small-molecule inhibitor of the Rac activator DOCK2. Chem Biol 19:488–497. https://doi.org/10.1016/j.chembiol.2012.03.008

327. England J, Loughna S (2013) Heavy and light roles: Myosin in the morphogenesis of

the heart. Cell Mol Life Sci 70:1221–1239. https://doi.org/10.1007/s00018-012-1131-1

328. Schaub MC, Hefti MA, Zuellig RA, Morano I (1998) Modulation of contractility in human cardiac hypertrophy by myosin essential light chain isoforms. Cardiovasc Res 37:381–404. https://doi.org/10.1016/S0008-6363(97)00258-7

329. Depre C, Shipley GL, Chen W, et al (1998) Unloaded heart in vivo replicates fetal gene expression of cardiac hypertrophy. Nat Med 4:1269–1275. https://doi.org/10.1038/3253

330. Berryman K, Buhimschi CS, Zhao G, et al (2019) Proteasome levels and activity in pregnancies complicated by severe preeclampsia and hellp syndrome. Hypertension 73:1308–1318. https://doi.org/10.1161/HYPERTENSIONAHA.118.12437.PROTEASOME

331. Panidis IP, Kotler MN, Ren JF, et al (1984) Development and regression of left ventricular hypertrophy. J Am Coll Cardiol 3:1309–1320. https://doi.org/10.1016/S0735-1097(84)80192-8

332. Mohamed BA, Asif AR, Schnelle M, et al (2016) Proteomic analysis of short-term preload-induced eccentric cardiac hypertrophy. J Transl Med 14:1–12. https://doi.org/10.1186/s12967-016-0898-5

333. Schott P, Asif AR, Gräf C, et al (2008) Myocardial adaptation of energy metabolism to elevated preload depends on calcineurin activity. Basic Res Cardiol 103:232–243. https://doi.org/10.1007/s00395-008-0696-1

334. Hill JA, Olson EN (2008) Cardiac Plasticity. N Engl J Med 358:1370–1380. https://doi.org/10.1056/nejmra072139

335. Rassier DE (2017) Sarcomere mechanics in striated muscles: From molecules to sarcomeres to cells. Am J Physiol - Cell Physiol 313:C134–C145. https://doi.org/10.1152/ajpcell.00050.2017

336. Stromer MH (1998) The cytoskeleton in skeletal, cardiac and smooth muscle cells. Histol Histopathol 13:283–291. https://doi.org/10.14670/HH-13.283

337. Brandenburger Y, Arthur JF, Woodcock EA, et al (2003) Cardiac hypertrophy in vivo is

associated with increased expression of the ribosomal gene transcription factor UBF. FEBS Lett 548:79–84. https://doi.org/10.1016/S0014-5793(03)00744-0

338. Wen Y, Alimov A, McCarthy J (2016) Ribosome Biogenesis is Necessary for Skeletal Muscle Hypertrophy. Exerc Sport Sci Rev 44:11–115. https://doi.org/10.1249/JES.0000000000000082.Ribosome

339. Hannan RD, Jenkins A, Jenkins AK, Brandenburger Y (2003) Cardiac hypertrophy: A matter of translation. Clin Exp Pharmacol Physiol 30:517–527. https://doi.org/10.1046/j.1440-1681.2003.03873.x

340. Baar K, Esser K (1999) Phosphorylation of p70(S6k) correlates with increased skeletal muscle mass following resistance exercise. Am J Physiol - Cell Physiol 276:. https://doi.org/10.1152/ajpcell.1999.276.1.c120

341. Zhou X, Liao WJ, Liao JM, et al (2015) Ribosomal proteins: Functions beyond the ribosome. J Mol Cell Biol 7:92–104. https://doi.org/10.1093/jmcb/mjv014

342. Strunk BS, Karbstein K (2009) Powering through ribosome assembly. Rna 15:2083–2104. https://doi.org/10.1261/rna.1792109

343. Kuo WW, Chu CY, Wu CH, et al (2005) The profile of cardiac cytochrome c oxidase (COX) expression in an accelerated cardiac-hypertrophy model. J Biomed Sci 12:601–610. https://doi.org/10.1007/s11373-005-7373-2

344. Schaper J, Kostin S, Hein S, et al (2002) Structural remodelling in heart failure. Exp Clin Cardiol 7:64–68

345. Gilda JE, Gomes A V. (2017) Proteasome dysfunction in cardiomyopathies. J Physiol 595:4051–4071. https://doi.org/10.1113/JP273607

346. Xu D, Shan B, Lee B-H, et al (2015) Phosphorylation and activation of ubiquitin-specific protease-14 by Akt regulates the ubiquitin-proteasome system. Elife 4:1–16. https://doi.org/10.7554/elife.10510

347. Koulich E, Li X, DeMartino G (2007) Relative Structural and Functional Roles of Multiple Deubiquitylating Proteins Associated with Mammalian 26S Proteasome Elena. Mol Biol Cell 18:3250–3263. https://doi.org/10.1091/mbc.E07

348. Haghikia A, Missol-Kolka E, Tsikas D, et al (2011) Signal transducer and activator of

transcription 3-mediated regulation of miR-199a-5p links cardiomyocyte and endothelial cell function in the heart: A key role for ubiquitin-conjugating enzymes. Eur Heart J 32:1287–1297. https://doi.org/10.1093/eurheartj/ehq369

349. Silva KAS, Dong J, Dong Y, et al (2015) Inhibition of Stat3 activation suppresses caspase-3 and the ubiquitin-proteasome system, leading to preservation of muscle mass in cancer cachexia. J Biol Chem 290:11177–11187. https://doi.org/10.1074/jbc.M115.641514

350. Machackova J, Barta J, Dhalla NS (2006) Myofibrillar remodelling in cardiac hypertrophy, heart failure and cardiomyopathies. Can J Cardiol 22:953–968. https://doi.org/10.1016/S0828-282X(06)70315-4

351. Hedhli N, Pelat M, Depre C (2005) Protein turnover in cardiac cell growth and survival. Cardiovasc Res 68:186–196. https://doi.org/10.1016/j.cardiores.2005.06.025

352. Lino CA, Demasi M, Barreto-Chaves ML (2019) Ubiquitin proteasome system (UPS) activation in the cardiac hypertrophy of hyperthyroidism. Mol Cell Endocrinol 493:110451. https://doi.org/10.1016/j.mce.2019.110451

353. Depre C, Wang Q, Yan L, et al (2006) Activation of the cardiac proteasome during pressure overload promotes ventricular hypertrophy. Circulation 114:1821–1828. https://doi.org/10.1161/CIRCULATIONAHA.106.637827

354. Hedhli N, Depre C (2010) Proteasome inhibitors and cardiac cell growth. Cardiovasc Res 85:321–329. https://doi.org/10.1093/cvr/cvp226

355. Baskin KK, Taegtmeyer H (2011) Taking pressure off the heart: The ins and outs of atrophic remodelling. Cardiovasc Res 90:243–250. https://doi.org/10.1093/cvr/cvr060

356. Costelli P, García-Martínez C, Llovera M, et al (1995) Muscle protein waste in tumor-bearing rats is effectively antagonized by a β2-adrenergic agonist (clenbuterol): Role of the ATP-ubiquitin-dependent proteolytic pathway. J Clin Invest 95:2367–2372. https://doi.org/10.1172/JCI117929

357. McKinnell IW, Rudnicki MA (2004) Molecular mechanisms of muscle atrophy. Cell 119:907–910. https://doi.org/10.1016/j.cell.2004.12.007

358. Lecker SH, Goldberg AL, Mitch WE (2006) Protein degradation by the ubiquitin-proteasome pathway in normal and disease states. J Am Soc Nephrol 17:1807–1819. https://doi.org/10.1681/ASN.2006010083

359. Taylor RG, Tassy C, Briand M, et al (1995) Proteolytic activity of proteasome on myofibrillar structures. Mol Biol Rep 21:71–73. https://doi.org/10.1007/BF00990974

360. Mearini G, Schlossarek S, Willis MS, Carrier L (2008) The ubiquitin-proteasome system in cardiac dysfunction. Biochim Biophys Acta - Mol Basis Dis 1782:749–763. https://doi.org/10.1016/j.bbadis.2008.06.009

361. Rodríguez JE, Schisler JC, Patterson C, Willis MS (2009) Seek and destroy: the ubiquitin----proteasome system in cardiac disease. Curr Hypertens Rep 11:396–405

362. Shang F, Taylor A (2011) Ubiquitin-proteasome pathway and cellular responses to oxidative stress. Free Radic Biol Med 51:5–16. https://doi.org/10.1016/j.freeradbiomed.2011.03.031

363. Shang F, Nowell TR, Taylor A (2001) Removal of oxidatively damaged proteins from lens cells by the ubiquitin-proteasome pathway. Exp Eye Res 73:229–238. https://doi.org/10.1006/exer.2001.1029

364. Dudek EJ, Shang F, Liu Q, et al (2005) Selectivity of the ubiquitin pathway for oxidatively modified proteins: relevance to protein precipitation diseases. FASEB J 19:1707–1709. https://doi.org/10.1096/fj.05-4049fje

365. Hilfiker-Kleiner D, Struman I, Hoch M, et al (2012) 16-KDa prolactin and bromocriptine in postpartum cardiomyopathy. Curr Heart Fail Rep 9:174–182. https://doi.org/10.1007/s11897-012-0095-7

366. Azakie A, Fineman JR, He Y (2006) Myocardial transcription factors are modulated during pathologic cardiac hypertrophy in vivo. J Thorac Cardiovasc Surg 132:. https://doi.org/10.1016/j.jtcvs.2006.08.005

367. Pentimalli F (2007) Technology: On the trail of transcription factors. Nat Rev Genet 8:655. https://doi.org/10.1038/nrg2191

368. Sartorelli V, Hong NA, Bishopric NH, Kedes L (1992) Myocardial activation of the human cardiac α-actin promoter by helix- loop-helix proteins. Proc Natl Acad Sci U S A

89:4047–4051. https://doi.org/10.1073/pnas.89.9.4047

369. Ardati A, Nemer M (1993) A nuclear pathway for α1-adrenergic receptor signaling in cardiac cells. EMBO J 12:5131–5139. https://doi.org/10.1002/j.1460-2075.1993.tb06208.x

370. Wang Y, Cao R, Yang W, Qi B (2019) SP1-SYNE1-AS1-miR-525-5p feedback loop regulates Ang-II-induced cardiac hypertrophy. J Cell Physiol 234:14319–14329. https://doi.org/10.1002/jcp.28131

371. Long Y, Wang L, Li Z (2020) SP1-induced SNHG14 aggravates hypertrophic response in in vitro model of cardiac hypertrophy via up-regulation of PCDH17. J Cell Mol Med 24:7115–7126. https://doi.org/10.1111/jcmm.15073

372. Physiology C (2018) Erratum: Epicatechin suppresses angiotensin II-induced cardiac hypertrophy via the activation of the SP1/SIRT1 sgnaling pathway (Cellular Physiology and Biochemistry (2017) 41 (2004-2015) DOI: 10.1159/000475396). Cell Physiol Biochem 44:2090. https://doi.org/10.1159/000485990

373. Ravi V, Jain A, Khan D, et al (2019) SIRT6 transcriptionally regulates global protein synthesis through transcription factor Sp1 independent of its deacetylase activity. Nucleic Acids Res 47:9115–9131. https://doi.org/10.1093/nar/gkz648

374. Nakayama M, Takeda M, Asaumi Y, Shimokawa H (2014) Identification and visualization of stimulus-specific transcriptional activity in cardiac hypertrophy in mice. Int J Cardiovasc Imaging 30:211–219. https://doi.org/10.1007/s10554-013-0314-7

375. Lu R, Medina KL, Lancki DW, Singh H (2003) IRF-4,8 orchestrate the pre-B-to-B transition in lymphocyte development. Genes Dev 17:1703–1708. https://doi.org/10.1101/gad.1104803

376. Sucharov CC, Mariner P, Long C, et al (2003) Yin Yang 1 is increased in human heart failure and represses the activity of the human α-myosin heavy chain promoter. J Biol Chem 278:31233–31239. https://doi.org/10.1074/jbc.M301917200

377. Patten M, Wang WZ, Aminololama-Shakeri S, et al (2000) IL-1β increases abundance and activity of the negative transcriptional regulator yin yang-1 (YY1) in neonatal rat

cardiac myocytes. J Mol Cell Cardiol 32:1341–1352. https://doi.org/10.1006/jmcc.2000.1169

378. Sucharov CC, Dockstader K, McKinsey TA (2007) YY1 Protects Cardiac Myocytes from Pathologic Hypertrophy by Interacting with HDAC5. Mol Biol Cell 18:3250–3263. https://doi.org/10.1091/mbc.E07

379. Asensio-Lopez MC, Lax A, Fernandez del Palacio MJ, et al (2019) Yin-Yang 1 transcription factor modulates ST2 expression during adverse cardiac remodeling post-myocardial infarction. J Mol Cell Cardiol 130:216–233. https://doi.org/10.1016/j.yjmcc.2019.04.009

380. Tan CY, Wong JX, Chan PS, et al (2019) Yin Yang 1 suppresses dilated cardiomyopathy and cardiac fibrosis through regulation of BMP7 and CTGF. Circ Res 125:834–846. https://doi.org/10.1161/CIRCRESAHA.119.314794

381. Li J, Cao Y, Wu Y, et al (2015) The expression profile analysis of NKX2-5 knock-out embryonic mice to explore the pathogenesis of congenital heart disease. J Cardiol 66:527–531. https://doi.org/10.1016/j.jjcc.2014.12.022

382. Ghosh TK, Aparicio-Sánchez JJ, Buxton S, Brook JD (2019) HDAC4 and 5 repression of TBX5 is relieved by protein kinase D1. Sci Rep 9:1–10. https://doi.org/10.1038/s41598-019-54312-w

383. Cha-Molstad H, Xu G, Chen J, et al (2012) Calcium channel blockers act through nuclear factor Y to control transcription of key cardiac genes. Mol Pharmacol 82:541–549. https://doi.org/10.1124/mol.112.078253

384. Jacob J, Chopra S, Cherian D, Verghese P (2013) Physiology and clinical significance of natriuretic hormones. Indian J Endocrinol Metab 17:83. https://doi.org/10.4103/2230-8210.107869

385. Nakagawa Y, Nishikimi T, Kuwahara K (2019) Atrial and brain natriuretic peptides: Hormones secreted from the heart. Peptides 111:18–25. https://doi.org/10.1016/j.peptides.2018.05.012

386. Emmerson PJ, Duffin KL, Chintharlapalli S, Wu X (2018) GDF15 and Growth Control. Front Physiol 9:1–7. https://doi.org/10.3389/fphys.2018.01712

387. Morkin E (2000) Control of cardiac myosin heavy chain gene expression. Microsc Res Tech 50:522–531. https://doi.org/10.1002/1097-0029(20000915)50:6<522::AID-JEMT9>3.0.CO;2-U

388. Somvanshi RK, Qiu X, Kumar U (2013) Isoproterenol induced hypertrophy and associated signaling pathways are modulated by Somatostatin in H9c2 cells. Int J Cardiol 167:1012–1022. https://doi.org/10.1016/j.ijcard.2012.03.077

389. Wang J, Gareri C, Rockman HA (2018) G-protein-coupled receptors in heart disease. Circ Res 123:716–735. https://doi.org/10.1161/CIRCRESAHA.118.311403

390. Chung E, Yeung F, Leinwand L a (2012) Akt and MAPK signaling mediate pregnancy-induced cardiac adaptation. J Appl Physiol 112:1564–75. https://doi.org/10.1152/japplphysiol.00027.2012

391. Goldstein J, Sites CK, Toth MJ (2004) Progesterone stimulates cardiac muscle protein synthesis via receptor-dependent pathway. Fertil Steril 82:430–436. https://doi.org/10.1016/j.fertnstert.2004.03.018

392. Qian W, Yu D, Zhang J, et al (2018) Wogonin attenuates isoprenaline-induced myocardial hypertrophy in mice by suppressing the PI3K/Akt pathway. Front Pharmacol 9:1–13. https://doi.org/10.3389/fphar.2018.00896

393. Pedram A, Razandi M, Aitkenhead M, Levin ER (2005) Estrogen inhibits cardiomyocyte hypertrophy in vitro: Antagonism of calcineurin-related hypertrophy through induction of MCIP1. J Biol Chem 280:26339–26348. https://doi.org/10.1074/jbc.M414409200

394. Haines CD, Harvey PA, Leinwand LA (2012) Estrogens mediate cardiac hypertrophy in a stimulus-dependent manner. Endocrinology 153:4480–4490. https://doi.org/10.1210/en.2012-1353

395. Oudit GY, Crackower MA, Eriksson U, et al (2003) Phosphoinositide 3-Kinase γ-Deficient Mice Are Protected From Isoproterenol-Induced Heart Failure. Circulation 108:2147–2152. https://doi.org/10.1161/01.CIR.0000091403.62293.2B

396. McMullen JR, Shioi T, Huang WY, et al (2004) The Insulin-like Growth Factor 1 Receptor Induces Physiological Heart Growth via the Phosphoinositide 3-

Kinase(p110α) Pathway. J Biol Chem 279:4782–4793. https://doi.org/10.1074/jbc.M310405200

397. Wende AR, O'Neill BT, Bugger H, et al (2015) Enhanced Cardiac Akt/Protein Kinase B Signaling Contributes to Pathological Cardiac Hypertrophy in Part by Impairing Mitochondrial Function via Transcriptional Repression of Mitochondrion-Targeted Nuclear Genes. Mol Cell Biol 35:831–846. https://doi.org/10.1128/mcb.01109-14

398. Frey N, Barrientos T, Shelton JM, et al (2004) Mice lacking calsarcin-1 are sensitized to calcineurin signaling and show accelerated cardiomyopathy in response to pathological biomechanical stress. Nat Med 10:1336–1343. https://doi.org/10.1038/nm1132

399. Ramlakhan KP, Johnson MR, Roos-Hesselink JW (2020) Pregnancy and cardiovascular disease. Nat Rev Cardiol 17:718–731. https://doi.org/10.1038/s41569-020-0390-z

400. Sliwa K, Förster O, Libhaber E, et al (2006) Peripartum cardiomyopathy: Inflammatory markers as predictors of outcome in 100 prospectively studied patients. Eur Heart J 27:441–446. https://doi.org/10.1093/eurheartj/ehi481

401. Sarojini A, Sai Ravi Shanker A, Anitha M (2013) Inflammatory markers-serum level of c-reactive protein, tumor necrotic factor-α, and interleukin-6 as predictors of outcome for peripartum cardiomyopathy. J Obstet Gynecol India 63:234–239. https://doi.org/10.1007/s13224-013-0428-9

402. Hilfiker-Kleiner D, Haghikia A, Berliner D, et al (2017) Bromocriptine for the treatment of peripartum cardiomyopathy: A multicentre randomized study. Eur Heart J 38:2671–2679. https://doi.org/10.1093/eurheartj/ehx355

403. Ago T, Sadoshima J (2006) GDF15, a cardioprotective TGF-β superfamily protein. Circ Res 98:294–297. https://doi.org/10.1161/01.RES.0000207919.83894.9d

404. Wesseling M, de Poel JHC, de Jager SCA (2020) Growth differentiation factor 15 in adverse cardiac remodelling: from biomarker to causal player. ESC Hear Fail 7:1488–1501. https://doi.org/10.1002/ehf2.12728

405. Nishijima David L; Wisner, David H; Holmes, James F DKS (2016) NAG-1/GDF15 Accumulates in the nucleus and modulates transcriptional regulation of the Smad

pathway. Physiol Behav 176:139–148. https://doi.org/10.1016/j.physbeh.2017.03.040

406. Conte M, Martucci M, Mosconi G, et al (2020) GDF15 Plasma Level Is Inversely Associated With Level of Physical Activity and Correlates With Markers of Inflammation and Muscle Weakness. Front Immunol 11:1–10. https://doi.org/10.3389/fimmu.2020.00915

407. Luan HH, Wang A, Hilliard BK, et al (2019) GDF15 Is an Inflammation-Induced Central Mediator of Tissue Tolerance. Cell 178:1231-1244.e11. https://doi.org/10.1016/j.cell.2019.07.033

408. Santos I, Colaço HG, Neves-Costa A, et al (2020) CXCL5-mediated recruitment of neutrophils into the peritoneal cavity of Gdf15-deficient mice protects against abdominal sepsis. Proc Natl Acad Sci U S A 117:. https://doi.org/10.1073/pnas.1918508117

409. Luan HH, Wang A, Hilliard BK, et al (2019) GDF15 Is an Inflammation-Induced Central Mediator of Tissue Tolerance. Cell 178:1231-1244.e11. https://doi.org/10.1016/j.cell.2019.07.033

410. Salles GF, Schlüssel MM, Farias DR, et al (2015) Blood pressure in healthy pregnancy and factors associated with no mid-trimester blood pressure drop: A prospective cohort study. Am J Hypertens 28:680–689. https://doi.org/10.1093/ajh/hpu204

411. Silva LM, Steegers EAP, Burdorf A, et al (2008) No midpregnancy fall in diastolic blood pressure in women with a low educational level: The generation R study. Hypertension 52:645–651. https://doi.org/10.1161/HYPERTENSIONAHA.108.116632

412. Grindheim G, Estensen ME, Langesaeter E, et al (2012) Changes in blood pressure during healthy pregnancy: A longitudinal cohort study. J Hypertens 30:342–350. https://doi.org/10.1097/HJH.0b013e32834f0b1c

413. Mesa A, Jessurun C, Hernandez A, et al (1999) Human Pregnancy

414. Wang F, Guo Y, Yu H, et al (2010) Growth differentiation factor 15 in different stages of heart failure: Potential screening implications. Biomarkers 15:671–676. https://doi.org/10.3109/1354750X.2010.510580

415. Kempf T, von Haehling S, Peter T, et al (2007) Prognostic Utility of Growth Differentiation Factor-15 in Patients With Chronic Heart Failure. J Am Coll Cardiol 50:1054–1060. https://doi.org/10.1016/j.jacc.2007.04.091

416. Xu XY, Nie Y, Wang FF, et al (2014) Growth differentiation factor (GDF)-15 blocks norepinephrineinduced myocardial hypertrophy via a novel pathway involving inhibition of epidermal growth factor receptor transactivation. J Biol Chem 289:10084–10094. https://doi.org/10.1074/jbc.M113.516278

417. Marjono AB, Brown DA, Horton KE, et al (2003) Macrophage inhibitory cytokine-1 in gestational tissues and maternal serum in normal and pre-eclamptic pregnancy. Placenta 24:100–106. https://doi.org/10.1053/plac.2002.0881

418. Petry CJ, Ong KK, Burling KA, et al (2018) Associations of vomiting and antiemetic use in pregnancy with levels of circulating GDF15 early in the second trimester: A nested case-control study [version 1; referees: 3 approved]. Wellcome Open Res 3:1–14. https://doi.org/10.12688/wellcomeopenres.14818.1

419. Tong S, Marjono B, Brown DA, et al (2004) Serum concentrations of macrophage inhibitory cytokine 1 (MIC 1) as a predictor of miscarriage. Lancet 363:129–130. https://doi.org/10.1016/S0140-6736(03)15265-8

420. Hoda Badr, Cindy L. Carmack, Deborah A. Kashy, Massimo Cristofanilli and TAR (2011) Circulating and Placental Growth-Differentiation Factor 15 in Preeclampsia and in Pregnancy Complicated by Diabetes Mellitus. Hypertension 23:1–7. https://doi.org/10.1161/CIRCULATIONAHA.110.956839

421. Paralkar VM, Vail AL, Grasser WA, et al (1998) Cloning and characterization of a novel member of the transforming growth factor-β/bone morphogenetic protein family. J Biol Chem 273:13760–13767. https://doi.org/10.1074/jbc.273.22.13760

422. Tanno T, Bhanu N V., Oneal PA, et al (2007) High levels of GDF15 in thalassemia suppress expression of the iron regulatory protein hepcidin. Nat Med 13:1096–1101. https://doi.org/10.1038/nm1629

423. Millard KN, Frazer DM, Wilkins SJ, Anderson GJ (2004) Changes in the expression of intestinal iron transport and hepatic regulatory molecules explain the enhanced iron absorption associated with pregnancy in the rat. Gut 53:655–660.

https://doi.org/10.1136/gut.2003.031153

424. Ha G, De Torres F, Arouche N, et al (2019) GDF15 secreted by senescent endothelial cells improves vascular progenitor cell functions. PLoS One 14:1–17. https://doi.org/10.1371/journal.pone.0216602

425. Ma Y, Chen Y, Yang Y, et al (2013) Proteasome inhibition attenuates heart failure during the late stages of pressure overload through alterations in collagen expression. Biochem Pharmacol 85:223–233. https://doi.org/10.1016/j.bcp.2012.10.025

426. Razeghi P, Sharma S, Ying J, et al (2003) Atrophic Remodeling of the Heart In Vivo Simultaneously Activates Pathways of Protein Synthesis and Degradation. Circulation 108:2536–2541. https://doi.org/10.1161/01.CIR.0000096481.45105.13

427. Wang X, Robbins J (2006) Heart failure and protein quality control. Circ Res 99:1315–1328. https://doi.org/10.1161/01.RES.0000252342.61447.a2

428. Hein S, Arnon E, Kostin S, et al (2003) Progression from compensated hypertrophy to failure in the pressure-overloaded human: Heart structural deterioration and compensatory mechanisms. Circulation 107:984–991. https://doi.org/10.1161/01.CIR.0000051865.66123.B7

429. Hedhli N, Lizano P, Hong C, et al (2008) Proteasome inhibition decreases cardiac remodeling after initiation of pressure overload. Am J Physiol - Hear Circ Physiol 295:1–18. https://doi.org/10.1152/ajpheart.00532.2008

430. Nair N, Gongora E (2018) Correlations of GDF-15 with sST2, MMPs, and worsening functional capacity in idiopathic dilated cardiomyopathy: Can we gain new insights into the pathophysiology? J Circ Biomarkers 7:1–8. https://doi.org/10.1177/1849454417751735

431. Xue H, Fu Z, Chen Y, et al (2012) The Association of Growth Differentiation Factor-15 with Left Ventricular Hypertrophy in Hypertensive Patients. PLoS One 7:3–8. https://doi.org/10.1371/journal.pone.0046534

432. Knight RA, Scarabelli TM, Stephanou A (2012) STAT transcription in the ischemic heart. Jak-Stat 1:111–117. https://doi.org/10.4161/jkst.20078

433. Pai P, Velmurugan BK, Kuo C, Anp ÁPPAÁEÁ (2017) 17 b -Estradiol and / or estrogen

receptor alpha blocks isoproterenol-induced calcium accumulation and hypertrophy via GSK3 b / PP2A / NFAT3 / ANP pathway. Mol Cell Biochem 434:181–195. https://doi.org/10.1007/s11010-017-3048-3

434. Van Eickels M, Grohé C, Cleutjens JPM, et al (2001) 17B-Estradiol Attenuates the Development of Pressure-Overload Hypertrophy. Circulation 104:1419–1423. https://doi.org/10.1161/hc3601.095577

435. DeBosch B, Treskov I, Lupu TS, et al (2006) Akt1 is required for physiological cardiac growth. Circulation 113:2097–2104. https://doi.org/10.1161/CIRCULATIONAHA.105.595231

436. Yeves AM, Villa-Abrille MC, Pérez NG, et al (2014) Physiological cardiac hypertrophy: Critical role of AKT in the prevention of NHE-1 hyperactivity. J Mol Cell Cardiol 76:186–195. https://doi.org/10.1016/j.yjmcc.2014.09.004

437. Dziennis S, Jia T, Rønnekleiv OK, et al (2007) Role of signal transducer and activator of transcription-3 in estradiol-mediated neuroprotection. J Neurosci 27:7268–7274. https://doi.org/10.1523/JNEUROSCI.1558-07.2007

438. Matsuda T, Junicho A, Yamamoto T, et al (2001) Cross-talk between signal transducer and activator of transcription 3 and androgen receptor signaling in prostate carcinoma cells. Biochem Biophys Res Commun 283:179–187. https://doi.org/10.1006/bbrc.2001.4758

439. Koenig T, Bauersachs J, Hilfiker-kleiner D (2018) Pathophysiology of Peripartum Cardiomyopathy and Experimental Data. Card Fail Rev 46–49. https://doi.org/10.1016/S0140

440. Ricke-Hoch M, Pfeffer TJ, Hilfiker-Kleiner D (2020) Peripartum cardiomyopathy: Basic mechanisms and hope for new therapies. Cardiovasc Res 116:520–531. https://doi.org/10.1093/cvr/cvz252

441. Powell SR (2006) The ubiquitin-proteasome system in cardiac physiology and pathology. Am J Physiol - Hear Circ Physiol 291:. https://doi.org/10.1152/ajpheart.00062.2006

Supplementary Tables

Supplementary Table 1: Gene ontology Biological process for proteins upregulated om Day 14 postpartum

GO BP Term	Description	FDR value	# Genes
GO.0060048	cardiac muscle contraction	2.03E-06	8
GO.0055008	cardiac muscle tissue morphogenesis	2.03E-06	8
GO.0055010	ventricular cardiac muscle tissue morphogenesis	2.25E-06	7
GO.0048738	cardiac muscle tissue development	2.27E-06	10
GO.0044281	small molecule metabolic process	2.27E-06	24
GO.0006518	peptide metabolic process	2.27E-06	14
GO.0061061	muscle structure development	2.56E-06	14
GO.0003012	muscle system process	1.13E-05	10
GO.0043603	cellular amide metabolic process	1.25E-05	15
GO.0014706	striated muscle tissue development	1.25E-05	11
GO.0006936	muscle contraction	1.25E-05	9
GO.0055002	striated muscle cell development	1.78E-05	8
GO.0003206	cardiac chamber morphogenesis	1.99E-05	8
GO.0031032	actomyosin structure organization	2.21E-05	7
GO.0030239	myofibril assembly	2.21E-05	6
GO.0008152	metabolic process	2.21E-05	59
GO.0007517	muscle organ development	2.76E-05	10
GO.1901564	organonitrogen compound metabolic process	5.04E-05	40
GO.0006412	translation	7.98E-05	10
GO.0003007	heart morphogenesis	1.20E-04	9
GO.0071704	organic substance metabolic process	1.30E-04	55

GO.0044237	cellular metabolic process	1.60E-04	53
GO.0044238	primary metabolic process	2.10E-04	53
GO.0044057	regulation of system process	2.10E-04	12
GO.0008015	blood circulation	2.80E-04	10
GO.0065008	regulation of biological quality	3.10E-04	32
GO.0032272	negative regulation of protein polymerization	3.10E-04	5
GO.0008016	regulation of heart contraction	4.00E-04	7
GO.0006996	organelle organization	4.20E-04	28
GO.0002026	regulation of the force of heart contraction	6.40E-04	4
GO.0033275	actin-myosin filament sliding	6.90E-04	3

Supplementary Table 2: Gene ontology Biological process for proteins upregulated om Day 28 postpartum

GO BP Term	Description	FDR value	# Genes
GO.0044281	small molecule metabolic process	7.94E-15	51
GO.0044248	cellular catabolic process	1.53E-13	46
GO.0051186	cofactor metabolic process	2.30E-13	27
GO.0009056	catabolic process	9.58E-13	47
GO.0055114	oxidation-reduction process	5.26E-12	36
GO.0008152	metabolic process	6.58E-12	119
GO.0017144	drug metabolic process	1.09E-11	27
GO.1901575	organic substance catabolic process	1.61E-10	40
GO.1901564	organonitrogen compound metabolic process	7.33E-10	79
GO.0008015	blood circulation	7.33E-10	22
GO.0019752	carboxylic acid metabolic process	1.74E-09	29
GO.0065008	regulation of biological quality	2.25E-09	66
GO.0009987	cellular process	4.07E-09	146
GO.0044237	cellular metabolic process	4.11E-09	105
GO.0003015	heart process	8.74E-09	12
GO.0010038	response to metal ion	3.11E-08	19
GO.0060047	heart contraction	3.85E-08	11
GO.0003012	muscle system process	4.53E-08	16
GO.0072521	purine-containing compound metabolic process	6.77E-08	20
GO.0010035	response to inorganic substance	6.77E-08	22
GO.0071704	organic substance metabolic process	7.19E-08	105
GO.0006936	muscle contraction	9.49E-08	14
GO.0061061	muscle structure development	9.52E-08	21
GO.0060048	cardiac muscle contraction	9.52E-08	10

GO BP Term	Description	FDR value	# Genes
GO.0022900	electron transport chain	1.17E-07	12
GO.0009205	purine ribonucleoside triphosphate metabolic process	1.49E-07	14
GO.0009123	nucleoside monophosphate metabolic process	1.53E-07	15
GO.0006091	generation of precursor metabolites and energy	1.68E-07	17
GO.0046034	ATP metabolic process	2.25E-07	13
GO.0009167	purine ribonucleoside monophosphate metabolic process	2.25E-07	14
GO.0006941	striated muscle contraction	2.64E-07	11
GO.1901565	organonitrogen compound catabolic process	2.90E-07	26
GO.0055086	nucleobase-containing small molecule metabolic process	2.90E-07	22
GO.0044283	small molecule biosynthetic process	4.97E-07	20
GO.0048738	cardiac muscle tissue development	6.79E-07	13

Supplementary Table 3: List of most significantly enriched transcription factor controlling expression of upregulated proteins on Day 14 postpartum

Rank	Transcription Factor	Hypergeometric p-value
1	SP1	0.006383
2	IRF1	0.02034
3	SOX2	0.03202
4	USF2	0.03463
5	SP2	0.04015
6	IRF3	0.04573
7	PBX3	0.0588
8	HNF4A	0.06047
9	ZKSCAN1	0.0822
10	GATA1	0.09657

Supplementary Table 4: List of most significantly enriched transcription factor controlling the expression of upregulated proteins on Day 28pp

Rank	Transcription Factor	Hypergeometric p-value
1	YY1	1.997e-10
2	NFYA	7.687e-7
3	TAF1	9.149e-7
4	NFYB	0.00002939
5	KAT2A	0.00005463
6	MAX	0.00009536
7	MYC	0.0002939
8	MYC	0.0003153
9	TAF7	0.0003332
10	SP1	0.0003642
11	SP2	0.001276
12	E2F1	0.001312
13	FOS	0.002403
14	KLF4	0.002694
15	EGR1	0.00371
16	NFE2L2	0.003967
17	ATF2	0.004032
18	ZMIZ1	0.00586
19	YY1	0.007627
20	UBTF	0.007897
21	PPARD	0.00962
22	TCF3	0.01237
23	SIX5	0.01621
24	CEBPB	0.01733
25	GABPA	0.0185
26	CEBPD	0.01864
27	PBX3	0.01895
28	PML	0.01981
29	BRCA1	0.01984
30	NRF1	0.02534
31	CREB1	0.02797
32	ZBTB33	0.02828
33	NR2C2	0.02836
34	IRF3	0.03977
35	E2F6	0.05099
36	IRF1	0.05451

APPENDICES

Appendix 1 : Animal Ethics Approval

UNIVERSITY OF CAPE TOWN
Faculty of Health Sciences
Animal Ethics Committee

Room G50 Old Main Building
Groote Schuur Hospital
Observatory 7925
Tel: 0216505057
Email: fhsanimalresearch@uct.ac.za
Website: www.health.uct.ac.za/fhs/research/animalethics/forms

03 June 2020

FHS AEC REF NO: 017_019

Prof K. Sliwa
Hatter Institute for Cardiovascular Research
Chris Barnard Building
Faculty of Health Sciences
University of Cape Town

Dear Prof Silwa

PROTOCOL TITLE: MECHANISMS INVOLVED IN THE REGRESSION OF CARDIAC REMODELLING IN PREGNANT MICE.

Thank you for submitting your revised amendment to the Faculty of Health Sciences (FHS) Animal Ethics Committee (AEC) for review

I am pleased to inform you that the FHS AEC has authorised the following amendments to the above-mentioned study:

- 12 months extension; and
- Addition 5 mice.

1. A Form for amendment is also available via Submittable at: universityofcapetown.submittable.com/submit/72588/fhs005-application-for-amendments-to-a-previously-approved-study-by-fhs-aec.
2. Annual progress report submitted to the ethics office is a requirement for on-going authorisation of studies.
3. Notification of study closure is a requirement.
4. Ethics authorisation letter and copy of the application form to be submitted to the Animal Unit when commencing the study for release of animals.
5. The principal investigator has to:
5.1 Ensuring that all study participants perform within the confines of the procedures and experimental design of the protocol as authorised, or as amended.
5.2 Ensuring that all study participants comply with all applicable national legislation, UCT policies, FHS AEC policies and standard operating procedures (SOPs) and national standards (SANS 10386: 2008).

5.3 Ensuring that you as the PI (principal investigator) immediately alert the FHS AEC to any event involving the welfare of the animals which has occurred during the course of the study, as well as the actions that were taken to respond to these events.
5.4 Ensuring that you as the PI (principal investigator) alert the FHS AEC to any new or unexpected ethical issues that arose during the course of the study, and how these issues were addressed.
5.5 Ensuring that all study participants are registered with or have been authorised by the South African Veterinary Council (SAVC) to perform the procedures on animals or will be performing the procedures under the direct and continuous supervision of SAVC-registered veterinary professionals or SAVC-registered para-veterinary professionals.
6. If the principal investigator or any study participant is in any way uncertain how to respond to any of these obligations or deal with any of the issues referred to above, they must consult with FHS AEC.
7. All animals found dead must be reported to the RAF on the appropriate form:
http://www.health.uct.ac.za/fhs/research/animalethics/forms
8. All animals found in distress must be reported to the RAF and AEC on the appropriate form.

Please quote the REC. REF in all your correspondence

Yours sincerely

Signature Removed

PROF G. LOUW
CHAIR, FHS AEC

Appendix 2: Cardiac Disease in Maternity (CDMII) ethics approval

UNIVERSITY OF CAPE TOWN

HUMAN RESEARCH ETHICS COMMITTEE 14 NOV 2019 HEALTH SCIENCES FACULTY UNIVERSITY OF CAPE TOWN

FACULTY OF HEALTH SCIENCES
Human Research Ethics Committee

Form FHS007: Amendment – study staff

HREC office use only (FWA00001637; IRB00001938)			
☑ Approved			
This serves as notification that all changes to the study staff and documentation described below are approved.			
Chairperson of the HREC signature	Signature Removed	Date	15/11/2019

Principal Investigator to complete the following:

1. Protocol information

Date (when submitting this form)	13 Nov 2019
HREC REF Number	173/2010 & 262/2015
Protocol title	Cardiac Disease in Maternity Phase 2 (CDM II)
Protocol number (if applicable)	Not Applicable
Principal Investigator	Prof Karen Sliwa
Department / Office Internal Mail Address	Dept of Medicine, HICRA, 4th Floor Chris Barnard Building, Faculty of Health Sciences, Anzio Road, Observatory

1.1 Does this protocol receive US Federal funding?	☐ Yes	✓ No

2.1 Staff changes (tick ✓)

Are new personnel being added to this research?	✓ Yes	☐ No
Are current personnel being removed from this research?	☐ Yes	✓ No
Is the principal investigator for this research being changed? If yes, please attach revised conflict of interest and PI declaration statements (Refer: sections 7 and 8.3 in the New Protocol Application Form - FHS013)	☐ Yes	✓ No
Do the consent and assent forms need modification to reflect these staff changes? If yes, please attach copies of the revised forms, with all changes highlighted or tracked and listed in the documents for approval.	☐ Yes	✓ No

2.2 Amended study staff details

Title, first name, surname	Department/Division	E-mail	Role of new staff member
Ms Aqeela Imamdin *(Add)*	Medicine/HICRA	aqeela.imamdin@alumni.uct.ac.za	Scientist
Mr Vitaris Kodogo *(Add)*	Medicine / HICRA	KDGVIT001@myuct.ac.za	Scientist

3. List of documentation for approval

Please list below all staff documentation such as CVs, declarations, GCP certificates and revised consent forms which need approval. This information must correspond to all 'yes' answers in 2.1 above. This form will be signed and returned to the PI as notification of approval. Please add extra pages if necessary.

CV's & Signed Declaration of Interest for both new study staff members listed above are attached.
Aqeela Imamdin has a valid GCP certificate but Mr Vitaris Kodogo's GCP certificate has expired and he is booked to re-do his beginners GCP course on the 3&4th Dec 2019 through CREDE.
As soon as Mr Kodogo has his GCP certificate, I will send a copy up to UCT HREC.

4. Signature

My signature certifies that I will maintain the anonymity and/ or confidentiality of information collected in this research. If at any time I want to share or re-use the information for purposes other than those disclosed in the original approval, I will seek further approval from the HREC.

Signature of PI	Signature Removed	Date	13 Nov 2019

Appendix 3: EURObservational Registry on Peripartum Cardiomyopathy (PPCM) ethics approval

UNIVERSITY OF CAPE TOWN

HUMAN RESEARCH ETHICS COMMITTEE
14 NOV 2019
HEALTH SCIENCES FACULTY
UNIVERSITY OF CAPE TOWN

FACULTY OF HEALTH SCIENCES
Human Research Ethics Committee

Form FHS007: Amendment – study staff

HREC office use only (FWA00001637; IRB00001938)			
☑ Approved			
This serves as notification that all changes to the study staff and documentation described below are approved.			
Chairperson of the HREC signature	Signature Removed	Date	15/11/2019

Principal Investigator to complete the following:

1. Protocol information

Date (when submitting this form)	13 Nov 2019
HREC REF Number	R033/2013
Protocol title	EURObservational Registry on Peripartum Cardiomyopathy (PPCM)
Protocol number (if applicable)	N/A
Principal Investigator	Prof. Karen Sliwa
Department / Office Internal Mail Address	Dept of Medicine, HICRA, 4th Floor Chris Barnard Building, Faculty of Health Sciences, Anzio Road, Observatory

1.1 Does this protocol receive US Federal funding?	☐ Yes	✓ No

2.1 Staff changes (tick ✓)

Are new personnel being added to this research?	✓ Yes	☐ No
Are current personnel being removed from this research?	☐ Yes	✓No
Is the principal investigator for this research being changed? If yes, please attach revised conflict of interest and PI declaration statements. (Refer: sections 7 and 8.3 in the New Protocol Application Form - FHS013)	☐ Yes	✓No
Do the consent and assent forms need modification to reflect these staff changes? If yes, please attach copies of the revised forms, with all changes highlighted or tracked and listed in the documents for approval.	☐ Yes	✓ No

2.2 Amended study staff details

Title, first name, surname	Department/Division	E-mail	Role of new staff member
Ms Aqeela Imamdin *(Add)*	Medicine/HICRA	aqeela.imamdin@alumni.uct.ac.za	Scientist
Mr Vitaris Kodogo *(Add)*	Medicine / HICRA	KDGVIT001@myuct.ac.za	Scientist

3. List of documentation for approval

Please list below all staff documentation such as CVs, declarations, GCP certificates and revised consent forms which need approval. This information must correspond to all 'yes' answers in 2.1 above. This form will be signed and returned to the PI as notification of approval. Please add extra pages if necessary.

CV's & Signed Declaration of Interest for both new study staff members listed above are attached.
Aqeela Imamdin has a valid GCP certificate but Mr Vitaris Kodogo's GCP certificate has expired and he is booked to re-do his beginners GCP course on the 3&4th Dec 2019 through CREDE.
As soon as Mr Kodogo has his GCP certificate, I will send a copy up to UCT HREC.

4. Signature

My signature certifies that I will maintain the anonymity and/ or confidentiality of information collected in this research. If at any time I want to share or re-use the information for purposes other than those disclosed in the original approval, I will seek further approval from the HREC.

Signature of PI	Signature Removed	Date	13 Nov 2019

Appendix 4 : Lowry Method of protein determination

Protein Assay

1. **CTC reagent**
   a) Na_2CO_3 20g/100ml
   b) $CuSO_4.5H_2O$ 0.2g

   K2 Tartrat 0.4g mix in 100ml
   Slowly add a) to b), while mixing on stirrer to prevent precipitation.
2. **SDS**
   10% SDS 20g/200ml
   Dilute from the 20% SDS
3. **NaOH**
   NaOH 0.4g/200ml

Solution A: Mix all three reagents together (equal amount). Better to keep separate to have a longer shelf life.
E.g., 1ml/ sample, so for 20 samples require 20ml. Thus, 7ml CTC+7ml SDS +7ml NaOH.

Solution B: 1/5 dilution from the stock solution (in fridge)

Standard curve:

Albumin Bovine Fraction V (BSA) 2mg/ml

So, 0.02g/10ml and aliquot 1ml into epps.

Dilution series of BSA	**Amount of BSA added**	**Amount of dH_2O must take out**
0	1ml dH_2O	-
5mg	1ml dH_2O + 2.5ul BSA	2.5ul dH_2O
10mg	1ml dH_2O +	5ul dH_2O
20mg	1ml dH_2O +	10ul dH_2O
50mg	1ml dH_2O +	25ul dH_2O
100mg	1ml dH_2O +	50ul dH_2O
150mg	1ml dH_2O +	75ul dH_2O
200mg	1ml dH_2O +	100ul dH_2O *final conc 200mg/ml

Then add 1ml of solution A.

Step 1: Add 1ml of dH_2O to each tube followed by 5ul of protein

Step 2: Add 1ml solution A, vortex and let stand for 10 minutes to ensure complete dissolution of the precipitate

Step 3: Add 0.5ml solution B, vortex IMMEDIATELY (recall $t_{1/2}$ of phosphomolybdate reagent at pH=10 is only 8 seconds) and incubate for 30minutes

Step 4: Measure absorbance at 750nm

Referenced document

Lowry, O, H.; Rosenbrough, N. J.;Farr, A.L.; Randall, R.J. (1951)" Protein measurement with the Folin Phenol Reagent" J Bio Chem 193, pp. 255-275

Appendix 5: Bicinchoninic acid (BCA) assay

Purpose

The purpose of this procedure is to quantify proteins that are in a high detergent buffer, such as 1x RIPA buffer, prior to tryptic digest using the Pierce BCA kit 'microplate' assay

Equipment and Materials

Incubator at 37°C, Spectrophotometer, Pierce BCA kit cat # 23225, Flat bottomed clear 96 well plate

Reagents

Pierce BCA reagent A (clear), Pierce BCA reagent B (blue), Pierce BSA standard at 2mg/ml (ampoule)

Procedure

Your protein sample should be fully homogenised and in an acceptable concentration of detergent, i.e.:

Brij™-35	5.0%
Brij-56, Brij-58	1.0%
CHAPS, CHAPSO	5.0%
Deoxycholic acid	5.0%
Octyl β-glucoside	5.0%
Nonidet P-40 (NP-40)	5.0%
Octyl β-thioglucopyranoside	5.0%
SDS	5.0%
Span™ 20	1.0%
Triton™ X-100	5.0%
Triton X-114, X-305, X-405	1.0%
Tween™-20, Tween-60, Tween-80	5.0%
Zwittergent™ 3-14	1.0%

Make up working reagent according to the following equation (round up to ensure you have enough for the blank!):

Vol WR = (# samples + # standards) x (# replicates) x (200 ul)

Make up your standard curve in the same buffer as your protein sample according to the following doubling dilution from the Pierce 2 mg/ml BSA ampoule:

1 mg/ml
0.5 mg/ml
0.25 mg/ml
0.125 mg/ml
0.0625 mg/ml

Make up 50 ul of each standard.

Pipette 10 ul of each sample and each standard in triplicate into a flat bottomed 96 well plate, and one blank of lysis buffer only

Add 200 ul of working reagent into each well and tap carefully to mix

Cover plate and incubate at 37°C for 30 minutes

Measure at or near 562 nm on a plate reader – NOTE: Our plate reader can only measure 595 nm – this is fine.

Check that your R2 value is approaching 1!

Calculate the concentrations of your samples

Referenced documents

Pierce BCA protein assay kit user guide (2019)

Appendix 6: Filter Aided Sample Preparation (FASP)

Purpose

The purpose of this procedure is to generate tryptic peptides from crude lysates for LC-MS analysis using a molecular weight cut-off (MWCO) filtration device. It is particularly suitable for studying complex proteomes and fractions containing cell membranes.

Scope

This procedure describes the reduction of cysteine bonds using dithiothreitol (DTT), denaturation of proteins using urea (UA), alkylation of cysteine residues with iodoacetamide (IAA), and digestion of proteins using trypsin.

Equipment

- Water bath set at 95°C
- Microcentrifuge up to 14000 x *g*
- Vortex 600rpm
- Incubator up to 37°C
- Wet chamber
- Microcentrifuge up to 4000 x *g* that can accommodate FASP filter
- speedyVac concentrator/condenser (switch on 30 minutes prior to use)
- -20°C freezer

Materials

- UFC503096 - 30K FASP filters 500ul (Amicon Ultra centrifugal filter units 30 KDa NMWL, MWCO, 96 PK). Capacity of 0.2-200ug of protein.
- 1.09535.0001: pH-indicator strips, non-bleeding, pH 0-14, Universal indicator, Merck
- 6090357: Tapered micro inserts 0.1ml. (Clear glass, tapper bottom, 100 p/k, 0.1ml / 31 x 6mm / 15mm top, BM Scientific, Separations)
- 702283: Autosampler flat screw neck vials, 1.5ml. (N9 screw neck vial, clear, label and scale flat bottom, 100/pk, 1.5ml / 11.6 x 32mm, BM Scientific, Separations)
- Protein samples in appropriate buffer (RIPA buffer or urea buffer) with known concentration
- Eppendorf tubes (1.5 and 2.0 ml)

Reagents

- P8101S: Trypsin and 2X buffer. (Trypsin-ultra, Mass Spectrometry Grade. New England Biolabs). Obtain beforehand and store in -20 freezer until use
- 00020-14261-1L/1.00029.2500: LiChrosolv Acetonitrile (ACN) hypergrade for LC-MS
- 00040-14265-1L: Formic acid (FA) LC-MS Ultra Eluent additive
- 43816-50ML: 1M DTT for FASP. (1,4 - DL - Dithiothreitol solution, BioUltra, for molecular biology, ~1M in H2O, Sigma-Aldrich)
- IAA
- Ammonium bicarbonate
- HPLC water

Solutions

- Urea buffer (UA): 24g urea in 50mL of 0.1M tris dilution in HPLC water from 1M tris
- Ammonium Bicarbonate (ABC): 0.2g ABC (from FASP fridge) in 50mL water
- 0.05M Iodoacetamide (IAA): Weigh out a small amount (~0.05g) and back-calculate the required volume of UA to obtain 0.05M
- Reduction buffer (RB): 1M DTT (aliquots stored in FASP freezer)
- 1 M $CaCl_2$ solution

Procedure

1. **Buffer exchange**

1.1. Set water bath to 95°C, assemble and label filters accordingly

1.2. Remove 100 ug aliquots of each protein sample into a clean eppendorf tubes

1.3. Add DTT to each sample to a final concentration of 0.1 M, and incubate at 95°C for 3 minutes (e.g., 5.5 uL of 1M **DTT** added to 55.55 uL of protein sample)

1.4. To prepare the filters, add 500uL of **UA** to each filter unit and centrifuge at 14000 x *g* for 10 minutes

1.5. Add each sample to a filter unit

1.6. Add 200 uL of **UA** and centrifuge at 14000 x *g* for 15 minutes. Repeat once

1.7. Discard the flow-through from the collection tubes, and place the filter into an empty collection tube

1.8. Add 100 uL of **IAA** solution and mix by vortexing at 600rpm for 1 minute

1.9. Incubate in the dark for 20 minutes without mixing

1.10. Centrifuge the filter units at 14000 x *g* for 10 minutes

1.11. Add 100 ul of **UA** to the filter unit and centrifuge at 14000 x *g* for 15 minutes. Repeat twice.

1.12. Add 100 ul of **ABC** to the filter unit and centrifuge at 14000 x *g* for 10 minutes. Repeat twice.

2. Tryptic digest

2.1. Replace collection tubes with a clean tube before adding trypsin

2.2. Check that the pH is approximately 9 using a pH strip and ~1ul of each sample

2.3. Reconstitute 20 ug of trypsin in 40uL of HPLC water (final concentration of 0.5 ug/ul).

2.4. For an enzyme to protein ratio of 1:100, add 1 ug of diluted Trypsin to your sample.

2.5. Add 40 ul of ABC or trypsin buffer, and ensure that the final concentration of $CaCl_2$ is 20 mM

2.6. Mix by vortexing or triturating

2.7. Place filters in a wet chamber and incubate at 37°C for 12-18hrs. Ensure length of tryptic digest is constant between experiments to maintain reproducibility

2.8. Transfer filters to new collection tubes before centrifuging at 14000 x *g* for 10 minutes. The flow through contains tryptic peptides.

2.9. Add 40uL of **ABC** before centrifuging at 14000g for 10 minutes. Transfer flow through containing tryptic peptides into fresh eppendorf tube

2.10. Acidify tryptic peptides with formic acid to a final concentration of 0.1%, or until the pH is 3

2.11. Proceed with desalting (see SOP for 'C18 desalting')

Referenced documents

1) Wisniewski *et al.* (2009) Universal sample preparation method for proteome analysis. Nature Methods. Vol 6 No 5, 259-363.

Appendix 7: Western blot gel preparation

Preparation of gels (Table for two gels of 0.75mm, double volume for 2 gels of 1.5 mm

		Resolving gel			**Stacking gel**
Reagent	**Stock**	**7.5% gel**	**10% gel**	**12% gel**	**4% gel**
dH_2O	**Distilled**	5.525 ml	4.9 ml	3.35 ml	3.05 ml
Tris – HCl	**1.5 M pH 8.8 (resolving gel)**	2.50 ml	2.50 ml	2.50 ml	1.50 ml
	0.5 M pH 6.6 (stacking gel)				
SDS	**10%**	100 µl	100 µl	100 µl	50 µl
Acrylamide	**40%**	1.875 ml	2.50 ml	3.0 ml	0.5 ml
APS	**10%**	50 µl	50 µl	50 µl	50 µl
Temed	**99%**	20 µl	20 µl	20 µl	10 µl

- APS and TEMED react immediately, add TEMED last. Stir solution and immediately add to assembly of plates with a Pasteur pipette. Make sure that no bubbled form
- Add a few drops of N-Butanol (or 70% ethanol) to prevent oxidation of gel. If exposed to air, the solution won't polymerize and form the gel.
- Allow to set for 30 minutes
- Remove N-Butanol with water
- Add the stacking gel on top of resolving gel. Insert the comb at an angle to prevent bubbles from forming.
- Allow to set (about 15 minutes).

Sample preparation

- Add the appropriate volume of sample (protein lysate) to 20 µl laemmli's loading buffer. Boil at 95˚C for 5 minutes. Store at -80˚C.
- Before use for protein separation
  - Boil again as mentioned above.
  - Centrifuge at 8000 rpm for 10 seconds to collect sample before loading into wells.

Assemble and load samples into gels

- Put gels on the electrophoresis stand and, click knobs in place
- Place in tank and add running buffer in the middle compartment
- To load the samples, run a bit of sample buffer in the wells with a Hamilton pipette to show where the wells are.
- Place the marker in in 1st well on the left, nearest to you.
- Add the samples in the wells after the marker, washing Hamilton x5 after every sample
- Place the 1x running buffer in the outer compartment of the tank, just past the wire, or if system leaks to the top of the compartment.
- Place green lid on and attach electrodes, red to red, black to black.
- Run 1st: 100 V; 200 mA; 10 minutes
- Run 2nd: 200 v; 200 mA; 50 mi

Appendix 8: Western blot buffers and recipes

Laemmli's loading buffer – sample preparation

Solution A:

- 38 ml ddH_2O
- 10 ml 0.5M Tris (pH 6.8) use HCl to pH
- 8 ml glycerol
- 16 ml 10% SDS
- 4ml 0.05% (w/v) bromophenol blue – this is only to colour the buffer

On the day of use make up a **working solution** of laemmli's as follows:

- For every 850 µl solution A, add 150 µL B-mercaptoethanol
- Do not store this mixture for more than 2 days as it oxidizes

10X Running Buffer:

For 200 ml:

- Dissolve the 6.06g Tris and 28.8g Glycine in 150 ml ddH_2O (takes about an hour)
- Add 2.0 g SDS
- pH to 8.6 with concentrated HCl and then make up to 200 ml
- **For use:** Dilute running buffer to 1x – 900 ml ddH_2O and 100 ml 10x Running Buffer. Mix well and do not adjust pH

Transfer buffer 2 L

- 6.06g Tris
- 28.83g Glycine
- 400 ml 20% Methanol
- Dissolve Tris, glycine and methanol in dH_2O and make up to full amount, no need to set pH. Store in fridge.
-

10X TBS

For 1L:

- Dissolve 24.2g Tris and 80g NaCl in 600 ml ddH_2O.
- Adjust pH to 7.6 with HCl
- Make up to 1 L with ddH_2O
- **For use:** Dilute to 1x add 1 ml tween 20 for 1x TBS-T

Appendix 9: Automated processing protocol

Step #	Solution	Time (minutes)	Temperature
1	70 % Ethanol	60	RT
2	70% Ethanol	60	RT
3	90% Ethanol	60	RT
4	95% Ethanol	60	RT
5	95% Ethanol	60	RT
6	100% Ethanol	60	RT
7	100% Ethanol	60	RT
8	100% Ethanol	60	RT
9	Xylene	60	RT
10	Xylene	60	RT
11	Paraffin wax	120	60
12	Paraffin wax	120	60

Appendix 10: H& E staining procedure

Step #	Solution	Time (minutes)	Repetitions
1	Xylene	5 minutes	X2
2	Ethanol 99%	2 minutes	X2
3	Ethanol 96%	2 minutes	X1
4	Ethanol 70%	2 minutes	X1
5	Tap water	2 minutes	X1
6	Haematoxylin	8 minutes	X1
7	Running water	5 minutes	X1
8	Scott's Tap water	2 minutes	X1
9	Running water	1 minute	X1
10	Eosin	30 seconds	X1
9	Running water	1 minute	X1
10	Ethanol 96%	1 minute	X2
11	Ethanol 99%	1 minute	X1
12	Xylene	1minute	X1
13	Xylene	1 minute	X1
14	Air dry and mount		